Investigation of Concrete Wall Systems for Reducing Heating and Cooling Requirements in Single Family Residences

Ian Ross Doebber

Thesis submitted to the faculty of the
Virginia Polytechnic Institute and State University
in partial fulfillment of the requirements for the degree of

Master of Science

in

Mechanical Engineering

Dr. Michael W Ellis, Chair
Dr. Yvan J Beliveau
Dr. Douglas J. Nelson

September 10, 2004
Blacksburg, Virginia

Keywords: concrete wall, residential, holistic analysis, thermal performance

Investigation of Concrete Wall Systems for Reducing Heating and Cooling Requirements in Single Family Residences

Ian Ross Doebber

ABSTRACT

The single family housing sector currently accounts for approximately 15% (US DOE 2002) of the total national energy consumption with the majority of the energy use associated with the HVAC system to provide comfort for the residents. In response to recent concern over the unpredictability of the energy supply and the pollution associated with its consumption, new methods are constantly being developed to improve the energy efficiency of homes. A variety of concrete wall systems including Multi-functional Precast Panel (MPP) systems and Insulating Concrete Form (ICF) systems have been proposed to not only improve the building envelope thermal performance but other important residential characteristics such as durability and disaster and fire resistance. MPPs consist of Precast Concrete Panels (PCPs) that incorporate structural elements, interior and exterior finishes, insulation, and even heating/cooling systems into a single manufactured building panel. The ICF system is a cast-in-place concrete panel system that does not offer the level of integration found in the MPP system but has become increasingly accepted in the building construction industry. This research evaluates the thermal performance benefits of concrete wall systems in detached, single family home applications.

The thermal performance benefits of two MPP systems and an ICF system are analyzed within the context of a representative or *prototypical home* in the U.S. and are compared to two wood frame systems; one representing a typical configuration and the other an energy efficient configuration. A whole wall approach is used to incorporate the two and three dimensional conduction and transient characteristics of the entire wall assembly, including the clear wall and wall detail regions, into a whole building simulation of the prototypical house. The prototypical house heating and cooling energy consumption associated with each wall system is determined for six representative climates throughout the U.S. to evaluate the effect of various ambient conditions on the relative energy savings. For each wall system, the effect of thermal bridging on overall R value, the effect of thermal capacitance, and the role of infiltration on energy use are investigated.

The results of the research include a comparison of the prototypical house energy savings associated with each of the wall systems; an assessment of the relative importance of the increased insulation, thermal mass, and improved air tightness on the overall energy load; and a comparison of the cost of ownership for the various wall systems. The results indicate that properly designed concrete wall systems can reduce annual heating and cooling costs. In

addition, the results show that the most significant impacts of improved wall systems are, from greatest to least: infiltration reduction, improved insulation configuration, and thermal capacitance. Finally, the results show that while there are energy savings associated with concrete wall systems, economic justification of these systems must also rely on the other attractive features of concrete systems such as greater durability and disaster resistance.

ACKNOWLEDGEMENTS

I would first like to thank my family, Tom, Lynne, and Rachel Doebber, for their unconditional love, support, and encouragement.

Special thanks to my advisor, Dr. Mike Ellis, for his guidance, support, encouragement, and giving me the opportunity to work with him. Thanks to Dr. Doug Nelson and Dr. Ivan Beliveau for their support and recommendations for further improvement of this work.

Finally, thanks to all my friends who have made my time in Blacksburg extremely enjoyable and one that I will never forget.

TABLE OF CONTENTS

NOMENCLATURE

A	area (ft^2) or (m^2)
A*	State Space coefficient matrix associated with the state variable vector [x]
B*	State Space coefficient matrix associated with the input vector [u]
C*	State Space coefficient matrix associated with the state variable vector [x]
C	Total thermal capacitance $\left(\frac{Btu}{lb \quad ft^2}\right)$
C_p	Specific Heat $\left(\frac{Btu}{lb \quad F}\right)$ or $\left(\frac{J}{kg \quad K}\right)$
D*	State Space coefficient matrix associated with the input vector [u]
H	Height of the house from ground level to ceiling
H_0	Reference height of a one story home (8 ft)
k	conductivity $\left(\frac{Btu/hr}{ft \quad F}\right)$ or $\left(\frac{W}{m \quad K}\right)$
n	number of nodes across a wall system for the finite difference implementation of the State Space Method
q''	surface heat flux $\left(\frac{Btu/hr}{ft^2}\right)$ or $\left(\frac{W}{m^2}\right)$
R	resistivity of a wall section defining its steady state performance $\left(\frac{hr \quad ft^2 \quad F}{Btu}\right)$
T	temperature (F) or (C)
t	current time step (seconds)
TP	referring to the other thermal properties of a wall system (i.e. structure factors and thermal capacitance)
u	vector of inputs associated with the State Space Method
V	volume (ft^3) or (m^3)

X^*	time series of internal response factors with an internal temperature pulse associated with the response factor equation
X	outside conduction transfer function coefficient
x	Vector of state variables associated with the State Space Method
Y^*	time series of internal response factors with an external temperature pulse associated with the response factor equation
Y	cross conduction transfer function coefficient
y	Vector of outputs associated with the State Space Method
Z*	time series of external response factors with an external temperature pulse associated with the response factor equation
Z	inside conduction transfer function coefficient
δ	time step associated with the response factor or conduction transfer function equations (seconds)
f	flux conduction transfer function coefficient (Btu/hr) or (W)
j_{ii}	internal structure factor associated with the equivalent wall method
j_{ie}	integral structure factor associated with the equivalent wall method
j_{ee}	external structure factor associated with the equivalent wall method
q	dimensionless temperature for the problem of steady-state heat transfer with interior and exterior surface temperatures equal to 0 and 1 respectively used to calculate the structural factors for the equivalent wall method
r	density $\left(\frac{lb}{ft^3}\right)$ or $\left(\frac{kg}{m^3}\right)$

SUBSCRIPTS

CW	Clear wall
i	internal surface of a wall system or the ith wall detail
o	external surface of a wall system

LIST OF FIGURES

LIST OF TABLES

CHAPTER 1: INTRODUCTION

The housing industry is an integral part of the US economy with housing and related services accounting for 14 percent of the Gross Domestic Product (Ellis 2002). Furthermore, the size of the housing industry is steadily increasing as shown by the plot of new single family home constructions within the United States from 1980 to 2002 in Figure 1.1 below (US DOE 2002). Yet to those who inhabit a house, these statistics pale in comparison to the value of comfort, safety, and financial stability that a home provides. Therefore, the significance of the housing industry is that it not only contributes to the health of the economy but the basic welfare of the people.

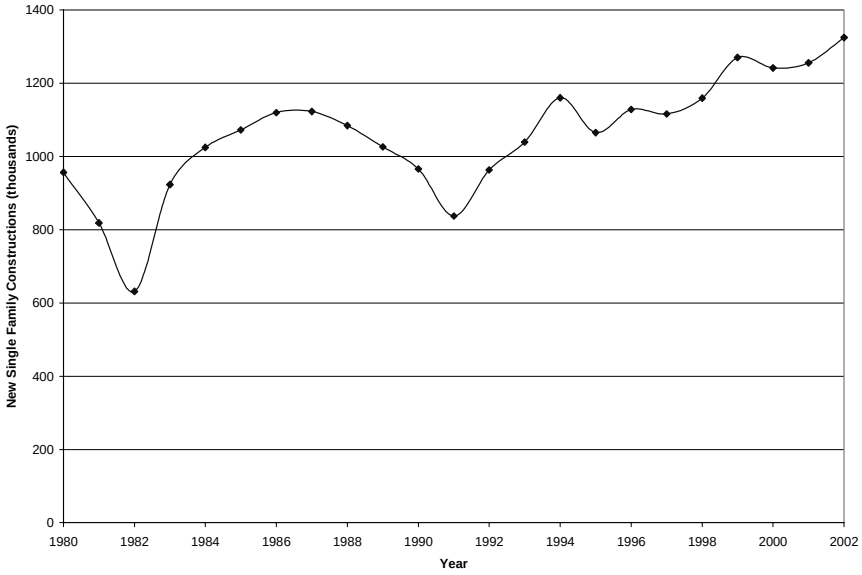

Figure 1.1. New single family home constructions from 1980 to 2001 (US DOE 2002)

In response to the obviously important role the housing industry has, the national government formed the Partnership for Advancing Technology in Housing (PATH). The organization is dedicated to the advancement of residential performance through new technological innovation and building practices. Several of the most important goals of PATH are developing new housing techniques that improve:

- Affordability,
- Safety and disaster mitigation,
- Quality and durability,
- Environmental performance, and
- Energy efficiency.

Within the past decade, the energy and environmental goals have become more of a predominant issue due to the increasing instability of the energy supply and growing public concern over the pollution associated with energy consumption. According to the 1997 Residential Energy Consumption (REC) survey (US DOE 1997), 73 percent of the 101.5 million residences are single-family homes. These single family homes contribute a significant portion to the national energy consumption as illustrated in Figure 1.2 which is based on Energy Information Administration (EIA) data for the year 2001 (US DOE 2002).

Figure 1.2. 2001 U.S. energy consumption end use splits
(US DOE 2002)

A typical household consumes 100 MBtu annually of on-site energy (amount of energy consumed within the home); roughly 50 percent for space heating, 22 percent for

appliances/lights, and 28 percent for air conditioning/hot water heating. Accounting for generation and transmission losses for the various energy types, a typical house consumes 172 MBtu per year of primary energy. This amount of energy usage results in a $1400 bill per household and $167 billion total residential sector expenditure annually (US DOE 1997).

Recognizing their appreciable energy consumption, the national government set minimum efficiency standards for many household related products. The National Appliance Energy Conservation Act (NAECA) enacted in the late 1980's regulated all large home appliances and space conditioning equipment. In conjunction, state and local governments set stricter building codes requiring greater insulation and tighter building construction. Essentially both initiatives were the same basic approach to tackling the problem, separate the major components affecting residential energy usage and optimize the efficiency of each independently. Looking back at annual energy consumption per household, these actions seemed to have worked. Typical household energy usage was down 27% from the 1978 REC survey to the 1997 REC survey mainly due to reduced space heating loads in the early to mid 1980's (US DOE 1997). Yet the most notable achievement is that household energy consumption has declined despite the enormous increase in household electronic equipment which nearly doubled from 1980 to 1997 (Wenzel et al 1997).

Although the regulations set forth by the NAECA and local building codes are continually updated, improvements in efficiency have begun to level off. Further efforts have only improved the performance of the individual components a fraction of that obtained during the initial years of the stricter standards. Fortunately, a completely different approach has started to gain popularity within the housing industry. Rather than separately optimizing the individual components that contribute toward the household energy consumption, a holistic method called the whole house approach can be implemented.

The whole house approach is the next logical step toward providing a significant improvement in energy efficiency and the other performance parameters highlighted by the PATH goals. This

method revamps the traditional technique which relies on the assembly of independently designed and fabricated components which may or may not share a common purpose. For example, the conventional construction practice configures the structural infrastructure without recognizing how it will affect the insulative behavior of the building envelope. The result is a complex management challenge allowing ample opportunities for failure and less than optimal performance of the overall system. Conversely, the whole house approach acknowledges the behavior of all the building components and integrates them in such a way to maximize the total system performance. From a fundamental standpoint, the whole house method is based upon the principle "a chain is only as strong as its weakest link". By evaluating the design to locate the weakest components, revisions to the total design can be made to eliminate or at least minimize these weak points.

Although the applicability of the whole building approach is by no means limited to design and construction (other areas include landscaping, operational conditions, and appliance interconnection), its adoption into these aspects of the housing industry has been the most prevalent thus far. This can be best explained by the flooding of the building market with inexpensive, often free, software over the past 20 years that provide engineers, architects, and contractors the ability to apply computational tools to help achieve whole house design. Rather than solely relying on experience and empirical data, algorithms based upon fundamental physical equations can describe the complex relationships between the many different building components. Repeated simulations analyzing various design strategies give the designer the ability to make an educated decision on which solution maximizes the desired performance. As computational power grows at an exponential rate, the capabilities of these programs will increase as well, affording greater complexity in whole house modeling.

While computational tools assist with applying whole house design to existing construction methods, the advent of entirely new construction techniques provides additional opportunities for improvement. For example, the Multi-functional Precast Panel (MPP) system inherently exemplifies the whole house approach and therefore has a large potential to improve the overall performance of a home. This technology consists of precast concrete panels (PCPs) that incorporate structural elements, interior and exterior finishes, insulation, and even

heating/cooling systems into a single manufactured panel. They epitomize the whole house design by forcing the architects, engineers, and contractors to optimize the overall system during the design phase since all of the construction elements are contained within one panel. A typical MPP is illustrated in Figure 1.3.

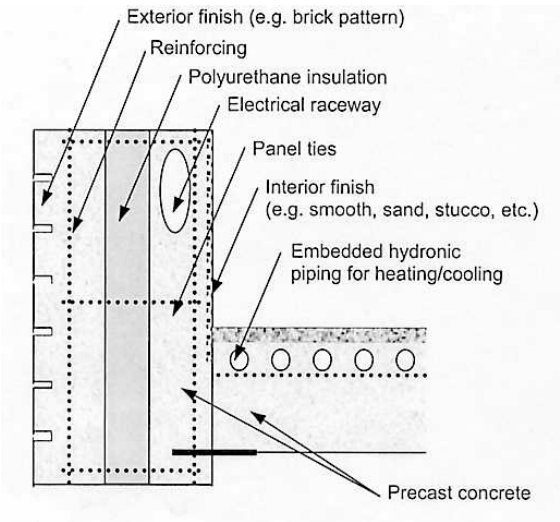

Figure 1.3. Typical MPP for residential construction
(Ellis 2001)

PCP[1] technology offers improvements to all the PATH goals. In fact, PCP systems were labeled number 10 in the top ten technologies to pursue in 2004 to improve the affordability, quality/durability, environmental impact, and energy efficiency of homes. The following paragraphs briefly explain how PCP systems meet each one of these goals outlined by PATH.

In terms of affordability, the material costs for panels are larger than wood frame systems. Yet PCP systems are designed for quick assembly in the field which reduces construction time and labor costs. A house that would normally take approximately a month to frame using wood frame construction would take roughly 3 days using a PCP construction and an experienced crew (Long 2004). PCP systems also eliminate the need for several of the tasks required for wood frame construction such as applying insulation, air ducts, or interior/exterior finishes since these

[1] Here PCP technology refers to precast concrete panels with or without the embedded energy systems characteristic of MPP systems

components can be cast within the panel. Therefore, with increased PCP production resulting in greater economies of scale, the material costs of panels can be reduced such that the overall material and construction cost of this system has the potential to be less then that of conventional wood frame technologies.

With respect to quality and durability, PCP systems far exceed wood frame technologies by the simple fact that reinforced concrete is much more resistant to bug infestation, natural disasters, and fire than wood. A study conducted at Texas Tech University shot wood studs at speeds over 100 miles per hour toward wood frame and concrete walls to simulate tornado or hurricane conditions. For all the tests, the wood stud penetrated the wood frame wall but was deflected away by the concrete wall. In another test, when both wall systems were exposed to hot flames at temperatures over 2000°F, the wood frame system structurally failed after 1 hour while the concrete wall system remained structurally sound for the entire 4 hours of testing.

Regarding environmental performance, according to a study conducted by Canada's natural resources council, the material extraction and production to build a concrete home produces slightly more greenhouse gas emissions than that for a wood frame home. Yet incorporating the greenhouse gas emissions associated with the energy consumption to heat and cool the house, the higher thermal performance of concrete homes results in significantly less emissions than that of the wood frame house. In fact, after one year of operation, the total emissions released including those associated with the materials and heating/cooling energy were roughly the same for the concrete and wood frame systems.

Three aspects of PCP technology make it ideal for improving residential energy efficiency. First, the majority of the panel consists of concrete, a large thermal capacitance material which helps in mitigating and delaying thermal loads through the absorption of large surpluses in energy. Second, PCPs reduce air leakage in the building envelope caused by wall details since they are fabricated in a controlled industrial environment which minimizes construction errors and results in a tight assembly. Third, PCPs can be designed with a more continuous insulation configuration preventing thermal bridging effects (Cornelissen 1998).

Currently, PCP technology has been limited to large or medium scale commercial buildings. Despite their benefits and level of integration with other energy efficient design concepts, PCP technology has not been able to penetrate the residential construction market due to price competition, the lack of established guidelines for their design, construction, and assembly, and an inability to distinguish their performance versus conventional wood frame constructions. On the other hand, a cast-in-place concrete construction method called Integrated Concrete Forms (ICFs) has had greater success at entering the housing market. First implemented 30 years ago, ICFs are praised by home owners for some of the same benefits PCP panels can provide; better thermal performance, reduced maintenance, improved noise reduction, and increased resistance to damage and fire. Basically, ICFs are a layer of concrete enclosed by a layer of insulation on either side. With the recent price fluctuations associated with wood frame construction, ICFs have rapidly gained attention among home owners and builders. Although they only accounted for 2.7% of homes constructed in 2001, they grew 29% from the previous year according to the National Association of Home Builders (NAHB) and the Portland Cement Association (PCA). The success of ICFs suggests that the housing market is ripe for the introduction of an PCP system which has the potential to provide greater benefits than ICFs.

The research presented here is motivated by the needs to understand the impact of PCP construction on energy costs and to demonstrate approaches for designing energy efficient PCP systems. The research is divided into three parts. First, an approach based upon the work of Kossecka and Kosny (1997) is applied to assess the transient thermal response of PCP systems. Second, a building energy modeling program is used to analyze the possible energy savings of a typical U.S. residence constructed using PCPs over wood frame and ICF technologies. Finally, the construction and life cycle costs associated with this technology will be compared to wood frame and ICF residential building practices.

CHAPTER 2: PROBLEM DESCRIPTION

The objectives of this research are to compare the thermal performance and economic costs of Multifunctional Precast Panel (MPP) technologies versus Wood Frame and Insulated Concrete Form (ICF) technologies for a "typical" home construction. First the approach developed by Kossecka and Kosny (1997) was used to characterize precast concrete panel (PCP) wall assemblies based on their overall resistance, thermal capacitance, and structure factors. Second, the EnergyPlus building modeling program was used to simulate a typical, detached, single family house constructed with different PCP, ICF, and wood frame technologies in six different US locations. The characteristics of a "prototypical" house which served as a basis for comparison for the different wall technologies were established by a thorough review of the literature. The effect of each wall system on the thermal performance of the building envelope and energy efficiency of different residential HVAC systems within the context of the prototypical house was then evaluated. In the course of this study, different modifications were made to the various wall systems to determine ways to improve their thermal performance. Finally, the initial construction and life cycle costs were calculated for each wall technology to determine the feasibility of MPPs to penetrate the household construction market.

From a strict terminology standpoint, precast concrete panels (PCPs) refer to the configuration of concrete and insulation elements that are comprised within the interior and exterior surface finishes. The multi-functional precast panel (MPP) incorporates the PCPs and the interior and exterior finishes as well as any additional space conditioning equipment such as the duct or hydronic radiant piping systems. Since the interior and exterior surface finishes are included in the analysis of the PCP wall assemblies and neither duct nor radiant systems are evaluated in this study, PCP and MPP will be used synonymously.

Essentially four different wall technologies were analyzed: wood frame construction, ICF construction, precast waffle panel construction, and sandwich PCP construction. For the wood frame and precast waffle panel technologies, two systems were simulated. The first represented the standard, base configuration commonly used by industry. The subsequent system represented different modifications that could be made to the base case to improve the thermal performance of that technology. With this approach, the thermal performance improvement of

each system to realistic enhancements would be understood. Table 2.1 reviews the four wall technologies modeled and describes the different modifications made to each. Chapters 4 and 5 explain how each of the different wall systems were modeled and present the energy performance results.

Table 2.1. Four different wall technologies

Wall Technology	Modifications
Waffle MPP	1. Base Case 2. Added Insulation
Sandwich MPP	1. Base Case
Wood Frame	1. Base Case 2. Energy Efficient
ICF	1. Base Case

The whole house approach was applied to the simulation of the prototypical home to fully analyze how the different wall systems affected all the elements directly associated with its energy performance. The house was modeled in six different US locations to understand how the behavior of the wall systems changed according to different climates experienced within the country. The construction and occupant characteristics were obtained mainly from the 1997 REC survey (US DOE 1997). The appliances and lights energy use profiles as well as the residential HVAC performance information were obtained from the 1997 RECS (US DOE 1997), 1997 Energy Data Sourcebook (Wenzel et al. 1997), and 1987 BEAG technical document (Huang et al. 1987). All these sources are reviewed in the literature survey presented in Chapter 3. Table 2.2 below covers the main information defining the prototypical home. Chapter 4 describes in detail the specific information gathered from the sources and the modeling decisions made from that information.

Table 2.2. Typical detached, single family home characteristics

Home Specifications	Description
Room Configuration	3 Bedrooms; 2 Bathrooms; 1 Living Room; 1 Dining Room; 1 Kitchen; 1 Basement; 1 Garage
Conditioned Floor Area	2275 ft^2
Number of Windows	14
Total Glazing Area	218 ft^2
Annual Appliance/Light Loads	32 MBtu
Thermostat Setpoints	Summer: 78°F Winter: 70°F
Heating Equipment	Gas Furnace / Heat Pump
Cooling Equipment	Central Air Conditioner / Heat Pump

For all the wall technologies evaluated, except the precast waffle panel system, two different cost estimates are presented. First, the initial cost to build the prototypical house was calculated using construction cost data associated with each wall system. Second, the annual energy consumption results and typical energy costs were used to determine the annual monetary savings associated with the greater heating and cooling energy performance provided by the ICF and PCP wall systems versus the conventional wood frame system. Chapter 4 reviews the method and assumptions to develop the construction costs for each wall system and energy costs for the different prototypical house locations. Chapter 5 shows the initial costs and annual heating and cooling bill savings associated with the ICF and MPP technologies. Note that the unit system convention used in the ensuing sections follows the standard used in the building construction industry; Imperial (English) Units for everything except electric energy consumption which is defined in kilowatt-hours (kW-hr).

CHAPTER 3: REVIEW OF LITERATURE

A literature survey was completed prior and throughout this research project to incorporate any existing studies that have conducted a similar analysis or developed methods to assist in characterizing the thermal performance of a wall system. Section 3.1 provides further insight into the current stage of development of PCP systems in regard to their viability as an alternative for the residential construction market. Section 3.2 presents the extensive capabilities of EnergyPlus and the rigorous verification testing it passed to prove its validity as a worthy program to use for this study. Section 3.3 reviews the recent research that developed the revolutionary building envelope analysis techniques that were used in this study. Section 3.4 covers the publications from which characteristic data and various methods were obtained to simulate a typical, detached, single family residence to the highest accuracy such that PCP performance could be confidently assessed in the applied environment. Section 3.5 states the references used to obtain the economic data associated with the different wall systems evaluated. Finally Section 3.6 shows several similar research initiatives to which the results of this study were compared and to emphasize the contribution of the current study toward the greater body of knowledge.

3.1 Background on Concrete Construction

The following subsections give a broader picture of the current status of PCPs for household construction and the important factors that will determine its penetration into that market. Subsection 3.1.1 briefly summarizes the different current concrete construction technologies. Subsection 3.1.2 highlights the ways in which PCP systems can potentially improve upon the important characteristics of a sustainable construction technology outlined by PATH over the ICF construction method described in 3.1.1. Finally, subsection 3.1.3 states the current level of the different concrete methods in home construction and the main factors inhibiting PCPs growth.

3.1.1 Different Concrete Constructions

In response to the increasing difficulty to meet new expectations with the same old wood framing technology, more methods of using concrete to build homes are appearing. All of them

provide the typical benefits with using concrete such as superior strength, minimal maintenance, fire resistance, and acoustic damping. The following paragraphs describe the different residential concrete construction approaches including concrete masonry, cast-in-place concrete, and precast concrete panels (PCPs).

Concrete masonry which refers to the assembly of individual concrete elements (i.e. blocks) has improved in strength, sound resistance, and energy efficiency with advances in rigid foam insulation and construction methods. These systems provide greater moisture protection and potentially lower costs by replacing wood studs and fiberglass insulation with metal brackets and rigid foam insulation. Several sub-variations of concrete masonry exist such as interior insulated block, exterior insulated block, and integrated block insulation. One of the most recent developments in concrete masonry is using blocks comprised of Autoclaved Aerated Concrete (AAC). AAC is made with all fine aggregates mixed with cement and a natural expansion agent that fills the block with small air pockets such that the resultant form is 80% air. The benefits of AAC are its light weight, flexibility (since it can be cut just like wood), and its significantly lower conductivity than normal concrete according to the Portland Cement Association.

The most traditional concrete construction method is cast-in-place construction using temporary forms typically made of aluminum. Rigid insulation is placed in between the forms and held in place with non-conductive ties. Once the concrete is poured and sets, the forms are removed and reused again. The greatest advantage of this method is its flexibility and speed. All the exterior walls can be poured at the same time with spaces for fenestration automatically cast with the amount of insulation decided upon by the builder.

A subtle variation to the cast-in-place method has resulted in the most popular energy efficient concrete technology currently in the home construction industry. Insulated Concrete Forms (ICFs) replace the temporary aluminum forms with insulation. As a result, concrete is poured in between two layers of insulation preformed into interlocking blocks or connected with plastic ties. The insulation layers provide a continuous insulation barrier and backing for dry wall on the inside and some sort of finish material on the outside. Table 3.1 describes the three different

varieties of ICFs that are available. ICFs first began in Europe and have been used in home construction for the past 30 years. They are accepted by all the major building codes in the U.S.

Table 3.1. Different varieties of ICFs

ICF Type	Concrete Description
Flat System	constant layer of concrete
Grid System	waffle pattern where the concrete is thicker at some points than others
Post-and-Beam System	discrete horizontal and vertical columns of concrete completely encapsulated in the foam insulation

PCP systems are usually lumped alongside tilt-up construction since both are based upon a panel system although the two are very different. PCPs are manufactured in an industrial environment and are shipped to the construction site. Tilt-up construction casts all the building envelope surfaces in forms on the floor slab which are than tilted up and held in place by columns or other fastening devices. Tilt-up construction is extremely effective if the building design is mostly right angles.

3.1.2 PCPs versus ICFs

Concrete construction, irregardless of the applied method, has the potential to provide benefits over wood frame construction including: improved thermal performance, increased strength, less maintenance, and reduced outside noise. Therefore concrete inherently provides the characteristics defined by PATH. Yet the magnitude of the increase in performance depends on the type of concrete construction and the details of the system. So far, ICFs have proven their worth to home owners and builders. In fact, the National Association of Home Builders (NAHB) Research Center, sponsored by the Portland Cement Association (PCA) and the U.S. Department of Housing and Urban Development (HUD), coordinated four demonstration projects in four locations (Virginia Beach, Austin, Sioux City, Chestertown) to evaluate the performance of ICFs. The following paragraphs describe how ICFs meet the goals defined by PATH according to a study done (NAHB Research Center 1997) on these four ICF homes and postulates how PCPs have the potential to perform even better.

The thermal testing of ICFs conducted for the NAHB association (NAHB Research Center 1997) included collecting air infiltration data and thermographic imaging. The testing showed that the ICF clear wall contained less cold spots than wood frame systems. Yet the wall details had a significant detrimental effect on the total system insulative efficiency. Winter infiltration rates varied from 0.15 to 0.55 air changes per hour (ACH) which is a lower range than for typical wood framing. Compared to ICFs, PCPs have the potential to further reduce infiltration and improve thermal resistivity of the overall wall system for two reasons. First, the PCP wall details would be controlled in the manufacturing environment to minimize thermal bridging and air leakage areas that cause infiltration. Second, PCP walls can be designed with the majority of the thermal mass inside the insulation barrier which has been proven in many studies to increase performance for continuously conditioned buildings (Kosny 1995; Christian 1991).

In terms of its environmental impact from raw material extraction to recyclability, concrete is both better and worse compared to other building materials. Although cement only accounts for 9-13% by mass of the raw materials used to produce concrete (water and coarse/fine aggregate being the other ingredients), it causes the greatest environmental damage through the emission of carbon dioxide. The two main sources of this carbon dioxide emission are the combustion of fossil fuels to power the energy intensive cement manufacturing process and decarbinization of limestone (calcination CO_2) that occurs during the pyroprocessing of the cement in kilns. Before the 1973 energy crisis, the emmission of carbon dioxide was approximately equal between the two sources. Since then, advancements in energy generation efficiency have resulted in the calcination CO_2 accounting for 59% of the carbon dioxide emission as of 1996. The greatest reduction in calcination CO_2 was due to supplementing cement with fly ash obtained from coil power plants. Despite these improvements, the cement industry is still targeted as one of the three worst carbon dioxide emitters (Cornelissen 1998).

Encouraged by the significant reduction in carbon dioxide emission associated with concrete production, the Canadian Portland Cement Association sponsored a study “to compare the environmental impacts of a concrete house and a wood frame house in terms of the total greenhouse gases (converted to carbon dioxide equivalents) emitted to the environment during a twenty-year period” (Cornelissen 1998). The concrete house was constructed using the ICF

system. The study employed a computer model that evaluates the environmental impact of buildings, called ATHANA, and a building energy modeling program called HOT2000. The three factors that comprised the total greenhouse gas emitted from each house were those associated with: the production and manufacturing of the building materials, the construction of the houses, and the heating and appliance used for daily operation of the houses. The conclusion of the study was that the concrete house emits more greenhouse gases than the wood frame construction in terms of the manufacturing and production of the building materials and the energy consumption to build the house. Yet the greenhouse gases emitted to heat the eight Canadian cities modeled in HOT2000 were so much larger than the other two aspects that the amount of carbon dioxide emitted from both houses were approximately the same after one year of operation. After five years of heating with a natural gas furnace, the wood house emitted 33 more tons of CO_2 than the ICF house. At the twenty year mark, the wood house emitted 94 more tons of CO_2 than the ICF house. Comparing the ICF and PCP systems, the PCP will have a longer break even point until the total CO_2 emitted equals that of the wood frame since the PCP system contains a greater amount of concrete. Yet, considering that PCP systems have the potential to have a greater thermal performance than ICF system, PCPs will emit less carbon dioxide during the entire life of the house.

Since ICFs and PCPs use concrete which is a much stronger and more fire resistant material than wood, they both improve durability, safety and disaster mitigation. In fire wall tests, ICF walls were subjected to continuous gas flames and temperatures of up to 2000°F for 4 hours in which none failed structurally compared to wood frame walls which collapsed after an hour or less. Disasters normally involve high winds that project debris at high speeds. According to a recent laboratory test at the Wind Engineering Research Center at Texas Tech University, a wood stud was shot out of a compressed air cannon at speeds over 100 mph. The stud was able to penetrate the exterior insulation layer but was unable to penetrate the internal concrete layer of the different ICF wall systems. Yet the stud did penetrate every wood and steel framed wall tested. In PCPs, two layers of concrete completely envelope the insulation layer. Thus PCPs have the potential to yield an even greater durability against fire and flying debris compared to ICFs where the insulation layers bear the brunt of the fire or projectile first.

Over the last ten years, concrete prices have been remarkably stable. Conversely, lumber prices have fluctuated substantially. According to the Portland Cement Association, due to these market changes, the cost of building with ICFs is comparable to that of ordinary 2x6 wood frame construction. The NAHB Research Center study (1997) estimates that ICF construction can range from 1 to 5 % more than conventional wood framing based on just the exterior wall construction cost. The increase in material costs is partially offset by the reduced labor costs during construction since ICFs are easy to assemble and consolidate several construction steps into one. The PCA claims that as construction crews become more experienced with ICFs, the increased cost over wood framing drops significantly. The cost of PCP construction is the greatest hindrance that prevents it from being market competitive. Compared to its European counterpart, the US precast manufacturing industry is far from state of the art and sparsely spread across the country (Donahey 2004). The limited size of production prevents precasting companies from taking advantage of economies of scale and limited factory locations requires a heavy surcharge for transportation. For instance, any construction outside of a 200 mile radius from the PCP manufacturer can increase the price per panel from $2 to $5 depending on the extra distance required for transportation (Long 2004). ICFs are much more cost effective currently because they are flexible enough to be used by the same contractors and construction crew who build with wood frame systems. On the other hand, PCPs requires a whole new group of contractors and construction crew specially trained to building with panelized systems. Consequently, two major changes need to take place before PCPs can become cost competitive. First, the precast manufacturing industry needs to expand to locations across the country, implement the same technology used in European precast factories, and increase production to drive down the cost per panel. Second, a whole new infrastructure of architects, engineers, contractors, and construction workers needs to be developed who are experienced in building with PCP technology. Until these two requirements are met, PCP systems will not be able to penetrate the market.

3.1.3 Penetration of PCP systems into the Home Construction Market

Although ICFs have been proven to perform better than wood frame construction, their growth mainly began as the prices of materials associated with wood frame construction, mainly lumber, became unstable. As with most other products, cost is the bottom line and factors such as safety

and energy efficiency will always be a second thought. Yet as the public is beginning to understand the increase in home quality associated with concrete construction, factors such as noise reduction and reduced maintenance are becoming more of a consideration. ICFs have proven that concrete construction can compete in the residential industry and may even provide the public awareness necessary for other techniques such as PCPs to enter the market.

Currently, PCPs major inroad into home construction has been through foundation walls and floors. For PCPs to compete with wood framing and ICFs for above grade construction, several major barriers need to be overcome. Although ICFs have been used successfully for roughly 30 years, their broader acceptance was due to the general publication of prescriptive requirements and structural design guidelines for residential applications according to the NAHB association and PCA. Once home builders, building code officials, and design professionals see how the technology works, it becomes accepted in all the major building codes which in turn sparks interest in home owners. The prescriptive method publication of a particular technology includes below-grade and above grade wall design tables, lintel tables, construction details, thermal guidelines, and other related information (NAHB Research Center 1998). When a home design falls under the requirements of the prescriptive method, any further engineering evaluation is eliminated which significantly reduces costs. The structural design guidelines provide a step-by-step procedure for the design of residential structures using the new technology.

Consequently, for PCPs to become broadly accepted, research pertaining to the development of a prescriptive method and structural design guidelines must be conducted. These research endeavors must include the development of:

- Conceptual plans of manufacturing systems to achieve the level of finish and system integration necessary for complete panelized systems,
- Techniques for on-site assembly, including interconnection of energy systems and maintenance of finish continuity,
- Concepts describing the insulating properties, thermal capacitances, infiltration rates, and opportunities for energy collection, and
- Implementation plans that identify key steps necessary to employ the new technology.

This study addresses one component (i.e insulation, thermal capacitance, and infiltration rates) of an entire research initiative to address these tasks to provide the necessary information for the

development of the prescriptive method and structural design guidelines to promote MPP technology in the home construction industry.

3.2 Energy Modeling Programs

Computational building modeling programs are a very useful tool to aid in evaluating the effect of MPP systems on the energy performance of single family homes. With the continual improvement in computational power, these programs are constantly increasing their capabilities to simulate the complicated fluid and energy transfer dynamics that occur within a building. The following subsections review the more popular ones and then reason why the EnergyPlus program was chosen for this study.

3.2.1 Predecessor Programs Overview

Many different whole building energy simulation programs have been developed by organizations throughout the world. Currently, the most popular programs are reaching maturity with some methods and codes originating in the 1960's. This section briefly reviews the history of the five most popular programs: ESP-r, TRNSYS, TAS, BLAST, and DOE2.1.

The most extensively used program outside the United States is called ESP-r. All the information pertaining to ESPr including downloading it for free can be obtained at the following URL address, **http://www.esru.strath.ac.uk**. The initial prototype was originally developed by a PhD student as a part of his doctoral research in the mid 1970's at the University of Strathclyde. Since that time, the program has been heavily funded and refined to make it a commercial software package for building simulators. Many researchers from all over the world have had a hand in its enhancement. Currently under the management of the Energy Simulation Research Unit (ESRU), its capability extends beyond thermal analysis to visual and acoustic performance and assessment of the energy use and gaseous emissions associated with environmental control systems and construction materials. At different resolutions, ESP-r can model heat, air, moisture, and electrical power flows. One of its most impressive features is its capability to conduct two dimensional CFD analysis throughout a building. Compared to the other programs in the industry, ESP-r has been the most extensively validated.

The TRNSYS (Transient Energy System Simulation Tool) program is a flexible tool designed to simulate the transient performance of thermal energy systems. The following information concerning TRNSYS including purchasing information can be obtained at the URL, **http://sel.me.wisc.edu/trnsys/**. Beginning as a joint project between the University of Wisonsin-Madison Solar Energy Lab and the University of Colorado Solar Energy Applications Lab, TRNSYS became a commercial program in 1975. It currently has a graphical interface, a library of 80 standard components, add on libraries offering over 300 other components, and a world wide user base. Written in Fortran, its structure is based upon linking individual subroutines consisting of mathematical equations or empirical data to form an entire system. Focusing mainly on the simulation of thermal energy systems, its whole building analysis application is recent relative to the other programs stated in this section.

Probably the most rigorous program currently on the market and most expensive, the TAS program combines a suite of three software products. All the information concerning the TAS program including the purchasing information can be found at the at the Environmental Design Solutions Limited (EDSL) company website, **http://212.23.11.237/**. The main module, TAS Building Designer, performs the dynamic building simulation with integrated natural and forced airflow. The TAS Systems module simulates the HVAC systems/controls. The TAS Ambient module is a robust two dimensional CFD package which produces a cross section of micro climate variation in a space. All of these modules can be directly coupled.

The BLAST and DOE2.1 programs were developed separately and supported by the U.S. Government for over two decades. Information concerning the BLAST and DOE2.1 programs can be found at **http://www.cecer.army.mil/td/tips/product/details.cfm?ID=506&TOP=1** and **http://www.doe2.com/**, respectively. They were both designed in the days of mainframe computers such that expanding their capabilities to keep up with ever increasing computational methods and power became difficult, time-consuming, and prohibitively expensive. The BLAST program, sponsored by the US Department of Defense (DOD), was developed at the U.S. National Bureau of Standards (now NIST) starting in the early 1970's. The DOE2.1 program, sponsored by the DOE, originally was created for the U.S. Post Office in the late 1960's. Often

the programs approach the many components of building simulation in two different ways. Since they have become so ingrained into the industry, both programs are still extensively used: BLAST by the DOD and DOE2.1 by the DOE and private sector (Crawley. et al 1999).

3.2.2 EnergyPlus Background

The first beta version of EnergyPlus was released in April 2001. Building on the strengths of BLAST and DOE2.1, EnergyPlus provides users a much wider array of modeling capabilities. All the publications concerning the development of EnergyPlus and its availability for download are contained on the following URL, **http://gundog.lbl.gov/EP/ep_main.html**. There were two motivations for EnergyPlus. First, the U.S. Government wanted to eliminate the funding necessary to maintain two programs that had the same purpose. Second, after years of enhancement, the DOE2.1 and BLAST codes turned into what can be best described as "spaghetti code" where the time, effort, and cost to further develop these two programs was not worth it. The DOE took the initiative in 1996 to streamline both programs into one. The EnergyPlus team included a variety of research institutions, the: U.S. Army Construction Engineering Research Laboratory, University of Illinois, Lawrence Berkeley National Laboratory, Oklahoma State University, GARD Analytics, Florida Solar Energy Center, and DOE. Early in the project, the developers realized that combining the two programs without starting from scratch would be too difficult. As a result, EnergyPlus became an all new program based on the most popular features and capabilities of BLAST and DOE2.1 (Crawley. et al 1999).

The source code is written in a modular format using Fortran 90, such that the addition of new modules and links to other programs is facilitated. Like BLAST and DOE2.1, EnergyPlus uses the lumped zone method such that the air in each zone is assumed to be well mixed and have constant properties throughout. The main advantage of EnergyPlus is simultaneous loads and systems simulation; loads are calculated by a heat balance engine and then passed to the building system simulation module at the same timestep. The benefit of this approach is that the program can simulate the inability of the HVAC system to meet a zone load and actually model the nonsetpoint conditions in that zone. Furthermore, an integrated simulation can model realistic system control, moisture adsorption and desorption in building elements, radiant heating and

cooling systems, and interzone air flow. Three tables in Crawley. et al (1999) illustrate the different general, loads, and HVAC features/capabilities of EnergyPlus compared to BLAST and DOE2.1.

The overall EnergyPlus structure is comprised of three components: simulation manager, heat and mass balance simulation module, and a building systems simulation module. The simulation manager controls the entire simulation, providing the input data and externally linked program features to the other modules. The heat and mass balance simulation module applies energy and mass conservation fundamentals to calculate the energy transfer through a zone. The building systems simulation handles the communication between the heat balance equation and various HVAC modules and loops, such as coils, boilers, chillers, and other equipment/components. It should be noted that the building systems module does not limit the users to predefined HVAC templates but allows a wide range of flexibility so the modeler can closely simulate their system. Since its first beta version, there have been eight releases, with EnergyPlus version 1.2.1 due out in September 2004. In addition to fixing problems found with the program, new features are constantly being added and the open source code allows any user the availability to generate their own program modules to simulate specific components.

3.2.3 EnergyPlus Validation

Much like any new software, especially scientific/engineering based programs, rigorous testing must be conducted to validate the simulation. For building energy simulation programs, this testing is extremely extensive and time consuming considering all the parametric variations to consider even for the simplest model. In addition, establishing actual experimental data for comparison is expensive and increasingly difficult for more complicated cases. Since its development, EnergyPlus has gone through many formal independent tests (Witte et al 2001). To date, EnergyPlus has been put through analytical, comparative, sensitivity, range, and empirical tests which are briefly described in Table 3.2 below. Obtained from Witte. et al (2001), the following paragraphs describe each of these tests and how EnergyPlus performed.

Table 3.2. Different validation tests for building energy simulation programs

Test Type	Description
Analytical Tests	Compares against mathematical solutions
Comparative Tests	Compares against other software
Sensitivity Tests	Compares small input changes versus a baseline run
Range Tests	Exercises the program over wide ranges of input values
Empirical Tests	Compares against experimental data

EnergyPlus has been tested by two separate *analytical tests*. The first was a wall conduction validation study published by the Building Energy Performance Analysis Club (BEPAC 1993) in the UK. Their tests check the accuracy of the conduction method which is the Conduction Transfer Function (CTF) method for EnergyPlus. From the first few tests, a significant error was found with calculating the CTF coefficients and subsequently fixed. Further verification with this test has been uneventful. The second analytical test was one developed by ASHRAE sponsored research project 1052 RP (ASHRAE 2000) which incorporated 16 analyses including conduction, convection, solar gains, shading, infiltration, internal gains, radiant transfer, and ground coupling. This is still the only test that encompasses all these physical areas. Similar to the previous analytical test, several more errors were found with the ASHRAE 1052 RP validation method. Most of these errors have been corrected. Those not yet fixed are minor and were concluded by Witte. et al (2001) to be negligible.

The *comparative tests* used the BESTEST suite which has been restated as ASHRAE Standard 140 (ASHRAE 2001c). The BESTEST compares the output from a single and double zone shoebox building configuration with varying mass, windows, overhang, and fins to eight different reference programs. Five of these reference programs are the ones reviewed in section 3.2.1. The results compared are the annual/peak heating and cooling loads. Applying this test helped identify several bugs and documentation deficiencies. Overall, EnergyPlus results were within the range of the other tested programs. To specify which of the program outputs were correct is impossible considering no experimental data exists.

EnergyPlus HVAC simulation was also validated against a hybrid *comparative/analytical test*. Entitled the HVAC BESTEST suite (Neymark and Judkoff 2002), this test analyzes the cooling loads and electric power consumption for a single zone DX cooling system. While EnergyPlus

results are within the range of results from the other programs, several minor issues were investigated and fixed.

Sensitivity and *range tests* are to systematically exercise many of the program inputs to confirm that basic elements are functioning properly. Since no standard sensitivity test exists, the EnergyPlus program was processed many times with an automated tool that altered various parameters for each simulation. Unfortunately, the results of this test were not published.

The final and probably most important validation is *real data test*. The IEA Validation Package (IEA 1994) was used. It contains two ten-day experiments on three highly monitored test rooms. The test is set up to exercise the following components:

- Opaque conduction and exterior solar gains
- Simple glazing, conduction, and solar gains
- Zone heat balance without internal loads, and
- Simple heating system.

The results are still in the process of being published.

3.2.4 Reason for Using EnergyPlus

With respect to the capability of EnergyPlus and its validation against all the tests, it was chosen over the other popular simulation programs summarized in 3.2.1 for the following reasons. The increased capability and rigor of EnergyPlus made it an obvious choice over BLAST and DOE2.1. The expense of the TAS and TRNSYS programs automatically ruled them out. The selection of EnergyPlus instead of ESP-r was made because of two reasons. First, the help documentation provided with EnergyPlus and the responsiveness of its list serve linking users to the developers substantially reduces the learning curve and the time for trouble shooting. Second, EnergyPlus was developed much later then ESP-r such that it was designed upon accumulated insight into what worked and with the inherent capability to continually expand. According to several conversations with leading building simulation experts at an International Building Performance Simulation Association (IBPSA) conference, EnergyPlus will soon become the standard in the US and will eventually exceed the capabilities of ESP-r. In other words, it is a long term investment that research presently conducted with EnergyPlus will be more useful in the future in an EnergyPlus standardized industry.

3.3 Building Envelope Analysis

The main whole building energy simulation programs use one dimensional conduction to model the heat transfer through the various construction elements. For light weight, wood frame technologies, several simple methods exist to account for the effects of structural elements (wood studs) in a one dimensional analysis. Yet, for wall details such as corners or junctions, complicated two and three dimensional heat transfer becomes so significant that these methods are not valid. Furthermore, the PCP systems in this study are thermally massive and therefore have an important dynamic behavior. Using these simple methods to also estimate the thermal capacitance distribution across the wall thickness would be extremely inaccurate. Consequently, the equivalent wall method, a more robust approach, was used. Sections 3.3.1 and 3.3.2 summarize the references that illustrate the steady state and transient modeling techniques of this method, respectively. Section 3.3.3 outlines the sources used to validate the mathematical relationship between the equivalent wall method and the one dimensional transient conduction approach used by EnergyPlus. Section 3.3.4 specifies the different types of wall systems evaluated and the sources from which their construction details were obtained. Finally, section 3.3.5 states the references used to define the material properties.

3.3.1 Whole Wall Techniques

Tuluca, et al. (1997) came to two conclusions by analyzing the variety of methods to determine the R-value of a wall system. First, several of these methods were inaccurate for wall systems that incorporate highly conductive materials such as metal. Second, even for the methods that were accurate, only analyzing the clear wall section of the envelope construction (surface area free of construction details such as corners or junctions) still yields inaccurate results compared to how the whole building envelope performs. They concluded that any over estimate of the thermal resistivity of a wall system would result in an inefficient construction and an increased susceptibility to moisture condensation problems.

In response to the inadequacies with standard wall system thermal analyses, Christian and Kosny (1996) developed a way to accurately model two and three dimensional heat conduction effects and account for thermal bridges in the clear and detailed construction areas. First they developed a three dimensional finite difference heat conduction program called Heating to simulate

different wall configurations. Then they determined an area weighted approach to apply this program to calculate the overall building envelope thermal performance including the most detrimental wall details. In the paper, they give examples of R-values calculated for typical wall technologies and indicate the difference between a clear and whole wall analysis. In a later publication (Kosny and Childs 2000), the Heating program was calibrated and validated using experimental data gathered from hot box testing. Currently, Dr. Jan Kosny is improving upon a web based "Whole Wall Calculator" that inputs user specified residential construction configurations and outputs the whole wall R-value for different wall technologies based upon previously evaluated data. The "Whole Wall Calculator" can be found at the following URL address, **http://www.ornl.gov/sci/roofs+walls/calculators/index.html**.

In another paper, Kosny and Christian (1995) describe in further detail how to use the Heating program temperature maps of the wall details to determine the area of the zones affected by the construction detail (area of influence). Using several configurations of insulation and metal structural elements, the authors show the extent that the thermal bridging effects can propagate into the clear wall area. Finally, two important calculations are introduced, one to illustrate the thermal efficiency of the insulation arrangement within a wall system and the other to combine the area of influence and R-value of a wall detail into one parameter.

A publication by McGowan and Desjarlais (1997) identified the thermal bridges which significantly degrade the whole wall performance for several different construction technologies used in this study. They implemented both experimental and computational analyses through hot box testing and Heating program simulations, respectively. The end of this reference and another investigation by Kosny (2001) show different design and construction methods to ameliorate the impact of thermal bridges. Both studies recommended rigid insulative sheathing to be the most basic, yet efficient solution. McGowan and Desjarlais (1997) go into further detail about rigid insulative sheathing stating that it increases the whole wall R-value more than the R-value of the material itself which they call "phantom resistance". They explain that this phenomena is due to the reduction in the area of influence of the thermal bridge.

3.3.2 Equivalent Wall Techniques

In a compilation of papers, Kossecka and Kosny (1996; 1997; 2002) describe the equivalent wall method, an approach that develops "a plane multilayer structure with dynamic characteristics similar to those of a complex structure in which three dimensional heat flow occurs" (Kossecka and Kosny 1996). In the 1997 publication, they illustrate the mathematical sequence behind the method starting from the Fourier heat conduction equation to the integrals defining three terms called structure factors. These terms essentially quantify the resistance and capacitance distribution across the thickness of the wall layer. By matching these structure factors, total resistance, and total capacitance between a complicated wall configuration and a simple one dimensional multilayer wall, similar transient behavior will be observed. The 1996 and 1997 papers outline the mathematical relationship between structure factors and response factors (transfer function coefficients). The significance of this relationship is that it shows that structural factors impose conditions on response factors and therefore influence the dynamic characteristics of a wall system. Another important conclusion from this relationship is that the equivalent wall method applies to the transient conduction method used in the EnergyPlus program which is described in greater detail in section 3.3.3.

In Kosny and Kossecka (2002), the authors put the equivalent wall method to the test. This reference shows a one dimensional multilayer wall developed using the equivalent wall method accurately simulating the heat fluxes measured from an experiment on a complicated three dimensional clear wall section of an insulated concrete form (ICF) system using a hot box test apparatus. Further useful information is explained concerning the incorporation of this technique in hourly energy simulation programs. Kossecka and Kosny (2002) implements the equivalent wall method for different arrangements of large thermal mass and insulation layers to show that wall systems with thermal mass inside the insulation barrier perform better. Finally, Kossecka (1999) draws mathematical correlations between the structure factors and the decrement factor/time lag terms explained in the *Conduction of Heat in Solids* book by Carslaw and Jaeger (1959). These relationships can be used for future studies of designing wall systems based upon frequency response parameters. The culmination of the equivalent wall analysis conducted by Kossecka and Kosny was the completion of the 1145-TRP report, Modeling Two- and Three-Dimensional Heat Transfer through Composite Wall and Roof Assemblies in Hourly Energy

Simulation Programs, for the Energy Calculations Technical Committee 4.7 of ASHRAE (ASHRAE 2001d).

3.3.3 State Space Method/Equivalent Wall Relationship

The engineering reference document that accompanies the EnergyPlus program (EnergyPlus 2004b) describes the Conduction Transfer Function (CTF) solution method that models the one dimensional transient conduction through all the building elements. Fundamentally, the CTF solution method reduces the second order differential Fourier conduction heat transfer function into a linear algebraic equation. Giaconia and Orioli (2000) show the acceptable accuracy of such a technique to model the smooth dynamic boundary conditions experienced by a typical wall and the appreciable increase in speed using it instead of the finite difference or finite element methods. There are two approaches to solve for the CTF coefficients necessary to apply the CTF method. Rather than using the older Laplace Transform method which is used by the BLAST program, the EnergyPlus program uses the State Space Method. Although slightly slower and requiring more CTF coefficients than the Laplace approach, the engineering reference document (EnergyPlus 2004b) sites three major advantages with the State Space method. First, its mathematical sequence has more of a physical interpretation by eliminating the need for complex functions. Second and third, two separate PhD theses, Seem (1987) and Strand (1995), have demonstrated the ability of the State Space method to solve for CTF coefficients at shorter time steps and for two and three dimensional geometries. Seem (1987) presents a clear outline on how to calculate the CTF coefficients from the Fourier conduction heat transfer function using the State Space method. For further validation, Celan and Myers (1980) and Ouyang and Haghighat (1991) address the accuracy of the State Space method against analytical and LaPlace techniques, respectively.

As stated in the previous section 3.3.2, the equivalent wall method structure factors are mathematically related to the thermal response factors. Since the thermal response factors form the basis of the CTF solution method, then the structure factors are mathematically related to the CTF coefficients. This association of response factors, CTF coefficients, and structure factors, reviewed by Kossecka (1998), demonstrates that the equivalent wall method can be applied to the CTF solution method implemented in the EnergyPlus program

3.3.4 Wall Technologies Evaluated

The importance of the equivalent wall method explained in the previous subsections is that the thermal performance of particular wall technologies can be accurately simulated using energy modeling software like EnergyPlus. Irregardless of their intrinsic dynamic behavior or excessive susceptibility to thermal bridging, the equivalent wall method can accurately model wall behavior even subject to the limitation of the one dimensional conduction analysis imposed by EnergyPlus. The following paragraphs describe the different wall technologies evaluated for this study, why they were chosen, and where their architectural details were obtained. As stated in the problem description in Chapter 2, two walls systems were analyzed for the wood frame and precast waffle panel technologies to evaluate the effects of different improvements. These wall systems are described in the following paragraphs as well. Appendix E shows the wall detail schematics for all the following wall systems.

Wood frame construction was used as the base case since it is the most common wall technology. Two different wall systems were evaluated for wood frame construction, a standard system and an energy efficient system. The standard system consisted of 2x4 stud walls at 16" on center (o.c.) with R13 insulation, 2x8 joist floor at 16" o.c. with R19 insulation, and 2x6 spar ceiling at 24" o.c. with R30 insulation. The energy efficient system consisted of the same floor and ceiling configuration but increased the walls to 2x6 studs at 16" o.c. with R19 insulation. The construction schematics for both these wall systems were obtained from Dr. Jan Kosny at the Building Technology Center in Oak Ridge National Lab (Hoke; Marino 1992).

The next wall technology was a precast waffle panel. It was used to represent the standard PCP configuration currently used in the housing market. The precast waffle panel modeled includes the interior finish, structure, and insulation but does not include exterior finish or embedded energy systems. Two different wall systems were analyzed for this technology. After the base case, a continuous layer of rigid insulative sheathing was applied just inside of the layer of gypsum board to evaluate the improvement recommended by McGowan and Desjarlais (1997) and Kosny (2001) at the end of 3.3.1.

A sandwich PCP, the third wall technology, simulated an improved configuration over the precast waffle panel system. It consists of a layer of insulation bound by concrete layers on either side. The configuration was modeled after the DOW Thermomass PCP product that has been distributed for the past 25 years mainly for commercial applications (Long 2004). It has most of the concrete at the inside layer in order to evaluate the claim made in Kosny (2002) and Christian (1991) that the wall performance improves the more the thermal mass exists inside the insulation barrier. Detailed construction schematics for the sandwich PCP were obtained from Composite Technologies Corporation, the designer of the DOW Thermomass PCP product (Composite Technologies 2004).

The last wall technology, an insulated concrete form, represented the most popular concrete construction method in the market. Although it represents a cast-in-place concrete application, it was evaluated to examine whether PCP systems performed better. Only one wall system was modeled. The ICF detailed construction specifications were obtained from the Reward Wall System Company, a manufacturer of several different types of ICF systems (Reward Wall Systems 2004).

3.3.5 Material Properties

Three properties are necessary to completely define the thermal characteristics of a material: conductivity, density, and specific heat. These thermal properties are not well known for many building materials whose primary purpose is not thermal insulation. For these materials, thermal properties are not regularly measured and for historic reasons, vary depending upon the reference. To maintain consistency in the thermal property data, one source was used almost exclusively for the materials modeled. That reference, (EMPA 1999), was a final report that consolidated material properties from numerous sources in many different countries. The project was funded to prepare a series of European Standards concerned with determination of thermal properties and methods of undertaking design calculations for the CEN Technical Committee TC 89 “Thermal Performance of Buildings and Building Components”. For the materials whose primary purpose is other than thermal insulation, the published thermal properties were obtained from existing tables in national standards and similar lists. For thermal insulating materials, the study implemented detailed design calculations based upon measured data obtained on the

particular material. When a statistical range of thermal properties was printed for a material, the mean value was obtained. For the materials where several different thermal properties were specified at different densities, the thermal properties associated with the standard density printed in the 2001 ASHRAE Fundamentals Handbook (ASHRAE 2001a) material property list was used. Similarly, for materials not included in the EMPA report, the thermal property list from the 2001 ASHRAE Handbook of Fundamentals was used.

3.4 Whole House Analysis Approach

In order to characterize the thermal performance of different wall systems, they must be simulated in a typical residence. Rather than comparing these systems individually through their R-value or dynamic heat flux based upon certain boundary conditions, this whole house approach evaluates the effect of the wall system on the overall home performance. The importance of such an approach is that it puts the significance of the wall thermal performance into perspective. For instance, a large difference in the R-value between two systems might be negligible if the wall component load on the overall house is insignificant compared to the other components such as infiltration, internal heat gain, etc. In fact in hot and temperate climates, a higher wall R-value actually increases the overall cooling load for reasons that are described in Chapter 5. Consequently, to design the whole house properly, the individual components affecting the house energy performance must be modeled as accurately as possible. The following subsections review the publications from which the building characteristics and analytical methods were obtained to model a typical U.S. home and then validate it.

3.4.1 Construction Specifications

The “typical” home used as a context for the wall analysis must contain the normal features of modern residences so that its characteristics will be representative of the recently built U.S. housing stock. The basic configuration of the typical detached single family house was modeled after a single story ranch specified in Huang. et al (1987) which subsequently has been used as the model for many other studies. It should be noted that this single story ranch design was among four other major residential building types defined by the NAHB Research Center survey of 1979 that encompassed over 90% of all new U.S. residences. Several modifications were

made, mainly increasing the conditioned floor area, to make the design more up-to-date. These changes were based upon the general trends of the 525 single family homes assessed from various Residential Energy Consumption Surveys (RECS) (US DOE: 1995a; 1995b; 1997). The window geometry and thermal design were based upon the National Fenestration Rating Council (NFRC 2002) base design, Windows 5.0 program (Windows 5.0 2001), and the minimum requirements specified by ASHRAE Standard 90.2 (2001b)

3.4.2 Occupant and Energy Consumption Profiles

Using a compilation of sources, the occupant thermal behavior and daily energy consumption profiles were defined. The basic information such as how many occupants in a home and typical appliances and their efficiencies were obtained from various RECSs (US DOE: 1990b; 1993c; 1995c; 1995d). The daily energy use profiles for each appliance were determined through extensive calculations from Wenzel. et al (1997), Huang. et al (1987), and the Building America program (US DOE 2003). Since the occupant and appliance heat emission can contribute a significant load to the conditioning system, considerable care was taken to verify the daily energy consumption profiles versus two other whole building simulation studies, Huang. et al (1987) and the Building America (US DOE 2003).

3.4.3 Foundation Heat Loss

The standard method used to model the heat flow through a residential basement wall and floor is based upon the experimental data by Latta and Boileau (1969) published in the 2001 ASHRAE Fundamentals Handbook (2001a). Field data originally from Latta and Boileau showed that isotherms near the basement wall and floor are not parallel lines but rather radial lines. Consequently, the heat flow path follows a concentric circular pattern and can not be estimated by simple one dimensional conduction. The 2001 ASHRAE Fundamentals Handbook recommended to calculate an effective heat transfer coefficient between the basement wall/floor and the outside air based upon experimentally calculated heat transfer coefficients obtained from Latta and Boileau. This standard method to calculate basement foundation heat loss will be called the ASHRAE Fundamentals method for future reference.

Sobotka, et al. (1994), published a study comparing four basement heat transfer models, including the ASHRAE Fundamentals method, to measured values from three different deep basement experiments. The results showed that the ASHRAE Fundamentals method always underestimated the basement wall and especially basement floor heat transfer. The method that was consistently closest to the measured results was the Mitalas method (Mitalas 1989), another well known and accepted approach. Introduced around 1982, the Mitalas method implemented two and three dimensional physical models of the basement using a finite element program. From the Sobotka, et al. literature review, the Mitalas method almost always predicted larger basement floor and wall heat transfer compared to other methods. Yet the greater the insulation applied to the basement walls, the more the predicted heat fluxes converged from the different methods. Since the Mitilas method consistently was the most accurate in the Sobotka, et al. (1994) paper and converged well with other methods for highly insulated basement walls, it was the method chosen to simulate the basement heat flux throughout the year.

The Mitilas method (Mitilas 1989) is based upon many two and three dimensional finite element analyses of different foundation arrangements. For verification, the Mitalas method simulations were compared to basement foundation heat transfer studies conducted by a collaboration between the buildings group at the Lawrence Berkeley Laboratory and the Underground Space Center. Specifically, two separate publications were used which gave the technical background to developing the “Building Foundation Design Handbook” , an all inclusive design guide for residential foundations. The first reference, Shen. et al. (1988), illustrated the finite difference and numerical scaling procedure to evaluate the different basement heat transfer in different climates. The second publication, Huang. et al. (1988), described how the information from the first paper was applied to the DOE-2.1C building energy simulation program. Overall, the Mitalas (1989) method was used to model the typical house basement foundation heat transfer which was than validated using data from the Shen. et al. (1988) and Huang. et al. (1988) references.

3.4.4 Infiltration

Compared to the other elements affecting residential thermal performance, the infiltration component is the most difficult to simulate. The parameters that influence infiltration are

numerous and the variation of each is even larger. Unfortunately, infiltration must be carefully estimated because of its significant impact on the conditioning loads of a house as shown by a component load analysis on residential heating and cooling energy consumption by Huang. et al (1999). According to Sherman and Dickerhoff (1998), infiltration can account for a quarter to a half of the heating energy load on a house. As a result, a considerable amount of time was invested to properly model infiltration.

According to the Input/Output reference document distributed with the EnergyPlus program (EnergyPlus 2004a), two separate methods are available to simulate infiltration. The first and much simpler option is based upon the Sherman-Grimsrud method (Sherman and Grimsrud 1980). Compared to the many other methods available, it is the most popular because it provides a well balanced approach between simplicity and incorporating the important fundamentals of infiltration. Based on experimental results of fan pressurization and weather data, the Sherman-Grimsrud method incorporates the geometry, leakage distribution, and terrain/shielding classifications into two reduced parameters. These two terms are used to define the relative magnitudes of the wind and stack induced infiltration based upon the wind speed and indoor/outdoor temperature difference, respectively. Using a total leakage area calculated using a fan pressurization test or estimated based on previous data, the infiltration can be calculated from any weather condition. Sherman and Grimsrud (1980) found that their method compares reasonably well with measured infiltration data from fifteen different sites.

The second option implements a stand alone program called COMIS (Conjunction of Multizone Infiltration Specialists). For each simulation, the COMIS program is called to calculate the air infiltration in the EnergyPlus model for each time step. The COMIS program was developed as a result of a symposium specifically conducted to create a computer model to simulate building air flow. COMIS also models natural ventilation so that the use of open windows can be reflected in the simulation. Feustel and Raynor-Hoosen (1990) explain the fundamentals behind COMIS and Feustel and Smith (1997) show how to use the latest version, COMIS 3.0, as a stand alone program. In addition to the standard input to model a building in EnergyPlus, numerous other criteria have to be defined. All the theory behind the equations and assumptions made by

COMIS is explained in the infiltration summary laid out chapter 26 of the 2001 ASHRAE Fundamentals Handbook (2001a).

Harrje and Born (1982) summarize the mathematical sequence to convert from the physical parameters describing the air leakage distribution in a building to the inputs necessary for the COMIS program. The publication basically focuses on how to relate the standard orifice flow equation to the power law equation. Colliver. et al (1992) presents an air leakage database of typical residential components. As part of ASHRAE Research Project RP-438, the authors compile, catalogue, and analyze available data on air leakage from a wide variety of building components. The final table, also printed in chapter 26 of the 2001 ASHRAE Fundamentals Handbook (2001a), contains the necessary information to define the air leakage distribution throughout a typical home. Two additional references, Arasteh. et al (1994) and Bursey and Green (1970), supplied more focused air leakage information for standard and advanced fenestration products, respectively.

Several ASHRAE Standards contain valuable infiltration specifications to classify the level of air leakage for detached, single family homes. ASHRAE Standard 119 (1988) establishes minimum performance requirements for air leakage of residential buildings for different U.S. climates in order to minimize infiltration conditioning loads. ASHRAE Standard 62 (1999) defines basic regulations concerning the outdoor ventilation rates to maintain the minimum quality of fresh air within a conditioned space. ASHRAE Standard 136 (2000) defines the parameters necessary to calculate the general infiltration rate for homes in different locations across the country using the Sherman and Grimsrud method.

Three different references provided information concerning the air flow around detached, low rise, rectangular shaped buildings. While chapter 16 of the ASHRAE Fundamentals Handbook summarizes how varying wind direction will effect the pressure distribution around the exterior building envelope, ASCE (1998) and Holmes (1986) define the actual wind pressure coefficients (Cp) experienced by different walls and roofs for various incident wind directions. These Cp profiles were required by COMIS for each construction surface facing the different cardinal directions to calculate the wind induced pressure differentials.

Infiltration rates measured from a wide variety homes located across the country obtained from various studies indicate one trend-new construction methods have made homes significantly tighter over the past several decades. Grimsrud. et al (1982) and Grot and Clark (1979) show the spread of infiltration rates for hundreds of homes representing new, energy efficient and older, low income constructions, respectively. Comparison of the two studies shows a tighter distribution of significantly lower infiltration rates for new homes compared to the wide spread, higher infiltration rates experienced by older homes. This trend is further reinforced by a more recent study, Parker (1990).

The Lawrence Berkeley National Lab Energy Performance of Buildings Group recently used a database describing the leakage area of 12,500 single family homes across the U.S. including their basic features such as number of stories, conditioned floor area etc. Two studies were conducted using this database. First, Sherman and Dickerhoff (1998) used standard regression techniques to determine the leakage trends of single family homes in the U.S. according to different demographics such as construction date, location etc. They concluded that the leakage area was more a function of date of construction and local construction practices rather than location. The second study by Sherman and Matson (1998) used the leakage areas and the Sherman-Grimsrud method (1980) to calculate the infiltration rates associated with the houses in the database to determine whether the general U.S. housing stock maintained a reasonably moderate infiltration rate and proper ventilation rate requirements according to ASHRAE Standard 62. The authors concluded that only 15% of the general U.S. single family housing stock met ASHRAE Standard 119 leakage requirements and all but 5% of the houses met the ventilation requirements.

3.4.5 Ventilation

Similar to infiltration, the EnergyPlus InputOutput reference document (EnergyPlus 2004a) gives two choices for modeling ventilation, the simple or COMIS approaches. The simple method is based on the identical equation obtained from the Sherman-Grimsrud method used for infiltration. In addition to specifying the coefficients in this equation, a schedule and temperature conditions have to be specified when ventilation can be allowed to occur. The COMIS ventilation option requires several more parameters defined in addition to the conditions

specified for the simple method to characterize the opening of the windows. These parameters were modeled after those used by the house energy studies of Huang (1987) and the Building America program (US DOE 2003). In addition, the proper attic ventilation requirements specified by ASHRAE 90.2 (2001b) were implemented.

3.4.6 Duct Modeling

The duct inefficiencies within a conditioning system can have a large impact on the overall house performance. According to several related studies, (Wenzel et al 1997; Siegel et al 2002, US DOE 2003), duct losses are normal around 15 to 25%. The duct losses are mainly due to two factors, air leakage and conduction, and depend significantly on the location of the duct within the house. Optimally, ducts should be placed within the conditioned space so that their inefficiency is negligible. Even ASHRAE Standard 90.2 (2001b) recognizes the importance of duct location since its minimum component performance requirements differ depending on whether the ducts are inside or outside the conditioned space.

Consequently, ASHRAE has developed a test method for evaluating residential thermal distribution systems based upon previous ASHRAE procedures and new experimental research. Still waiting for acceptance, ASHRAE Standard 152P (ASHRAE 2004), "Method of Test for Determining the Design and Seasonal Efficiencies of Residential Thermal Distribution Systems", has been shown to calculate measured duct performance within 5 percentage points as long as the weather data, duct leakage, and air handler flow are well known (Siegel et al 2002). Using the procedure developed in ASHRAE Standard 152P, the Building America program (US DOE 2003) created an extensive excel program that automates all the calculations of the duct efficiency according to certain features associated with the duct system mainly their location within the house. This excel program can be found at **http://www.eere.energy.gov/buildings/building_america/pa_resources.html**.

Understanding the importance of duct efficiency, the developers of EnergyPlus developed a separate module that models the air leakage and conduction losses associated with the performance of duct systems. Although limited to certain HVAC configurations, the fundamental equations that characterize the duct system are similar to the information provided

by the ASHRAE Standard 152P procedure. The inputs necessary to create the air distribution system simulating a duct system are defined in the EnergyPlus InputOutput Reference document (EnergyPlus 2004a).

3.4.7 HVAC System Performance

The characteristics of the heating and cooling equipment in the prototypical house were based upon the standard HVAC systems determined from the latest REC survey (US DOE 2002). The rated efficiencies and performance curves to define the system efficiency at non-rated conditions are required by EnergyPlus to properly simulate the behavior of the conditioning equipment for each of the climates. This information is described in the EnergyPlus InputOutput document (EnergyPlus 2004a) and was obtained from standard manufacturing data on actual HVAC systems commercially available from the Carrier Coporation (Carrier 2004).

The sizing of each of these systems was based upon the "autosizing" feature built into the EnergyPlus program, described in the InputOutput reference document (EnergyPlus 2004a). The logic behind the autosizing feature is based upon the heat balance method described in Chapter 29 of the 2001 ASHRAE Fundamentals Handbook (ASHRAE 2001a). Therefore, it is a viable option to size actual building equipment like the Trace program which was developed by the Trane Corporation to help contractors size the conditioning equipment for a house which can be found at the following URL, **http://www.trane.com/commercial/software/trace/**.

3.5 Residential Economic Information

Unlike the thermal performance of a wall system which is based on constant physical characteristics, construction costs are based upon a variety of variables that fluctuate depending on the market conditions. The two most important construction cost variables are material and labor costs. According to a NAHB Research Center study (2001), there are two main methods to estimate the construction cost of the various wall systems. The first and more common method is to use a guide book that estimates the construction costs based upon a wide compilation of previous construction data. The second and one of the most reliable is to conduct a detailed time-and-motion study of an actual construction. Based upon either of these methods, the final

construction cost estimate is compressed into the cost per square foot of wall area. Therefore, the exterior wall construction cost can be quickly approximated by multiplying this value to the exterior wall area of a home (minus the window and door openings).

For the wood frame systems, the first method of using a guide book described in the previous paragraph was used to estimate the cost of construction since the costs associated with wood systems have been extensively investigated considering the commonality of this technology. The guide book used was the RSMeans Residential Cost Data guide book, 22th Annual Edition (RSMeans 2003). This source of construction cost data allows for a detailed assessment of the cost of a traditional house. Although it does not account for job specific variables such as the experience of the contractor, local material availability, and cyclic market trends, the RSMeans guide book is considered a valid approach to estimating construction costs for a well known wall system, namely wood frame.

The ICF system construction costs were based upon a compilation of references. First, a NAHB Research Center study (2001) compared the costs to construct three small homes (one wood frame and two ICF) using the time and motion study method described in the first paragraph of this subsection. The authors determined that the ICF construction costs are approximately $2 to $5 more per square foot of net wall surface area (excluding the fenestration cut outs) than wood frame construction. This trend correlated well with the typical increase in construction costs determined by the Insulated Concrete Form Association (ICFA 2004).

The construction cost for the sandwich PCP system was based upon general trend information obtained from personal communication with the Composite Technologies corporation who developed the DOW T-mass sandwich panel used as the basis for the sandwich PCP system in this study. The general trend specified that typical MPP systems incorporating a PCP system and exterior finish normally cost $12 to $15 per square foot of net wall surface. These figures can vary considerably across the United States due to massive transportation fees, mainly starting 200 miles outside from any of the PCP manufacturers. For example, a recent home built in San Diego cost an extra 5 dollars per square foot of exterior surface area since the panels were shipped from the precast factory in Nevada. For simplification, the construction costs assigned to

the MPP wall systems were independent of any additional transportation expense, essentially assuming that the house was within 200 miles of the precast plant.

3.6 Similar Research Initiatives

Three separate references conducted a very similar analysis to this study but focused entirely on ICF and wood frame wall systems. The first was an NAHB Research Center study (1999). This study provided both experimental and simulation results for comparison. The second study was conducted by several research scientists at the Building Technology Center at ORNL concerning the influence of several characteristics of an exterior wall, specifically thermal mass, thermal bridging, and airtightness, on the overall energy performance of a typical home (Kosny et al 1999). The results from their analysis provided valuable insight into methods to compare the performance of different wall systems. The last reference was a survey study comparing the annual energy savings from different ICF systems over wood frame systems (VanderWerf 1988).

The NAHB study was based upon the results of a study to compare the performance of ICF walls to wood frame walls. Three identical homes were built of either an ICF plank system, an ICF block system, or a conventional 2x4 wood frame system. All of these homes were located side by side one another in Maryland. Each home was extensively equipped to monitor its energy performance and provide data for a thermal comfort analysis. During the one year experiment, the weather data was collected and entered into the BLAST program to compare the predicted energy performance of the homes to the actual energy use. Several important conclusions were made from this study.

1. There was not a significant difference between the air leakage tests for each of the homes. This lack of difference may be attributed to the limited wall area and reduced wall details of these simple homes.
2. The two ICF homes were approximately 20% more energy efficient than the wood frame house mainly due to their higher effective R-value and continuous insulation at the slab.
3. The BLAST modeling program produced very similar results to the actual energy end use. The results suggest that the contribution of thermal mass and ground-coupling effects to overall energy efficiency of the ICF homes was not significant.

4. No dramatic thermal comfort differences were apparent between the ICF and wood frame homes. Yet several thermal comfort measures showed slightly better performance for the ICF homes.

The publication by the Building Technology Center at ORNL identified the building characteristics on which to focus to evaluate the thermal performance of several different wall systems (Kosny et al 1999). Most importantly, the authors used the equivalent wall method to properly incorporate the steady-state and dynamic behavior of an ICF and wood frame wall system in the DOE2.1C program to compare their resultant annual energy consumption. The publication compares the ICF clear wall parameters obtained from the heat transfer program to experimental data gathered from a hot box test. Using a slightly smaller configuration of the prototypical house used in this study, the authors determine the effective R-value for the ICF based upon its thermal mass and reduced infiltration benefits. The wall systems are evaluated for the same locations used for this study. Several important conclusions were obtained from the resultant data.

1. The ICF wall will perform at least as well as a wood frame system of similar clear wall R-value.
2. The thermal mass benefits are mostly apparent in the warm and temperature climates and least apparent in the extreme cold climates. An ICF clear wall with a R-value of $11.6\frac{\text{hr ft}^2\ \text{F}}{\text{Btu}}$ will behave as a wood frame system with an R-value of roughly $21\frac{\text{hr ft}^2\ \text{F}}{\text{Btu}}$ for warm and temperature climates and roughly 16 $\frac{\text{hr ft}^2\ \text{F}}{\text{Btu}}$ for extremely cold climates.
3. Assuming that ICF systems maintain approximately 20% less infiltration than wood frame systems, the effective R-value for all of the six climates will range $26\frac{\text{hr ft}^2\ \text{F}}{\text{Btu}}$ to 44 $\frac{\text{hr ft}^2\ \text{F}}{\text{Btu}}$.

The VanderWerf (1988) study involved a survey of the annual conditioning energy consumption of 29 pairs of homes, each pair consisted of a wood frame house and an ICF house which were similar in location and construction features. From the raw data, the author determined that ICF system saves approximately 44% and 27% of heating and cooling energy respectively. Then using several normalization techniques, the author adjusts the 29 pairs of house data to obtain a home with:

1. 2100 square feet of conditioned space,
2. 2 stories above grade,
3. 3 regular occupants,
4. average winter and summer thermostat setpoints of 69°F and 74°F, respectively,
5. 100% efficient heating equipment,
6. 285% efficient cooling equipment, and
7. a full basement foundation.

Finally, the reference uses the normalized data to determine the annual monetary energy savings for different house sizing.

CHAPTER 4: ANALYSIS

The following sections outline the methods used and assumptions made to compare the thermal performance and economic costs of Precast Concrete Panels (PCPs) versus Insulated Concrete Forms (ICFs) and Wood Frame construction technologies. Section 4.1 describes the different wall systems that were analyzed in this study including their insulation configuration. Section 4.2 summarizes the techniques used to characterize the steady state and transient performance of the wall systems including the clear wall and wall details. Section 4.3 covers the references used, choices made, and methods incorporated to model a typical detached, single family home in the EnergyPlus program to implement the whole house approach for evaluating the thermal performance of the different wall systems in their applied environment. For future reference, the "prototypical residence" is defined as a house that represents the most common construction specifications and operating conditions for new single family, detached homes within the United States (Huang et al. 1987). Section 4.5 describes the methods used to calculate the exterior wall construction costs associated with each of the wall technologies. Note that the unit system convention used in the ensuing sections follows the standard used in the building construction industry; Imperial (English) Units for everything except electric energy consumption which is defined in kilowatt-hours (kW-hr).

4.1 Wall Construction Types

To assess the impact of PCP construction on residential energy use and cost, two types were evaluated: waffle PCPs and sandwich PCPs. These wall systems were compared to wood frame and ICF systems. Therefore, four different building envelope technologies were modeled:

1. Waffle PCP construction (Two Way Slab),
2. Sandwich PCP construction,
3. Wood Frame construction, and
4. Flat ICF construction.

For the Wood Frame and Waffle PCP constructions, two different systems were evaluated. The first system represented the conventional construction configuration for that particular technology. The second system represented practical modifications that could be made to improve the thermal performance of the construction.

The Waffle PCP technology was modeled because it represents an industry standard precast concrete panel configuration. Two different wall systems were evaluated for this technology. The first represents typical Waffle PCP assemblies used in residential construction. Figure 4.1, Figure 4.2, and Figure 4.3 show the Waffle PCP wall, ceiling, and floor schematics, respectively. The second system had a half inch of rigid insulative sheathing uniformly applied across the entire wall surface just under the gypsum board. The resulting wall center-of-panel R-values for system one and two were 26 $\frac{\text{hr ft}^2 \text{ F}}{\text{Btu}}$ and 28 $\frac{\text{hr ft}^2 \text{ F}}{\text{Btu}}$, respectively. Note that these R-values represent the amount of insulation applied to the center-of-cavity of each assembly independent of the thermal effects from the structural elements, exterior façade, or interior gypsum board. The ceiling and floor construction specifications were identical for both systems except for the half inch of rigid insulative sheathing applied to the second system.

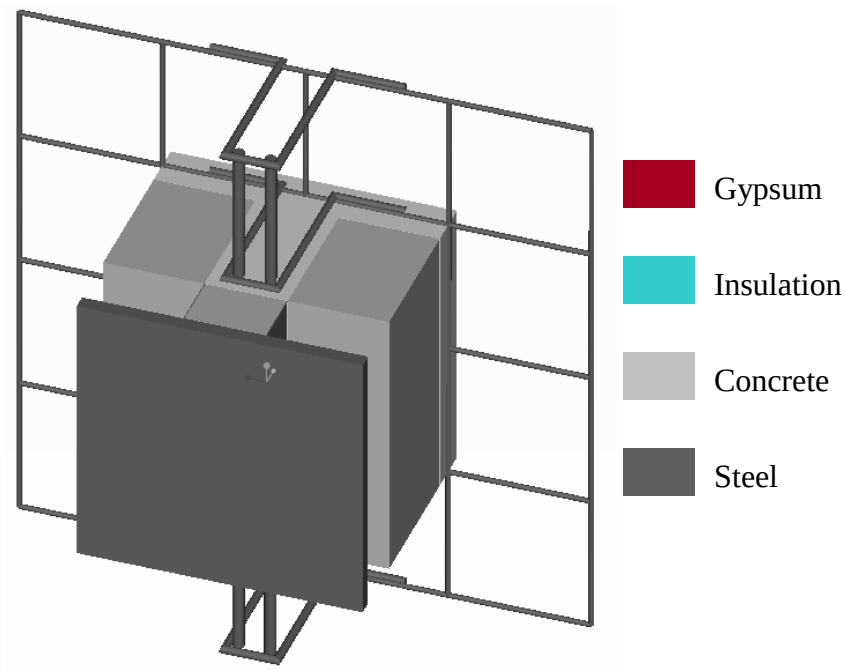

Figure 4.1 Waffle PCP wall schematic

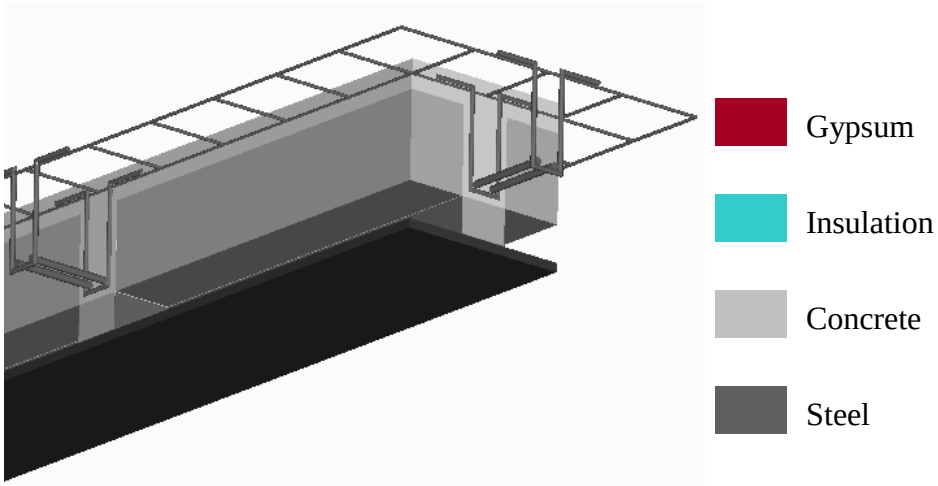

Figure 4.2. Waffle PCP ceiling schematic

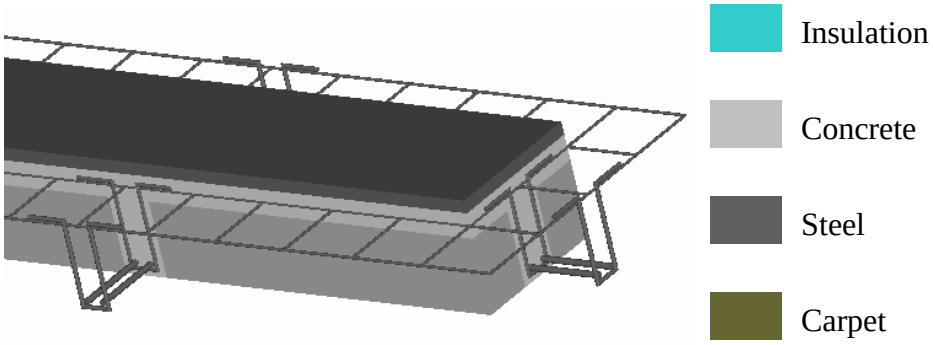

Figure 4.3. Waffle PCP floor schematic

The Sandwich PCP technology was modeled to evaluate a higher thermal performance PCP construction by assessing the influence of two features: reduced thermal bridging across the insulation barrier and the majority of the thermal mass located inside the insulation barrier. The Sandwich PCP technology was modeled after a commercially available Sandwich PCP product called "DOW Thermomass" which was designed by Composite Technologies and bought by the Building Construction Department of DOW Chemical. The resulting wall center-of-panel R-value for was 13 $\frac{\text{hr ft}^2 \quad \text{F}}{\text{Btu}}$. Figure 4.4 (a) shows the basic assembly of the Sandwich PCP system with a layer of rigid insulation in between two layers of concrete. Figure 4.4 (b) shows the fiber composite connectors that span the interior insulation and connect the two layers of concrete.

(a) (b)

Figure 4.4 Sandwich PCP assembly schematic

(a) Sandwich PCP assembly of rigid insulation in between two layers of concrete

(b) Sandwich PCP fiber composite connectors connecting two layers of concrete (Composite Technologies 2004)

The wood frame technologies were modeled to represent the base thermal performance currently provided in the housing industry to which the PCP and ICF technologies can be compared. For the Conventional Wood Frame construction, the wall structural configuration was assumed to be 2x4's at 16" on center (o.c.) for all the prototypical house locations. This system reflects the typical wood frame configuration used for new homes based upon data from the 2001 REC survey (US DOE 2002). The Energy Efficient Wood Frame construction was assumed to have a structure composed of 2x6's at 16" o.c. The Energy Efficient Wood Frame system represents the standard practice to improve the envelope performance by increasing the stud and insulation thickness to the next standard stud width (Kosny 2001; McGowan and Desjarlais 1997). The Conventional and Energy Efficient Wood Frame wall R-values were 13 $\frac{\text{hr ft}^2 \text{ F}}{\text{Btu}}$ and 19 $\frac{\text{hr ft}^2 \text{ F}}{\text{Btu}}$, respectively. Figure 4.5 shows the general schematic of the walls for the Conventional and Energy Efficient Wood Frame constructions.

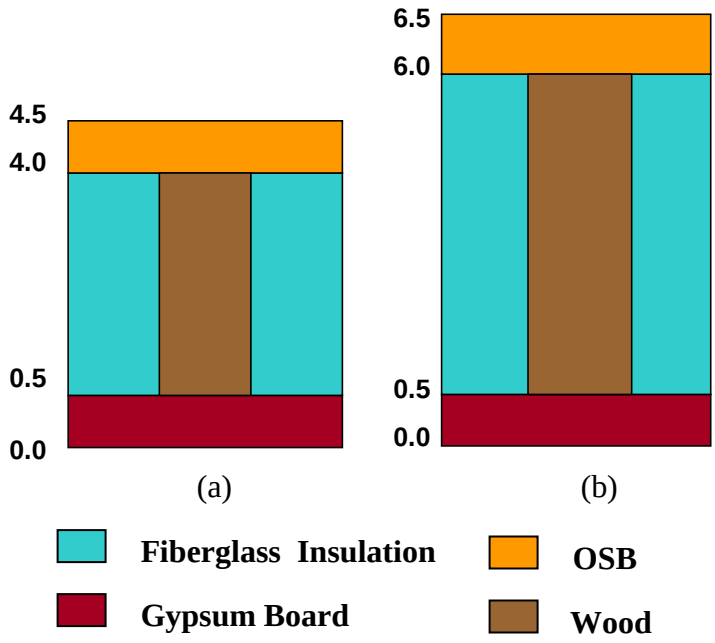

Figure 4.5. Wood Frame construction schematics

(a) Conventional Wood Frame wall construction - 2x4 @ 16" o.c.

(b) Energy Efficient Wood Frame wall construction – 2x6 @ 16" o.c.

The ICF construction was modeled to evaluate the thermal performance of a technology that has already proven itself in the field and been accepted as an energy efficient alternative to wood framing by the housing industry. There are two basic ICF types, "Flat" and "Grid", which are shown in Figure 4.6 (a) and (b), respectively. The "Flat" systems yield a continuous thickness of concrete, like a conventionally poured wall. The "grid" systems are composed of discrete horizontal and vertical columns of concrete that are completely encapsulated in foam insulation. Only the Flat ICF construction was analyzed since it represents the standard used and is more energy efficient. The resulting wall center-of-panel R-value for the Flat ICF was 21 $\frac{\text{hr ft}^2 \text{ F}}{\text{Btu}}$.

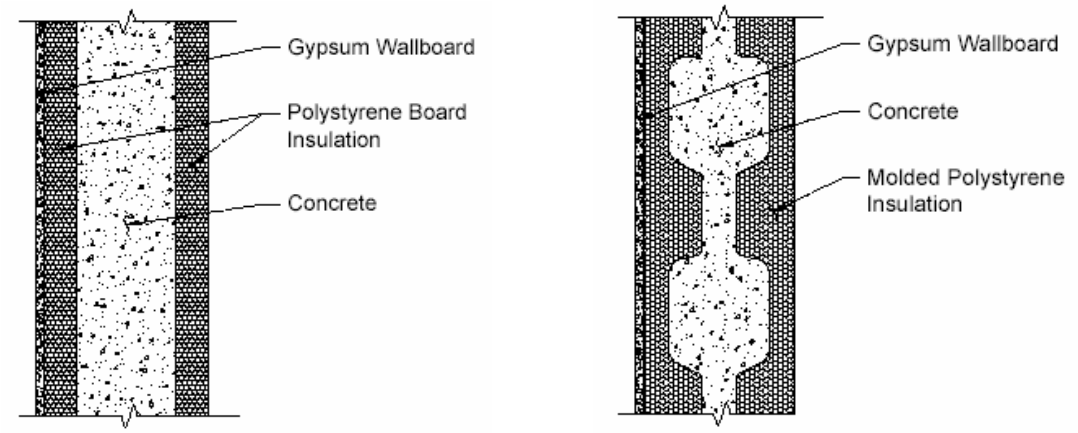

(a) (b)

Figure 4.6. Insulated Concrete Form types

(a) "Flat" ICF system type

(b) "Grid" ICF system type

The Sandwich PCP, Conventional and Energy Efficient Wood Frame, and ICF systems had the same ceiling and floor configurations. Therefore, the analysis was solely focused on the thermal performance effects of these exterior wall systems. The ceiling and floor structural configurations were assumed to be comprised of 2x6's at 24" o.c. and 2x8's at 16" o.c., respectively. The resulting floor and ceiling center-of-cavity R-values were 19 $\frac{\text{hr ft}^2 \text{ F}}{\text{Btu}}$ and 30 $\frac{\text{hr ft}^2 \text{ F}}{\text{Btu}}$, respectively. The floor and ceiling configurations are shown in Figure 4.7 and Figure 4.8, respectively.

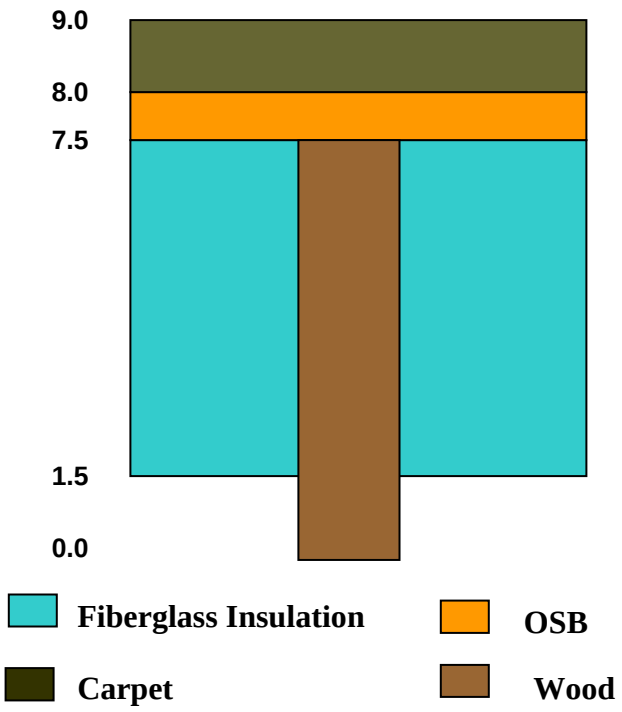

Figure 4.7. Floor schematic for all wall systems (except waffle PCP)

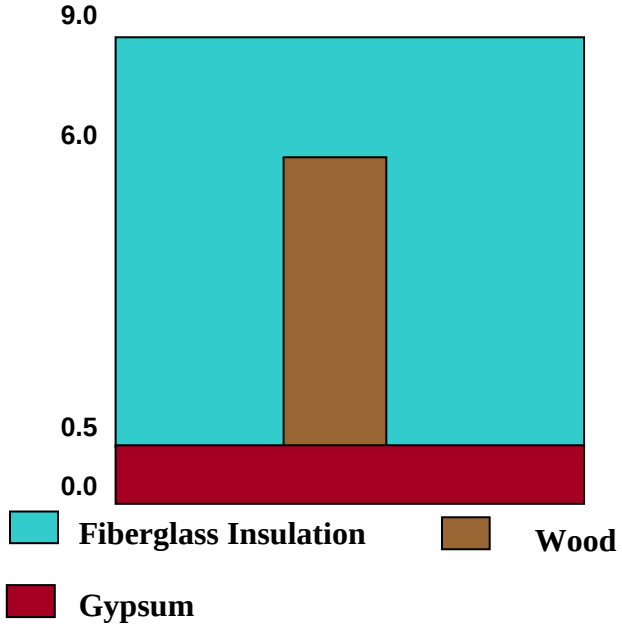

Figure 4.8. Ceiling schematic for all wall systems (except waffle PCP)

The construction descriptions above apply to only the walls, floor, and ceiling that separate the conditioned zones of the prototypical home from the exterior environment and unconditioned zones. Other construction surfaces of the prototypical home were controlled in such a way to normalize their effects. This way the focus was on the relative performance of the different wall technologies. For example, the exterior finish for all the systems was chosen to be a thin layer of paint. Consequently, the performances of the different wall constructions were independent of the exterior surface radiative properties. The following paragraphs summarize how several different construction aspects were constrained.

The garage wall construction was the same for all the construction technologies. Since the garage zone was not a conditioned space, the walls had no insulation or gypsum board. As a result, the garage walls were modeled simply as paint on ½" OSB. The floor of the garage was simulated as 4" of concrete slab on grade. The detail applied to the basement foundation described in section 4.3.10 or the conditioned walls in section 4.2 was not applied to the garage envelope because its infiltration due to leaky walls and continual opening of the garage door dominated the internal conditions. In other words, going into further depth concerning the garage envelope heat transfer would have had a negligible effect on the garage zone conditions.

Much like the garage walls, the roof construction was constant for all the wall technologies. The roof assembly consisted of asphalt shingles over ½" OSB. The roof gable wall constructions were modeled identically to the garage walls with paint on ½" OSB. The reason that considerable detail was not used to model the heat transfer through the roof zone envelope was due to two reasons. First, there was almost no resistivity or capacitance within the roof zone surfaces except for the floor which separated the roof and conditioned spaces. Therefore, the heat flux through these thermally dynamic surfaces was almost strictly one dimensional so applying the equivalent wall method to these surfaces would have had a negligible effect. Second, according to ASHRAE 90.2 (ASHRAE 2001b), a free ventilation area of 1.0 ft^2 for each 300 ft^2 of attic floor area is required for an attic with a vapor retarder, which the prototypical house roof was assumed to have. This amount of ventilation area results in a large infiltration rate of approximately 9 ACH throughout the year. Consequently, other than the heat

flux from the absorbed solar radiation on the asphalt shingles, the roof conditions were dominated by the large ventilation rate.

The interior wall and basement foundation constructions were the same for all the different construction technologies. The interior walls were simulated as two layers of gypsum board separated by 3.5” of air space to modeled the typical 2x4 studs at 16” o.c. covered on either side by gypsum board. The basement foundation configuration is described in subsection 4.3.10.

4.2 Detailed Building Envelope Analysis

A wide variety of methods exist to characterize the steady-state and transient performance of a wall system. Yet many of them were developed for light weight, wood frame, wall constructions which contain little to no highly conductive metal components nor large thermal capacity materials. As a result, these methods are inadequate to model wall systems that incorporate numerous metal elements and have a large thermal mass such that their thermal response is slow. The following subsections describe a more rigorous approach called the equivalent wall method (Kossecka and Kosny 1997) that can accurately account for two and three dimensional conduction effects as well as large capacitance wall systems. Subsection 4.2.1 summarizes the transient conduction technique employed by the EnergyPlus program. Subsection 4.2.2 reviews the important effects thermal bridging have on the building envelope performance. Subsection 4.2.3 describes the computer program used to analyze the different wall technologies. Subsection 4.2.4 explains the equivalent wall method and the mathematical theory behind it. Subsection 4.2.5 explains how to apply the equivalent wall method to the entire building envelope.

4.2.1 Background of Whole Building Envelope Heat Transfer

All of the whole building simulation programs use one dimensional conduction to evaluate the heat transfer through the building envelope. The reason for this simplification is two fold. First, whole building analysis programs were originally developed around and calibrated against field data for light weight, wood framed walls in which two and three dimensional heat transfer effects were not extremely important (ASHRAE 2001). Second, to account for heat transfer in more

than one dimension significantly increases computation time which has always been a precious commodity. For the same two reasons, building envelopes were often characterized only by their steady-state performance, R-value, without considering their dynamic behavior.

Although the main whole building simulation programs still use one dimensional conduction, various mathematical methods have been employed that account for transient heat transfer without increasing computation time. Table 4.1 below shows the different conduction heat transfer methods used by various building simulation programs. Despite being mathematically related to varying degrees, the attributes associated with each affects the whole building simulation in very distinct ways.

Table 4.1. Conduction heat transfer methods
(CTF represents conduction transfer coefficient)

Whole Building Simulation Programs	**Conduction Heat Transfer Methods**
DOE 2.1	Response Factors
TRNSYS/BLAST	CTF/Laplace Method
EnergyPlus	CTF/State Space Method

All the methods shown in Table 4.1 involve time series solutions in which the desired output is based upon current and previous inputs and/or previous outputs. In the case of conduction heat transfer through building elements, the desired output is the surface heat flux and the inputs are internal and external temperatures. The most basic time series solution is the response factor equation which relates the heat flux at one surface to an infinite series of internal/external temperature histories (EnergyPlus 2004b). Equation 4.1 shows this relation below:

$$q''(t) = \sum_{j=0}^{\infty} X_j^* T_{o,t-j\delta} - \sum_{j=0}^{\infty} Y_j^* T_{i,t-j\delta} \qquad \textbf{(4.1)}$$

where: q” is the surface heat flux,

T is temperature,

i and o subscripts represent the inside and outside surfaces respectively,

t is the current time,

δ is the time step,

and X* and Y* are the response factors.

The response factors are determined from heat fluxes recorded at uniform time intervals from either of the wall surfaces after the application of a unit triangular temperature excitation shown graphically in Figure 4.9. Table 4.2 below shows the surface to which the temperature excitation is applied and the surface at which the heat flux is measured for each of the response factors. Since the main focus for this study is the interior heat flux affecting the internal zone, the Z* response factor which represents the external heat flux is often ignored.

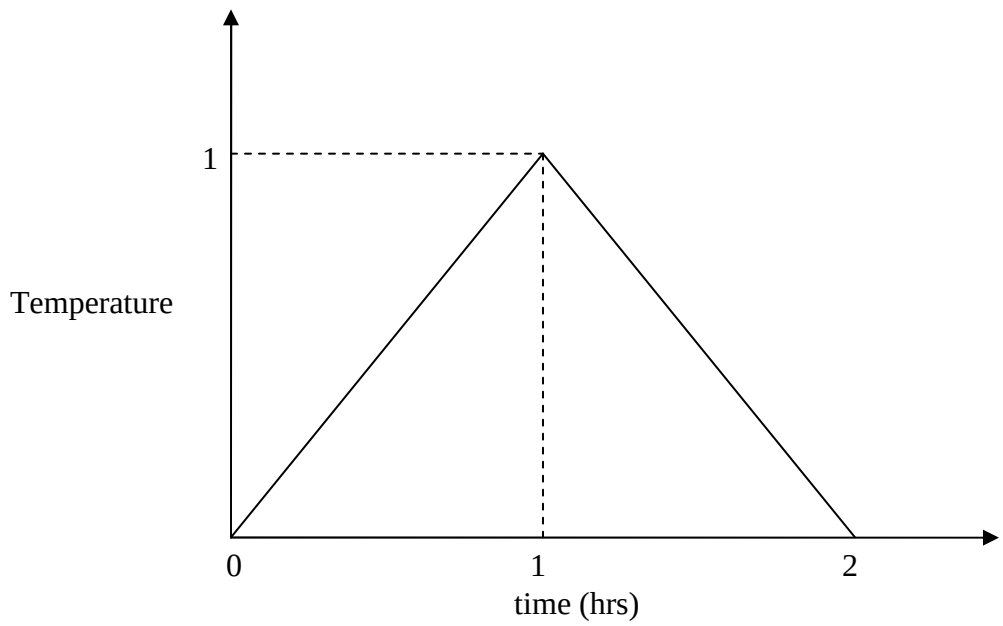

Figure 4.9. Unit triangular temperature excitation used to calculate response factors

Table 4.2. Response factor descriptions

	Surface of Applied Unit Temperature Pulse	**Surface of Measured Heat Flux**
X*	Interior	Interior
Y*	Exterior	Interior
Z*	Exterior	Exterior

For most cases, especially light weight envelope constructions, the response factor series decays rapidly. Yet the infinite terms needed for an exact response makes it less than desirable. Consequently, the conduction transfer function (CTF) method was developed, refining the response factor method by eliminating the need for infinite terms to obtain an exact solution.

The similar higher order terms were replaced with interior heat flux history terms resulting in Equation 4.2 and 4.3:

$$q_i''(t) = -Z_0 T_{i,t} - \sum_{j=1}^{nz} Z_j T_{i,t-j\delta} + Y_0 T_{o,t} + \sum_{j=1}^{nz} Y_j T_{o,t-j\delta} + \sum_{j=1}^{nq} f_j q_{i,t-j\delta}'' \qquad \textbf{(4.2)}$$

$$q_o''(t) = -Y_0 T_{i,t} - \sum_{j=1}^{nz} Y_j T_{i,t-j\delta} + X_0 T_{o,t} + \sum_{j=1}^{nz} X_j T_{o,t-j\delta} + \sum_{j=1}^{nq} f_j q_{o,t-j\delta}'' \qquad \textbf{(4.3)}$$

where: X_j is the outside CTF coefficient (j = 0,1,…nz),

Y_j is the cross CTF coefficient (j = 0,1,…nz),

Z_j is the inside CTF coefficient (j = 0,1,…nz),

and f is the flux CTF coefficient (j = 0,1,…nq).

Note that nz and nq represent the number of terms in the temperature and heat flux series, respectively. The first term in each series denoted with subscript 0 have been separated from the summation terms to facilitate solving for the current temperature in the solution scheme.

In general, the CTF method linearly relates the heat flux on either surface of a building system to current and several previous interior and exterior surface temperatures as well as previous heat fluxes. These coefficients only need to be calculated once for each construction configuration. The formulation does not require any knowledge of temperatures within the wall, only CTF coefficients and a limited number of internal and external surface temperatures and internal heat fluxes.

Two distinct methods can be used to calculate the CTF coefficients, the more common Laplace method (Hittle 1979; Hittle & Bishop 1983) or the more recent State Space method (Ceylan and Myers 1980; Seem 1987; Ouyang and Haghighat 1991). A previous study directly comparing these methods found almost no difference in their calculated response factors (Ouyang and Haghighat 1991). Yet different positive and negative attributes are associated with either method. Even though the number of temperature and flux history terms are identical, the State Space method requires more coefficients and is more time consuming than the Laplace method. However, the State Space method is better suited than the Laplace method for the analysis of building envelope heat transfer because:

1. State Space method eliminates the need to solve for roots in the Laplace domain resulting in a methodology that has more physical meaning and is easier to follow than complex functions required by the Laplace transform method,
2. State Space method can yield CTF coefficients for much shorter time steps, and
3. State Space method can solve for two and three dimensional CTF coefficients.

As a result, the State Space method was used to calculate the CTF coefficients in the EnergyPlus Program (EnergyPlus 2004b).

The basic State Space system is defined by two linear matrix equations shown in Equation 4.4 and 4.5 below:

$$\frac{d[x]}{dt} = [A^*][x] + [B^*][u] \qquad \textbf{(4.4)}$$

$$[y] = [C^*][x] + [D^*][u] \qquad \textbf{(4.5)}$$

where: x is a vector of state variables,
u is a vector of inputs,
y is an output vector,
and A, B, C, and D are coefficient matrixes.

In the application of transient heat conduction, a one dimensional finite difference grid subdivides the various layers of the wall element. The resulting nodal temperatures are represented by the state variable [x], the interior/exterior temperatures are the inputs [u], and the interior/exterior heat fluxes are the output [y]. Therefore, the State Space Equation 4.4 and 4.5 above implemented with the finite difference variables becomes:

$$\frac{d\begin{bmatrix} T_1 \\ \vdots \\ T_n \end{bmatrix}}{dt} = [A^*]\begin{bmatrix} T_1 \\ \vdots \\ T_n \end{bmatrix} + [B^*]\begin{bmatrix} T_i \\ T_o \end{bmatrix} \qquad \textbf{(4.6)}$$

$$\begin{bmatrix} q_i'' \\ q_o'' \end{bmatrix} = [C^*]\begin{bmatrix} T_1 \\ \vdots \\ T_n \end{bmatrix} + [D^*]\begin{bmatrix} T_i \\ T_o \end{bmatrix} \qquad \textbf{(4.7)}$$

where: n is the number of nodes.

Through the use of matrix algebra, Equation 4.6 and 4.7 are reconfigured such that the vector of state variables, the nodal temperatures, are eliminated. As a result, the output vector (interior and exterior heat fluxes) is directly related to the input vector (interior and exterior temperatures) and time histories of these input and output vectors.

4.2.2 Thermal Bridging Effects

Although the one dimensional heat transfer methods described in section 4.2.1 are adequate for light weight wood frame construction, they inaccurately model building envelope technologies that incorporate significant thermal bridging. Thermal bridging can be described as locations within the envelope assembly that compromises the thermal resistance due mainly to structural elements (Carpenter 2001). The most recognized thermal bridges include studs or joists located within the clear wall region[2]. Yet recent studies have shown the significant degradation of the overall envelope resistance due to other wall details such as wall/floor connections or window/door framing (McGowan and Desjarlais 1997; Carpenter 2001; Kosny et al. 1999; Tuluca et al. 1997).

The most obvious way thermal bridging affects wall systems is in their steady-state performance. Certain construction materials with extremely large conductivities can act as thermal "escalators" causing excessively large heat fluxes across the insulation barrier. Metal, in particular, which has a conductivity several orders of magnitude larger than other common building materials has become extremely common within the building structure. Since its incorporation into residential buildings is fairly recent, the negative effects of metal on the overall wall performance is not well understood. Consequently, metal elements often compromise the effectiveness of the insulation barrier. For example, wood studs that span across the insulation barrier are often simply replaced by thin steel supports as shown in Figure 4.10 below. Although extremely thin, the steel supports have a conductivity over 400 times that compared to soft woods (spruce, pine, and fir) which undermines the resistance provided by the insulation. In general, any highly conductive material arranged perpendicular to the interior/exterior surfaces, especially across the insulation barrier, will result in a significant degradation of the R-value.

[2] Clear wall region: surface area free of construction details such as corners or junctions

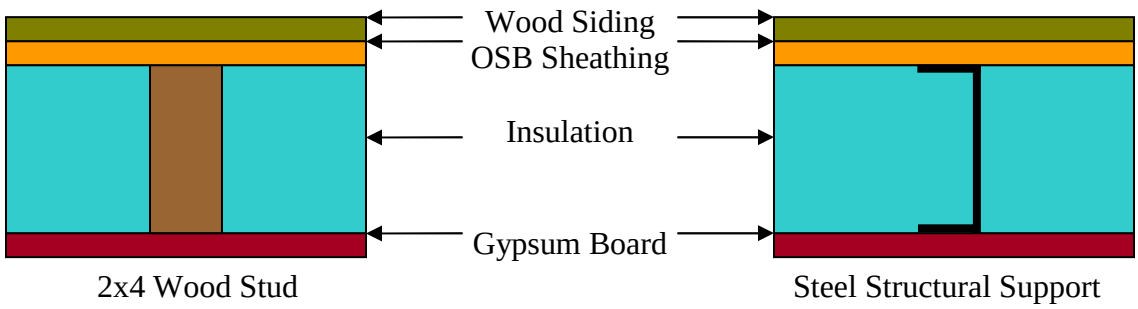

Figure 4.10. Standard practice to replace wood studs with steel supports

Less acknowledged, thermal bridging has a large impact on the transient performance of a wall system by altering the temperature distribution and dynamic characteristics. This aspect has become more of a pressing issue as massive wall systems have penetrated all sectors of the building market. Massive wall systems consisting of concrete, brick, or stone material inherently have a strong time-dependent behavior due to their large thermal capacitance. Ignoring the effects of thermal bridging when simulating these wall systems would result in inaccurate computer models.

4.2.3 Wall Detail Simulation Methods

With the complexity of building envelopes increasing, better simulation techniques are necessary to enable engineers, contractors, and architects to evaluate the effect of thermal bridging on both the steady-state and transient performance. Many different methods have been developed throughout the past several decades to meet this need. The complication and detail associated with each method varies over a wide range. Tuluca et al (1997) summarizes the more popular methods. Unfortunately, many of the methods inadequately simulate wall technologies that incorporate highly conductive elements and/or thermally massive materials like PCPs. Yet the rapid advancement of numerical methods associated with ever increasing computational power has resulted in two robust methods, the Finite Difference (FD) and Finite Element (FE) methods. Both function on the same fundamental level, by discretizing the conduction heat transfer equation into discrete, algebraic equations. Similarly, the one, two, or three dimensional wall detail is discretized into discrete elements in which the algebraic conduction heat transfer

equation is applied to each. Finally some predetermined function (linear, polynomial etc) is used to define the relationship between the elements. The FD method breaks the wall detail into rectangular elements aligned with the Cartesian Coordinate directions and therefore has difficulty evaluating curved or diagonal surfaces. The FE method breaks the wall detail into any predetermined element shape (triangular, rectangular etc.) and therefore can model more complicated geometries (Patankar 1980).

Both the FD and FE methods were used to evaluate the different wall technologies in this study to capitalize on the beneficial attributes from both schemes. Initially, the ANSYS FE program was used but discarded since importing complicated wall assemblies from the CAD/CAM software package ProEngineer proved to be too difficult and limited. Instead, the FEMLAB FE program was used due to its extremely user friendly interface. Unfortunately, FEMLAB was not rigorous enough to model the complicated wall geometries in three dimensions. Therefore, FEMLAB was used to evaluate the wall details in two dimensions as a verification method for the three dimensional simulations and as a tool to investigate the area of influence for each wall detail since it provided a simple means to quickly change the simulation. The main numerical program used was a simple but very robust FD program called Heating 7.3 (Kosny and Christian 2000). Although Heating 7.3 was limited to rectangular geometries and had no preprocessor interface, it was capable of conducting three dimensional steady-state and transient simulations quickly. Two other aspects made Heating 7.3 a reliable tool. First, it was the program used in the development of the equivalent wall method, explained in section 4.2.4. Second, Heating 7.3 was extensively calibrated against experimental data on different steady-state and dynamic wall performances from Hot Box Testing (Kosny and Childs 2000).

4.2.4 Equivalent Wall Method

Although the application of the FD and FE numerical techniques improve the steady-state and transient analysis of building envelope assemblies that include extensive thermal bridging, the problem of how to incorporate these effects into the whole building simulation programs still remains. The option to implement either method to simulate the three dimensional heat transfer throughout the envelope while simultaneously modeling the whole building would result in ridiculous simulation times. Consequently, the equivalent wall method was developed to meet

the demand to account for thermal bridging effects without requiring any changes to the one dimensional conduction heat transfer approaches used by the main whole building simulation programs discussed in section 4.3.1 above. The following paragraphs will describe the equivalent wall method, its methodology, and how it relates to the various time series solution methods.

The general explanation of the equivalent wall method is the creation of a one dimensional multi-layer wall whose fictitious thermal properties (conductivity, specific heat, and density) gives it the same steady-state and transient performance as the three dimensional intricate wall assembly being evaluated. The steady-state performance is simply mirrored by setting the equivalent wall total R-value identical to that of the wall detail. The dynamic behavior is mirrored by setting the basic thermal characteristics of the wall detail and equivalent wall equal to one another. The basic thermal characteristics are defined by five parameters: the overall resistance value, overall thermal capacitance, and three structural factors. The overall thermal capacitance can be solved by integrating the density and specific heat of all the material elements within the assembly over the total volume. This procedure has been incorporated into the Heating 7.3 program such that the capacitance is calculated separately during a steady-state or transient analysis. The calculation of the three structure factors requires a more rigorous process. Structure factors are defined as "dimensionless quantities representing the fractions of heat stored in the wall volume, in transition between two different states of steady heat flow, which are transferred across each wall surface" (ASHRAE 2001d). Essentially, structure factors describe the resistance and capacitance distribution across the thickness of the wall detail.

The structure factors were developed from the integral formula for heat flow across a wall assembly in a finite time interval (Kossecka 1992). Equations 4.8, 4.9, and 4.10 show how to calculate the structure factors for j_{ii}, j_{ie}, and j_{ee} respectively:

$$\jmath_{ii} = \frac{1}{C_{Total}} \int_V \rho C_P (1-\theta)^2 dv \qquad \textbf{(4.8)}$$

$$\jmath_{ie} = \frac{1}{C_{Total}} \int_V \rho C_P (1-\theta)\theta dv \qquad \textbf{(4.9)}$$

$$\jmath_{ee} = \frac{1}{C_{Total}} \int_V \rho C_P \theta^2 dv \qquad \textbf{(4.10)}$$

where:

C_{Total} is the total thermal capacity of the wall element within volume V $\left(C = \int_V \rho C_P dv \right)$ and

θ is the dimensionless temperature for the problem of steady-state heat transfer with interior and exterior surface temperatures equal to 0 and 1 respectively.

These three equations above result in the following relation,

$$\jmath_{ee} + 2\jmath_{ie} + \jmath_{ii} = 1. \qquad \textbf{(4.11)}$$

General rules defining the behavior of the structure factors can be derived from Equations 4.8 – 4.11. In steady-state heat flow through layers of different material, the temperature slope is large for materials with low conductivity and small for materials with high conductivity material. Therefore, the relative magnitudes of the structure factors describe the location of the thermal mass versus resistance. For example, $\jmath_{ii}$ is large if most of the thermal mass is located on the interior of the wall while most of the resistance is located at the exterior of the wall and visa versa for a large $\jmath_{ee}$. A large $\jmath_{ie}$ represents the majority of the resistance distributed on either side of most of the thermal mass (Kossecka and Kosny 2001).

The fundamental principle behind the equivalent wall method is the mathematical relationship between the structure factors and response factors. As evident from section 4.3.1, response factors are the basic features describing the transient behavior of a wall system. Therefore, by imposing conditions on the response factors through the structure factors, this method controls

the transient behavior of the one dimensional thermally equivalent wall. The resultant mathematical relationships, are shown in Equations 4.12, 4.13, and 4.14 (Kossecka 1998) below:

$$d\sum_{n=1}^{\infty} nX^*_n = -Cf_{ii}, \qquad \textbf{(4.12)}$$

$$d\sum_{n=1}^{\infty} nY^*_n = -Cf_{ie}, \text{ and} \qquad \textbf{(4.13)}$$

$$d\sum_{n=1}^{\infty} nZ^*_n = -Cf_{ee}. \qquad \textbf{(4.14)}$$

In other words, the thermal structure factors along with the total thermal resistance and capacitance determine the dynamic thermal properties of a wall element by the conditions they impose on the response factors. Yet these conditions do not determine the response factors in a unique way but rather play a role of constraints. Therefore, several different equivalent walls can be created which all have similar dynamic thermal behavior (and thus similar values for resistance, total capacitance, and structure factors). Since response factors form the basis of the CTF method, the structure factors are also mathematically related to the CTF coefficients. As a result, the equivalent wall method can be incorporated within the EnergyPlus program which uses the State Space version of the CTF method.

The entire methodology of the equivalent wall method is outlined in the following steps and further highlighted in the flow chart shown in Figure 4.11.

1. Develop a two or three dimensional model of the building element in the FEMLAB or Heating 7.3 programs respectively.
2. Conduct a steady-state simulation of the model to calculate the total resistance of the wall element. Use boundary conditions of the first kind, (i.e. constant surface temperatures), in order to omit the effects of the surface convection on either side since EnergyPlus will account for this effect separately.
3. Integrate the density and specific heat of the materials that comprise the wall element across its entire volume to determine the total thermal capacitance.
4. Determine the dynamic behavior of the building element by calculating the thermal structure factors. Two separate methods can be used.

a. The first involves using a specific equivalent wall module within the Heating 7.3 program that applies a unit temperature pulse to the wall detail and determines its response factors. Using the mathematical relationships in Equations 4.12, 4.13, and 4.14, the thermal structure factors are calculated.

b. The second involves simulating the steady-state solution of the wall element within the FEMLAB FE program for a unit temperature on the exterior surface and zero temperature on the interior surface. The resultant temperature distribution represents the dimensionless temperature, θ or $\left(\frac{T - T_{interior}}{T_{exterior} - T_{interior}}\right)$, where T is the temperature at each node within the building element. Integrating across the entire building element subdomain using Equations 4.8, 4.9, and 4.10, yields the thermal structure factors.

5. A basic optimization program written in Matlab, can calculate the necessary thermal properties of a multilayer wall system such that the total resistance, total capacitance, and thermal structure factors are identical to those calculated for the building element. The optimization program is shown in Appendix F. An equivalent wall consisting of six layers was found to be adequate to model the transient performance of all of the wall details considered here.

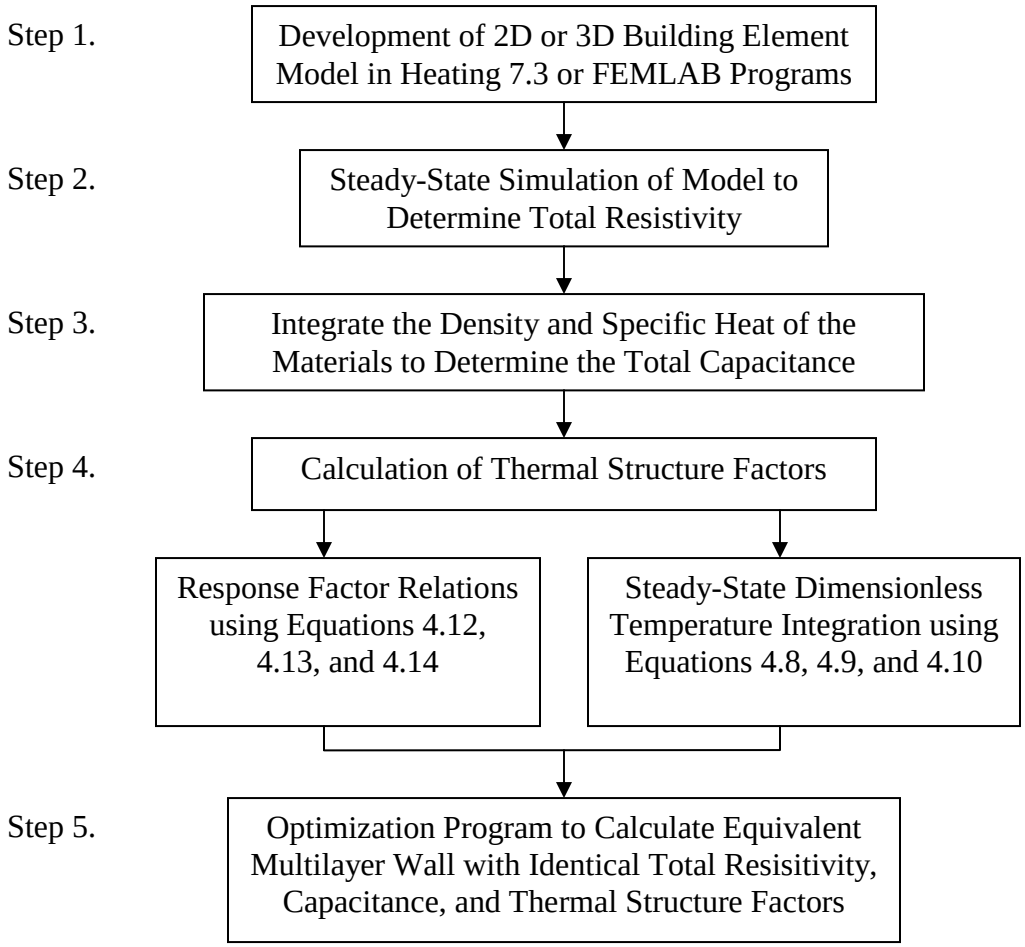

Figure 4.11. Flow chart of equivalent wall method

ASHRAE Project 1145 report (ASHRAE 2001d) compares the simulation results for the dynamic performance of a simple wall element obtained using the Heating 7.3 program with results from a thermally equivalent wall to assess the validity of the equivalent wall method. Comparing the equivalent wall model to three dimensional simulation, although the response factors look familiar, slight differences were still apparent due to the fact that parallel flow paths of different conductance may not be completely reproduced by a one-dimensional model. Therefore, under rapid temperature excitations such as those used to determine the response factors, the equivalent wall produces a small delay and amplitude amplification of the resulting heat flux (ASHRAE 2001d). Similar trends are shown when the three dimensional and equivalent wall simulations are compared using the frequency response method (ASHRAE 2001d; Carslaw and Jaeger 1959; Hittle 1979). The frequency method showed that these discrepancies increased with a larger oscillation frequency of the temperature excitation.

Fortunately, the environmental conditions experienced by wall elements will not be rapid temperature fluctuations but smooth, continuously varying outdoor temperatures. ASHRAE project 1145 compared the interior surface heat flux in response to typical daily environmental conditions (ASHRAE 2001d). Differences between the three dimensional and equivalent wall simulations were extremely small for smooth temperature changes compared to the disagreements shown for rapid temperature oscillations. The equivalent wall only showed slightly more dynamic behavior, amplifying the internal heat flux a minute amount. This deviation was found to increase with a larger thermal mass of the wall element. Yet for all the wall systems analyzed in this study, these discrepancies between the three dimensional and equivalent wall transient behaviors were considered negligible compared to the other sources of inconsistency associated with predicting heat transfer such as the large variability that can occur in the thermal-physical properties of a material. To put things into perspective, the precision of standard hot box testing is roughly 8% (ASTM 1993), significantly larger than the error between three dimensional and equivalent wall simulations of internal heat fluxes (Kosny and Childs 2000).

4.2.5 Whole Wall Analysis

Predicted heat transfer through building envelopes is typically based upon measurements of the clear wall area using ASTMC 236 techniques or calculations using ASHRAE Fundamentals respectively (Kosny and Desjarlais 1994). The clear wall area is defined as “the part of the wall system that is free of thermal anomalies due to building envelope subsystems, or thermally unaffected by intersections with other surfaces of the building envelope” (Kosny and Desjarlais 1994). This coincides with the statement made in Section 4.3.2 that the most recognized location of a thermal bridge in a building envelope is the structural components within the clear wall (i.e. wood studs or metal supports). Therefore, in a typical whole building analysis, only the clear wall, clear floor, and clear ceiling dynamic behavior is incorporated into the thermal effects on the interior zone. Consequently, the effects of the wall details (i.e. wall/ceiling or wall/window connections) are often ignored despite the fact that their effect on the overall building performance can be significant.

The troubling aspect is the cumulative effect this standard practice has; little to no attention given to wall details in building simulations most likely means the same apathy during the design of the wall configuration resulting in poor thermal performance of these details. In other words, the scenarios where no thermal evaluation of wall details took place would be the times when it would be most necessary since the insulation is probably inefficiently integrated within the wall detail. The saying "A chain is only as strong as its weakest link" applies perfectly to this situation. A supposed energy efficient envelope technology that has proper insulation configuration in the clear wall but improper insulation in the wall details will perform poorly.

To properly evaluate the overall performance of the building envelope, a whole wall calculation method was used to account for both the clear wall and wall detail thermal effects. The steady-state and transient performance for each clear wall and wall detail was simulated using two or three dimensional models in FEMLAB or Heating 7.3, respectively. The resultant resistance, capacitance, and thermal structure factors for each clear wall or wall detail were then summed based upon an area weighted method to calculate an equivalent wall for each exterior surface of the prototypical house. The area weighted method to calculate the total resistance and other thermal properties (capacitance and structure factors) of the thermally equivalent wall is shown in Equations 4.15 and 4.16 respectively:

$$R_{Total} = \left[\left(\frac{A_{CW}}{A_{Total}} \right) \frac{1}{R_{CW}} + \sum_{i=1}^{n} \left(\frac{A_i}{A_{Total}} \right) \frac{1}{R_i} \right]^{-1} \quad \textbf{(4.15)}$$

$$TP_{Total} = \left[\left(\frac{A_{CW}}{A_{Total}} \right) TP_{CW} + \sum_{i=1}^{n} \left(\frac{A_i}{A_{Total}} \right) TP_i \right] \quad \textbf{(4.16)}$$

where: R is the resistance,

TP is the other wall thermal properties (total capacitance and structure factors),

A is the wall detail areas,

n is the number of details for that particular exterior surface, and

subscripts Total, CW, and i are the overall wall, clear wall, and i^{th} wall detail respectively (Kosny and Christian 1994).

For example, to calculate the overall resistance of the east facing wall on the prototypical house, the total exterior opaque wall minus the window and door openings would first be split up into

areas associated with either the clear wall or a specific wall detail. **Error! Reference source not found.** below shows the breakdown of the prototypical house east facing wall. Table 4.3 gives representative resistivity values and areas associated with each clear wall and wall detail. Finally, (4.17 shows how to calculate the overall resistance of the east facing wall using the information in Table 4.3. The resultant total resistance value from solving Equation 4.17 is $7.6\frac{hr \quad ft^2 \quad F}{Btu}$.

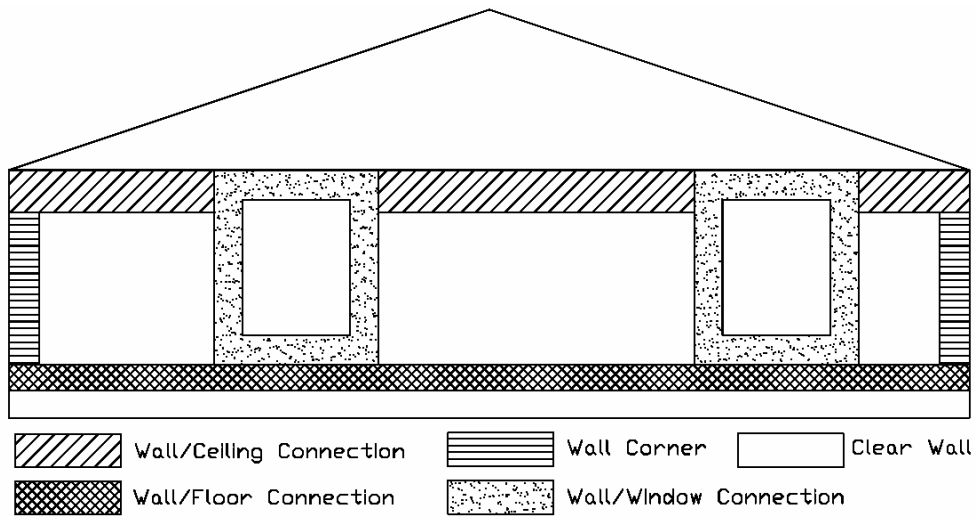

Figure 4.12. Prototypical house east facing wall wall detail breakdown

Table 4.3. Representative resistances and areas with the clear wall and wall details

	Total Resistance $\left(\frac{hr \quad ft^2 \quad F}{Btu}\right)$	**Detail Area** (ft^2)
Clear Wall	7.5	116
Wall/Ceiling Connection	7.0	35
Wall/Floor Connection	6.5	32
Wall Corner	5.5	12
Wall/Window Connection	6.0	47

$$R_{Total} = \left[\begin{array}{l} \left(\frac{116\,ft^2}{242\,ft^2}\right)\frac{1}{7.5\frac{hr\,ft^2\ F}{Btu}} + \left(\frac{35\,ft^2}{242\,ft^2}\right)\frac{1}{7.0\frac{hr\,ft^2\ F}{Btu}} + \left(\frac{32\,ft^2}{242\,ft^2}\right)\frac{1}{6.5\frac{hr\,ft^2\ F}{Btu}} + \\ K\left(\frac{12\,ft^2}{242\,ft^2}\right)\frac{1}{5.5\frac{hr\,ft^2\ F}{Btu}} + \left(\frac{47\,ft^2}{242\,ft^2}\right)\frac{1}{6.0\frac{hr\,ft^2\ F}{Btu}} \end{array} \right]^{-1} \quad \textbf{(4.17)}$$

Based upon a previous study highlighting the most important architectural details affecting the overall building envelope performance, the wall details analyzed were the roof/wall connection, floor/wall connection, window/wall connection, and wall corners (Kosny and Desjarlais 1994). For simplification purposes, the door/wall connection was simulated with the same thermal properties as the window/wall connection yet with its own associated area. The construction configurations for these details were ascertained from standard architectural drawings for the Conventional and Energy Efficient Wood Frame systems (Hoke; Marino 1992) and system manufacturers design guides for the Waffle PCP and Sandwich PCP systems (Composite Technologies 2004).

Determining the areas of each external surface thermally influenced and therefore associated with each of the wall details described above was the hardest aspect of the whole wall analysis. The area affected by a wall detail was termed the area of influence which was defined as "that area where the existence of the detail changed the slope of the isotherm more than 5°" (Kosny and Desjarlais 1994). This slope was roughly a 1°F change in temperature per inch of length along the wall surface. Therefore, the area that contained isotherms that were impacted by the presence of a certain wall detail was defined as the area of influence for that wall detail. The area of influence often extended well within the clear wall section adjacent to the wall detail. Often up to 2 times the actual wall detail area of clear wall area was absorbed within its area of influence.

Mainly two dimensional models of the different wall details were developed in the FEMLAB FE program to evaluate the isotherms and determine the different zones of influence. Although three dimensional conduction can vary the size of the area of influence of the wall detail, the two dimensional simulations were considered adequate to characterize the extent that each wall detail

affected its surroundings. For the same wall detail, the area of influence varied depending on the wall construction type (wood frame, PCP etc.). Therefore, the area of influence for each detail was varied depending on the wall technology. Note that the 5° isothermal slope constraint used to define the area of influence was used more as a general constraint rather then a necessary condition. From the two dimensional FE solution, the isotherms were analyzed and the area of influence dimensions were set such that without a doubt, the entire effect from the wall detail was incorporated. More clear wall was encompassed within the area of influence than necessary which was acceptable considering that the excess clear wall area would still have an effect on the final thermal properties of the wall detail. The clear wall area was the total opaque exterior wall minus the area of influences of all the wall details associated with that surface. When two zones of influences overlapped, the area of influence of the wall detail with the lower resistivity was applied to that area.

There are many ways to compare the influence of wall details on the overall building envelope performance. The area of influence and thermal resistance are the two most important aspects that play a vital role in gauging the significance of wall details. Therefore, these factors were incorporated into one parameter called the "detail influence factor" (DIF) which combines the effects of both so that the impact from each wall detail can be quantified and compared (Kosny and Christian 1994). Basically, the DIF is a measure of the amount of heat loss that can be attributed to each wall detail of the overall wall system. Equation 4.18 below shows how to calculate the DIF:

$$DIF = \frac{R_{Total} / A_{Total}}{R_i / A_i} * 100\% \qquad \textbf{(4.18)}$$

where R_i is the R-value of the ith wall detail and

A_i is the area of influence of the ith wall detail (Kosny and Christian 1994).

Another way to characterize the performance of a wall system based upon its wall details is to determine the effectiveness of the insulation configuration of the system. For future reference, this parameter will be referred to as the *insulation effectiveness*. Essentially, the insulation effectiveness is the percentage of the total possible R-value for a given quantity of insulation that the actual insulation configuration within the wall system provides. The maximum R-value of a

wall system is the resistance of a uniform layer of insulation that covers the entire clear wall area that is comprised of the consolidation of the actual insulation configuration in the clear wall. Finally, the whole wall R-value divided by this maximum R-value is the insulation effectiveness.

4.3 Prototypical House Specifications

The following section describes a "prototypical residence" which is defined as a house that represents the most common construction specifications and operating conditions for new single family, detached homes within the United States (Huang et al. 1987). It serves as a basis of comparison for which the different construction technologies can be analyzed in their applied environment to determine how each wall system affects the overall thermal performance of the home. Simulating a typical home built from different wall systems applies the whole house approach described in the literature. Rather than simply evaluating the wall systems independently, this approach investigates how the wall construction affects the other components associated with the thermal performance of the home and optimizes the whole system. The practices used to define the prototypical home are based on data from several sources. Already summarized in the literature review, they are the:

- 1995 Residential Energy Consumption (REC) surveys (US DOE 1995a; US DOE 1995b; US DOE 1995c; US DOE 1995d),
- 1987 LBL BEAG technical document (Huang et al. 1987),
- 1997 Energy Data Sourcebook by the LBL End-Use Forecasting group (Wenzel et al. 1997),
- 2003 Building Energy Databook by the Energy Efficiency Renewable Energy (EERE) Office of the DOE (US DOE 2002), and
- Building America Research Benchmark Definition by the DOE Building America Program (US DOE 2003).

The subsequent subsections describe in detail the information used from these references as well as the weather conditions employed and analytical/numerical tools used to accurately simulate a house to determine the effects of each wall type on overall energy use. The characteristics and assumptions regarding the prototypical house developed in sections 4.3.2 to 4.3.10 are summarized in Table 4.4.

Table 4.4. Summary of prototypical house characteristics and assumptions

Home Specifications	Description
Room Configuration	3 Bedrooms; 2 Bathrooms; 1 Living Room; 1 Dining Room; 1 Kitchen; 1 Basement; 1 Garage
Conditioned Floor Area	2275 ft^2
Number of Windows	14
Total Glazing Area	218 ft^2
Annual Appliance/Light Loads	32 MBtu
Thermostat Setpoints	Summer: 78°F Winter: 70°F
Heating Equipment	Gas Furnace / Heat Pump
Cooling Equipment	Central Air Conditioner / Heat Pump

4.3.1 Weather Locations

Six cities were chosen within the continental United States as representative climates to evaluate the behavior of the different construction technologies[3]. Table 4.5 below lists these cities and their corresponding heating degree days (HDD) and cooling degree days (CDD). Using EnergyPlus, the prototypical house incorporating each of the different construction technologies was exposed to the annual weather for each city. The weather data was based on the TMY2 information. For future reference, Minneaopolis and Denver represent cold cities, Washington D.C. and Atlanta represent temperate cities, and Phoenix and Miami represent hot cities.

Table 4.5. Six cities representative of typical U.S. climates

	HDD		CDD	
Cities	18.3°C	(65°F)	18.3°C	(65°F)
Minneapolis	4298	(7736)	394	(709)
Denver	3379	(6082)	352	(634)
Washington D.C.	2795	(5031)	609	(1096)
Atlanta	1751	(3152)	973	(1751)
Phoenix	628	(1130)	2280	(4104)
Miami	64	(115)	2369	(4264)

[3] These cities were chosen to correspond to those used by Kosny et al (1999) so that the results from the current study could be compared to those from the Kosny reference

4.3.2 Room Configurations and Dimensions

Based on the 1995 REC surveys, the prototypical house is a one story ranch located in the suburbs with three bedrooms, two full baths, and three other main rooms which are a living room, kitchen, and dining room. According to the 1995 REC surveys, the median heated floor area is within a range of 2000-2500 ft^2 (186-232 m^2) and for this study, is assumed to be 2275 ft^2 (211 m^2). The median unheated floor area from the 1995 REC survey is between 500-1000 ft^2 (46-93 m^2). This contradicted the BEAG document (Huang et al. 1987) which specifies that most homes have a basement foundation and thus an unheated floor area that is comparable to the heated floor area. To be consistent with the BEAG document, the prototypical house is assumed to have a 2275 ft^2 (211 m^2) unheated basement and a 484 ft^2 (45 m^2) unheated garage. Appendix A shows the spread by percentages of the 525 houses surveyed for each of the house specifications previously mentioned. Figure 4.13 and Figure 4.14 below show the first floor schematic and front elevation of the prototypical house, respectively. Although larger, this house configuration is almost identical to a 1540 ft^2 (143 m^2) typical ranch style house used in several previous studies (Huang et al. 1987; Christian and Kosny 1996; Kosny and Desjarlais 1994; Kosny et al 1999).

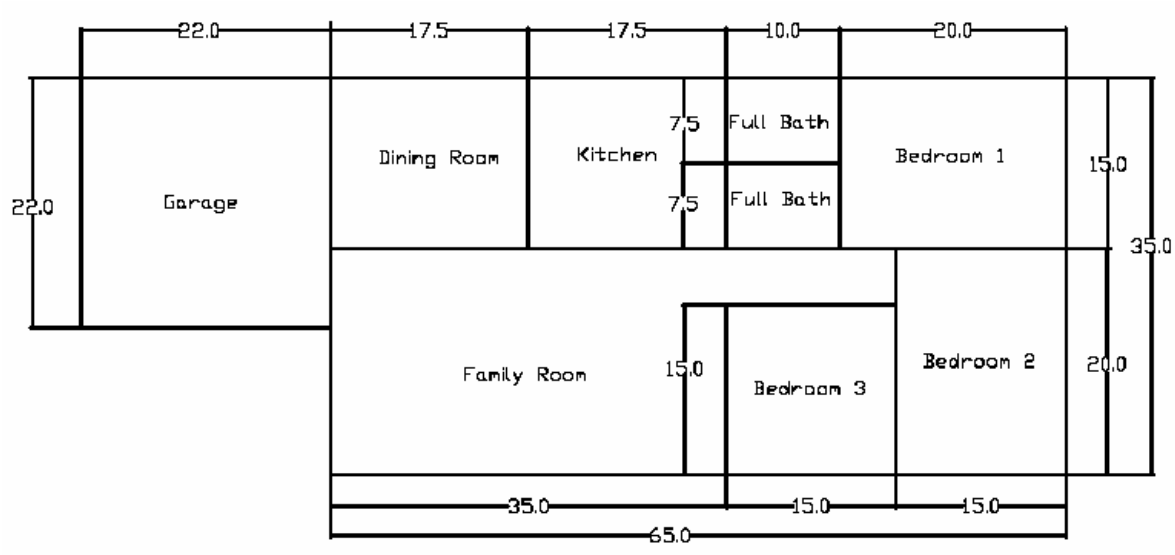

Figure 4.13. Prototypical house first floor schematic dimensioned in feet

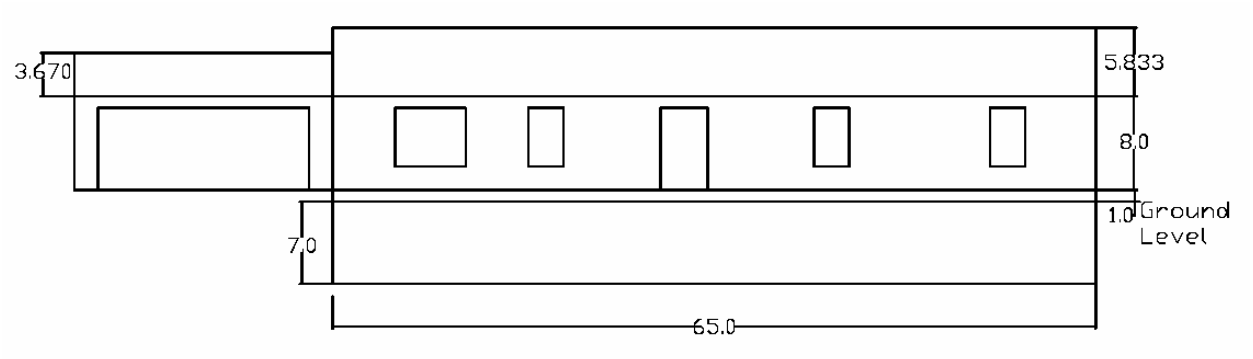

Figure 4.14. Prototypical house front elevation dimensioned in feet

For modeling in the EnergyPlus building simulation program, the prototypical house is divided into zones that represent distinct thermal environments. More specifically, each zone does not necessarily represent one room but could include several adjacent rooms that maintain similar air temperature and humidity conditions throughout the year. As a result, the prototypical house is split into 5 zones as shown in Figure 4.15: the garage, the basement, the attic, the living area consisting of the living room, dining room, and kitchen, and the bedroom area consisting of all the bedrooms and full baths.

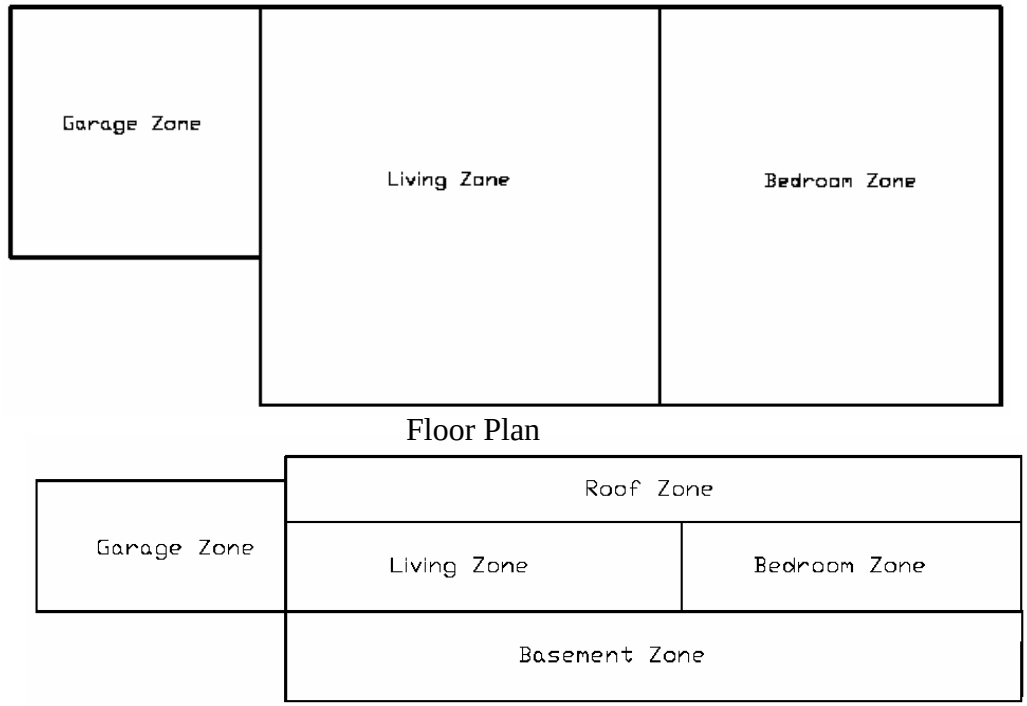

Figure 4.15. Division of the prototypical house into thermal zones

The thermal mass in each zone was determined by two separate calculations, thermal mass due to interior walls and thermal mass due to furniture. Only the bedroom and living room zones have interior walls which span 90 ft (27 m) and 50 ft (15 m), respectively. For the total exposed surface area to the zone air, both sides of the interior walls are taken into account. The material composition of these interior walls is two layers of ½" gypsum separated by 3.5" of air to represent the standard interior wall construction excluding 2x4 studs at 16" o.c.

The furniture thermal mass located in each of the zones is based upon data developed by Mayflower Transit Moving Company (Mayflower Transit 2004) and the DOE Building America Program (US DOE 2003). Table 4.6 shows the furniture weight, volume, and surface area for each thermal zone. The conditioned zones are assumed to contain 8 pounds of furniture per square foot of floor surface while the unconditioned zones contain a flat 1,250 pounds each. The exposed surface area of the thermal mass is based upon an estimate that all the furniture has a density of 7 pounds per cubic foot, all the furniture is cubic in shape, and each zone contains 15 items of furniture each. Assuming that all the furniture is composed of wood, the conductivity and specific heat properties of all the furniture is based upon that of spruce/pine/fir.

Table 4.6. Furniture specifications in each thermal zone

	Weight	**Volume**	**Volume per Furniture Item**	**Expose Surface Area per Furniture Item**
	(lb)	(ft^3)	(ft^3)	(ft^2)
Living	9800	1400	93	103
Bedroom	8400	1200	80	93
Garage	1250	179	12	26
Basement	1250	179	12	26
Roof	1250	179	12	26

4.3.3 Fenestration Configurations and Dimensions

From the 1995 REC surveys, shown in Appendix A, the number of windows in a new house ranges from 10 to 14. Consequently, the conditioned zones of the prototypical house have 14 windows and the garage zone has 2 windows with the base 2 feet above ground level. The gross window size including frame is 3.9'x4.9' based upon the standard window size of the National Fenestration Rating Council (NFRC). Considering only the 14 windows surrounding the

conditioned zones, the window area including the framing comprises roughly 12% of the conditioned floor area which is the same estimate cited for typical homes in the BEAG report (Huang et al. 1987). Figure 4.16 shows the schematic of the window simulated for this study including its frame and dividers.

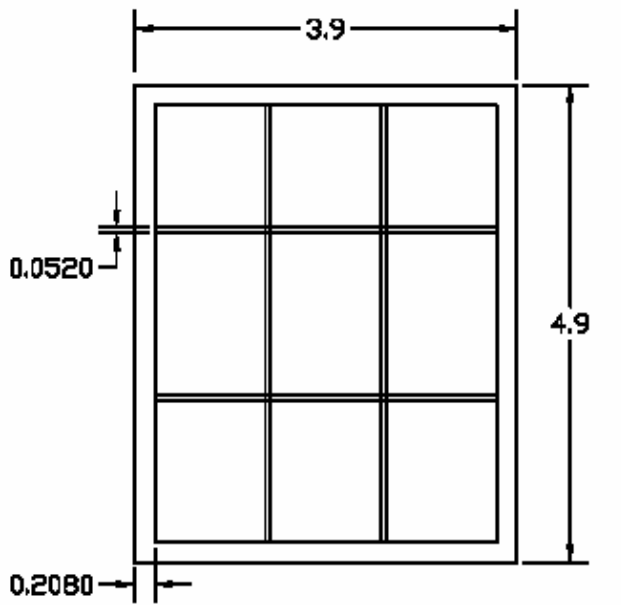

Figure 4.16. Window dimensions (feet)

The windows included in the EnergyPlus program including the framing, dividers, and glazing area were modeled using Window 5.0 (Windows 5.0 2001) to determine overall U-values, shading coefficients, and other window properties required by EnergyPlus. Developed by the LBNL Window and Daylighting Group, Window 5.0 thermally evaluates any fenestration that incorporates some type of glazing. The exact dimensions shown in Figure 4.16 were specified in the Window 5.0 program. The program then creates a text file containing all the important thermal properties of the window that can be directly referenced by the EnergyPlus program. These thermal properties, which include the effects of the frame and dividers, are the thermal conductance (U-value), shading coefficient, and the absorptance, reflectance, and transmittance of the window averaged over the entire solar spectrum for every 10° from 0° to 90° angle of incidence. The shading coefficient (SC) is a ratio of solar heat gain through the glazing design to that through a single pane of 3 mm clear glass under identical conditions. Figure 4.17 shows the

user interface associated with the Windows 5.0 program including the graphical representation of the picture window used for the prototypical house.

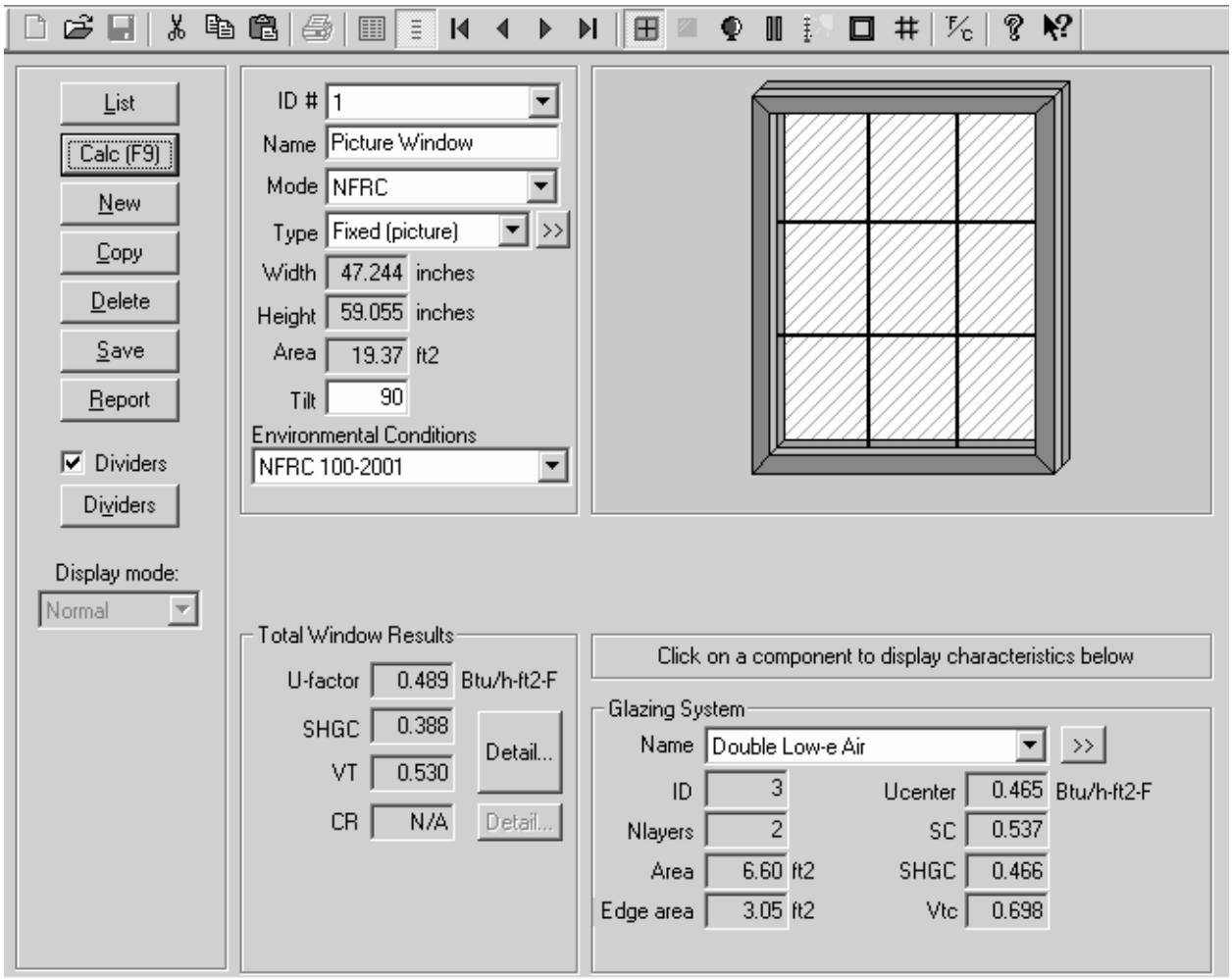

Figure 4.17. Graphical user interface for the Window 5.2 program

Since this study compares different wall technologies, the same window constructions are used for the different wall systems so that the window effects are independent. According to ASHRAE Standard 90.2 (ASHRAE 2001b), each climate region has minimum thermal conductance and maximum SC values to meet for the gross window area, including frame and dividers, for a house to be considered energy efficient. According to the 2003 Building Energy Databook (US DOE 2002), wood frame windows still represent the major window type used in new construction accounting for roughly 46% of the entire new construction window market in 2002. In terms of the glazing configuration, the 2003 Building Energy Databook (US DOE

2002) indicates that the amount of double-pane, low-emissivity windows in the market has rapidly increased such that it comprised 36% of the window sales market in 1996. Consequently, wood frame, double-pane, low-emissivity windows were used in the prototypical house for all the city locations. The resultant window U-value of 0.48 $\frac{\text{Btu}}{\text{hr}\ \ \text{ft}^2\ \ \text{F}}$ and SC of 0.54 met the minimum ASHRAE Standard 90.2 (ASHRAE 2001b) window requirements for all the cities and was very close to the average U-value of 0.47 $\frac{\text{Btu}}{\text{hr}\ \ \text{ft}^2\ \ \text{F}}$ and SC of 0.52 of all the residential windows available in 1999 (US DOE 2002).

According to a residential fenestration modeling program developed by the LBNL Windows and Daylighting group called ResFen (Resfen 3.1 1999), typical windows in a house experience solar gain reduction from: overhangs attached to the house, exterior obstructions from neighboring houses and flora (trees and bushes), dirt, and interior shading devices. The parameters that define these features were modeled identical to those defined as “Typical” in the ResFen program. To account for a house with no overhang and a two foot overhang, a one foot horizontal overhang was attached to the entire prototypical house perimeter at the top of the exterior walls. Fifteen foot vertical obstructions with 67% transmittance were applied to cover 1/3 of each of the prototypical house exterior surfaces at 20 feet away to represent neighboring houses and flora. To account for dirt and insect screens, the SC was reduced 10% manually in the Window 5.0 output text file. Finally, every window in the prototypical house, except for the two garage windows, was assumed to have an indoor shading device that is drawn across the entire glazing region, excluding the frame area. The shading device represented a semi-open weave, light colored drapery with a low reflectance and high transmittance whose thermal properties were obtained from a data set of shading devices incorporated in the EnergyPlus program. The interior shade further reduced the SC of the window by 10%.

From a heat transfer perspective, only doors between thermal zones or separating a zone from the exterior environment are significant in affecting the total building energy load. Therefore only four doors in the prototypical house are modeled; the main door leading into the living room measures 3’x7’, the door connecting the living room to the garage measures 3’x7’, the door

separating the living and bedroom zones measures 3'x7', and the garage door measures 18'x7'. The rest of the doors are considered a part of the interior thermal mass inside the bedroom and living zones discussed in section 4.3.2. The door constructions are independent of the prototypical house location or wall technology. The main door, the door connecting the living and garage zones, and the garage door are modeled as rigid insulation between two ½" layers of SPF wood with an R-value of 5.76 $\frac{ft^2 - F - hr}{Btu}$. This door insulation met the minimum requirement of 5.26 $\frac{ft^2 - F - hr}{Btu}$ based upon ASHRAE Standard 90.2 (ASHRAE 2001b). The door between the living and bedroom zones is made of two ½" layers of OSB separated by a ½" air space resulting in a R-value of 0.934 $\frac{ft^2 - F - hr}{Btu}$. Yet specifying the resistivity of this door is unnecessary because it is modeled constantly open throughout the year as stated in Section 4.3.7. The location of all the windows and doors in the prototypical house is shown in **Error! Reference source not found.** below. Figure 4.19 shows a three dimensional view of the prototypical house including the fenestration and the solar heat gain reduction features such as the detached obstructions and overhangs.

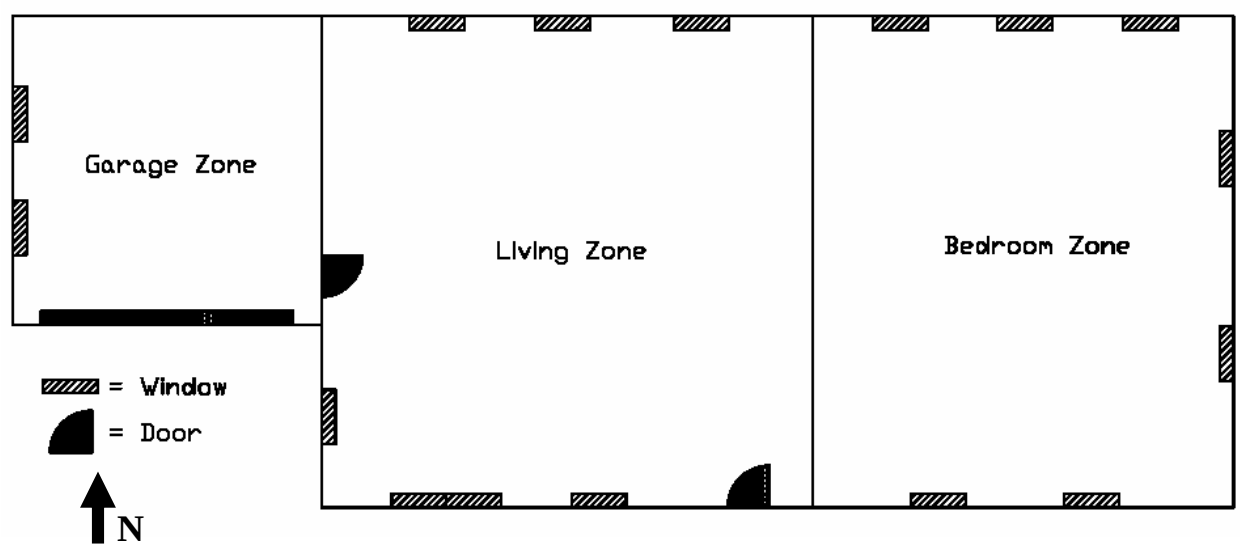

Figure 4.18. Fenestration location throughout the prototypical house

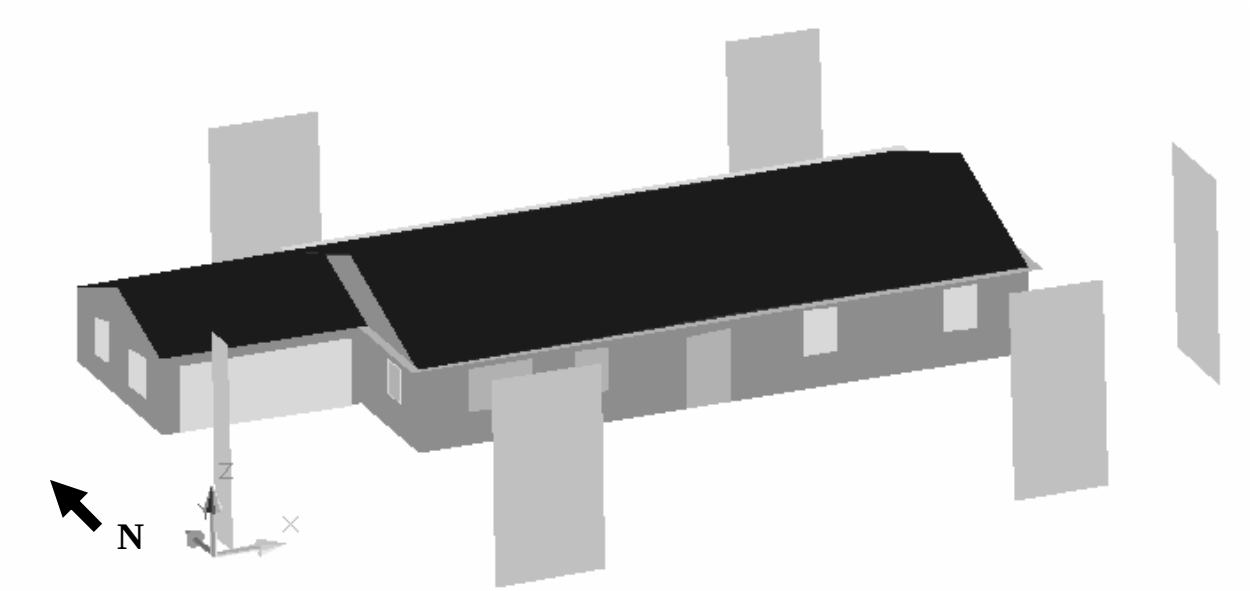

Figure 4.19. Three dimensional view of the prototypical house (including the solar gain reduction)

4.3.4 Internal Loads

The heat emitted by people, lighting, and appliances, termed *internal load*, contributes a significant amount to the total sensible and latent heat gains within a house. Especially today where residences contain a large amount of electronic equipment, the internal heat gain can offset 10 to 15% of the total heating load and contribute to 20 to 25% of the total cooling load (Huang et al. 1987). The energy consumed and heat emitted by the people, lighting, and all the appliances, except the hot water heater, are assumed to be independent of the house location. Since the prototypical residence exemplifies high efficiency, the appliances are modeled at a higher performance than that required by the minimum government standards (Wenzel 1997). Table 4.7 below summarizes all the occupants and appliances, except for the hot water heater, within the prototypical house including their thermal zone location, yearly energy consumption, and the percentages of energy consumed that enters their respective zones, classified by type of heat: sensible, latent, or radiative. Figure 4.20 shows the hourly electric consumption simulated for every day of the year itemized to show the contribution of each appliance to that total. Appendix B contains a more detailed description of how the people, lighting, and appliances are modeled within EnergyPlus.

Table 4.7. Summary of people, lighting, and appliance annual energy consumption

		Annual Cons.	Heat Gain Percentage				
Zone	**Component**	(kW-hr)	Conv	Latent	IR Rad	Visible	Lost
Living	Incandescent Lights	1290	18%	-	72%	10%	-
	Fluorescent Lights	143	50%	-	30%	20%	-
	Dishwasher	178	30%	15%	30%	-	25%
	Refrigerator	648	50%	-	50%	-	-
	Range/Oven	822	20%	30%	20%	-	30%
	Microwave	132	20%	30%	20%	-	30%
	TV	276	50%	-	50%	-	-
	Misc. Electronics	1000	45%	10%	45%	-	-
	Occupants	768	~35%	~30%	~35%	-	-
Bedroom	Incandescent Lights	758	18%	-	72%	10%	-
	Fluorescent Lights	84	50%	-	30%	20%	-
	TV	199	50%	-	50%	-	-
	Misc. Electronics	1000	45%	10%	45%	-	-
	Occupants	721	~35%	~30%	~35%	-	-
Basement	Clothes Washer	103	40%	-	40%	-	20%
	Clothes Dryer	1002	8%	5%	8%	-	79%
Garage	Incandescent Lights	100	18%	-	72%	10%	-
Outdoor	Incandescent Lights	250	18%	-	72%	10%	-

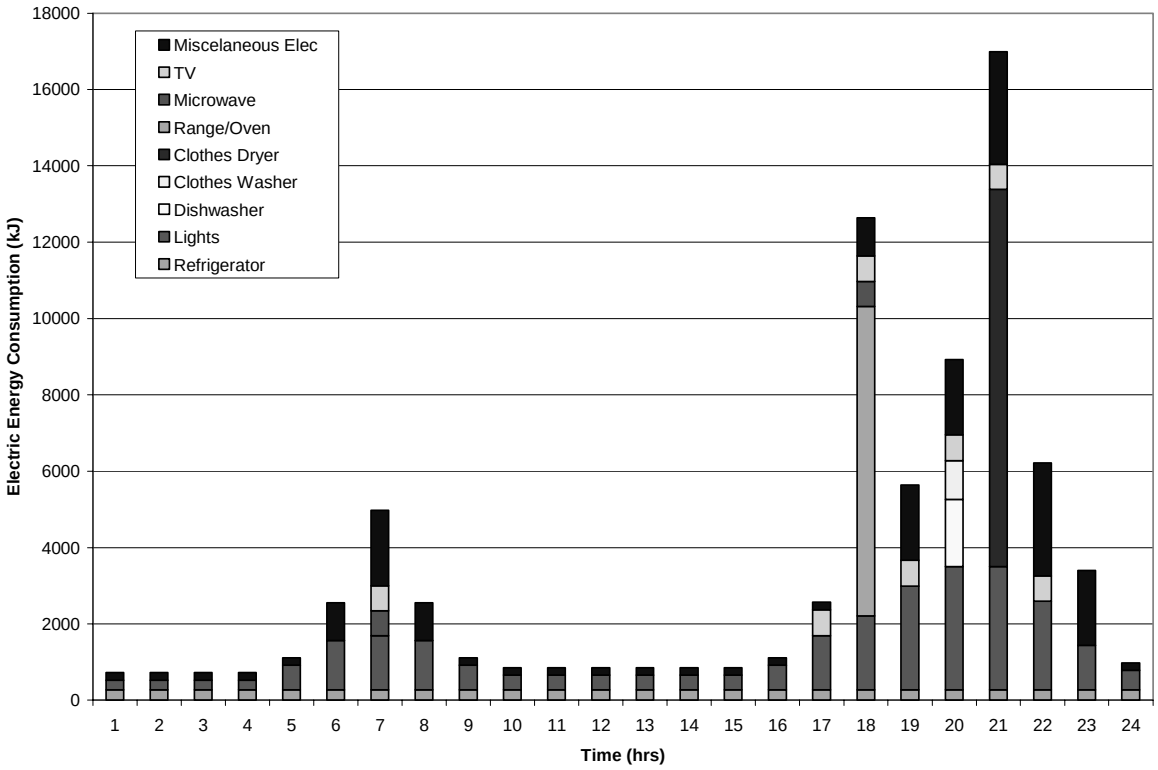

Figure 4.20. Daily electrical energy consumption broken up by appliance

Since the information to determine these internal loads is substantial and can vary considerably, the resultant annual sensible heat gains from the various internal loads were compared to those from two similar studies, the Building America Program (US DOE 2003) and the BEAG technical document (Huang et al. 1987), as shown in Figure 4.21. Table 4.8 compares the total annual energy consumption of the people and appliances (except for the hot water heater) and the amount of that energy emitted as sensible and latent heat for the prototypical house with data for the houses described in Building America with BEAG. As evident from Figure 4.21and Table 4.8, the main difference between the internal loads stems from inconsistent miscellaneous equipment loads. This load which mostly represents electronic equipment has the greatest variability and has significantly increased over the past decade in residences as the consumer market has become saturated with electronic equipment (Wenzel et al. 1997). This explains the major underestimate of the miscellaneous equipment loads in the BEAG Technical Document since it was published in 1987.

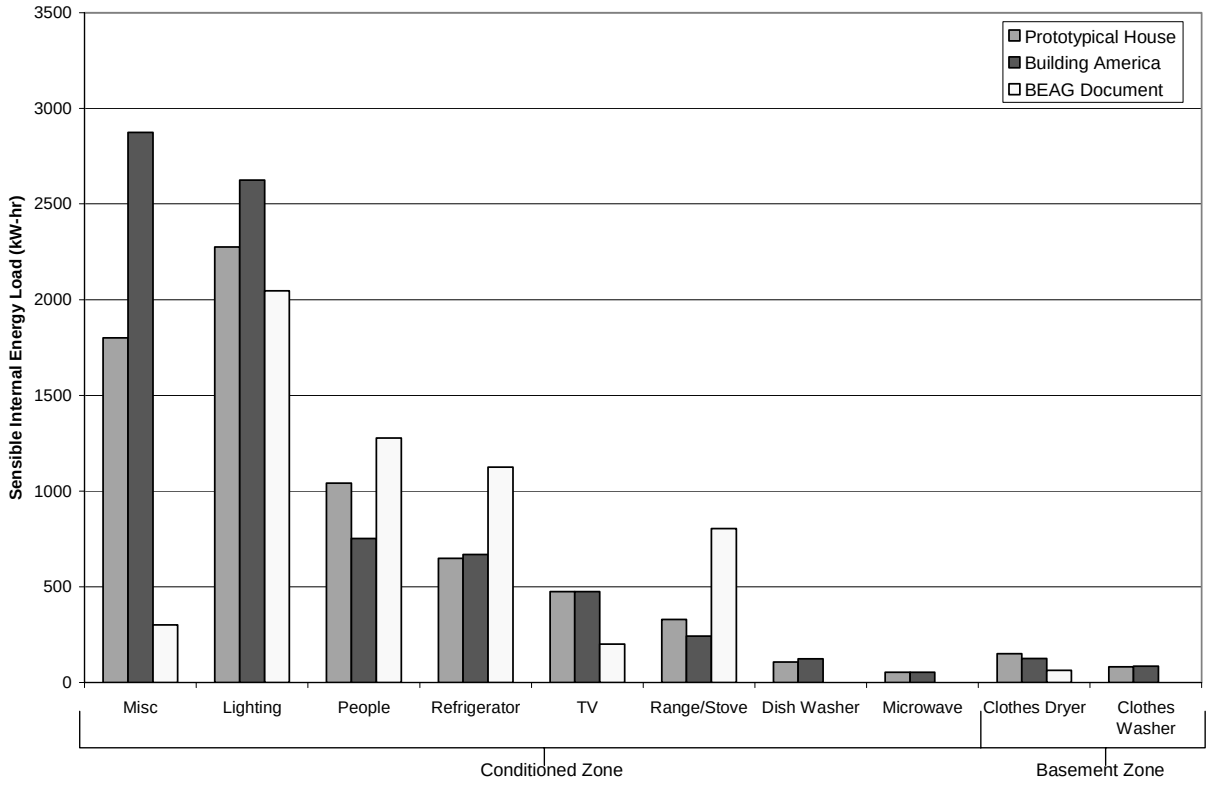

Figure 4.21. Annual sensible internal heat gain

Table 4.8. Total annual energy consumption with emitted sensible and latent heat (except hot water heater)

	Prototypical House	Building America (US DOE 2003)	BEAG Document (Huang et al. 1987)
	(kW-hr)	(kW-hr)	(kW-hr)
Energy Consumption	9475	10290	7701
Sensible Heat Gain	7212	7940	5726
Latent Heat Gain	1010	1328	570

The only appliance modeled to vary depending on the prototypical house location and HVAC system is the water heater. When the heating system is a gas furnace, the house contains a gas water heater. Conversely, when a heat pump is used, the house contains an electric water heater. Using a program developed by the Building America Program (US DOE 2003) to calculate the water mains monthly temperature for each prototypical house location and knowing the hot water setpoint temperature, the annual energy consumption by the hot water heater was calculated for each climate. Table 4.9 shows annual gas and electricity consumption associated with the water heater for each location. The energy that is not lost by the inefficiencies of the hot water heater is consumed by the dishwasher, clothes washer, and shower. Table 4.10 below shows how the water energy is distributed between each of these items in terms of their zone location and the percentages of that energy that enters the zone as heat. Appendix B reviews the calculations and assumptions made to simulate the water heater in more detail.

Table 4.9. Water heater energy consumption for each prototypical house location

Cities	**Electric Energy Consumption** (kWhr/year)	**Gas Energy Consumption** (kWhr/year)
Minneapolis	4468	7282
Denver	4164	6786
Washington D.C.	3915	6380
Atlanta	3461	5640
Phoenix	2683	4373
Miami	2478	4037

Table 4.10. Hot water annual energy consumption and description of heat emitted

Zone	Component	Percentage of Water Energy	Heat Gain Percentage				
			Conv	Latent	IR Rad	Visible	Down the Drain
Living	Dishwasher	12%	-	-	-	-	100%
Bedroom	Shower	67%	2%	11%	-	-	87%
Basement	Clothes Washer	21%	-	-	-	-	100%

4.3.5 Thermostat Setpoints

Although the conditioned area is broken into 2 zones, the thermostat is located in the living zone such that all control over the conditioning equipment is solely based upon the living zone temperature. The bedroom zone is allowed to have a floating temperature. The setpoint temperature deadband was set to the median heating and cooling season temperatures specified from the REC survey information shown in Appendix A. During the heating season, the thermostat is set to 70°F. During the cooling season, the thermostat is set to 78°F.

4.3.6 Infiltration Modeling

The air flow through the exterior shell and zones of a building is based upon pressure differentials caused by exterior wind pressure, mechanical ventilation, and air density variations due to air temperature differences called buoyancy or stack effects. These air flows can contribute a significant amount to the annual energy load of a building due to air leakage in or out of the conditioned zones called infiltration or exfiltration, respectively. According to Sherman and Dickerhoff (1998), infiltration can account for a quarter to a half of the heating energy load on a house. The standard unit used to measure infiltration is the air change per hour (ACH) or how many times the zone volume is replaced with outside air every hour.

Many studies on typical homes in North America indicate that infiltration rates can vary by as much as a factor of ten, from new tight constructions with about an average of 0.2 ACH to old loose constructs with an air exchange rate of 2.0 ACH. Two studies in particular show this infiltration rate deviation in North American homes. Figure 4.22 shows an average seasonal infiltration rate of 0.5 ACH for 312 homes located throughout the U.S. and Canada which mostly represent new, energy-efficient homes (Grimsrud et al. 1982). Also, Figure 4.22 below shows an average seasonal infiltration rate of 0.9 ACH for 266 homes located in 16 cities throughout the

U.S. that mainly represent older, low-income homes (Grot and Clark 1979). More recent studies have shown that average air infiltration rates for new constructions have achieved 0.25 ACH (Parker et al. 1990).

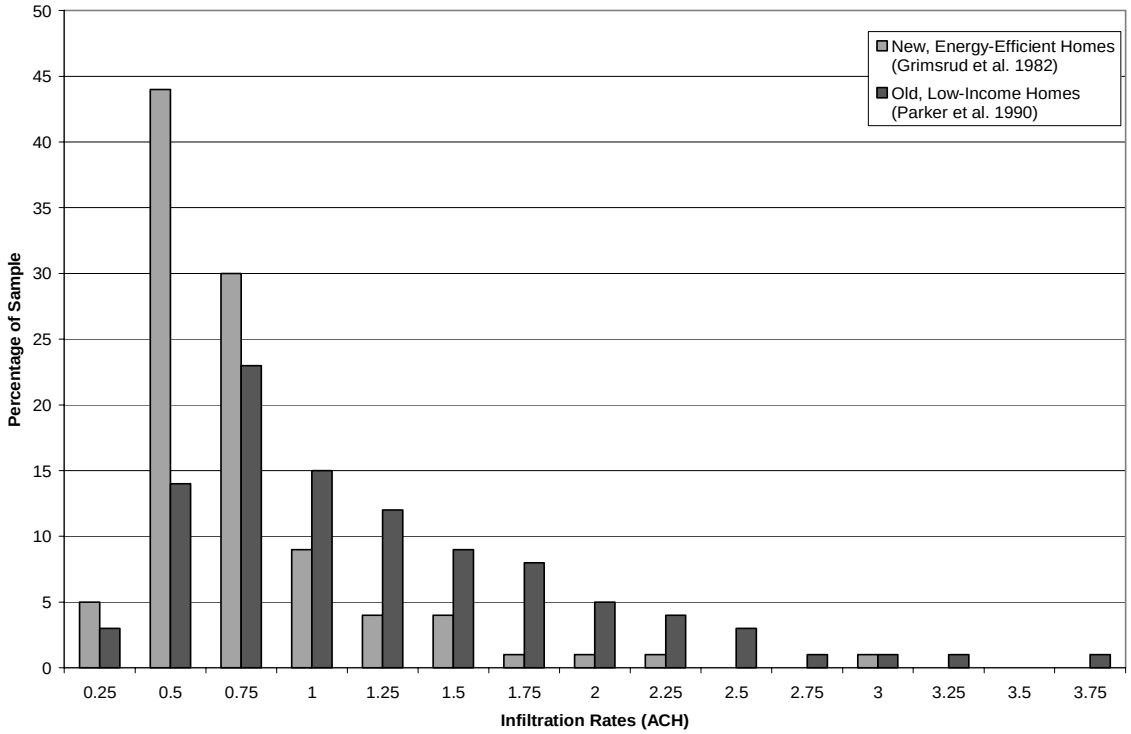

Figure 4.22. Air infiltration rates for energy efficient versus older homes

Since newer residential constructions are becoming considerably more airtight than previous generations, countries such as Canada are mandating mechanical ventilation in new residences to sustain proper air quality. Since no such mandates exist within the US, the majority of residences within the United States meet the minimum ventilation requirements for humans solely based upon infiltration. ASHRAE Standard 62 (ASHRAE 1999) provides that proper indoor air quality is maintained if the minimum outside air ventilation per person is 15 cfm regardless of the space type. This minimum air flow rate is based upon maintaining the indoor carbon dioxide concentration to 0.07% to that of the outdoor air assuming a typical carbon dioxide generation rate per occupant. To assure the proper indoor air quality for three occupants, a minimum annual average infiltration rate of 0.35 ACH has to be maintained for the conditioned zones.

In 1988, ASHRAE Standard 119 (ASHRAE 1988) was created to specify an acceptable range of leakage areas distributed around the building envelope in order to reduce the infiltration load and improve the thermal performance of new homes. The standard is based on a parameter called the effective leakage area (ELA) introduced by Sherman and Grimsrud (1980) to represent the effective area of an orifice with a unity discharge coefficient (C_D) to produce the same amount of flow at a reference pressure as the summation of the flows through all the leaks in a building component. It should be stressed that the ELA is not the actual leakage area. ASHRAE Standard 119 normalizes the ELA to make it independent from the size or height of the house using (4.19:

$$ELA_N = 1000 \frac{ELA}{A} \left[\frac{H}{H_0} \right]^{0.3} \qquad \textbf{(4.19)}$$

where:

ELA_N is the normalized effective leakage area,

ELA is the total effective leakage area $(1.78\ ft^2)$,

A is the conditioned floor area $(2275\ ft^2)$,

H is the height of the prototypical house (9 ft),

and H_0 is the reference height of a one story home (8 ft).

Table 4.11 shows the minimum normalized ELA requirement specified in ASHRAE Standard 119 for each of the prototypical house locations.

Table 4.11. ASHRAE Standard 119 Leakage Class Classification (ASHRAE 1988)

Normalized ELA Range	Leakage Class	Minimum City Requirements
$ELA_N < 0.10$	A	
$0.10 \le ELA_N < 0.14$	B	
$0.14 \le ELA_N < 0.20$	C	
$0.20 \le ELA_N < 0.28$	D	
$0.28 \le ELA_N < 0.40$	E	Minneapolis
$0.40 \le ELA_N < 0.57$	F	Denver
$0.57 \le ELA_N < 0.80$	G	Atlanta, Miami, Washington DC
$0.80 \le ELA_N < 1.13$	H	Phoenix
$1.13 \le ELA_N < 1.60$	I	

The ELA_N is determined experimentally from a fan pressurization measurement during a blower door test. Developed first in Sweden (Sherman and Dickerhoff 1998), the blower-door test involves using a high powered fan tightly sealed in a doorway to pressurize or depressurize the conditioned spaces with all the windows and other doors closed. Measuring the pressure across the fan and the air flow rate can determine the ELA of the building envelope.

A study by the Energy Performance of Buildings Group at LBNL (Sherman and Dickerhoff 1998) determined the ELA_N distribution throughout the U.S. using a database comprised of 12,500 blower door test results for single-family, detached homes from around the country. Using the characteristics of each house in the database, the authors employed standard regression techniques to determine the leakage trends in terms of different demographics such as climate and date of construction. They concluded that the "trends in leakage are more dominated by construction quality, local practices, age distribution, etc. than they are by weather" (Sherman and Dickerhoff 1998). As a result, the ELA_N of the prototypical house was constant irregardless of the city location.

In a separate study (Sherman and Matson 1998), the same ELA_N database in Sherman and Dickerhoff (1998) was used to calculate the infiltration rate of homes throughout the country applying the Sherman and Grimsrud (1980) method which calculates the air flow through the conditioned spaces using the ELA_N and local weather conditions (inside/outside temperature difference and wind speeds). The authors found that only 15% of the homes in the U.S. meet the ELA_N range requirements specified in ASHRAE Standard 119. Yet all but 5% of the homes met the proper ventilation rate of 0.35 ACH specified in ASHRAE Standard 62.

The leakage area of the prototypical house was distributed across a variety of building components such as windows, plumbing, and electrical wall penetrations. The leakage area of each component was taken from a leakage area database developed by ASHRAE Research Project RP-438 (Colliver et al. 1992). Unfortunately, since the majority of the building construction occurs on site where quality control is difficult, the ELA for a specific building component can range dramatically. Therefore, the database developed by Colliver is an

extensive table cataloging the minimum, maximum, and best estimate[4] of the ELA for a wide variety of typical residential building components measured with a discharge coefficient of 1.0 and reference pressure difference of 0.016 in of water. The values in ASHRAE Research Project RP-438 present the results in terms of the ELA per component, per unit surface area, or per unit length of crack/sash, whichever is appropriate.

The total ELA for each surface is calculated by summing all the individual ELAs that affected that particular surface. For example, the total living zone ceiling ELA was based upon the ELA of: 1225 ft^2 of exposed ceiling surface, one installed ceiling fan, two surface mounted lights, one installed kitchen fan with an open damper, and 240 linear feet of ceiling-wall joints. Table 4.12 shows the calculation of the total living zone ceiling ELA based upon the best estimate ELA for the different aforementioned components associated with the ceiling.

Table 4.12. Example calculation of the total ELA for the living zone ceiling surface

	Area/Length/ Number	**Best Estimate ELA**	**Total ELA**
General Ceiling	1225 ft^2	0.026 in^2/ft^2	31.85 in^2
House Fan	1 unit	3.1 in^2 each	3.1 in^2
Surface Mounted Lights	2 units	0.13 in^2 each	0.26 in^2
Tight Gasket Kitchen Fan	1 unit	6.2 in^2 each	6.2 in^2
Ceiling-Wall Joints	240 ft	0.07 in^2/ft	16.80 in^2
		Total =	58.21 in^2

Following the procedure just described, a crack comprised of several relevant component ELA's from the ASHRAE Research Project RP-438 is specified for every surface surrounding the conditioned zones in the prototypical house. Therefore, the air leakage through each wall, ceiling, closed window/door, or floor is represented by a crack designed to replicate the effective leakage area (ELA) of that building component. The most energy efficient components, such as weatherstripped windows or caulked wall/floor joints, were chosen so that the resultant ELA was representative of a tightly constructed home. To establish a base case, the typical wood frame construction surrounded by rigid sheathing is used along with the ELA for each component. The

[4] Best estimate refers to the ELA value repeated the most from the various references that published ELAs for specific building components

maximum ELA of every component was used since it provided a resultant ELA_N of 1.21 which was close to the average 1.72 ELA_N from the leakage area database in Sherman and Dickerhoff (1998) and which was determined to be an acceptable leakage area to provide the proper outside air ventilation according to ASHRAE Standard 62. As a result, none of the conditioning equipment in the prototypical house brought in outside air and the pressure differentials were induced only by wind and stack effects.

Since there are no mechanical ventilation effects on pressure differentials, a program called COMIS (Conjunction of Multizone Infiltration Specialists) (Feustel and Raynor-Hoosen 1990) was used in conjunction with the EnergyPlus program to model the air flow through the prototypical residence. During each EnergyPlus time step, the COMIS program uses the zone/outside air temperatures and the wind pressure distribution to calculate the air flows throughout the prototypical house. Figure 4.23 below shows a simple air flow network constructed for a three zone building. The air flow pattern shown is just one that would be possible if all the windows and doors in the building were open. The air flow through the interzonal doors depends solely on the air temperature differences between the zones. The air flow through the exterior windows depends on the inside/outside temperature differences (stack effects) and the wind pressure distribution on the exterior building surface represented by the external nodes. Appendix C contains a list of what COMIS can and can not model.

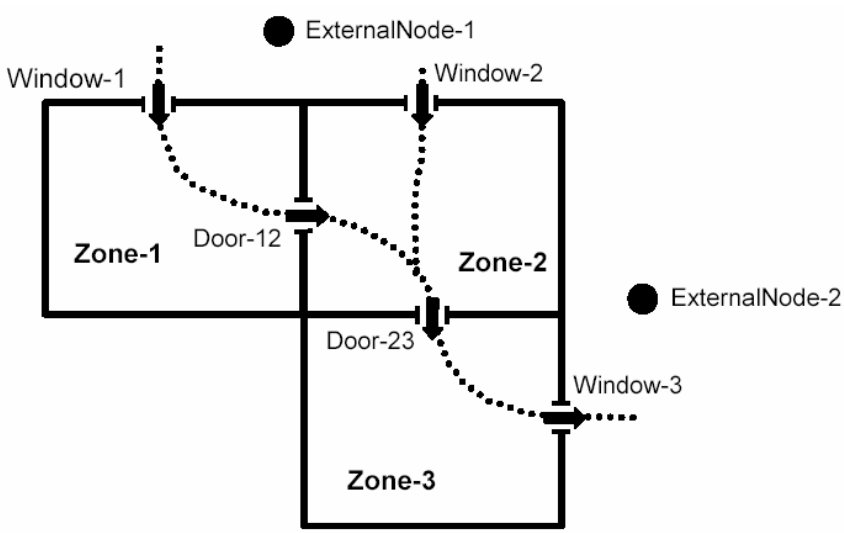

Figure 4.23. Example air flow network through three zone building

The information needed by the COMIS program to construct an air flow network throughout the prototypical house includes the zone volumes and the location/orientation of surface cracks through which air flows. Therefore, in addition to the building construction description already provided in the EnergyPlus program, several parameters describing the behavior of the air flow through the cracks distributed throughout the prototypical house are required. Essentially these parameters can be separated into two categories. The first category includes all the criteria necessary to calculate the wind pressure loads on each external surface of the prototypical house. The second category involves specifying the parameters that describe the ELA for each of the prototypical construction surfaces. The detailed information for both these categories is summarized in Appendix C.

The base case was further validated by comparing its ELA distribution among the prototypical house surfaces to that stipulated in the 2001 ASHRAE Handbook Fundamentals. Table 4.13 compares the typical ranges and best estimates of the percentage of the total ELA that is comprised within the basic components of a residential envelope versus those for the base case. Although the base case ELA distribution deviates in several instances from the best estimate, it always is within the typical range. Therefore, the base case ELA distribution was considered legitimate as a reference to evaluate infiltration effects on the residential energy load.

Table 4.13. Comparison of the typical ELA distribution to the base case ELA (ASHRAE 2001a)

	Typical Range	Best Estimate	Base Case
Walls	18-50%	35%	34%
Ceiling	3-30%	18%	27%
Floor	3-28%	15%	21%
Windows/Doors	6-22%	15%	7%
Fireplace	0-30%	12%	5%
Exhaust Vents	2-12%	5%	5%

The next step for the base case was to specify the leakage characteristics for the basement, garage, and attic zones. Much like the conditioned envelope, the basement ELA was determined using components from ASHRAE Research Project RP-438. Consequently, the maximum ELA for lightweight unfinished concrete block was used for the one foot of basement wall that was above ground which maintained the infiltration of the basement around 0.1 ACH. According to

ASHRAE Standard 62, the garage infiltration has a required a minimum ventilation of 100 cfm of outside air per vehicle in the garage (ASHRAE 1999). Therefore, the ELA for the garage zone was distributed equally among all of the exterior facing surfaces and manipulated for each prototypical house location such that an annual average infiltration rate of 1.0 to 2.0 ACH was maintained. The infiltration of the garage zone was ambiguously specified because the operation of the garage door exposes the garage zone to the outside conditions to such a degree that modeling its infiltration with extreme precision would be impossible. For the attic zone, ASHRAE Standard 90.2, Energy-Efficient Design of Low-Rise Residential Buildings, states that for an attic with a vapor retarder, there must be a free ventilation area of at least 1.0 ft^2 for each 300 ft^2 of attic floor area. Although this ventilation area corresponds to no pressure difference across the roof, 8.33 ft^2 of open area was equally distributed as the ELA to all the exterior facing surfaces of the attic. The resultant infiltration of the attic maintained roughly 12 ACH for all six prototypical house locations. The annual average infiltration rates for the basement, garage, and attic zones were considered acceptable based upon the criteria defined by Lau (2004).

There is considerable controversy regarding whether concrete wall systems reduce the ELA such that the infiltration load is significantly reduced. Of the few experimental analyses conducted on this topic, the results obtained have contradicted each other. According to a study by the NAHB Research Center (1999) in which three small single-family homes, two ICF constructions and one wood frame construction, were built in Maryland, both blower door tests and tracer gas tests[5] showed an average infiltration rate of approximately 0.5 ACH. Yet a study conducted by an infrared camera company for seven ICF houses in the southwestern U.S., determined a leakage area ranging from 0.27 to 0.60 ELA_N (Thompson 1995). As a result, in addition to the base leakage area distribution, the prototypical house was modeled with reduced leakage areas for each concrete wall system in each location to evaluate the energy savings associated with the wall systems and a reduced infiltration rate.

[5] Tracer gas method measures the infiltration rate for a home based upon the exponential decay of a measurable gas concentration in the conditioned room over a period of time

ASHRAE Research Project RP-438 did incorporate the leakage area per square foot of wall surface for precast and cast-in-place concrete wall systems.

Table **4.14** shows the ELA per square foot of wall surface for the wall system construction of sheathing, precast concrete, and cast-in-place concrete. As shown in

Table **4.14**, except for the best estimate, the ELA for the concrete walls are larger then that for the sheathing wall construction. Changing the wall system ELA from sheathing to the respective ELA for each concrete wall system has a negligible effect on the final leakage area distribution such that the ELA_N changes by 0.02 at the most. Therefore, the air leakage through the clear wall comprises an extremely small portion of the total leakage area.

Table 4.14. Effective leakage area (ELA) for the different wall construction systems (ASHRAE Research Project RP-438)

	Minimum	**Best Estimate**	**Maximum**
	(in^2/ft^2)	(in^2/ft^2)	(in^2/ft^2)
Sheathing	0.005	0.0042	0.006
Precast Panel	0.017	0.0004	0.024
Cast-in-Place	0.007	0.0007	0.026

Therefore, a leakage area distribution for the low leakage concrete wall systems was modeled using the identical components to define the ELA distribution as the base case except instead of using the maximum ELAs, the best estimate ELAs were used. For future reference, the different leakage area distributions are refered to as the maximum ELA and best estimate ELA. The best estimate ELA resulted in a normalized leakage area of $0.76\ ELA_N$ which met all of ASHRAE Standard 119 requirements except Denver and Minneapolis. For the basement, garage, and attic leakage areas, the natural ventilation requirements described in subsection 4.3.7 and wind input information in Appendix D remained the same regardless of the wall system evaluated.

In summary, the prototypical house was modeled with two different leakage areas to analyze the effect of reduced infiltration on energy savings. The concrete wall systems were modeled with the maximum ELA base case to focus solely on the energy savings associated with the wall thermal performance independent of any varying infiltration rates. The best estimate ELA

represented the energy savings that were possible with the concrete wall systems if they are inherently tighter in construction.

4.3.7 Ventilation

Converse to infiltration, the pressure differentials across the building envelope can be used to drive natural ventilation and reduce the cooling energy consumption of a building. The COMIS program was used to calculate the air flow through the prototypical house when the windows were open. Unlike the surface cracks which were limited to unidirectional flow, COMIS could also simulate the open windows with bidirectional flow depending on the stack effects and wind conditions. COMIS required several parameters to denote the conditions under which the fenestration could be opened, the degree to which they could be opened, and the discharge coefficient describing the air flow through the openings. When natural ventilation was allowed to occur, only the windows in the conditioned zones were allowed to be opened. The doors were always kept closed except for the door between the living and bedroom zones which was always open to provide significant thermal interaction between these zones.

Natural ventilation was only allowed in either zone from April 1 to September 30, if the enthalpy of the indoor air was greater than the outdoor enthalpy, and the outdoor temperature was above 23°C. To prevent large temperature swings within the conditioned zones, the degree to which the windows were open was modulated based upon the relative indoor/outdoor environmental conditions. Figure 4.24 shows how the window opening was varied from half of its glazing area ($7.75\ ft^2$) to $1/200^{th}$ of its glazing area ($0.0775\,ft^2$) as the inside enthalpy to outside enthalpy difference went from 0 to 0.043 Btu/lb respectively. Specifications of this range led to ventilation rates between 8 and 10 ACH similar to those specified in other studies (Huang et al 1987; US DOE 2003). For simplification, the discharge coefficient for all the windows was set to 1.0. The ventilation conditions just described were specified for all house locations and construction types.

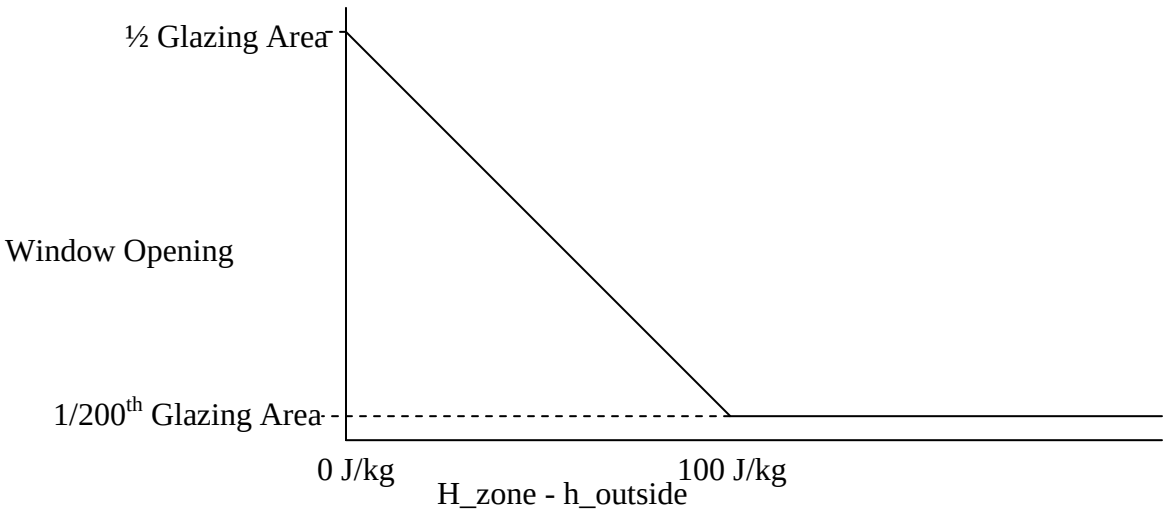

Figure 4.24. Modulation of the window opening due to zone versus outside enthalpy difference

4.3.8 Conditioning Equipment

Three distinct conditioning systems were modeled for the prototypical house. The first was an ideal system used to simplify the component load analysis and obtain a general estimate about the performance requirements for actual conditioning equipment. The second system modeled was the most popular heating/cooling combination in the US, the gas furnace and central air conditioner (CAC). The third system modeled was the second most popular heating and cooling system in the US, the air-to-air heat pump.

In order to evaluate the efficiency of different wall systems without the influence of the complicated conditioning and distribution equipment performance, the prototypical residence was conditioned by a theoretical system which EnergyPlus calls “purchased air”, that is 100% efficient at delivering heated and cooled air and that has an infinite capacity. More specifically, the purchased air system provides the required sensible heating or cooling load to meet the instantaneous load at all times. With the purchased air feature, the required air flow rate to meet the load is calculated based upon the difference between the set-point temperatures and predefined heating or cooling coil exiting air temperatures of 105°F or 55°F respectively. The latent load met by the purchased air system is based upon the calculated air flow rate and the

predefined heating or cooling coil exiting air humidity ratios of 0.005 or 0.0094 $\frac{lb\,water}{lb\,air}$, respectively. The resultant simulation, although ideal, provides the component loads that comprise the entire prototypical house load if the thermal comfort in the zones is maintained exactly and gives a general estimate of how the actual conditioning equipment should behave.

The performance of the furnace and CAC systems were modeled with the average shipment weighted efficiencies according to the 2003 Energy Databook (US DOE 2002). The efficiency of a gas furnace is measured on an Annual Fuel Utilization Efficiency (AFUE) corresponding to the percentage of the annual output of heat to the annual energy input. Although the AFUE is an annual efficiency calculation, the efficiency of a gas furnace fluctuates very little over any period of time. Consequently, the gas furnace efficiency was modeled at a constant 88% according to the 2003 Energy Databook (US DOE 2002). The remaining 12% of the energy input into the furnace was assumed to be lost to the outside air thereby having no effect on the house internal load. The furnace was assumed to be completely sealed such that it had no effect on the leakage area of the basement and all the combustion air was provided from the outside such that the conditioned zones were not depressurized.

The CAC performance was modeled with a 10 kBtu/kWhr Seasonal Energy Efficiency Ratio (SEER), 3.51 COP equivalent, which represents the ratio of the total seasonal cooling requirement (kBtu) to the total seasonal energy used (kWhr). The SEER provides a convenient single number rating to characterize the system performance. However, the actual EER (or COP) varies depending on the indoor/outdoor temperature and humidity conditions and partial loading. The equations used to describe the CAC performance based upon these variables are shown in Appendix D.

Similar to the CAC, the heating and cooling operations of the air-to-air heat pump were modeled using specified information at rated conditions and curve fitted equations to simulate the performance variation due to deviations from rated and full load conditions. The SEER of the air-to-air heat pump cooling mode was set identical to that of the CAC, 10 kBtu/kWhr. The equations used to model the cooling performance of the air-to-air heat pump due to variations

from full load and rated conditions were almost identical to those used to model the CAC system as shown in Appendix D.

The efficiency of the air-to-air heat pump heating mode was modeled with a Heating Seasonal Performance Factor (HSPF) that corresponded to commercially available heat pumps with a 10 kBtu/kWhr cooling mode SEER. Consequently, the heat pump HSPF was set to 7.0, 2.05 COP equivalent. Several other constraints were defined for the heating mode of the air-to-air heat pump to realistically define its annual behavior. To prevent frost accumulation on the outdoor coil, the heat pump was run in reverse 3.5 minutes each hour of the day whether or not frost had accumulated. This defrost mode was disabled if the outdoor air dry-bulb temperature was above 41°F. To assist the heating operation of the heat pump, especially when the outdoor air dry-bulb temperature was low, a supplemental 100% efficient electric resistive heater was modeled within the system. Its total capacity and maximum supply air temperature were different for each prototypical house location. The supplemental heater was only allowed to function when the outdoor air dry-bulb temperature was lower than 50°F. The compressor was not allowed to run when the outdoor air dry-bulb temperature was below 10°F. Finally, while the outdoor air dry-bulb temperature was below 50°F, a 200 W crankcase heater was on while the compressor was not running. The equations used to describe the heating and defrost mode of the air-to-air heat pump performance based upon the indoor/outdoor air conditions and partial loading are shown in Appendix D.

The conditioning equipment was sized using an integrated "autosizing" feature within EnergyPlus based upon the heat balance method described in Chapter 29 of the 2001 ASHRAE Fundamentals Handbook (ASHRAE 2001a). The logic behind the autosizing feature is summarized in the following four steps.

1. The autosizing module determines the necessary heating or cooling loads to maintain the thermal zone conditions at the thermostat set-point for two design days representing the worst winter and summer weather conditions respectively. These design days were previously defined from the TMY2 data sets for each prototypical house location.
2. The autosizing module then calculates the required air flow rates to meet these loads based upon the difference between the thermostat set-points and predefined exiting air

conditions from the conditioning equipment. These air conditions, which included dry-bulb temperature and humidity ratio, vary depending on the type of HVAC system modeled.

3. The maximum heating or cooling flow rates from each of the thermal zones are summed to determine the maximum flow rate through the HVAC system. Note that since both the heating and cooling operations of the conditioning equipment use the same air distribution system, the maximum flow rate was the same for both modes of operation.
4. The maximum flow rate is used along with the difference between the current zone conditions and predefined heating or cooling coil exiting air conditions to calculate the maximum capacities. These predefined air conditions, referring to the dry-bulb temperature and humidity ratio, were identical to those used in step 2. These capacities were specified as the conditioning equipment sizes at rated conditions.

Except for the furnace, the predefined exiting coil air conditions for the different conditioning equipment were based upon the test conditions used for commercial rating standards, especially the Air-Conditioning and Refrigeration Institute (ARI) rating procedures (ARI 2004). The exiting coil air conditions for the CAC and cooling mode of the heat pump were 55°F dry bulb and 0.0094 $\frac{lb\ water}{lb\ air}$ humidity ratio. The exiting coil air conditions for the heating mode of the heat pump were 105°F and 0.005 $\frac{lb\ water}{lb\ air}$ humidity ratio.

Unfortunately, there was not an option in EnergyPlus to have a two speed fan, one speed for each of the furnace/CAC system operation modes. Consequently, for cold and temperate climates, the CAC system capacity was sized based on the larger air flow rate for the furnace system to meet the large heating loads. Realistically, the FCAC system should be sized based upon the CAC system. Thus the furnace temperature was taken to be sufficiently high to allow the heating loads to be met with the airflow rate selected for cooling. The exiting coil humidity ratio condition for the furnace was set to 0.005 $\frac{lb\ water}{lb\ air}$ humidity ratio.

For the cooling operations, the calculated Sensible Heat Ratio (SHR), sensible capacity divided by total capacity, depended mainly on the air flow rate to capacity ratio. The larger the flow rate to capacity ratio, the larger the SHR. The typical SHR range for residential cooling systems is 0.72-0.78. All the autosizing done during this study maintained the SHR within this range.

Instead of using standard commercially available equipment sizes at rated flow rates, the autosizing feature was used as a way to normalize the effects of the conditioning equipment. Except for the furnace system, the performance of the conditioning equipment varies due to part load conditions. Therefore, the annual efficiency of a system depends on how large its capacity is compared to the hourly loads required by the zones. Thus, overly sized equipment results in a system that operates at much less than full load for most of the time and therefore inefficiently. The autosizing feature was used along with the assumption that equipment of any desired size is available. This approach standardizes the sizing procedure for the system studies so that the results are not affected by an arbitrary choice of system size.

4.3.9 Distribution System

The air circulation between the heating/cooling equipment and the conditioned zones was maintained by a blow through fan for the gas furnace/CAC system and a draw through fan for the air-to-air heat pump system. Shown in Figure 4.25 below, the blow through fan was located between the exit ducts of the conditioned zones and the entrance to the heating or cooling coil of the furnace or CAC respectively. For the heat pump, the draw through fan was located between the exits of the heating/cooling coils and the supplemental heater as shown in Figure 4.26.

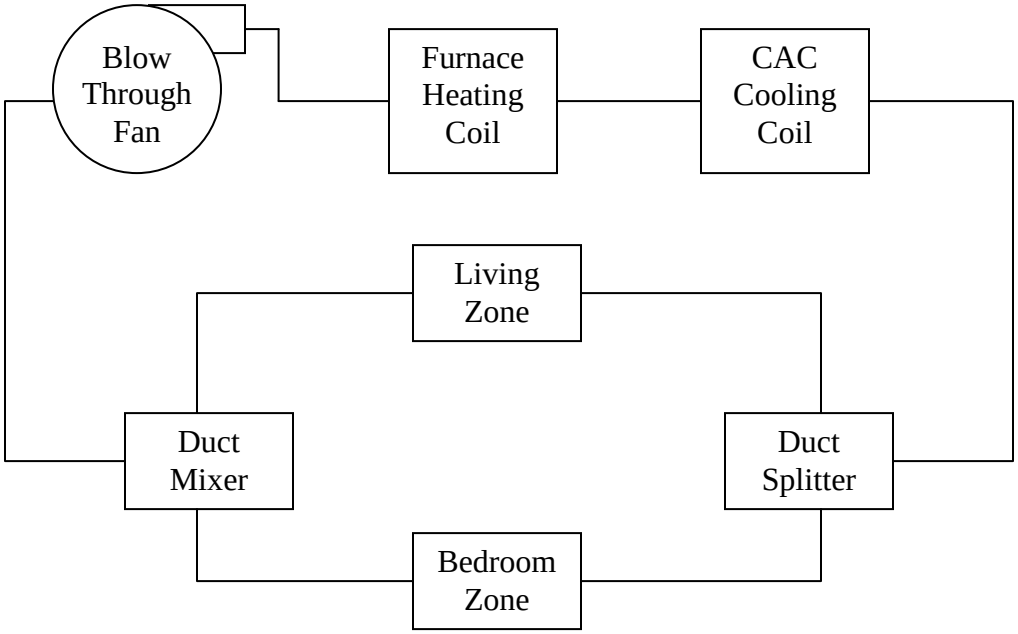

Figure 4.25. Furnace/CAC air circulation schematic

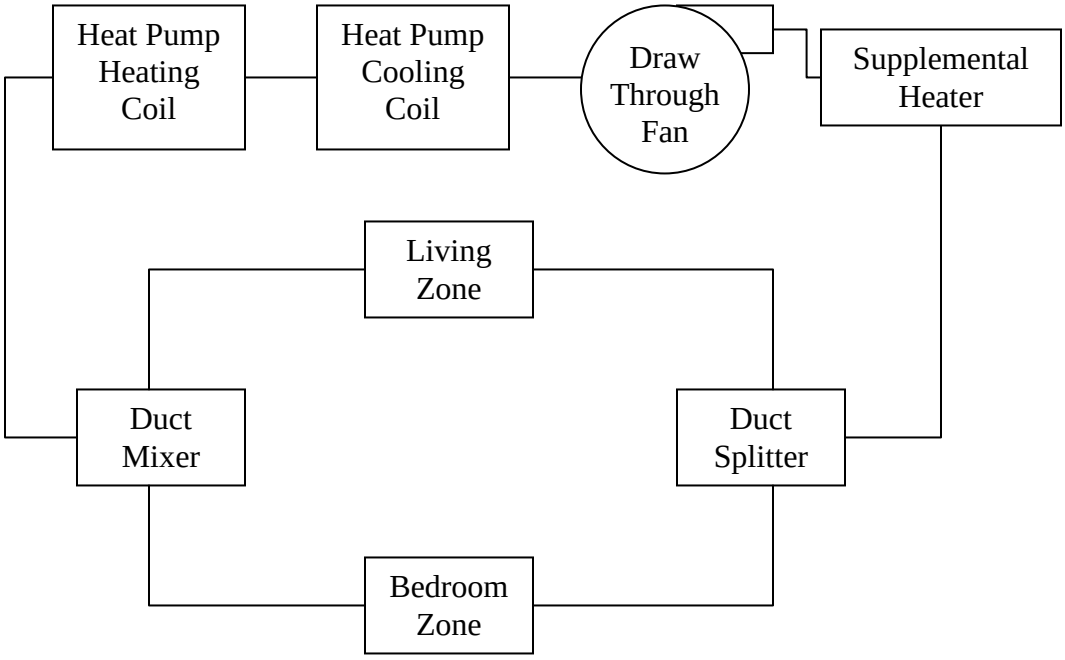

Figure 4.26. Heat pump air circulation schematic

The fan performance and control was identical for both systems. The fan supplied a constant air volumetric flow rate and was jointly controlled with the heating/cooling system such that they both cycled on and off together. The fan maintained a total efficiency of 45% with a pressure rise of 225 Pa at full flow and standard conditions (20°C and 101325 Pa) (Alspach 2004). The motor efficiency was 90% with the lost energy added as sensible heat to the air passing through the fan.

As summarized in section 3.4.6, duct efficiency can have a significant effect on the efficiency of the overall conditioning system. Based upon a test method for evaluating residential thermal distribution system efficiency (ASHRAE 2004), the duct losses due to conduction and air leakage can reduce the energy provided to the circulated air by the heating and cooling coils by 15 % to 25 %. Duct performance is so significant that the ASHRAE Standard 90.2 (ASHRAE 2001b) building envelope requirements are based upon duct location. Since the prototypical house is representative of relatively modern energy efficient construction, the ducts were located inside the conditioned space such that their losses were negligible. Consequently, the duct system was modeled in EnergyPlus with a 100% efficiency.

4.3.10 Foundation Heat Transfer

As the thermal performance of the building envelope increases, the heat loss to the slab-on-grade or basement foundations has become much more influential on the overall home energy consumption. Consequently, a wide variety of experimental and numerical studies have recently focused on foundation heat transfer and resulted in a multitude of methods to improve its simulation. Unfortunately, earth contact heat transfer is extremely complicated to model especially with the varying and often unknown ground thermal properties. Moisture, the main variable affecting the soil properties, depends on immediate site conditions such as rainfall, drainage, groundwater level, and freezing/thawing cycles (Walton 1987). For example, Sobotka et al (1994) showed that varying the soil thermal conductivity and capacitance even within a limited range could change the predicted annual heat loss of a basement using several simulation methods anywhere from 10 to 212 percent. Taking into consideration the large sensitivity of simulation techniques and rapid variability of ground thermal properties at specific site locations,

several foundation modeling methods were used to determine a reasonable heat flux range and final simulation approach to calculate the prototypical house foundation heat transfer.

Figure 4.28 below shows the six elements involved in affecting the basement heat transfer: outside environment, basement wall above grade, basement wall/floor below grade, ground surface adjacent to the basement, lower thermal boundary at a constant temperature equal to the mean ground temperature, and the conducting soil between the basement, ground surface, and lower thermal boundary (Mitalas 1983). Research conducted by Latta and Boileau (Latta 1969) showed that the isotherms near the basement wall and floor are not parallel lines but rather radial lines such that the heat flows in a concentric circle pattern as shown in Figure 4.29. Therefore, heat transfer across the foundation wall and floor boundary can not be approximated by one dimensional conduction. As insulation is applied to the basement wall or floor, the heat flow paths flatten out and the isotherms approach horizontal lines, parallel to the ground surface.

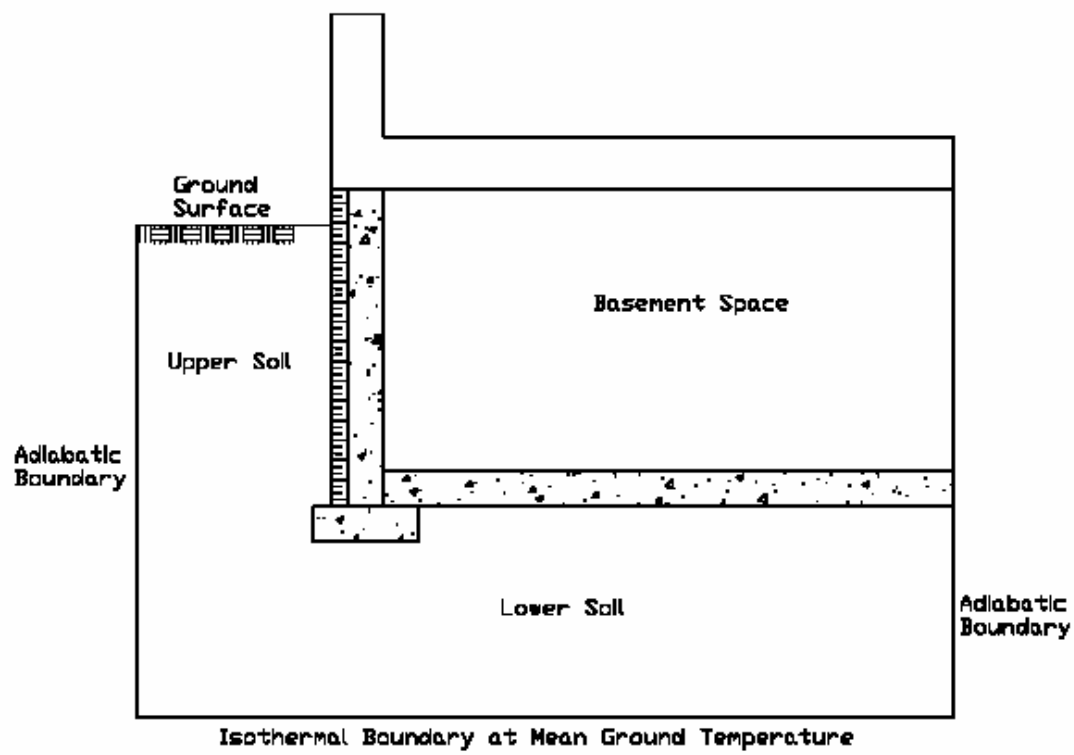

Figure 4.27. Physical basement foundation model

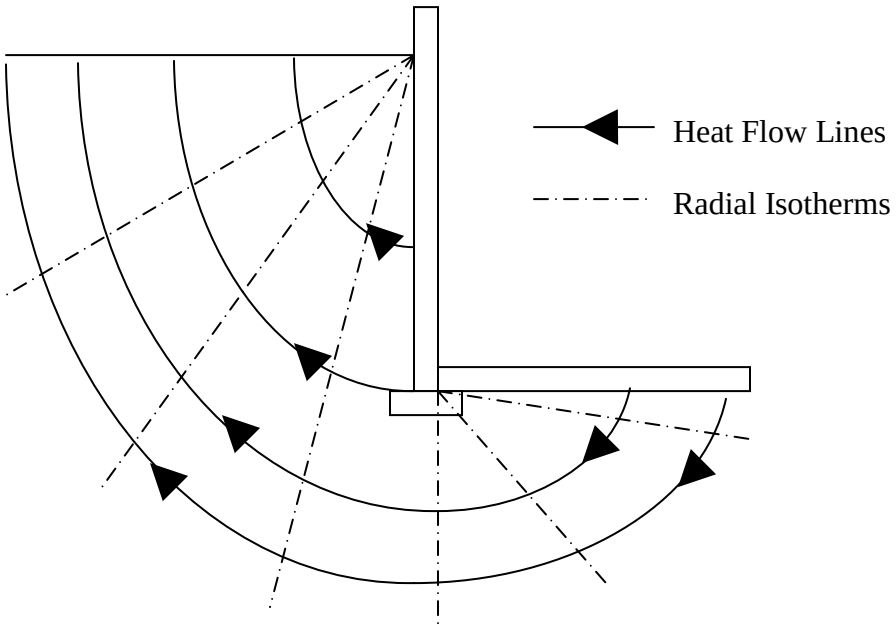

Figure 4.28. Typical heat flow pattern from a basement foundation (ASHRAE 2001a)

Before any foundation modeling was done, the configuration of the basement wall and floor was established. Since the entire goal of this study was to evaluate different wall construction technologies incorporated with various HVAC systems, the foundation construction was set constant. As a result, the effects of the foundation heat transfer behavior were independent of each wall technology and HVAC system combination evaluated. According to a study by Peony (Peony et al. 1979) and reinforced by a couple more recent analyses (Mitalas 1983; Huang et al 1988), the same amount of insulation applied to the exterior of a basement wall can increase the foundation performance by 10-20% compared to internal insulation. Therefore, the prototypical basement wall was simulated with rigid polystyrene spanning the entire exterior wall composed of four inch thick light weight concrete block. Since the ground temperatures under the basement floor are higher than outside the basement walls (ASHRAE 2001a), no insulation was applied to the prototypical basement floor. Figure 4.27 above, shows a two dimensional schematic of the prototypical basement configuration. Along with the above grade wall constructions, the amount of basement wall insulation was set to the minimum specified by ASHRAE 90.2 (ASHRAE 2001b) for each prototypical house location as shown in Table 4.15.

Despite the large amount of insulation supplied by the surrounding soil and insulation levels shown in Table 4.15 and the internal heat gains from the hot water heater, cloths washer, and cloths dryer the basement temperature was not maintained within 10°F of the living and bedroom zones for the entire year. Therefore, the basement was considered an unconditioned space according to ASHRAE Fundamentals (ASHRAE 2001a).

Table 4.15. Minimum basement wall insulation determined by ASHRAE 90.2

Cities	**Basement Wall R-Value** $\left(\frac{hr \quad ft^2 \quad F}{Btu}\right)$
Minneapolis	16
Denver	16
Washington D.C.	16
Atlanta	6
Phoenix	5
Miami	0.3

The standard approach for the calculation of foundation heat transfer determines the overall heat transfer coefficient between the wall to outside air and floor to outside air based upon experimental results (Latta 1969). Figure 4.29 below shows the thermal resistance for increasing depths below grade for uninsulated and insulated concrete walls. This plot shows that the increase in resistance above the uninsulated condition at each foot below grade is exactly equal to the R-value of the insulation added to the basement wall. Averaging across all seven feet of the basement depth, the uninsulated basement wall resistance would be $8.48\frac{\text{hr} \quad \text{ft}^2 \quad \text{F}}{\text{Btu}}$ plus any additional insulation applied to the wall. Similarly, an unisulated basement floor with the geometry of that in the prototypical house would have a resistance of $47.62\frac{\text{hr} \quad \text{ft}^2 \quad \text{F}}{\text{Btu}}$. This approach, termed ASHRAE Fundamentals method for future reference, then applies these R-values to determine the heat flux at the walls and floor based upon the difference between the outside and basement temperatures.

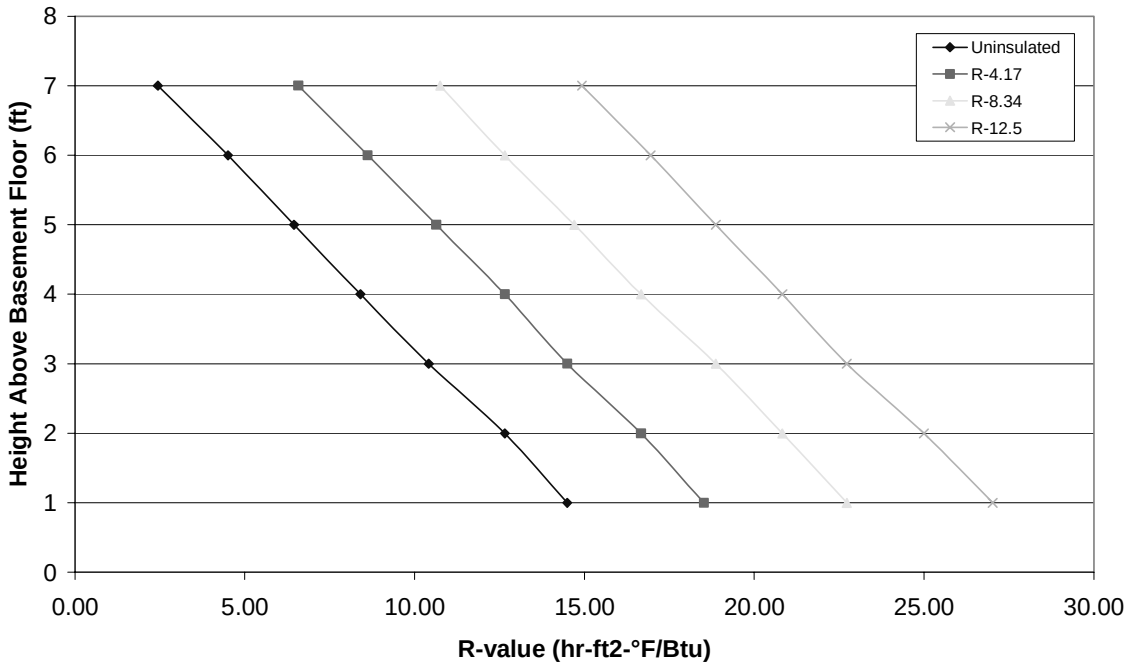

Figure 4.29. Basement wall R-value for each foot below grade (Latta 1969)

Although based upon experimental data, the ASHRAE Fundamentals method ignores several important aspects that play an important role in the overall basement heat transfer. Two of the most important are the two and three dimensional conduction effects that occur mainly at the basement corners and the large thermal capacitance of the ground which causes an appreciable thermal lag. One of the more recent studies on foundation heat transfer (Sobotka et al 1994) compared the ASHRAE Fundamentals method and two more complicated simulation techniques to experimentally measured heat transfer data for three different basement configurations. All three basements had a rectangular shape and were 8 feet in height in which 7 feet was below grade. The largest basement, roughly 30 feet by 28 feet, had a layer of rigid insulated applied across the entire wall interior. The other two basements which were identically in size, roughly 20 feet by 17 feet, had slightly different insulation configurations on the wall exterior. One method used a two dimensional transient finite element program which incorporates the effects of the wall to floor connection. The third and most complicated was the Mitilas method which

can be classified as a steady state method with a time-varying component. This technique uses precalculated factors based upon previous two and three dimensional numerical heat transfer programs fine-tuned from measurements. The result of the study showed that for all three basement comparisons, the Mitilas method was the most accurate followed by the FEM and then the ASHRAE Fundamental method. Table 4.16 gives the percentage error of each method when compared to the measured total basement heat loss for all three basements modeled. Other authors that conducted a similar comparison noticed the same trends; the ASHRAE Fundamentals Method consistently predicts significantly lower foundation heat transfer and the Mitalas method always predicts a slightly larger heat loss than that by the 2D FEM due strictly to increased basement floor heat loss.

Table 4.16. Percentage difference from the measurement basement annual heat loss (Sobotka et al 1994)

	Mitalas	**2D FEM**	**ASHRAE Fund.**
Basement A	4	24	42
Basement B	8	19	-
Basement C	14	32	-

Since the Mitilas method was the most accurate in the study by Sobotka et al (1994), it was combined with a simple optimization program to determine the foundation floor and wall heat loss for the prototypical home. First, the Mitilas method was used to calculate the monthly heat transfer for the basement walls and floor for each of the prototypical house climates using the different exterior wall insulation values listed in Table 4.15. Knowing the monthly heat flux distribution over an entire year and the annual average ground temperature from the TMY2 data, an optimization program was implemented to determine the overall wall and floor resistivities and the exterior foundation wall and floor ground temperatures. Appendix K reviews the components of the optimization routine and the objective function. These wall and floor resistance values and ground temperatures were then input into the EnergyPlus program. As a test, the basement was conditioned to the same setpoint temperature used in the Mitilas method and the resulting monthly heat transfer distribution for the year matched that calculated by the Mitilas method for each of the prototypical house locations. Once the foundation heat fluxes were verified, the basement was reset to an unconditioned zone. The benefit of this approach

was that it used the Mitilas method as a basis which has proved its accuracy and did not comprise the physics of the process by setting the resistivity values or ground temperatures to unreasonable values.

4.4 Construction Cost Information

Since wood frame systems are the standard construction technology, a large amount of economic information exists about it thereby making cost estimates, which are based on a wide variety of actual home constructions, reliable. Therefore, the RSMeans Residential Cost Data was used to calculate the construction cost for the Conventional and Energy Efficient Wood Frame systems (RSMeans 2003). Appendix G shows the estimates made to determine the framing and insulation costs per wall square foot of R13, 2x4 at 16" o.c. and R19, 2x6 at 16" o.c. wall systems. Appendix G also shows the steps to calculate the interior and exterior finishing costs to determine the entire cost per square foot of exterior wall surface.

Since the Sandwich PCP and ICF wall systems are not as widely applied as wood framing, the cost estimates were not based upon RSMeans data. The ICF system cost was determined using the ICF analysis conducted by the NAHB Research Center (2001). This study calculates the ICF cost per square foot using a detailed time-and-motion investigation of the three homes actually constructed for the analysis. Table 4.17 details the cost per square foot of wall surface area for the ICF system, conventional wood frame system, and the difference between the two. On average, the ICF construction costs $3 to $5 more per square foot of net wall area[6] than conventional wood frame systems, varying within this range depending on the size and complexity of the home. This figure correlates well to the ICF construction cost market average according to the ICF Association (ICFA 2004).

[6] Net wall area is the gross wall area minus the window and door openings

Table 4.17. ICF versus conventional wood frame costs per square foot of wall surface (NAHB Research Center 2001)

	ICF	Conventional Wood Frame	Difference
Economy One-story/1,008 sq ft $90,000-$100,000	$4.56	$2.37	$2.19
Custom One-Story/two-story mix/3,894 sq ft	$5.95	$2.25	$3.70
Custom One-story/2,775 sq ft	$6.65	$2.14	$4.51
Average	$5.72	$2.25	$3.47

The Sandwich PCP system cost information was based upon personal communication with the company that first designed the commercially available Sandwich PCP system, DOW T-Mass, and the company that currently distributes it (Bergtold 2004; Long 2004). The price of PCP systems is very regionally dependent since transportation costs outside of a 200 mile radius from a distributor can add anywhere from $2 to $5 per square foot of wall surface depending on the distance to be traveled. To prevent a complicated transportation cost assessment, the cost of the Sandwich PCP systems will be based on the price within 200 miles of a distributor. For a one inch stucco exterior, Sandwich PCP systems range from $11 to $13 per square foot of wall surface. For a brick or stone veneer, that range shifts to $13 to $15 per square foot. Note that these figures also include the interior gypsum finish.

Table 4.18 compares the Conventional Wood Frame, Energy Efficient Wood Frame, ICF, and Sandwich PCP systems cost per square foot including the interior and exterior finishes and labor costs. These figures were then multiplied by the $1290\,\mathrm{ft}^2$ total prototypical house wall surface area to obtain the exterior wall construction costs. Then the additional Energy Efficient Wood Frame, ICF, and Sandwich PCP construction costs over the Conventional Wood Frame cost were calculated. These cost differentials were finally multiplied by scaling factors obtained from RSMeans (2003) to account for different labor costs throughout the US. These scaling factors for the prototypical locations are shown in **Table 4.19** below.

Table 4.18. Wall systems price per square foot of wall surface

Wall System		Price per sq ft of wall surface
Conventional Wood Frame		$8.43
Energy Efficient Wood Frame		$8.91
ICF	Lower Bound	$11.43
	Upper Bound	$13.43
Sandwich PCP	Lower Bound	$11.00
	Middle	$13.00
	Upper Bound	$15.00

Table 4.19. Scaling factors (RSMeans 2003)

	Scaling Factors
Minneapolis	1.17
Denver	1
Washington	0.94
Atlanta	0.85
Phoenix	0.91
Miami	0.83

CHAPTER 5: RESULTS

The following sections summarize the results from the various analyses specified in the chapter 4 sections. Section 5.1 validates the prototypical house EnergyPlus model heating and cooling energy consumption versus survey data obtained from the 1997 REC survey (EIA 1999) and simulation data from a LBNL study (Huang et al 1999) conducted to evaluate typical residential energy component loads. Section 5.2 reviews the results from the detailed building envelope analysis described in section 4.2 for each of the wall systems described in section 4.1 including the whole wall R-value and the parameters that affect the dynamic performance of the wall system. Section 5.3 shows the prototypical house energy savings associated with the various wall systems compared to the base case Conventional Wood Frame system due to increased insulation and thermal mass benefits and independent of the HVAC system performance. Section 5.4 shows the energy savings of the HVAC systems associated with each of the wall systems with respect to the base case Conventional Wood Frame system. Section 5.5 evaluates the effect of reduced infiltration on the HVAC energy savings shown in Section 5.4. Section 5.6 uses the energy savings calculated in sections 5.4 and 5.5 to compare the reduction in annual energy expenses to the increase in the annual mortgage payment due to the increased construction cost associated with each wall system over the base case. Note that the unit system convention used in the ensuing sections follows the standard used in the building construction industry; Imperial (English) Units for everything except electric energy consumption which is defined in kilowatt-hours (kW-hr).

5.1 Prototypical Home EnergyPlus Model Validation

Despite the extensive amount of research conducted on residential energy performance, very limited experimental results exist that contain specific end-use energy consumption data with which to compare the results from this study. Instead, data has been derived from the 1997 REC survey (EIA 1999), giving broad estimates of residential energy consumption based upon limited demographics such as residence type, location, and vintage. Conversely, there is an extremely large amount of specific residential energy consumption information calculated from other studies using various energy modeling software. One, recently conducted in 1999 by the Building Technologies Department of LBNL, uses DOE2.1E to calculate the conditioning loads of a typical US home very similar to the prototypical house in many different US climates,

including the six locations analyzed for this study (Huang et al 1999). Consequently, both references were used to validate the EnergyPlus model of the prototypical home; the REC survey to provide a general comparison to actual HVAC energy consumption data which is covered in subsection 5.1.1 and the LBNL reference to provide specific heating and cooling component loads which is reviewed in subsection 5.1.2. For both comparisons, the Conventional Wood Frame system was used in the EnergyPlus prototypical house model since it is the standard construction method. Note that the whole wall approach was incorporated in this model, the validity of which is covered in Section 5.2.

5.1.1 Comparison of Prototypical House Energy Consumption to REC Survey

Although the latest REC survey was conducted in 2001, the data from the 1997 REC survey was used since a program called Electronic RECS (Electronic RECS 2001) was currently available for use with the 1997 data. Developed by the Pacific Northwest Laboratory for the U.S. DOE, Electronic RECS organizes all the information from the 1997 REC survey into an electronic database which can than be parsed into tables and graphs according to different specifications. To obtain the heating and cooling energy consumption with which to validate the EnergyPlus prototypical house model, Electronic RECS was used to select homes that were located in the vicinity of the prototypical house locations such that they experienced similar heating degree days (HDDs) and cooling degree days (CDDs). Figure 5.1 shows the geographic categories into which the surveyed homes could be parsed using Electronic RECS. First, the U.S. was broken into the four different census regions. Than each region was further discretized into zones experiencing distinct ranges of HDDs and CDDs. Figure 5.1 also indicates the location of each of the prototypical house locations.

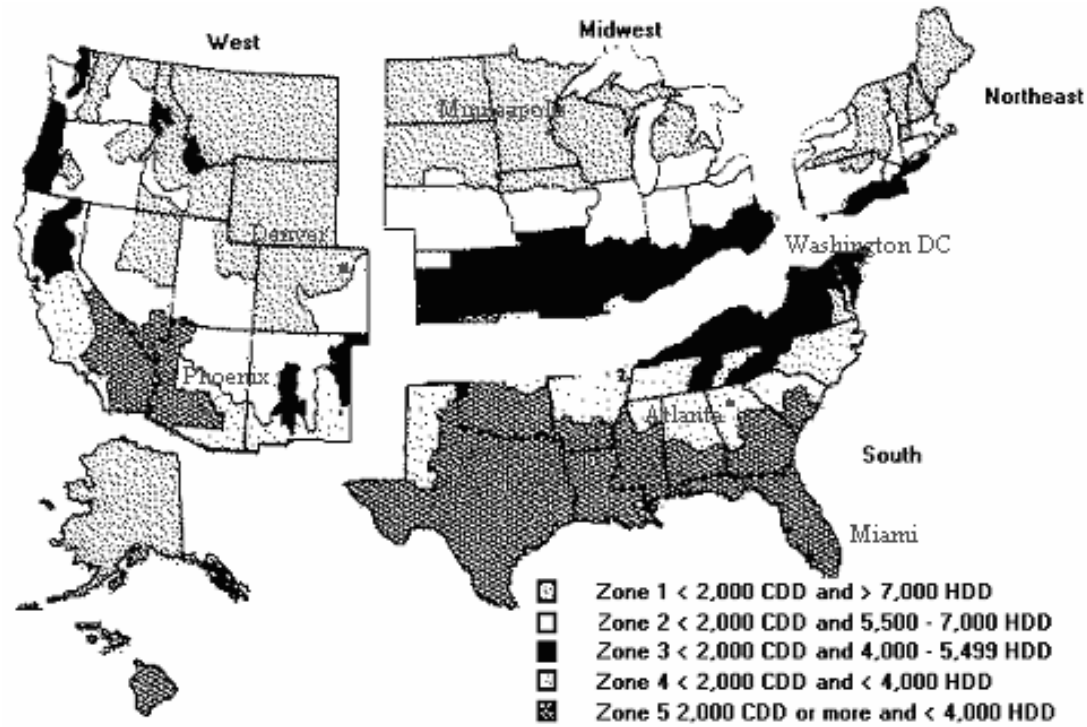

Figure 5.1. Highest resolution capability of the Electronic RECS program

The 1997 REC survey data was further filtered to focus on adequate to well insulated detached, single family homes built after 1980 that were conditioned by a gas central furnace and CAC system. Note that the EnergyPlus prototypical house model was only validated with the furnace/CAC system because the 1997 REC survey had an extremely limited set of heat pump energy consumption data. Comparing only the residential energy consumption with the furnace/CAC system was considered acceptable to provide the necessary validation of the EnergyPlus prototypical house model against actual HVAC energy consumption information. Finally, as long as the remaining sample size for each location contained more than 10 survey homes[7], homes with furnaces and/or CAC systems built before 1991 were eliminated. This way older conditioning systems with low efficiencies were ignored. Table 5.1 shows the resultant sample size, sample average HDDs and CDDs, and whether the additional constraint regarding the furnace/CAC system manufacturing date was incorporated for all six cities. Table 5.1 also includes the HDDs and CDDs of the TMY2 weather data used in the EnergyPlus simulation for

[7] Ten homes is the minimum sample size to ensure a statistically valid sample according to the Energy Information Administration (EIA)

verification against the average sample HDDs and CDDs from the 1997 REC survey data. Finally, the sample average gas heating and electric cooling consumption per square foot of conditioned space was multiplied by 2275 ft^2 to obtain a general expectation of the heating and cooling energy consumption of the prototypical house.

Table 5.1. General information concerning the resultant 1997 REC survey (EIA 1999) samples

		Minneapolis	**Denver**	**Washington**	**Atlanta**	**Phoenix**	**Miami**
Sample Size		12	10	11	10	10	11
HDD65	Sample Avg.	7747	5946	4480	2990	1316	1308
	TMY2	7736	6082	5031	3152	1130	115
CDD65	Sample Avg	560	479	1146	1432	2856	3067
	TMY2	709	634	1096	1751	4104	4264
Furnace Built after 1993		X	X		X		X
CAC Built after 1993		X	X				X

To illustrate how different operating conditions can significantly affect heating and cooling energy consumption, the prototypical house was modeled at a normal setpoint temperature deadband of 70°F to 78°F and a reduced setpoint temperature deadband of 72°F to 76°F. The proceeding heating and cooling energy consumption figures include the results from both simulations to demonstrate how shifting the setpoint temperature deadband even by 4°F can have a large effect on the annual energy consumption. In addition, Figure 5.1 shows how vague the breakdown of the REC survey data by location can be which results in samples that incorporate homes which experience climate conditions considerably different than those of the prototypical house locations. As a result, the annual heating and cooling energy consumption data can be skewed. Thus considering the many possible operating conditions such as the setpoint temperature deadband and the climate variations within regions, the comparison to the REC survey should be understood as a general validation of trends rather than an attempt to match data exactly.

Figure 5.2 compares the 1997 REC survey (EIA 1999) sample annual furnace energy consumption to that calculated from the EnergyPlus model for each prototypical house location. Of the six cities, the Atlanta, Phoenix, and Miami REC survey results are significantly larger than both the normal and reduced deadband prototypical house results. The discrepancy in

Miami can be simply explained by the larger REC sample average HDD of 1308 Fahrenheit degree days compared to the TMY2 HDD of 115 Fahrenheit degree days used in the EnergyPlus model. The main explanation for the Atlanta and Phoenix discrepancy is that the heating load in the more temperate and hotter climes are building envelope features (ceiling and walls) which were modeled in the prototypical house with a higher thermal performance than what is characteristic in these climates. Warmer cities incur heating loads that are dominated by the wall and ceiling component loads (Huang et al 1999). Therefore, the heating load generated by these envelope components were much smaller in the EnergyPlus model than those in the 1997 REC survey samples because the prototypical house was modeled with considerably more insulation than the wide range of insulation used in the homes that comprise the 1997 REC survey samples. Conversely, the colder cities have a heating load dominated by infiltration. For example, the infiltration load represents 38% and 24% of the total heating load for the Minneapolis and Phoenix component loads respectively. As noted in subsection 4.3.6, the infiltration was modeled with a typical normalized leakage area (ELA_N) of 1.21 based upon many blower door test results compiled by Sherman and Dickerhoff (1998) and not with the ELA_N of 0.70 that would represent a tight, energy efficient construction. Therefore the heating loads of the colder cities which were dominated by the infiltration load correlated better with house samples from the REC survey. Had the prototypical house features such as the walls and ceiling not been modeled with a higher thermal performance than the standard practice in existing buildings, the Atlanta and Phoenix heating loads would correlate better to those of the 1997 REC survey data.

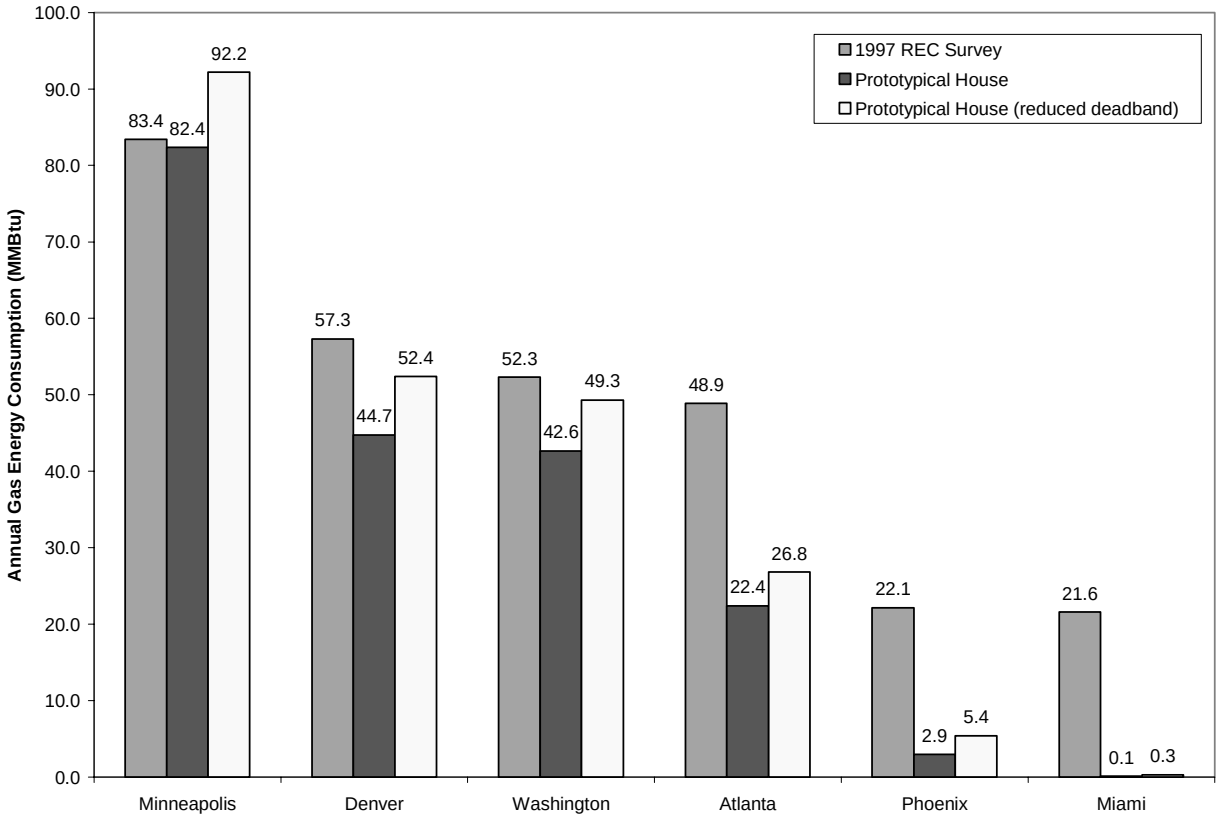

Figure 5.2. Annual gas heating energy consumption comparison

Figure 5.3 compares the 1997 REC survey sample average CAC energy consumption to that calculated from the EnergyPlus model for each prototypical house location. Unlike the gas heating energy consumption in Figure 5.2, the electric cooling energy consumption data correlates well for all the cities except Phoenix. The significantly larger energy consumption calculated by the Phoenix prototypical house is due to the fact Phoenix is such a dry climate that most homes use an evaporative cooler which requires much less electricity than the 10 SEER CAC used in the EnergyPlus model. Therefore, the discrepancy in the Phoenix electric cooling consumption can be disregarded.

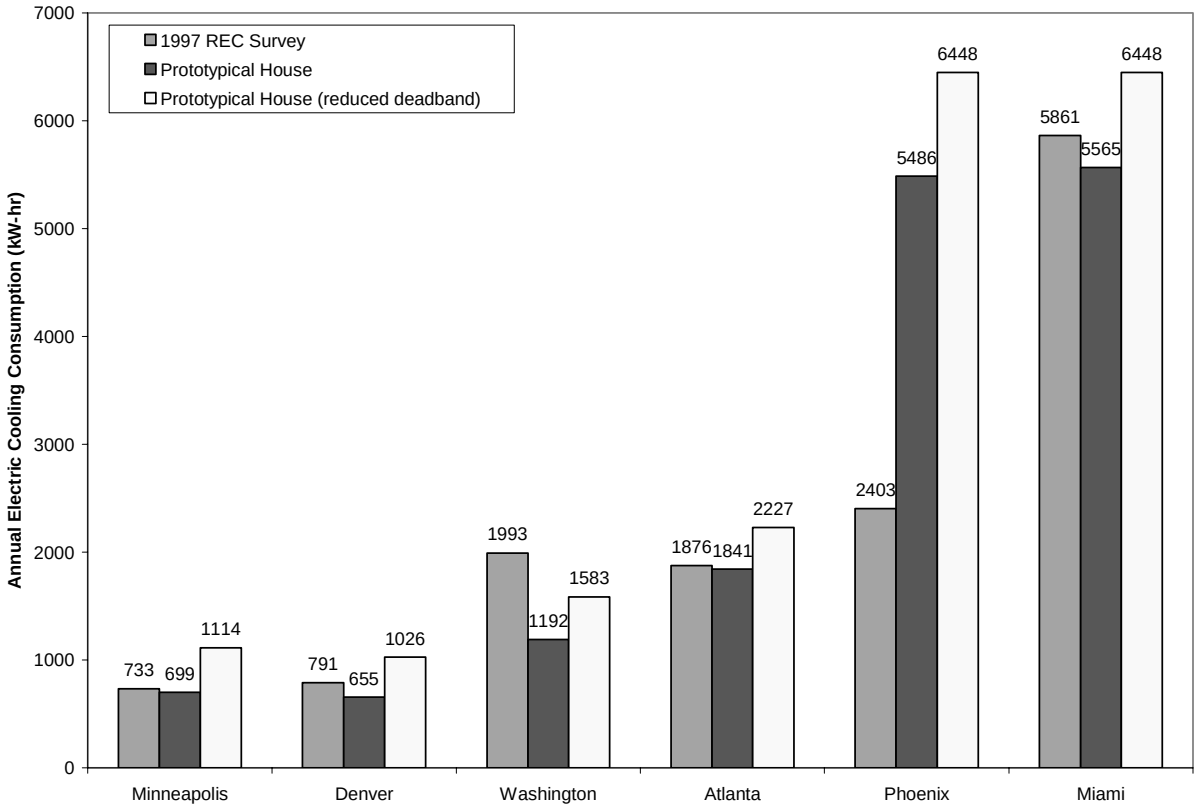

Figure 5.3. Annual electric cooling energy consumption comparison

The reason that the CAC energy consumption correlates better than the furnace energy consumption is because the cooling loads are dominated by the internal and solar heat gain components. For example, Figure 5.4 shows the influence of the various component loads on the total cooling load for Washington DC. The top half of the circle represents the sources that transfer heat into the conditioned space. The bottom half of the circle shows the sinks that remove heat from the conditioned space and the total annual cooling energy provided by the CAC to maintain the setpoint temperature. It is obvious that the solar and internal component loads dominate the cooling energy consumption. The diminuative effects of the other component loads minimizes the variability of the overall cooling load thereby making it much easier to match cooling energy consumption for the REC survey samples.

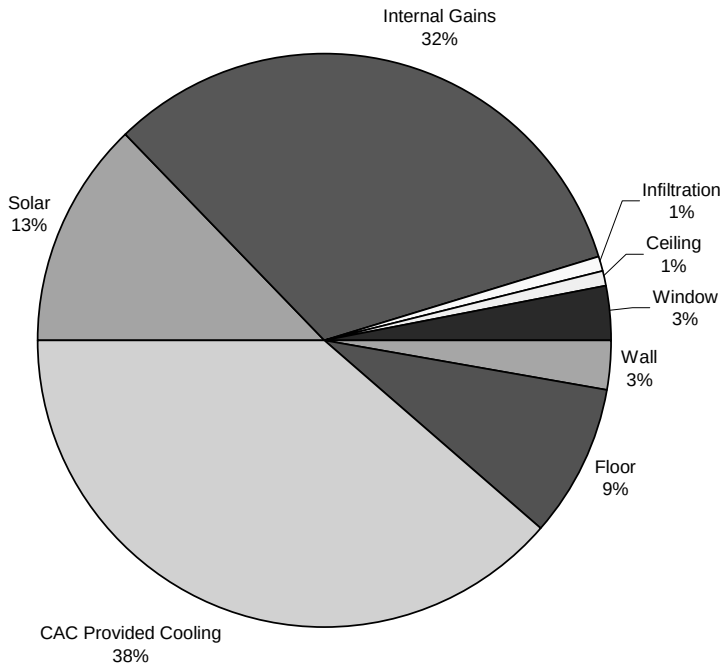

Figure 5.4. Washington DC component loads for the total annual cooling energy

Although the energy consumption results are not identical, especially for heating, the comparison with the 1997 REC survey data validated the range and general trends for the space conditioning energy consumptions in the various cities calculated from the EnergyPlus prototypical house model. Overall, the EnergyPlus prototypical house model was deemed acceptable as a context within which to study the effects of various wall construction types on residential energy use.

5.1.2 LBNL Reference Heating and Cooling Component Comparison

The LBNL report was the most recent publication of an on-going research effort by the US DOE and the Gas Research Institute to quantify the contributions of the various residential building components to the overall heating and cooling loads of a home (Huang et al 1999). These components consist of roofs, walls, floors, windows, infiltration, and internal heat gains. The results give the residential construction industry an indication of what components contribute the most to the overall conditioning loads so that methods can be investigated to reduce their impact.

The report uses the DOE2.1E program to model several different residential building prototypes developed from a previous study (Ritschard et al. 1992) to incorporate the various classifications and configurations of common US residences. The heating and cooling loads of the prototypes that represented the newest construction in each of the prototypical house locations were used to compare against the simulation results from the EnergyPlus model. Although several aspects of each prototype were different from the prototypical house such as the number of stories, those features that had a significant thermal impact were similar. Table 5.2 compares several of the important characteristics between the homes used from the LBNL study to those of the prototypical house used in the current work. Much like the REC survey comparison in subsection 5.1.1, the LBNL results were used to validate the range and trends of the various component loads of prototypical house in the various locations rather than matching the data exactly.

Table 5.2. Comparison of various features between the LBNL study prototype houses used and the prototypical house used for the current study

	Prototypical House for Current Study	**Prototype Houses for LBNL Study (Huang et al 1999)**		
	Conventional Wood Frame	Atlanta/ Washington/ Miami	Denver/ Phoenix	Minneapolis
Number of Stories	1	2	1	2
Conditioned Area (ft^2)	2275	2180	1660	2220
Window Area (ft^2)	267	270	179	262
Foundation	Basement	Basement	Slab-on-Grade	Basement
Wall Insulation $\left(\frac{hr\ ft^2\ F}{Btu}\right)$	13	11	13	19
Ceiling Insulation $\left(\frac{hr\ ft^2\ F}{Btu}\right)$	30	27	29	32
Floor Insulation $\left(\frac{hr\ ft^2\ F}{Btu}\right)$	20	19	0	0

Figure 5.5 compares the heating loads between the EnergyPlus model and the LBNL study for all six cities. Except for Minneapolis, all the heating loads are very similar. The same explanation for the discrepancy between the REC survey and prototypical house gas energy consumption applies to the heating load difference for Minneapolis in Figure 5.5. The LBNL study modeled the Minneapolis house with a tight construction such that the infiltration component represented ~35% of the heating load. The current study modeled the Minneapolis prototypical house with a looser construction resulting in the infiltration load accounting for ~52% of the heating load. Therefore, the different leakage areas resulted in the difference between the LBNL study and prototypical house Minneapolis heating load.

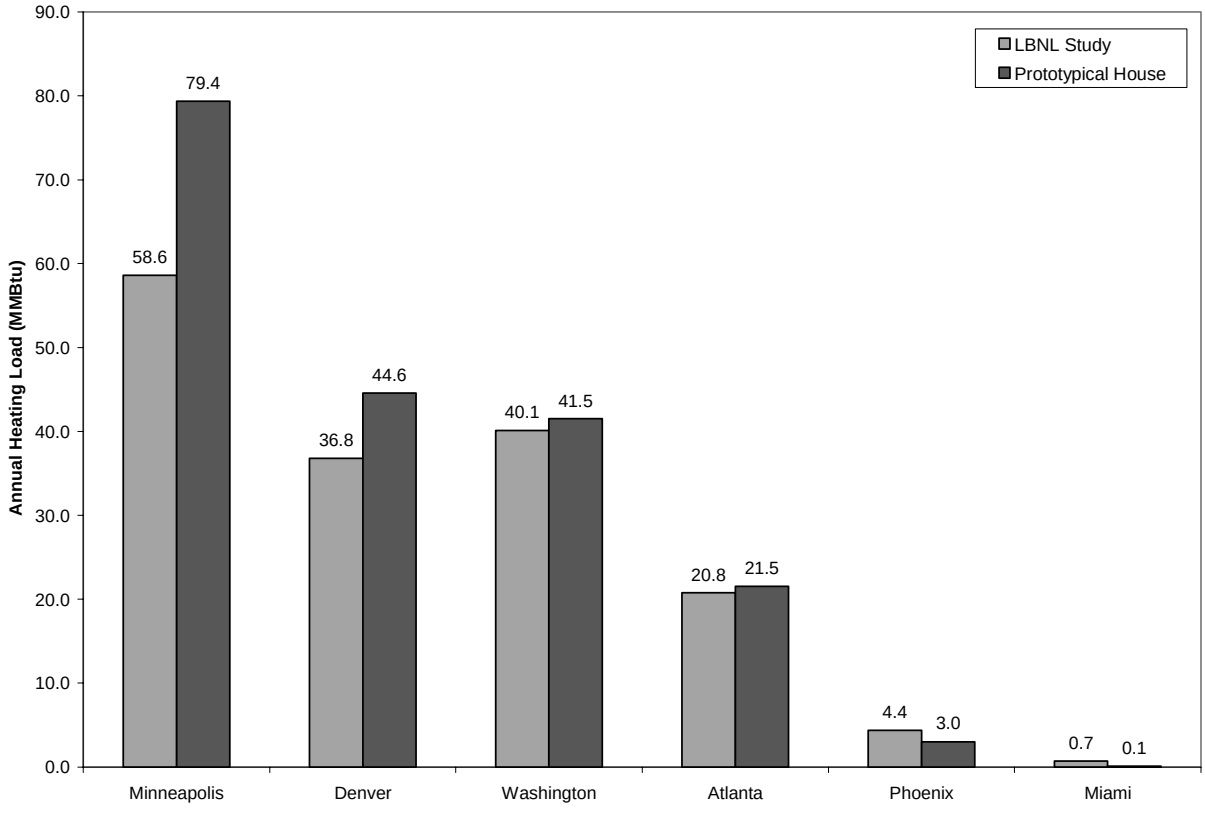

Figure 5.5. Heating load comparison of Huang et al (1997) vs prototypical house

Figure 5.6 compares the cooling loads between the EnergyPlus model and the LBNL study for each of the prototypical house locations. The Miami and Phoenix prototypical houses require considerably more cooling energy than their respective LBNL homes due to a combination of

floor and internal heat gain component load differences. The LBNL study applies the ASHRAE Fundamentals technique to model the heat loss through the foundation. Discussed in detail in subsection 4.3.10, this method has been shown by Sobotka et al (1994) to consistently over estimate the insulation level between the conditioned space and foundation. Therefore, for the cold and temperate climates where the ground temperature stays well below the outside air temperature during the cooling season, the LBNL study calculates a much smaller heat loss through the floor compared to the prototypical house. In the hot climates, the ground temperature is very close to the outside air temperature during the cooling season such that both the LBNL study and prototypical house calculate almost negligible heat loss through the floor. Already described in subsection 4.3.4, the internal heat gains specified in the LBNL study are significantly lower than those modeled in the prototypical house and even smaller than those used by the Building America house model (US DOE 2003). Therefore, during the cooling season, the prototypical house higher internal heat gains are offset by the larger floor heat losses in the cold and temperature climates such that the cooling energy loads are similar to those of the LBNL study. Yet the hot climates higher internal heat gains of the prototypical house are not offset by the small floor heat losses such that the cooling energy load is larger than for the LBNL study. Figure 5.7 shows the floor heat loss and internal heat gain for the LBNL study and the prototypical house model for Minneapolis and Miami to illustrate why the cooling energy load for the prototypical house is larger for the hot climates.

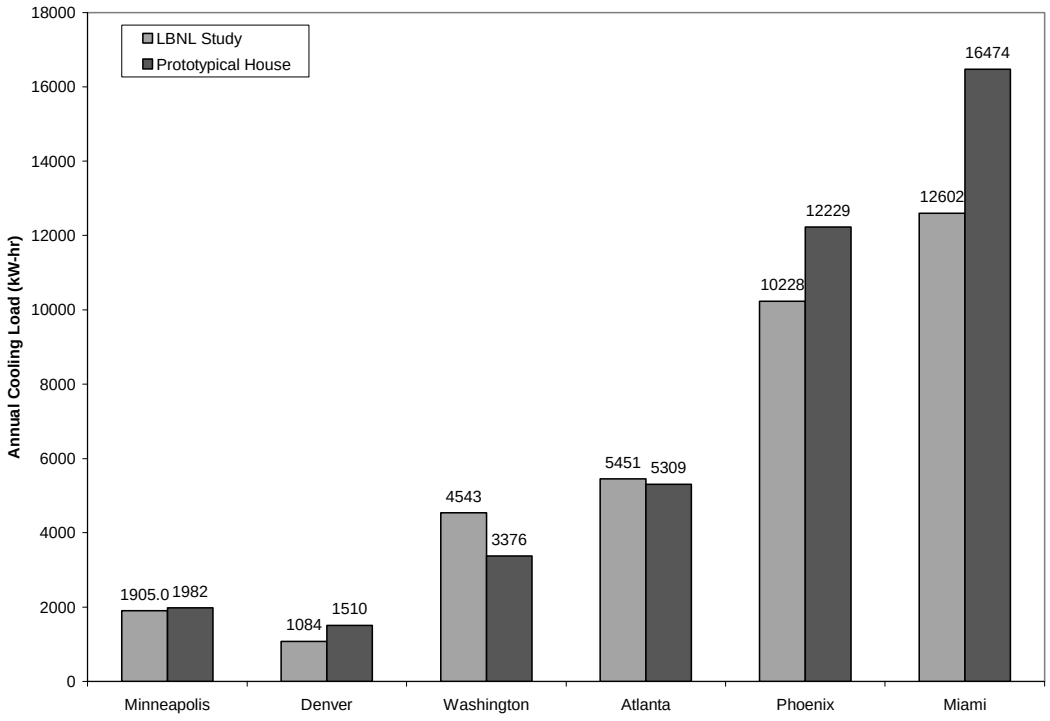

Figure 5.6. Cooling load comparison of Huang et al (1997) vs prototypical house

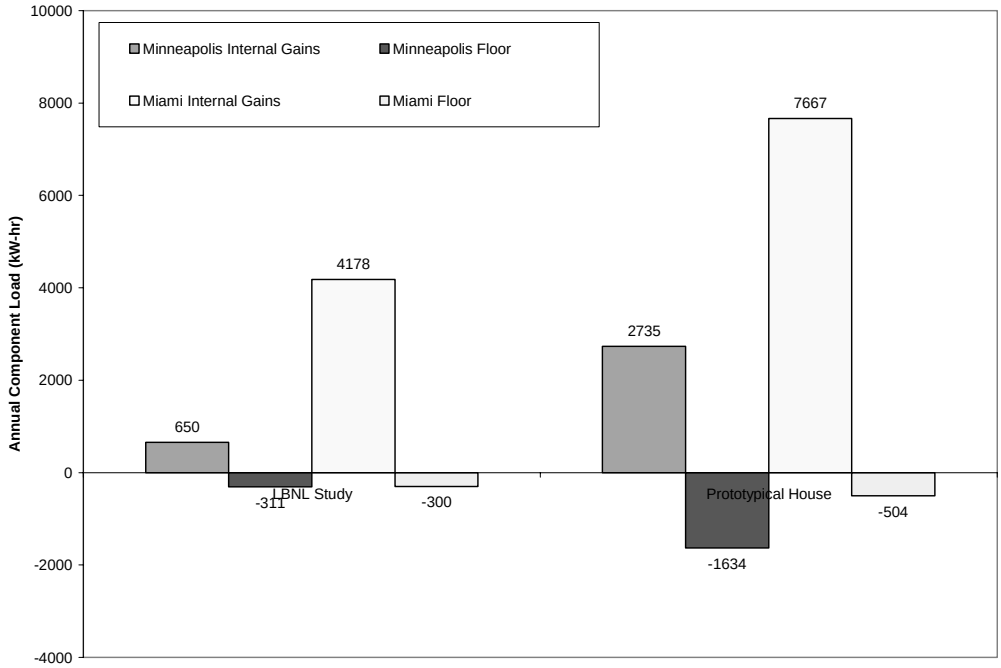

Figure 5.7. LBNL study and Prototypical house model internal heat gain/floor component loads for the Miami and Minneapolis locations

The prototypical house heating and cooling component loads resulted in trends similar to that shown by the LBNL study (Huang et al 1999). For the cities where the loads did not match, a reasonable difference in modeling approaches between the LBNL study and prototypical house model explained the discrepancy. Overall, the prototypical house model was determined to be acceptable to use as a context within which to study the effects of various wall construction on residential energy use.

5.2 Whole Wall Analysis

With the basis for comparison of the wall technologies established in the form of a validated prototypical house model, the next step was to apply the whole wall analysis approach to each wall system. The following section summarizes the results from the steady-state and dynamic performance investigations of the various wall systems. Subsections 5.1.1 through 5.1.4 review the relevant information for the different wall technologies and compare the resulting R-values to those published in several references calculated by means of computational modeling and/or hot box testing. The Conventional and Energy Efficient Wood Frame system R-values were compared to those published in Christian and Kosny (1996) whose clear wall R-values were validated against hot box test results in Christian (1993). The calculated ICF R-values were verified against the published R-values by a major producer of ICF systems (Reward Wall System 2004) and from results of another study evaluating the thermal performance of ICF versus wood frame systems (NAHB 1999). The Sandwich PCP system clear wall R-value was validated against the clear wall R-value of a similar Sandwich PCP configuration measured in a hot box test by Kosny et al (2001). Finally, subsection 5.1.5 compares several aspects between the different wall technologies.

5.2.1 Wood Framing

Figure 5.8 (a) and (b) shows the clear wall[8] schematic of the Conventional and Energy Efficient Wood Frame wall systems, respectively. The Conventional Wood Frame wall system was comprised of 2x4 wood studs at 16” on center. The Energy Efficient Wood Frame wall system was comprised of 2x6 wood studs at 16” on center. The clear wall R-value for the Conventional

[8] Clear wall refers to the area of the exterior wall surface free of wall details such as wall/floor connections

and Energy Efficient Wood Frame wall systems were approximately 15% less than the center-of-cavity[9] R-value. Yet the reduction from the center-of-cavity to whole wall R-value was different between the two systems; the R-value of Conventional Wood Frame construction was reduced 29% while the R-value of Energy Efficient Wood Frame construction was reduced 33%. This bigger decrease is explained by the larger susceptibility of higher thermal performance systems to detrimental thermal bridging. In other words, identical thermal bridging will cause a greater degradation in the whole envelope performance when the difference between the center-of-cavity and wall detail R-values is larger.

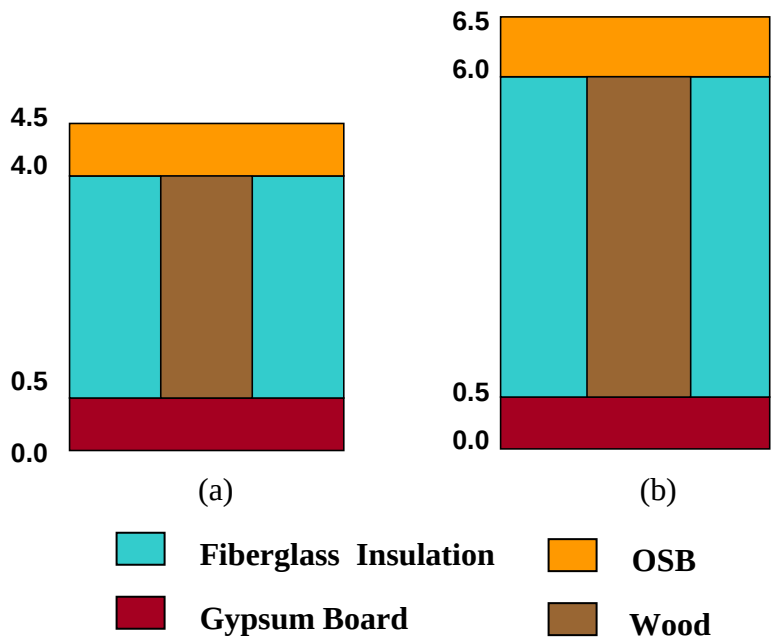

Figure 5.8 Wood frame wall construction schematics

(a) Conventional Wood Frame wall construction - 2x4 @ 16" o.c.

(b) Energy Efficient Wood Frame wall construction – 2x6 @ 16" o.c.

Table 5.3 (a) and (b) show the R-values calculated for the Conventional and Energy Efficient Wood Frame wall configurations, respectively, and how they compare to the values determined by Christian and Kosny (1996). It should be noted that Christian and Kosny (1996) used slightly

[9] Center-of-cavity refers to the area of the exterior wall that contains the most insulation and disregards any structural elements such as wood studs

different material heat transfer property values and a smaller version of the prototypical house than used in this study which affects the area weighted whole wall R-value. Despite these minor discrepancies, the R-values calculated for this study were consistent with those calculated by Kosny and Christian (1996).

Table 5.3. Center-of-Cavity, clear, and whole wall R-values $\left(\frac{\text{hr ft}^2\ \text{F}}{\text{Btu}}\right)$ for:

(a) Conventional Wood Frame construction (R-13)

	Center-of-Cavity	**Clear Wall**	**Whole Wall**
Calculated	13.5	11.4	9.5
Reference*	13.6	10.6	9.6

(b) Energy Efficient Wood Frame construction (R-19)

	Center-of-Cavity	**Clear Wall**	**Whole Wall**
Calculated	20.7	17.4	13.8
Reference*	20.7	16.0	13.7

*publication (Christian and Kosny 1996)

The plot of the different wall detail R-values in Figure 5.9 shows that, except for the clear wall, all the wall detail R-values are approximately $7.5\frac{\text{hr ft}^2\ \text{F}}{\text{Btu}}$ and $11\frac{\text{hr ft}^2\ \text{F}}{\text{Btu}}$ for the Conventional and Energy Efficient Wood Frame constructions, respectively. Yet Figure 5.10 indicates that each wall detail comprises a different percentage of the whole wall area and therefore affects the whole wall performance differently. Only one pie chart was necessary since the area of influence of each wall detail was the same for the Conventional and Energy Efficient Wood Frame systems.

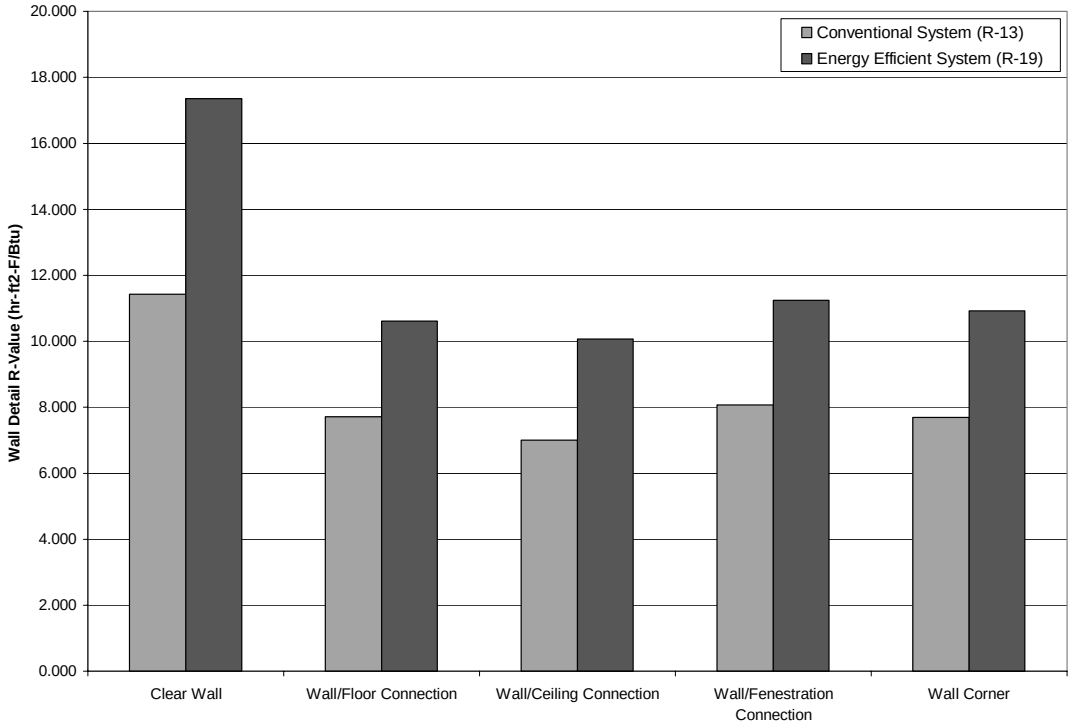

Figure 5.9. Wall Detail R-values $\left(\frac{\text{hr}\ \ \text{ft}^2\ \ \text{F}}{\text{Btu}}\right)$ of both wood frame constructions

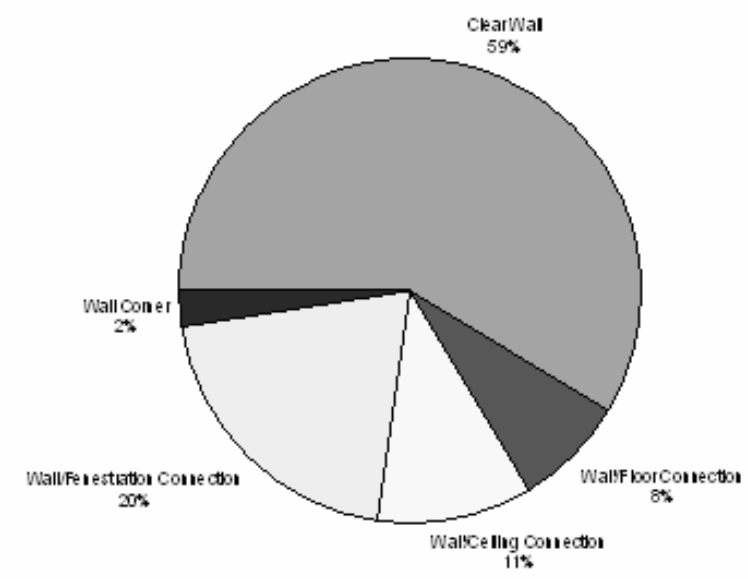

Figure 5.10. Area distribution of the wall details over the entire wall envelope surface for the Conventional and Energy Efficient Wood Frame systems

The wall "Detail Influence Factor" (DIF) described in Section 4.2.5. incorporates the resistivity and area of influence of a wall detail into one parameter. The DIF for the different wall details of the Conventional and Energy Efficient Wood Frame systems were essentially the same and are plotted in Figure 5.11. Figure 5.11 indicates that the heat transfer through the clear wall is approximately 50% of the heat transfer through the entire wall assembly. The remaining 50% of the heat transfer is attributable to the other wall details which, listed from most to least influential, are the: wall/fenestration connection, wall/ceiling connection, wall/floor connection, and wall corners. This sequence showing the relative importance of the various wall details is consistent with that determined in Kosny and Desjarlais (1994). Consequently, a design based upon the clear wall performance only accounts for roughly 50% of how the entire wall will perform. Ignoring the importance of wall details would result in building simulations that inaccurately predict the annual and maximum heating and cooling loads of the building.

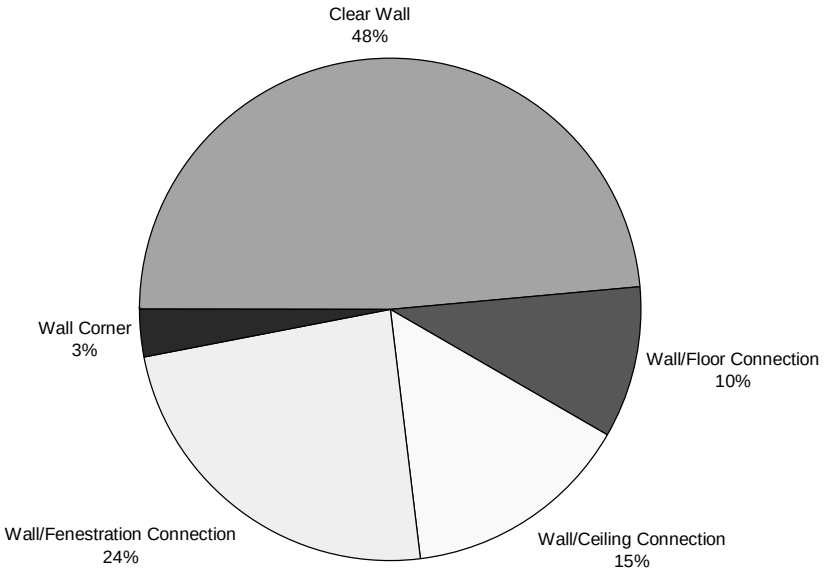

Figure 5.11. DIF for each wall detail for the wood frame systems

The Conventional and Energy Efficient Wood Frame systems implemented the same floor and ceiling configurations. Therefore, the center-of-cavity and clear wall R-values were identical for

both systems. Although the floor/wall and ceiling/wall connections were different, the difference in the whole wall floor and ceiling R-values between the two systems was extremely small. Therefore, the whole wall floor and ceiling R-values were modeled identically. Table 5.4 shows the center-of-cavity, clear wall, and whole wall R-values for the ceiling and floor of both wood frame systems.

Table 5.4. Floor and ceiling center-of-cavity, clear wall, and whole wall R-values $\left(\frac{\text{hr ft}^2 \text{ F}}{\text{Btu}}\right)$ for the Conventional and Energy Efficient Wood Frame systems

	Center-of-Cavity	**Clear Wall**	**Whole Wall**
Ceiling	30.9	28.8	28.1
Floor	24.6	21.2	20.8

Figure 5.12 shows the annual heating and cooling energy load to maintain the Atlanta prototypical house within the setpoint temperature deadband for both the Conventional and Energy Efficient Wood Frame construction systems. As expected, with the clear and whole wall R-values lower than the center-of-cavity R-value, the predicted heating loads increase. Yet, unexpectedly, the lower R-values of the clear and whole walls reduce the cooling conditioning load from that calculated for the center-of-cavity R-value. This behavior is due to the significant impact of the prototypical house internal loads which cause the conditioned zones to require cooling even though the exterior temperatures are lower than the interior temperatures. Consequently, the summation of all the wall heat fluxes when cooling is taking place in Atlanta results in a negative number, heat is transferring from the interior to the exterior of the walls. Either way, Figure 5.12 demonstrates that thermal bridging in the clear wall and wall details can appreciably affect the energy performance of a building envelope. Note that the energy loads in this figure were determined using the Purchased Air conditioning system option in EnergyPlus described in section 4.3.8 in order to evaluate the prototypical house thermal loads independent of the complicated HVAC system behavior.

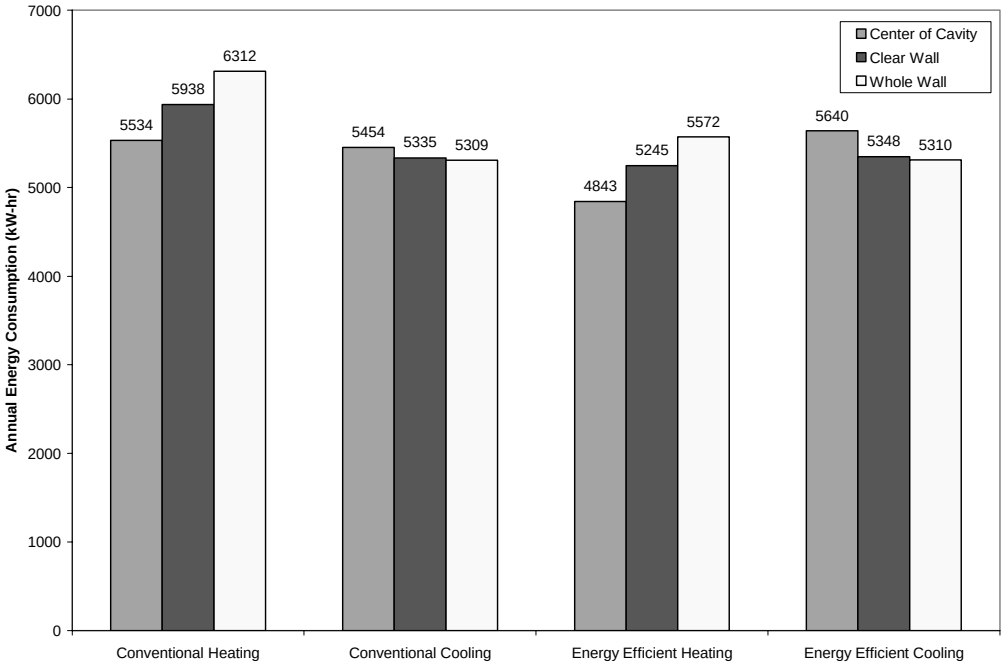

Figure 5.12. Annual heating and cooling loads to maintain the setpoint temperature deadband of the Atlanta prototypical house modeled with the center-of-cavity, clear wall, and whole wall analyses for the Conventional and Energy Efficient Wood Frame systems

5.2.2 Waffle PCP Panel

The Waffle PCP system ideally illustrates how a wall system that replaces wood studs and joists with highly conductive materials such as metal and concrete can exacerbate thermal bridging effects. The conductivity of steel and high density concrete is roughly 385 and 15 times that of spruce/pine/fir (SPF), respectively (EMPA Duebendorf 1999). To give a basic analogy indicating how large conductivity differences affects heat flow, Figure 5.13 shows what the widths of steel, concrete, and SPF wood elements would have to be for an identical amount of heat to conduct from the bottom to the top of the elements. Note that the depth, height, and temperature differential from the bottom to top of the elements were identical. Figure 5.13 gives a clear example of how even an extremely thin piece of steel penetrating the insulation barrier can significantly reduce the performance of a wall system.

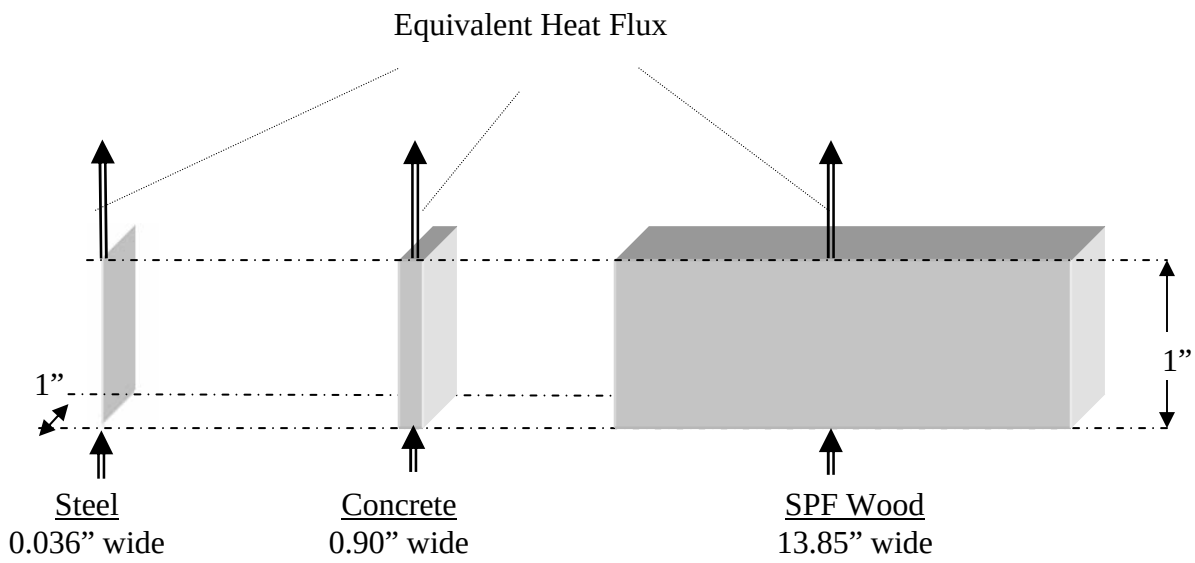

Figure 5.13. Dfference in width for unit depth and height elements composed of steel, concrete and SPF wood to transfer the same amount of heat from the bottom to the top of the element given identical temperature differentials

The Waffle PCP system has a configuration of supports comprised of concrete and steel that penetrate the main insulation layer. Figure 5.14 shows the two dimensional schematic of the clear wall of the Waffle PCP system analyzed for this study including the 3.5” thick reinforced concrete support tipped at the end with a 32 gauge metal nailer that protrudes completely through the main six inch batt insulation barrier at 2 feet on center. An additional 2.5” of batt insulation was inserted in between the concrete rib and metal nailer as shown in Figure 5.14 to try and reduce the heat flux through the concrete support.

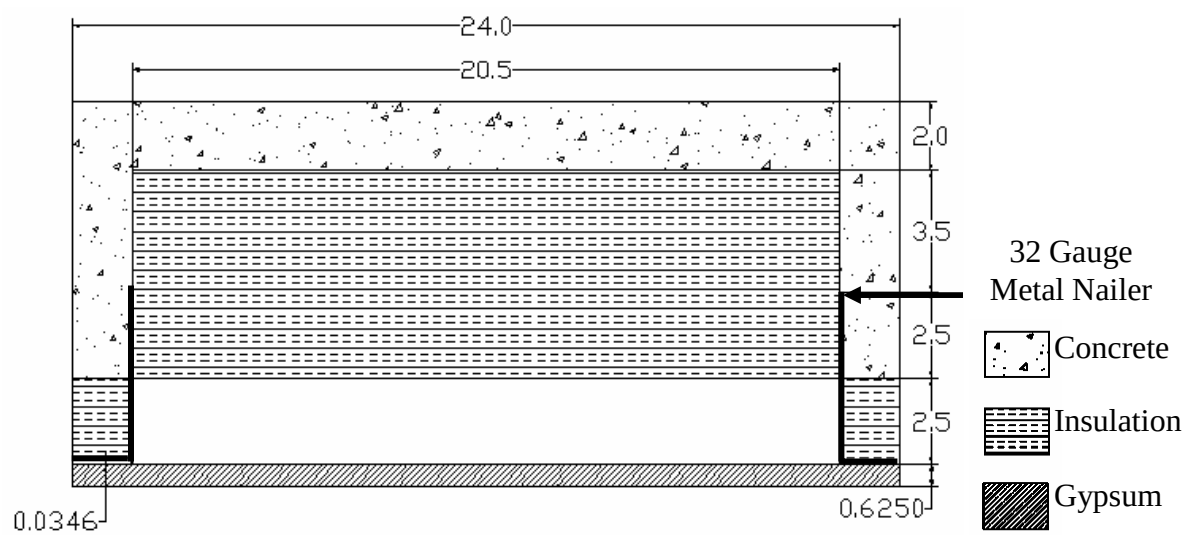

Figure 5.14. Waffle PCP system two dimensional schematic

At first glance, the design seems acceptable from a thermal performance standpoint. Even though 3.5" of highly conductive reinforced concrete spans across the main insulation layer every 2 feet along the clear wall, there is 2.5" of insulation located between the concrete and the interior gypsum. At a closer look, the 16 gauge steel nailer bridges the insulation between the concrete and the gypsum and, using the same analogy from Figure 5.13, essentially provides a heat transfer path comparable to a 0.9" wide concrete connection (or a 13.85" wide wood connection) from the concrete rib to the interior gypsum layer.

To properly model the Waffle PCP configuration, several different numerical heat transfer analyses were conducted, each subsequent analysis more complex than the previous. First, the center-of-cavity R-value was calculated to be 26.1 $\frac{\text{hr ft}^2 \text{ F}}{\text{Btu}}$. Second, a simple two dimensional analysis (applied to the section shown in Figure 5.14), using both the "Heating" Finite Difference and "FEMLAB" Finite Element programs, was conducted ignoring the steel reinforcement within the concrete. The two dimensional analysis reduced the R-value by approximately 77% of the center-of-cavity value to 6.3 $\frac{\text{hr ft}^2 \text{ F}}{\text{Btu}}$. Note that the Heating and FEMLAB results were almost identical. This enormous reduction in R-value is almost entirely

attributed to the heat flow through the concrete stud and steel nailer which penetrates the insulation barrier as shown by the FEMLAB vector plot of the heat flow in Figure 5.15.

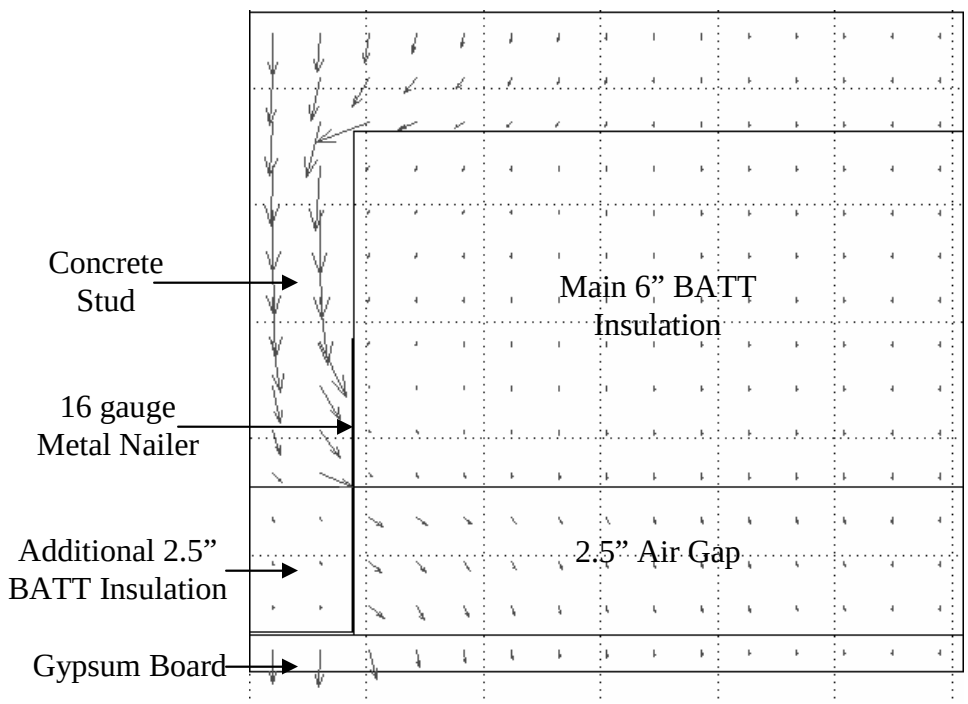

Figure 5.15. Two dimensional Waffle PCP system FEMLAB vector plot

Next, the influence of the steel reinforcement embedded within the concrete was analyzed. Figure 5.16 illustrates the steel rebar configuration within the Waffle PCP system clear wall. Initially, the high density concrete thermal conductivity was increased to account for a uniform distribution of steel at 1% and 2% composition by weight (EMPA Duebendorf 1999) which resulted in an R-value of 6.0 $\frac{\text{hr ft}^2 \text{ F}}{\text{Btu}}$ and 5.9 $\frac{\text{hr ft}^2 \text{ F}}{\text{Btu}}$, respectively. Then, a three dimensional model of the clear wall including the steel rebar was simulated in the Heating program and calculated an R-value of 6.1 $\frac{\text{hr ft}^2 \text{ F}}{\text{Btu}}$. Even though the Waffle PCP system has approximately a 2% composition of steel by weight, the two dimensional analysis that implemented a reinforced concrete conductivity based upon a 1% steel composition predicted a closer R-value to the three dimensional analysis than the reinforced concrete conductivity based

upon a 2% steel composition. The thermal performance results from the three dimensional clear wall analysis that included the steel rebar was used as the input into the EnergyPlus program to evaluate the Waffle PCP system clear wall. Table 5.5 summarizes the different calculated clear wall R-values.

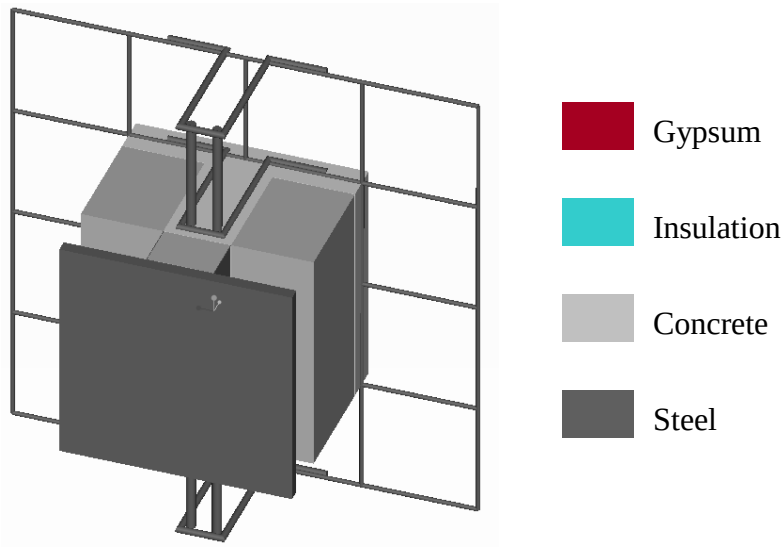

Figure 5.16. Three dimensional schematic of the Waffle PCP system clear wall

Table 5.5. Waffle PCP system calculated R-values $\left(\frac{\text{hr ft}^2\ \text{F}}{\text{Btu}}\right)$ for the different analyses

	Center -of- Cavity	**2D Clear Wall (no steel)**	**2D Clear Wall (1% mass weighted concrete and steel)**	**3D Clear Wall (with rebar configuration)**
R-value	26.1	6.3	6.0	6.1

The two dimensional clear wall analysis using the 1% mass weighted average conductivity for the reinforced concrete was considered acceptable to represent the steel rebar configuration embedded within the concrete. Therefore, for simplification, the concrete in the Waffle PCP wall details was modeled with the same estimated reinforced concrete conductivity to eliminate the need to model the complicated rebar arrangement for each detail. The same wall details were evaluated as for the wood frame systems. Much like the clear wall, excessive thermal bridging occurred within the Waffle PCP wall details resulting in low R-values which are shown in Table 5.6. The resultant whole wall Waffle PCP R-value was $2.7\frac{\text{hr ft}^2\ \text{F}}{\text{Btu}}$. In conclusion, the

Waffle PCP system whole wall R-value was 90% less than its center-of-cavity R-value, a significantly greater reduction than the 29% and 33% reduction experienced by the Conventional and Energy Efficient Wood Frame systems, respectively. Schematics of the Waffle PCP system wall details are provided in Appendix E.

Table 5.6. Waffle PCP system wall detail R-values $\left(\frac{\text{hr ft}^2\ \text{F}}{\text{Btu}}\right)$

3D Clear Wall	Wall/Floor Connection	Wall/Ceiling Connection	Wall/Fenestration Connection	Wall Corner
6.06	1.6	1.7	2.3	2.5

To evaluate how the Waffle PCP system thermal performance could be improved, a continuous half inch of rigid insulation was applied just under the gypsum board. For future reference, the Waffle PCP system without the rigid insulative sheathing will be referred to as the *original system* and the Waffle PCP system with the half inch of rigid insulative sheathing will be referred to as the *modified system*. Table 5.7 compares the center-of-cavity, clear wall, and whole wall R-values between the original and modified Waffle PCP systems.

Table 5.7. Original and modified Waffle PCP systems R-values $\left(\frac{\text{hr ft}^2\ \text{F}}{\text{Btu}}\right)$ for the center-of-cavity, clear wall, and whole wall

Waffle PCP System	Center-of-Cavity	Clear Wall	Whole Wall
Original	26.1	6.1	2.7
Modified	28.5	10.6	6.7

Amazingly, the difference between the original and modified clear and whole wall R-values is significantly greater than the 2.33 $\frac{\text{hr ft}^2\ \text{F}}{\text{Btu}}$ that the half inch of rigid insulative sheathing provides by itself. This phenomenon is described by McGowan and Desjarlais (1997) as "phantom resistance" due to the reduction in the effective area of the thermal bridge (i.e. "reduced lateral heat transfer in the specimen, in addition to the more obvious reduction in longitudinal heat transfer" (McGowan and Desjarlais 1997)). Therefore, the cost benefit of incorporating a continuous layer of rigid insulative sheathing is unquestionable. Figure 5.17 compares the clear wall and wall detail R-values between (a) the original configuration, (b) the

original configuration with ½" of rigid insulation and considering only longitudinal effects, and (c) the modified configuration. It is obvious that the half inch of rigid insulative sheathing provides "phantom resistance" for all the wall details as well.

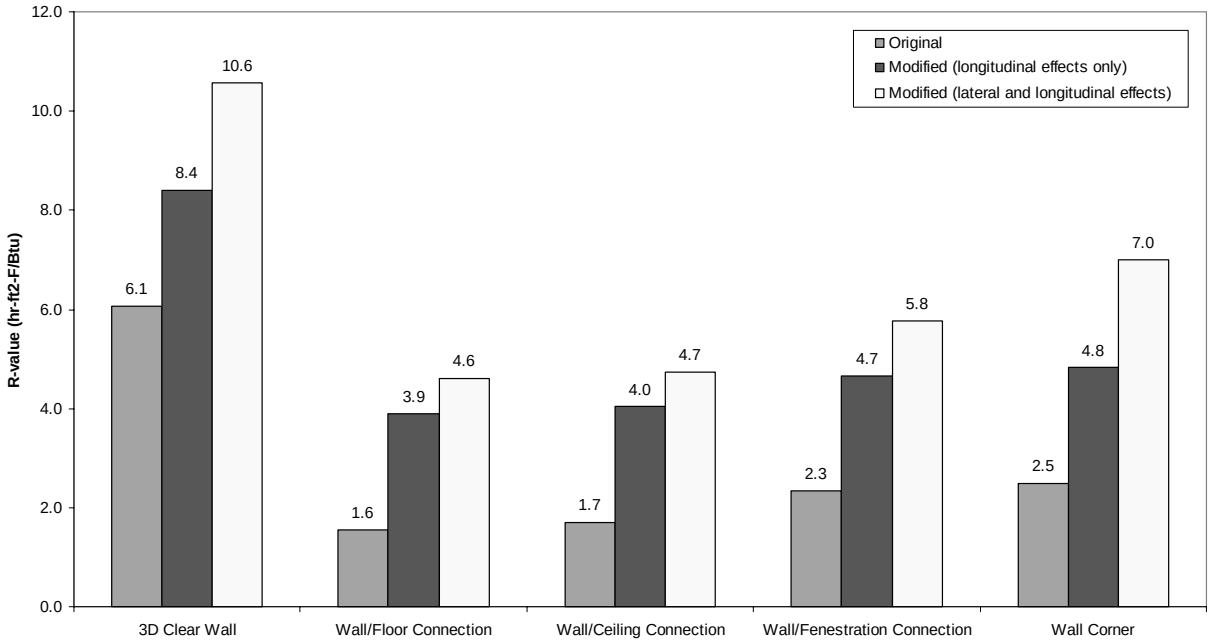

Figure 5.17. Clear wall and wall detail R-values for the original, original plus 2.33 $\frac{hr\ ft^2\ F}{Btu}$, and modified Waffle PCP systems

The behavior of the original and modified Waffle PCP floor and ceiling configurations was similar to that of the wall systems. Figure 5.18 (a) and (b) shows the original Waffle PCP ceiling and floor construction, respectively.

Table **5.8** presents the center-of-cavity, clear wall, and whole wall R-values for both the original and modified Waffle PCP ceiling and floor constructions.

Table **5.8** shows how significant thermal bridging and the existence of phantom resistance occurs with the Waffle PCP ceiling and floor constructions.

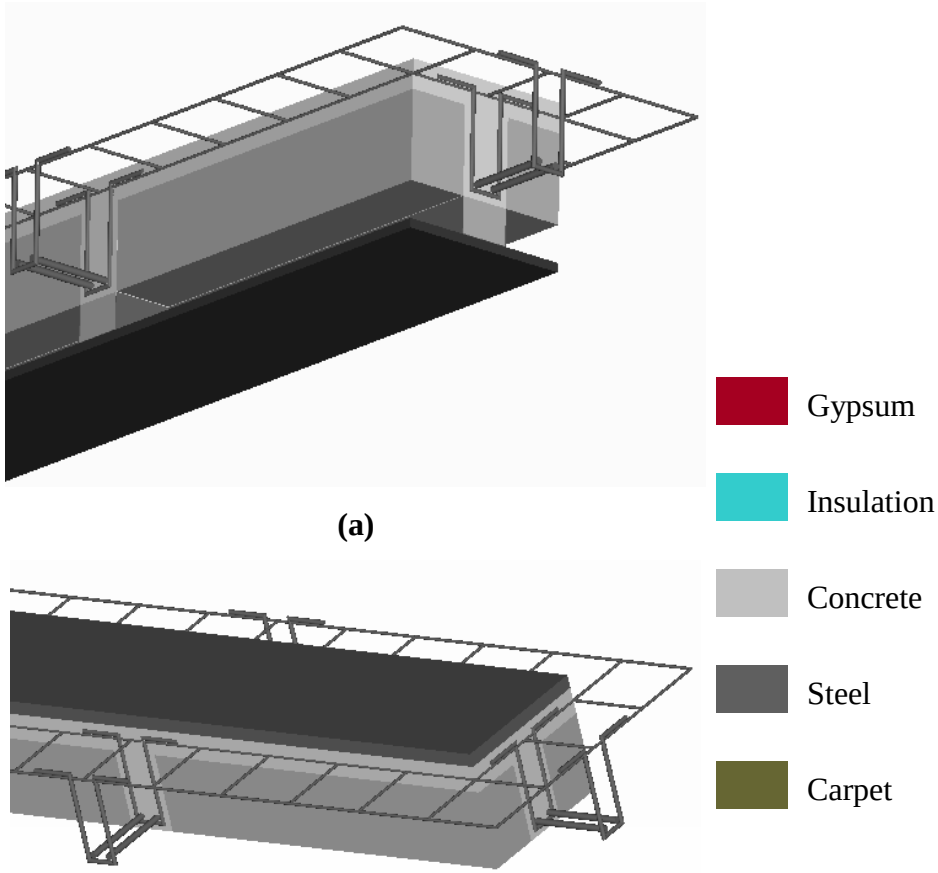

(a)

(b)

Figure 5.18. Waffle PCP ceiling and floor configurations
(a) Waffle PCP ceiling configuration
(b) Waffle PCP floor configuration

Table 5.8. Original and modified Waffle PCP floor and ceiling R-values $\left(\frac{\text{hr ft}^2\ \text{F}}{\text{Btu}}\right)$ for the center-of-cavity, clear wall, and whole wall

	Center of Cavity	**Clear Wall**	**Whole Wall**
Original Floor	24.1	4.9	4.8
Modified Floor	26.5	10.5	10.1
Original Ceiling	32.1	5.2	5.0
Modified Ceiling	34.5	10.5	10.3

Figure 5.19 and Figure 5.20 compare the original versus modified Waffle PCP system resultant heating and cooling loads, respectively, for the Atlanta prototypical house. Figure 5.19 shows how effective a half inch of insulative sheathing can be at reducing the heating load on a typical residence. Figure 5.20 shows the same unusual behavior as the cooling loads for the wood frame systems in Figure 5.12 where the decrease in the R-value from the center-of-cavity to whole wall analysis decreases the cooling load. Although the Modified Waffle PCP system has a larger wall R-value than the Original Waffle PCP system, it has a lower cooling load. This is due to the Modified Waffle PCP system having a larger floor and ceiling R-value than the Original Waffle PCP system. In other words, increasing the wall R-value increases the cooling load but increasing the floor and ceiling R-value decreases the cooling load. Note that the addition of the half inch of rigid insulative sheathing provides such a large improvement in performance in this case because the original Waffle PCP system was an extremely thermally inefficient wall technology. The same modification made to a higher performance wall system would provide less of an improvement.

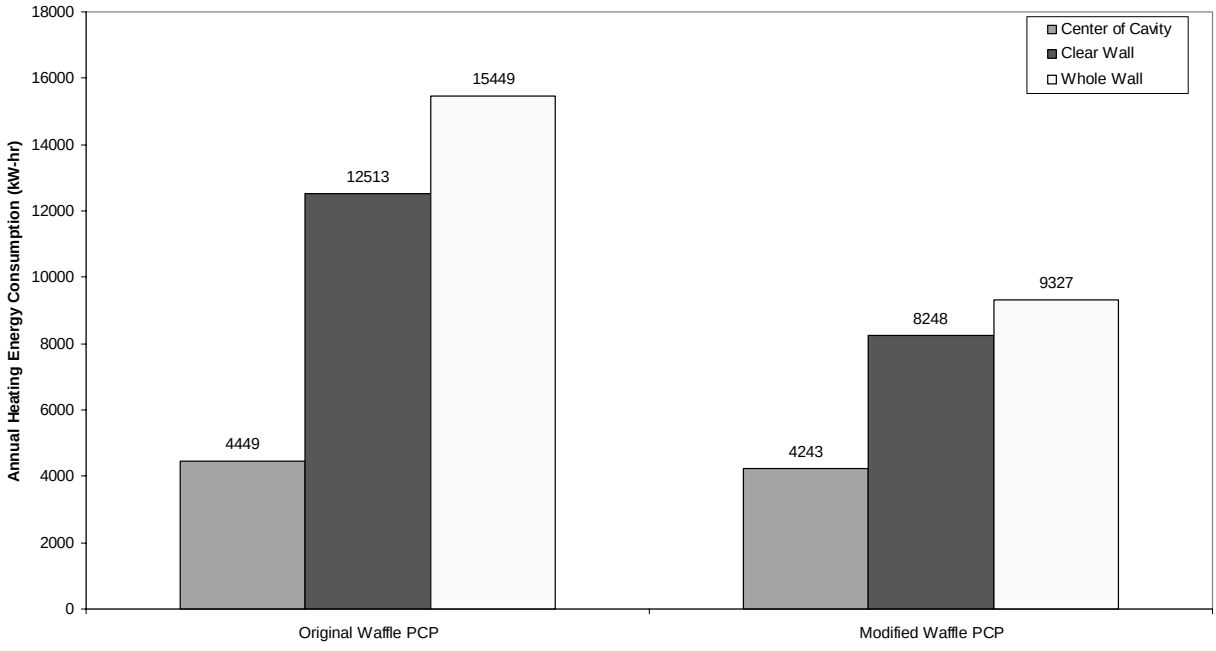

Figure 5.19. Original versus Modified Waffle PCP system heating energy load

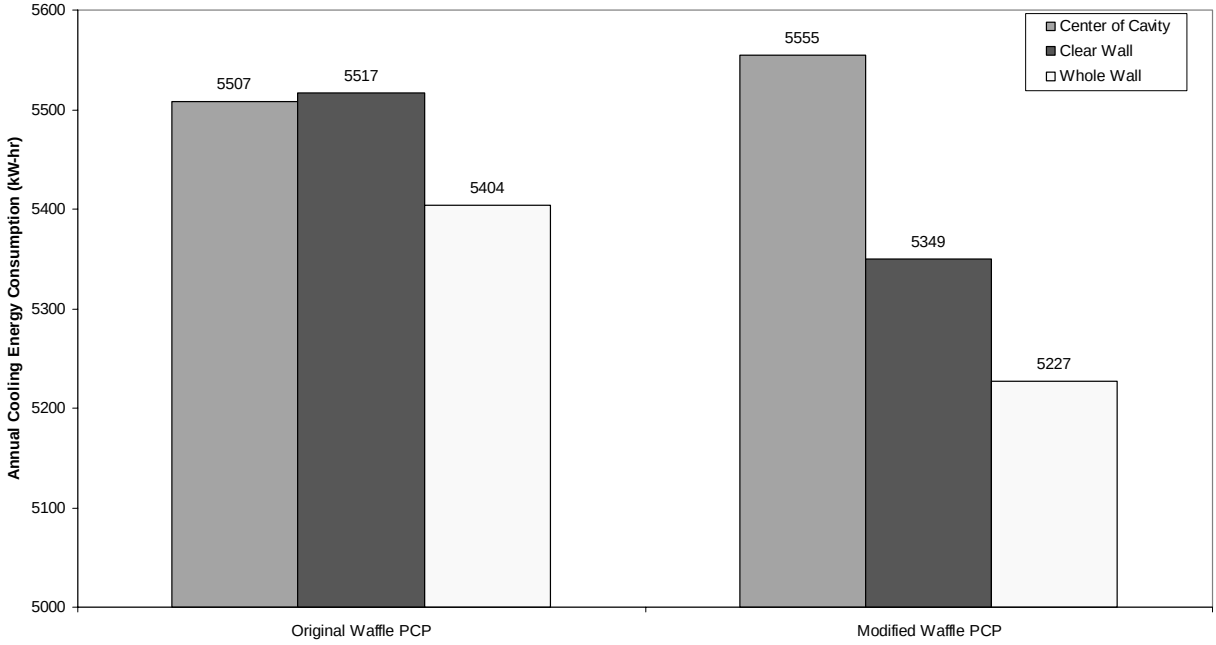

Figure 5.20. Original versus Modified Waffle PCP system cooling energy load

5.2.3 Insulated Concrete Form (ICF)

The ICF system proved to provide a more continuous insulation barrier for the entire wall assembly, including all the wall details, than the wood frame systems. Described in Section 4.1, the ICF configuration consisted of a four inch layer of concrete between two 2.5 inch layers of expanded polystyrene insulation connected by low conductive plastic ties as shown in Figure 5.21. Table 5.9 shows the center-of-cavity, clear wall, and whole wall R-values for the ICF system. The calculated clear wall R-value was very close the published clear wall R-value of 22 $\frac{\text{hr ft}^2 \text{ F}}{\text{Btu}}$ by the Reward Wall System company (Reward Wall System 2004) who makes the ICF wall configuration used for this study and 20 $\frac{\text{hr ft}^2 \text{ F}}{\text{Btu}}$ by the NAHB HUD ICF study (NAHB Research Center 1999). Figure 5.22 illustrates how the two, almost continuous, layers of insulation results in large wall detail R-values. Schematics of the ICF system wall details are provided in Appendix E.

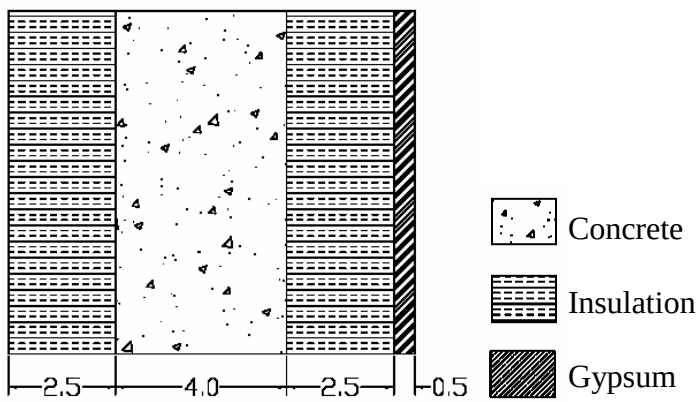

Figure 5.21. ICF Waffle PCP system two dimensional schematic

Table 5.9. R-values $\left(\frac{\text{hr ft}^2 \text{ F}}{\text{Btu}}\right)$ for ICF system for the Center-of-cavity, clear wall, and whole wall analyses

	Center-of-Cavity	**Clear Wall**	**Whole Wall**
Calculated	21.2	20.3	16.6

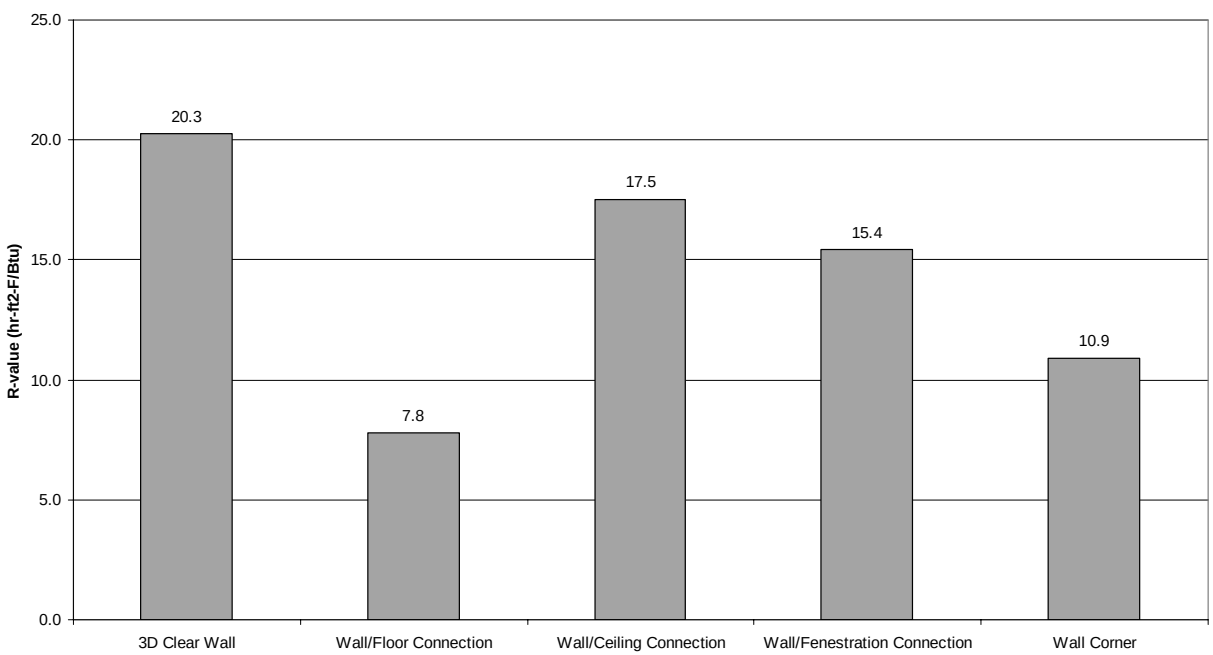

Figure 5.22. ICF system wall detail R-values $\left(\frac{\text{hr ft}^2 \text{ F}}{\text{Btu}}\right)$

The prototypical house construction with the ICF system had the same ceiling and floor configurations as the wood frame systems. Therefore, the center-of-cavity, clear wall, and whole wall R-values for the floor and ceiling were identical to those in Table 5.4. Figure 5.23 demonstrates how a high performance wall system with a design focused on a continuous insulation barrier can maintain approximately the same heating and cooling energy loads for the center-of-cavity, clear wall, and whole wall ICF analyses. Compared to the 29% and 33% reduction from center-of-cavity to whole wall R-value experienced by the Conventional and Energy Efficient Wood Frame systems, respectively, the ICF configuration only experienced a 21% reduction.

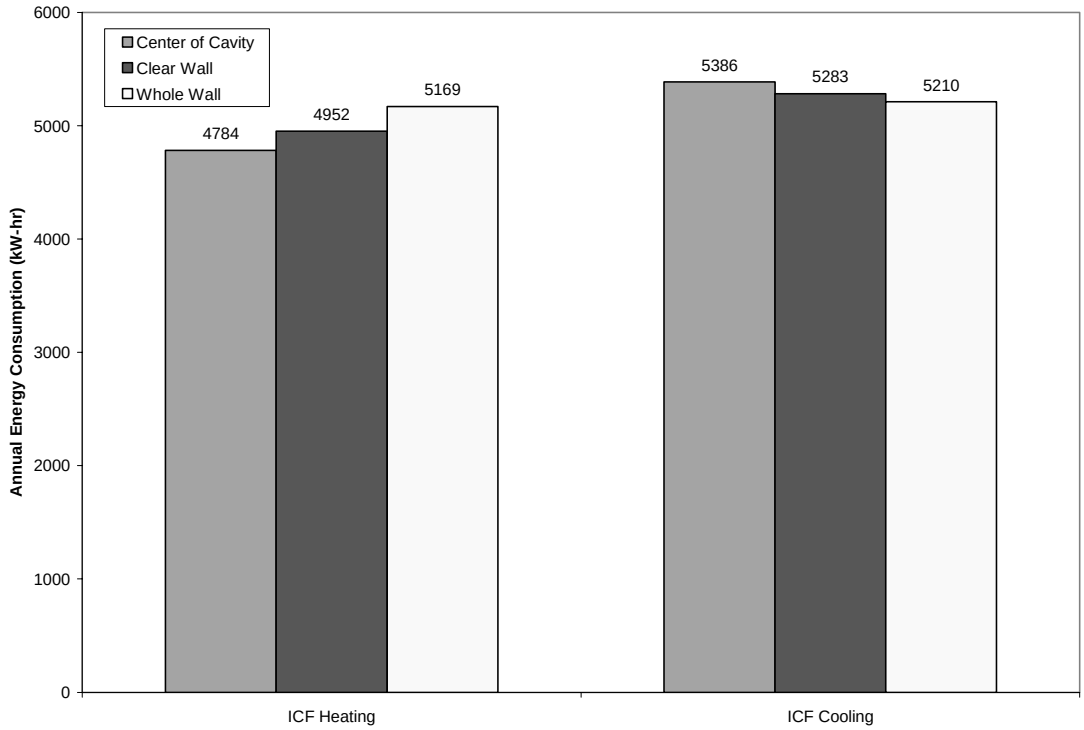

Figure 5.23. ICF system cooling annual energy consumption using the center-of-cavity, clear wall, and whole wall heating analyses

5.2.4 Sandwich PCP Panel

Much like the ICF system, the Sandwich PCP panel was able to maintain a whole wall R-value similar to that of the center-of-cavity. The clear wall of the Sandwich panel consisted of a three inch layer of expanded polystyrene in between two layers of concrete, two inch exterior and four

inch interior, connected by fiber composite connectors installed at 12 inches on center as shown in Figure 5.24.

Table **5.10** shows the center-of-cavity, clear wall, and whole wall R-values for the Sandwich PCP panel. Figure 5.25 plots the Sandwich PCP system wall detail R-values.

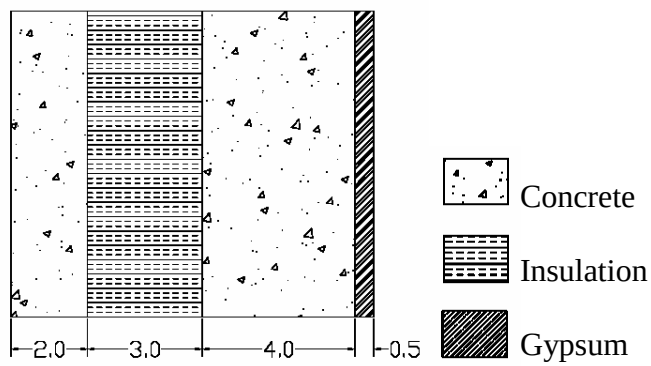

Figure 5.24. Sandwich PCP system two dimensional schematic

Table 5.10. R-values $\left(\frac{\text{hr ft}^2\ \text{F}}{\text{Btu}}\right)$ for the Sandwich PCP system for the center-of-cavity, clear, and whole wall analyses

	Center-of-Cavity	**Clear Wall**	**Whole Wall**
Calculated	13.1	13.0	10.6

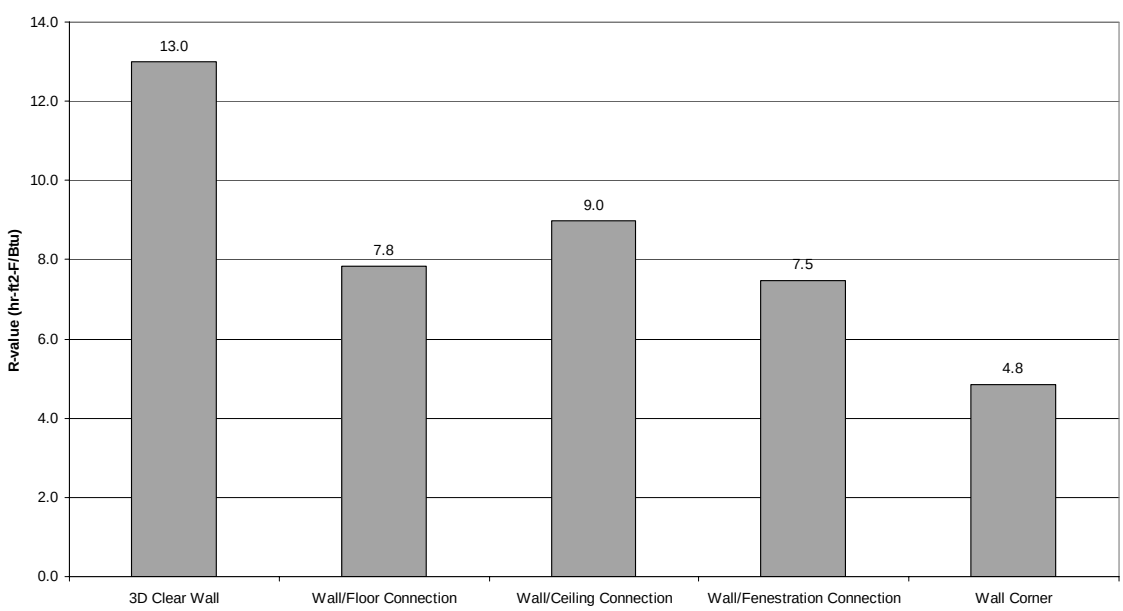

Figure 5.25. Sandwich PCP system wall detail R-values $\left(\frac{\text{hr ft}^2\ \text{F}}{\text{Btu}}\right)$

The prototypical house construction with the Sandwich PCP system had the same ceiling and floor configurations as the wood frame systems. Figure 5.26 shows how the Sandwich PCP system kept the prototypical house heating and cooling energy loads essentially constant for the center-of-cavity, clear wall, and whole wall analyses. Overall, the Sandwich PCP system center-of-cavity to whole wall R-value reduction of 19% was slightly better than the 21% reduction by the ICF system and much better than the 29% and 33% reduction for the Conventional and Energy Efficient Wood Frame systems, respectively.

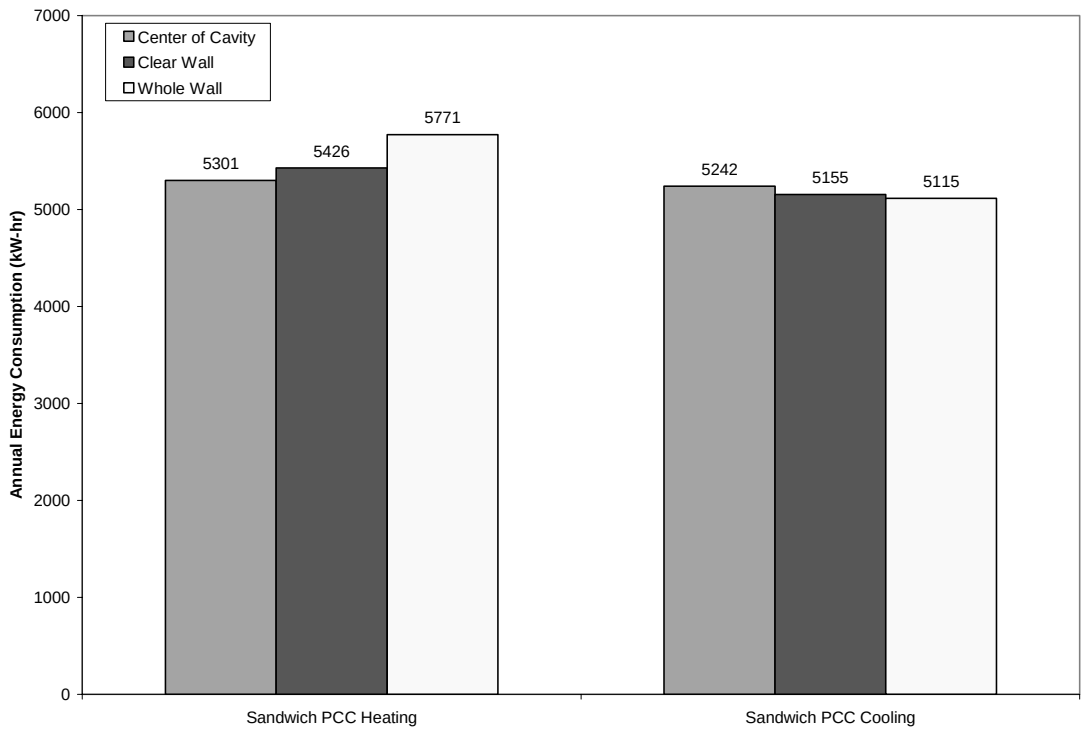

Figure 5.26. Sandwich PCP system heating and cooling annual energy consumption for the center-of-cavity, clear wall, and whole wall analyses

5.2.5 Comparison

This subsection compares several characteristics of the different wall technologies. Figure 5.27 plots the Detail Influence Factors (DIF) for all the wall systems which is defined in section 4.2.5 as a parameter that encompasses the area of influence and local R-value of the different wall details. The larger the DIF of the clear wall, the closer the whole wall system will be toward

behaving like its clear wall characteristics. Since the other wall details have lower R-values than the clear wall, the wall system should be designed to maximize the clear wall DIF.

As expected, the ICF and Sandwich PCP systems have the largest clear wall DIF followed by the wood frame systems and finally the Waffle PCP systems. Figure 5.27 shows that the influence of the wall corner detail remains constant for the different wall systems while the DIF values for the other wall details vary significantly. Focusing on the ICF and Sandwich PCP systems, Figure 5.27 indicates that the wall/floor configuration should be altered to reduce its large DIF. This makes sense because the wall/floor connection is the only detail for the ICF and Sandwich PCP systems where the continuous insulation barrier is broken. For the wood frame systems, the wall/fenestration connection is the most detrimental wall detail.

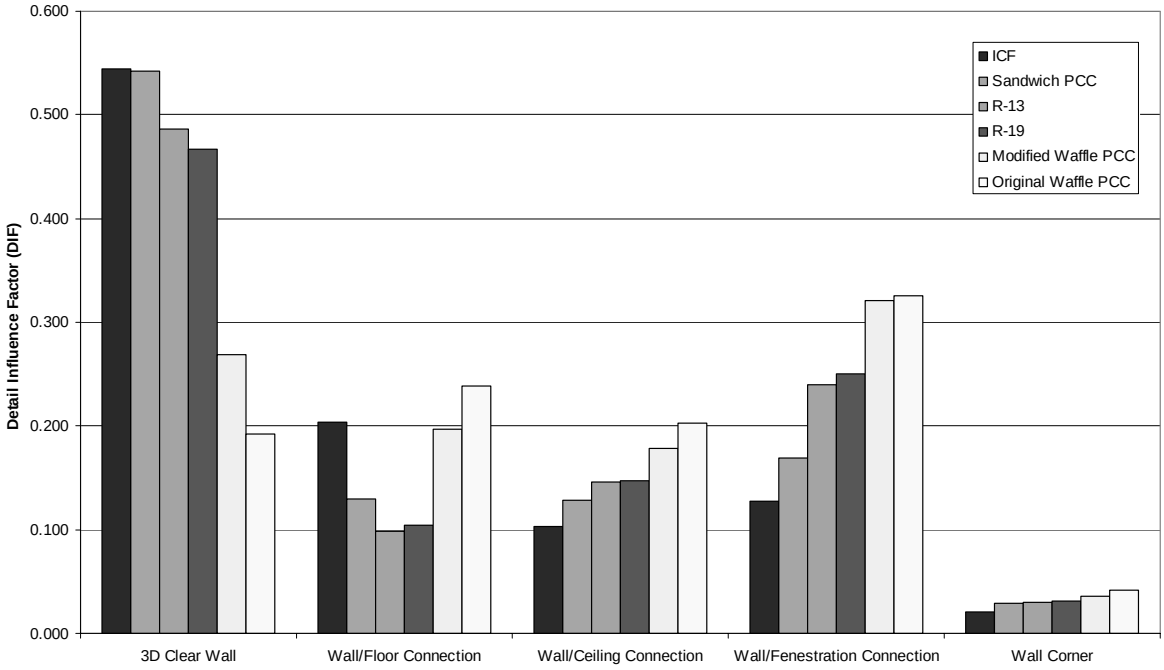

Figure 5.27. Detail Influence Factor for the various wall systems

Table 5.11 gives the percent reduction from the center-of-cavity to whole wall R-value for each wall system. As shown, the Sandwich PCP panel experiences a smaller R-value reduction than the ICF system. This can be explained by the center-of-cavity R-value of the Sandwich PCP system being lower than that of the ICF system. Therefore, the effectiveness of the Sandwich

and ICF systems at minimizing the harmful effects of the wall details can be approximated to be the same. Either way, both systems perform better than the Conventional and Energy Efficient Wood Frame systems.

Table 5.11. Percentage reduction from center-of-cavity to whole wall R-value $\left(\frac{\text{hr ft}^2 \text{ F}}{\text{Btu}}\right)$ for the different wall systems

	Percent Reduction
Sandwich PCP	18.6
ICF	21.4
R-13	29.4
R-19	33.0
Modified Waffle PCP	76.5
Original Waffle PCP	89.5

Table 5.12 presents another way of comparing the effectiveness of the insulation within a wall system. Defined in subsection 4.2.5, the insulation effectiveness calculates the percentage of the total possible R-value for a given quantity of insulation that the actual insulation configuration within the wall system provides. Not surprisingly, the wall systems are in the same order as in Table 5.11. There is no effective insulation value for the Original Waffle PCP systems because it had such a poor design that based upon the calculation procedure, it would have had a negative effective insulation. To prevent confusion, no value was entered.

Table 5.12. Insulation effectiveness of the different wall systems

	Effective Insulation
Sandwich PCP	80.4%
ICF	78.0%
R-13	74.1%
R-19	71.1%
Modified Waffle PCP	12.2%
Original Waffle PCP	-

Figure 5.28 presents the heat capacitance of the different wall systems. The International Energy Conservation Code and ASHRAE Standard 90.2 (ASHRAE 2001b) requires that a wall system

must have at least a heat capacitance of 6 $\frac{\text{Btu}}{\text{ft}^2\ \text{F}}$ in order to apply for thermal mass benefits. Not surprisingly, both wood frame wall systems fall severely short of this requirement. Interestingly though, the original and modified Waffle PCP systems heat capacities significantly increase from the center-of-cavity to clear wall analyses and even more from the clear wall to whole wall analyses. This can be explained by the large amount of concrete at the wall details for the Waffle PCP system especially since the ceiling and floors are concrete configurations as well. The other wall systems increase in capacitance from center-of-cavity to whole wall analysis for the same reason but to a much smaller degree than the Waffle PCP systems do. Another point to notice is the much greater heat capacity of the Sandwich PCP system, six inches of concrete in the clear wall, over the ICF system, four inches of concrete in the clear wall.

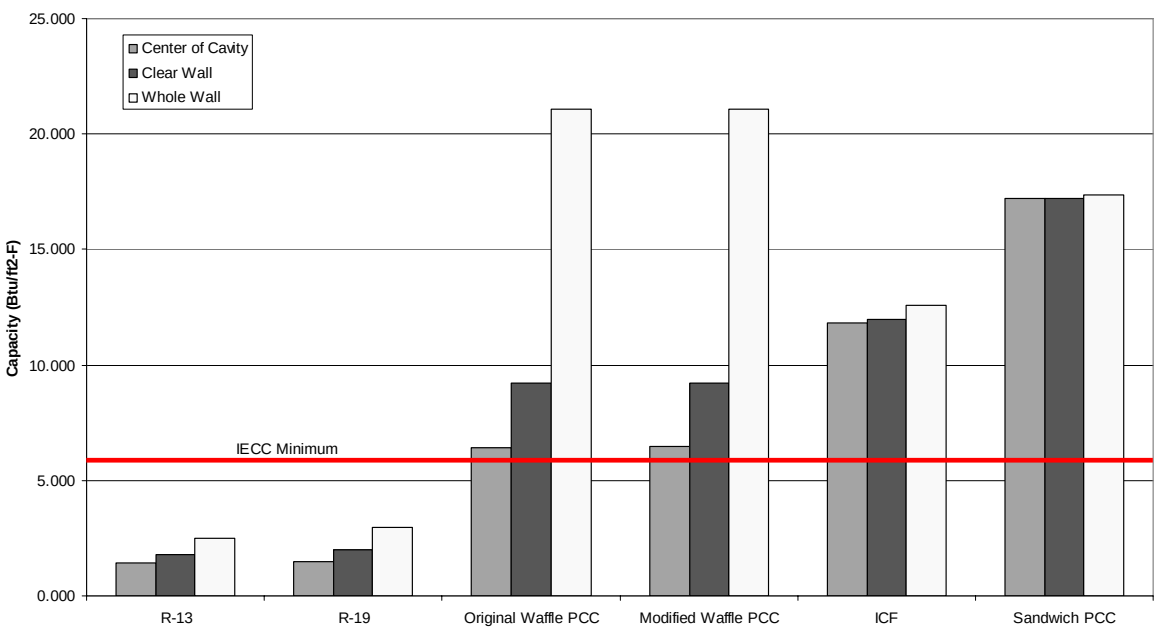

Figure 5.28. Heat capacitance of the different wall systems $\left(\frac{\text{Btu}}{\text{ft}^2\ \text{F}}\right)$

Figure 5.29 presents the heat capacitance distribution across the thickness of each wall system by plotting the structure factor terms (j_{ii}, j_{ie}, j_{ee}). Described in section 4.2.4, j_{ii} is the largest when most of the thermal mass lies inside the insulation barrier. Conversely, j_{ie} is the largest

when most of the thermal mass lies outside the insulation barrier. According to several studies (ASHRAE 2001b; Christian 1991; Kossecka and Kosny 2002), thermally massive walls provide the best performance when the thermal mass is inside the insulation barrier. Therefore, thermally massive walls should be designed to maximize j_{ii}. According to Figure 5.29, the Sandwich PCP system contains the largest j_{ii}.

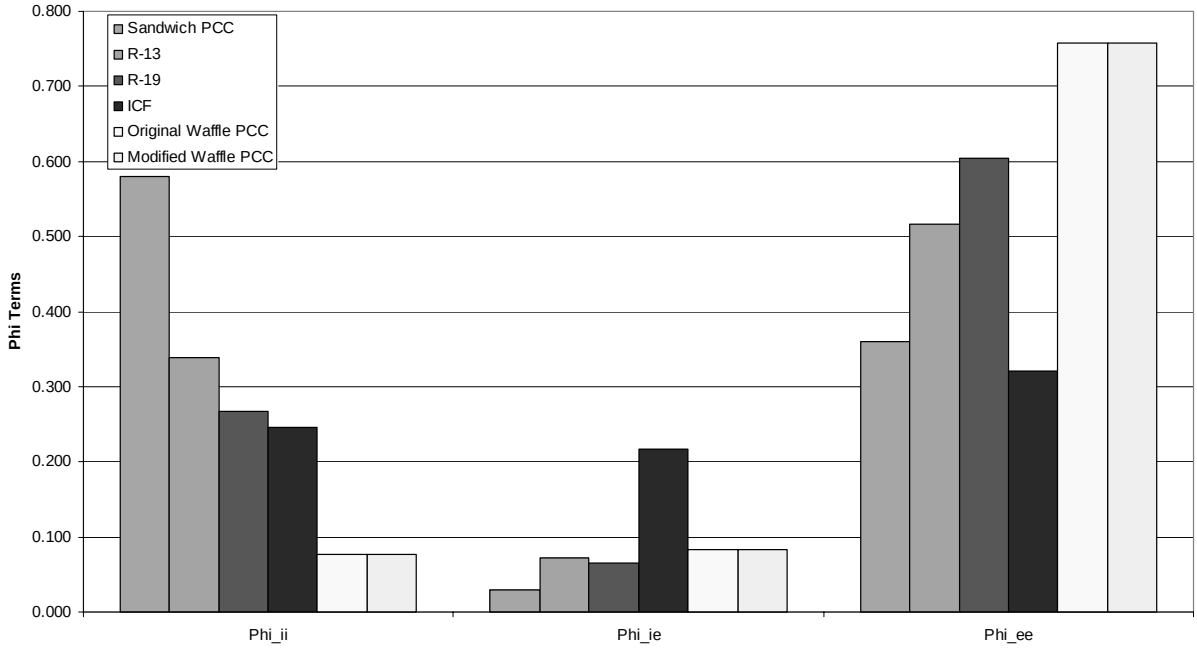

Figure 5.29. Structure factors for the different wall systems

5.3 Thermal Performance of Wall Technologies

The following subsections summarize the thermal performance of the Conventional Wood Frame, Energy Efficient Wood Frame, ICF, and Sandwich PCP wall systems in terms of the annual heating and cooling energy consumption. Both Waffle PCP systems were omitted from this aspect of the analysis because their excessive thermal bridging, reviewed in subsection 5.1.2, resulted in an extremely poor performance. Further modifications to the Waffle PCP systems are necessary before their energy performance is comparable to the other wall technologies. The ensuing annual energy consumptions were calculated with the "purchased air" feature in EnergyPlus described in subsection 4.3.8 as a 100% efficient conditioning system with an

infinite load capacitance. Essentially, the "purchased air" system supplies (heating) or removes (cooling) energy as necessary to maintain the conditioned zones at the proper setpoint temperature. Therefore, the following comparisons are solely based upon the thermal performance of the wall systems independent of any HVAC system behavior. Subsection 5.3.1 summarizes the annual energy savings of the Energy Efficient Wood Frame, ICF, and Sandwich PCP technologies over the Conventional Wood Frame system for all of the prototypical house locations. Subsection 5.3.2 highlights the percentage of the ICF and Sandwich PCP energy savings, shown in the previous subsection, attributable to thermal mass. Subsection 5.3.3 shows the wood frame R-value that provides the same energy performance as the ICF and Sandwich PCP systems for each prototypical house location, also known as the Effective R-value.

5.3.1 Annual Energy Consumption Comparisons

The heating and cooling energy savings were evaluated separately because thermal mass benefits perform differently for the two different conditioning types. The typical mindset is that thermally massive systems improve energy performance the most in temperate to hot climates where the daily outside temperature range often goes into the setpoint temperature deadband which is 70°F to 78°F for the prototypical house. In cold climates, thermal mass should have the smallest effect since the outside temperature is well below the lowest setpoint temperature. For future reference, Minneapolis and Denver represent cold climates, Washington and Atlanta represent temperate climates, and Phoenix and Miami represent hot climates.

Figure 5.30 shows the annual heating energy savings of the Energy Efficient Wood Frame, Sandwich PCP, and ICF systems over the Conventional Wood Frame system. For the cold and temperate climates, the wall system R-values were directly related to the heating energy savings; the ICF system with a whole wall R-value of $16.6\frac{\text{hr ft}^2\ \ \text{F}}{\text{Btu}}$ saved the most heating energy followed by the Energy Efficient Wood Frame system ($13.8\frac{\text{hr ft}^2\ \ \text{F}}{\text{Btu}}$ whole wall R-value) and the Sandwich PCP system ($10.6\ \frac{\text{hr - ft}^2\ \text{- 0F}}{\text{Btu}}$ whole wall R-value). The trend changed for the hot climates where the Sandwich PCP system performed better than the Energy Efficient Wood

Frame system. This can be explained by the mild winters experienced in Phoenix and Miami where the daily temperature range entered the setpoint temperature deadband resulting in larger thermal mass benefits. In fact, the Sandwich PCP and ICF systems almost completely eliminated the need for a heating system in Miami.

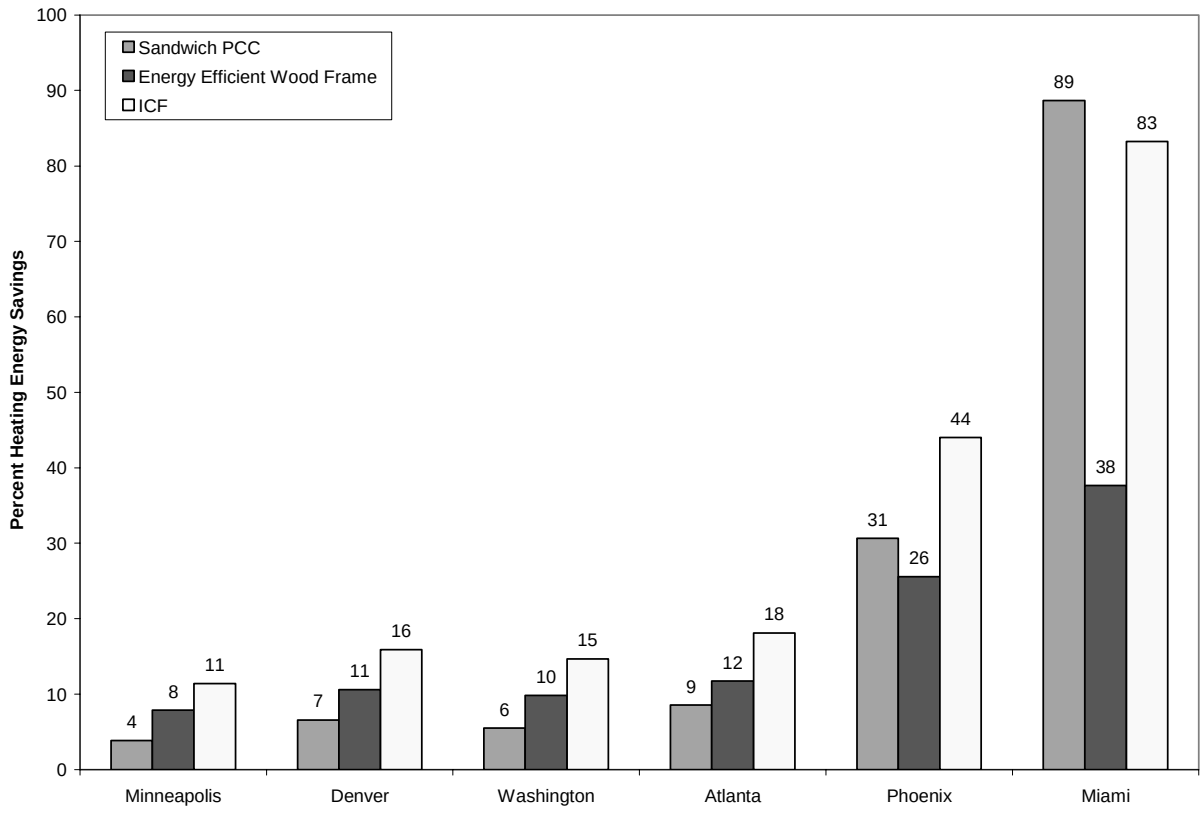

Figure 5.30. Annual heating energy savings of the Sandwich PCP, Energy Efficient Wood Frame, and ICF wall systems over the Conventional wood frame system

Figure 5.31 shows the annual cooling energy savings of the Energy Efficient Wood Frame, Sandwich PCP, and ICF systems over the Conventional Wood Frame system. The resultant trends are drastically different than those for the heating energy savings in Figure 5.30. For the cold and temperate climates, increasing the R-value from the Conventional to Energy Efficient Wood Frame system increases or has no effect on the cooling energy load. Although this may seem incorrect, from further investigation, it makes sense. These climates experience mild summer temperatures, thus, during the cooling season, the outdoor temperatures are often below

the thermostat setpoint with cooling required primarily to offset the internal and solar loads. Under these conditions, the walls transfer energy *out of the conditioned zone*. Consequently, the larger the R-value of the walls, the less the walls can remove energy from the conditioned space.

The concrete systems reduce the need for cooling by shifting the period of maximum heat gain from the walls to a time when the outside conditions are colder. For example, the light weight wood frame systems present very little delay between the peak radiative/convective heat flux into the exterior wall surface and the maximum heat emitted into the conditioned space from the interior wall surface. As a result, the peak wall heat transfer coincides with the peak internal heat gain in the late afternoon resulting in the requirement for a significant amount of cooling. The concrete systems delay the peak wall heat flux into the conditioned zones to early the next morning when the internal loads are minimal and the cooler exterior temperature has had time to reabsorb some of the energy stored inside the wall. This explanation is strengthened by the Sandwich PCP system reducing the annual cooling energy more than the ICF system which has a higher R-value but a lower capacitance. The benefits of thermal capacitance outweigh the detrimental effect of higher R-value walls trapping heat within the space during mild summer conditions. *In general, to reduce the wall loads on the annual cooling energy for a cold or temperate climate, the wall system capacitance should be increased, not the R-value.*

For the hot climates, the cooling energy saving trends were very different. The ICF system with a higher R-value but lower capacitance performed better than the Sandwich PCP system. Yet the Sandwich PCP system still performed as well as the Energy Efficient Wood Frame system even though it had a lower R-value. *Therefore, for climates with hot summers, both thermal mass and R-values are important in reducing annual cooling energy.*

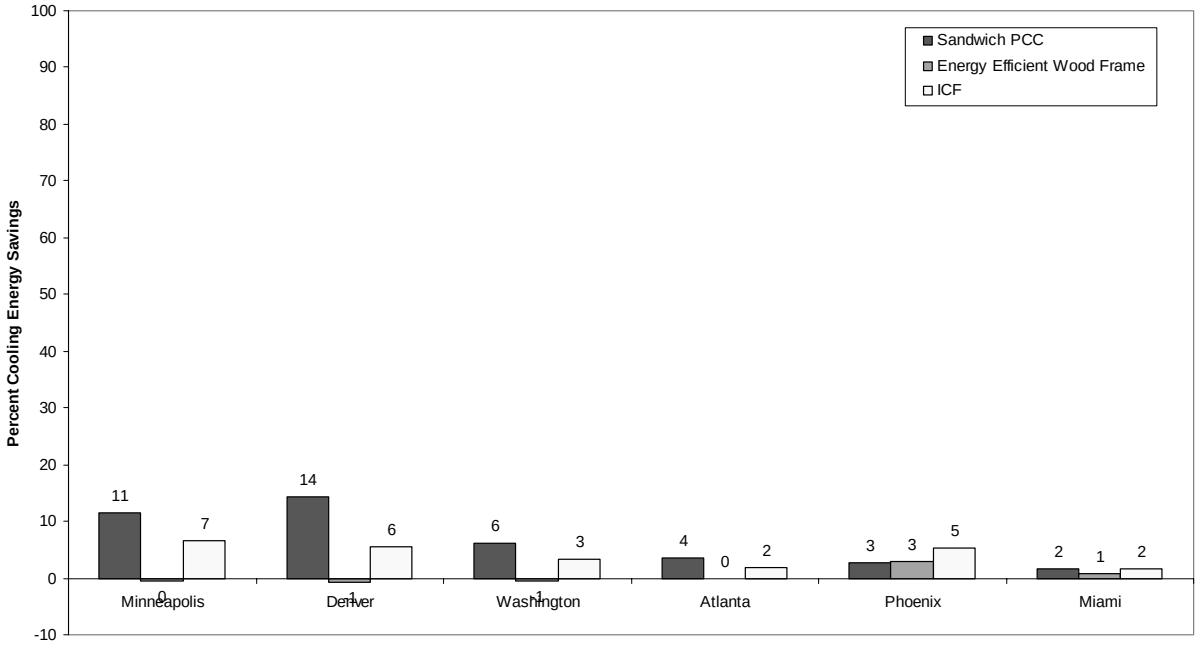

Figure 5.31. Annual cooling energy savings of the Sandwich PCP, Energy Efficient Wood Frame, and ICF wall systems over the Conventional wood frame system

5.3.2 Thermal Capacitance Component of Energy Savings

The graphs in subsection 5.3.1 combine the increased R-value and thermal mass benefits together for the energy savings associated with the Sandwich PCP and ICF wall technologies compared to the Conventional Wood Frame system. To evaluate the thermal mass contribution separately, the heating and cooling energy consumption of typical wood frame systems with the same whole wall R-value as the Sandwich PCP and ICF systems were compared to the Conventional Wood Frame system. These energy savings solely represented the result of increasing the whole wall R-value. Therefore, subtracting these energy savings from the total energy savings of the Sandwich PCP and ICF systems resulted in the energy savings from the thermal capacitance effects.

Figure 5.32 shows the percentage of the wall system heating energy savings that is due to thermal mass for both the Sandwich PCP and ICF systems. As expected, the Sandwich PCP system thermal mass benefits are substantially larger than those for the ICF system. Except for Denver, the heating thermal mass benefits increase for warmer climates.

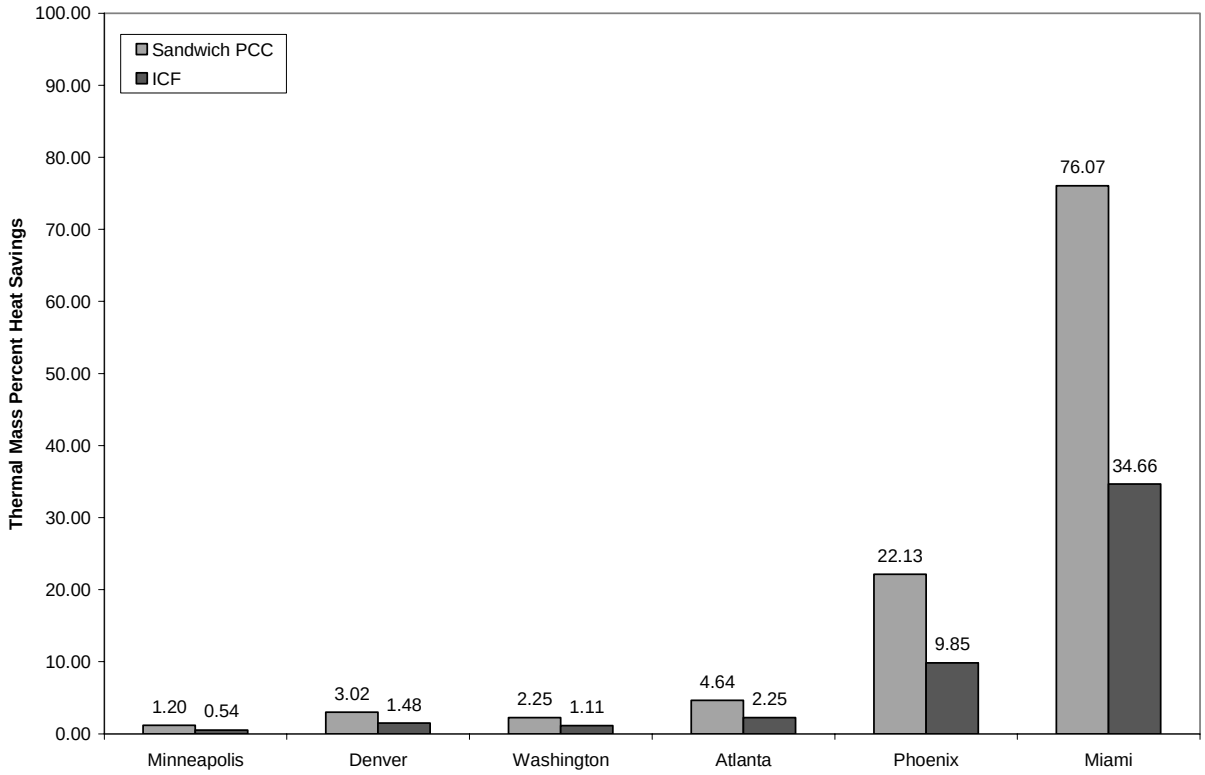

Figure 5.32. Heating energy savings from thermal mass of the Sandwich PCP and ICF systems

Figure 5.33 shows the percentage of the wall system cooling energy savings that is due to the thermal mass for both the Sandwich PCP and ICF systems. Much like Figure 5.32, the Sandwich PCP system experiences much larger thermal mass benefits than the ICF system. Except for Denver, the cooling thermal mass benefits are larger for colder climates.

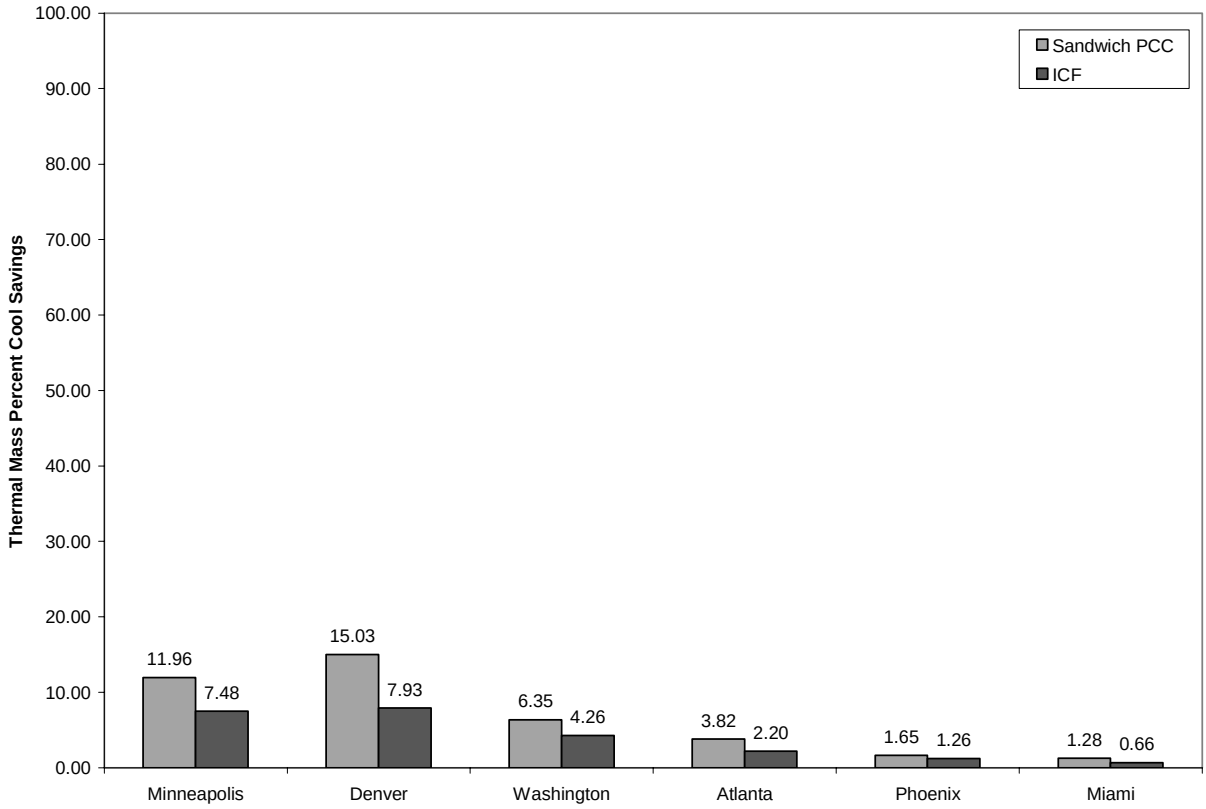

Figure 5.33. Cooling energy savings from thermal mass of the Sandwich PCP and ICF systems

The results in Figure 5.32 and Figure 5.33 contradict the common belief that temperate and hot climates experience the greatest thermal mass benefits. Instead, thermal mass benefits are most apparent for mild seasons in any climate where the daily temperature swing goes into the setpoint temperature deadband. *In other words, the heating season for hot climates and the cooling season for cold climates incur the greatest thermal mass benefits.*

The significantly larger thermal mass savings shown for the heating season in hot climates than those for the cooling season in cold climates is somewhat of an illusion. Miami and Phoenix only require between 1 to 3 MMBtu to heat during the cold season. Minneapolis and Denver require between 5 to 7 MMBtu to cool during the hot season. Therefore, the heating season in hot climates is much more mild than the cooling season in cold climates. Consequently, thermal mass savings are much larger in more mild climate conditions. Unfortunately, while the heating

thermal mass savings are large in hot climates, the absolute savings in energy is extremely small since homes in these climates consume very little heating energy in general.

5.3.3 Effective R-value of ICF and Sandwich PCP Wall Systems

The current housing industry uses the R-value as the benchmark from which to compare the thermal performance of different wall systems. Therefore, contractors or home owners will not understand the thermal performance difference between wall systems of varying capacitance. As a result, the R-value and thermal mass of a wall system can be combined into one parameter, called the Effective R-value that incorporates both performance factors. Described in Kosny et al (1999), the Effective R-value represents the wood frame system R-value that results in the same energy performance as the thermally massive system. This is the same procedure used to develop the thermal mass credit tables in ASHRAE 90.2 and the IECC 2001 (ASHRAE 2001b; IECC 2001; Christian 1991).

Heating and cooling Effective R-values were calculated for the Sandwich PCP and ICF systems for all six climates. First, the prototypical house was modeled with ten different wood frame wall systems keeping all the parameters identical to the Conventional Wood Frame whole wall system except for the R-value. Each wall system represented a different clear wall wood frame configuration ranging in R-value from 2.3 to 37.0 $\frac{\text{hr ft}^2 \text{ F}}{\text{Btu}}$ listed in Table 5.13. This procedure was obtained from Kosny et al (1999).

Table 5.13. Configurations and R-values of clear wall wood frame systems (Kosny et al 1999)

Clear Wall R-Value $\left(\frac{hr\ ft^2\ F}{Btu}\right)$	**Wall Configuration**
2.3	Alum. siding, 2” insul. sheathing, 3.5” wood stud, empty cavity, 2” gypsum board
4.7	Alum. siding, 2” insul. sheathing, 1” EPS foam, 3.5” wood stud, empty cavity, 2” gypsum board
6.8	Alum. siding, 2” insul. sheathing, 2” EPS foam, 3.5” wood stud, empty cavity, 2” gypsum board
12.5	Alum. siding, 2” insul. sheathing, 3.5” wood stud, R-11 BATTs, 1/2” gypsum board
15.0	Alum. siding, 1/2” insul. sheathing, 1/2” EPS foam, 3.5” wood stud, R-11 BATTs, 1/2” gypsum board
17.0	Alum. siding, 1/2” insul. sheathing, 1” EPS foam, 3.5” wood stud, R-11 BATTs, 1/2” gypsum board
20.0	Alum. siding, 1/2” insul. sheathing, 5.5” wood stud, R-19 BATTs, 1/2” gypsum board
23.0	Alum. siding, 1/2” insul. sheathing, 1/2” EPS foam, 5.5” wood stud, R-19 BATTs, 1/2” gypsum board
29.0	Alum. siding, 2” insul. sheathing, 1.5” EPS foam, 5.5” wood stud, R-19 BATTs, 1/2” gypsum board
37.0	Alum. siding, 2” insul. sheathing, 2” polyurethane foam, 5.5” wood stud, R-30 BATTs, 2” gypsum board

The annual heating and cooling loads were calculated for each wood frame system and plotted versus the clear wall R-value as shown in Figure 5.34. Then a curve was fit to the data points. Finally, the heating or cooling load of the ICF or Sandwich PCP system was pinpointed on the curve fit to determine the wood frame R-value that resulted in the same load. An example of this step is shown in Figure 5.34. The resultant R-value represents the “Equivalent R-value” or the R-value of a typical wood frame system that would provide the same heating or cooling performance as the thermally massive system.

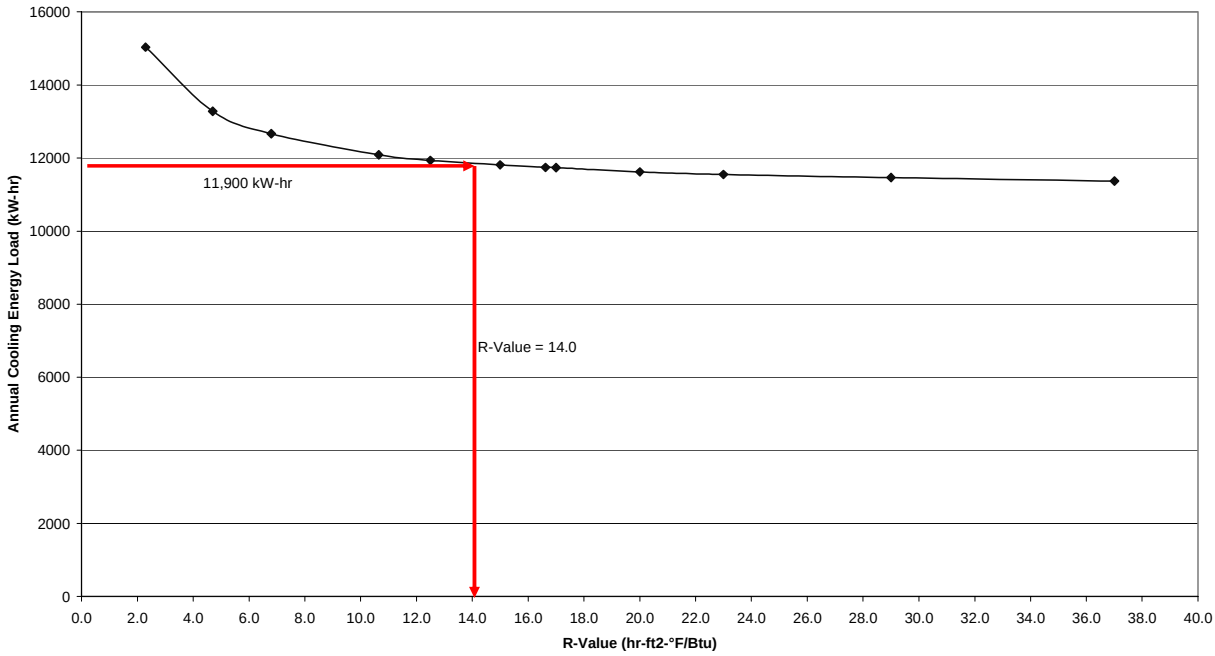

Figure 5.34. Example procedure to calculate the cooling Effective R-value for the Sandwich PCP system in Phoenix

The above procedure was repeated for the heating and cooling load of each of the prototypical house locations to determine the Effective R-value of the ICF and Sandwich PCP systems. Figure 5.35 and Figure 5.36 plot the heating and cooling Effective R-values for the ICF and Sandwich PCP systems, respectively. The ">37.0" means that the wall system being analyzed actually had less of a heating or cooling load the any of the wood frame systems and therefore had an Effective R-value above 37.0 $\frac{\text{hr ft}^2 \text{ F}}{\text{Btu}}$. The general trends between the two figures are the same; the heating Effective R-value increases the warmer the climate and the cooling Effective R-value is above 37.0 $\frac{\text{hr ft}^2 \text{ F}}{\text{Btu}}$ for all the climates except for Phoenix. It is interesting that Phoenix has the worst effective R-value for the cooling season since it is normally thought of as the climate that will incur the greatest thermal mass benefits. Another surprise was that both thermal mass systems perform better than 37.0 $\frac{\text{hr ft}^2 \text{ F}}{\text{Btu}}$ for the heating and cooling season in Miami. Yet this trend makes sense considering the small effect the wall component load has on the total heating and cooling load in Miami as shown by the plot of total

heating and cooling energy load versus wood frame R-values in Figure 5.37. The only difference between the ICF and Sandwich PCP panel performance was that the Phoenix cooling effective R-value increase over the whole wall R-value for the Sandwich PCP panel was significantly less than that of the ICF system.

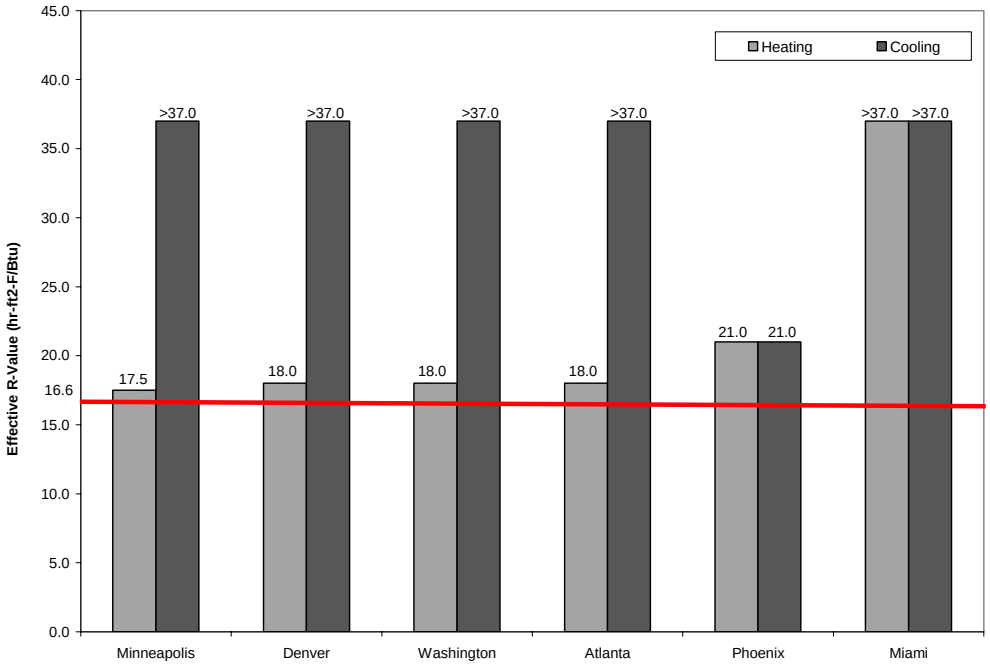

Figure 5.35. Effective R-value for the ICF system $\left(\frac{\text{hr}\ \ \text{ft}^2\ \ \text{F}}{\text{Btu}}\right)$

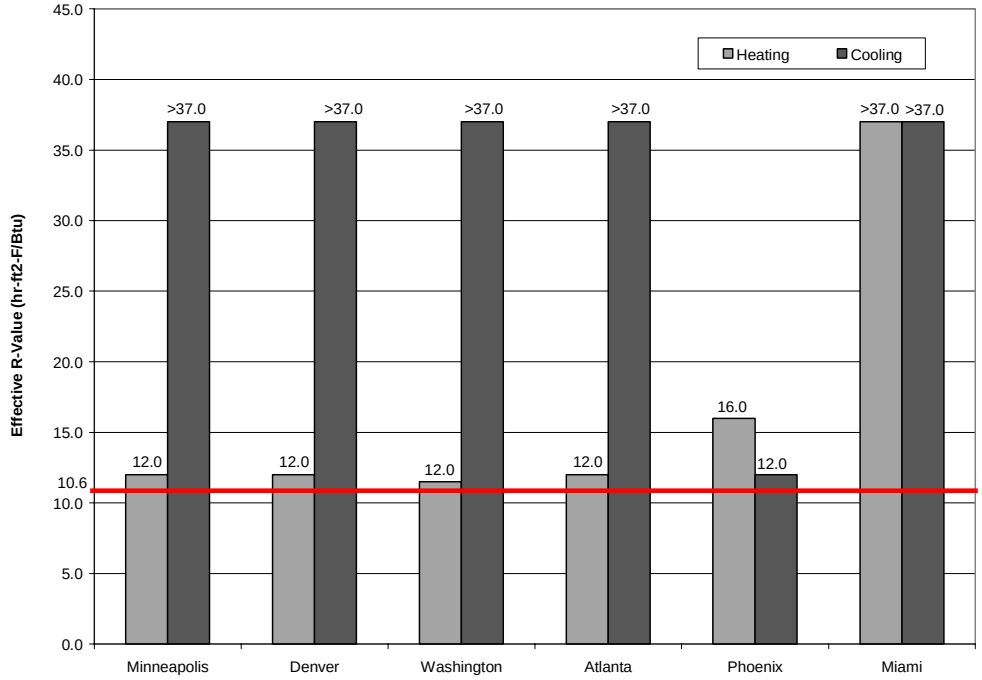

Figure 5.36. Effective R-value for the Sandwich PCP system $\left(\frac{hr\ \ ft^2\ \ F}{Btu}\right)$

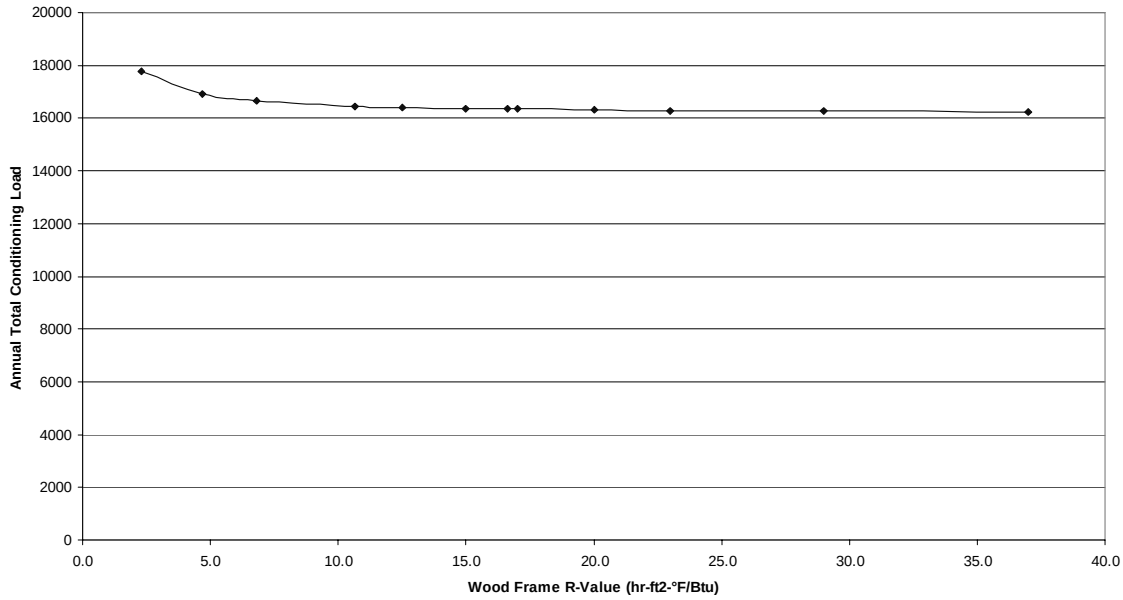

Figure 5.37. Miami total heating and cooling energy loads versus the R-value $\left(\frac{hr\ \ ft^2\ \ F}{Btu}\right)$ of the wood frame wall

In order to compare the ICF system Effective R-value results to those calculated by Kosny et al (1999), the heating and cooling Effective R-values were combined into a total Effective R-value for each prototypical house location. Essentially, the same procedure was used as the heating or cooling Effective R-value shown in the example in Figure 5.34, except the total conditioning energy was used. Table 5.14 compares the ICF system Effective R-value calculated for this study and by Kosny et al (1999). Although the Effective R-values follow the same trend relative to the climates and are very similar except for Miami, Kosny et al (1999) used a smaller ICF whole wall R-value of 12.0 $\frac{\text{hr ft}^2 \text{ F}}{\text{Btu}}$ compared to the ICF whole wall R-value of 16.6 $\frac{\text{hr ft}^2 \text{ F}}{\text{Btu}}$ used for this study. Therefore, Kosny et al (1999) calculated a significantly larger thermal mass benefit from the ICF system by obtaining similar Effective R-values for a much smaller whole wall R-value. Note that the whole wall capacitances reported in Kosny et al (1999) and in this study were very similar, 11.6 and 12.574 $\frac{\text{Btu}}{\text{ft}^2 \text{ F}}$, respectively.

Table 5.14. Effective R-value for the ICF system compared to Kosny et al (1999) $\left(\frac{\text{hr ft}^2 \text{ F}}{\text{Btu}}\right)$

	Kosny	**Calculated**
Minneapolis	16.2	18.0
Denver	20.0	18.5
Washington	19.2	19.0
Atlanta	21.1	21.0
Phoenix	22.0	21.0
Miami	21.1	37.0

Table 5.15 compares the total Effective R-value between the Sandwich PCP system from this study and a similar Sandwich PCP configuration evaluated by the Oak Ridge National Laboratory Building Technology Center (Kosny et al 2001). The Sandwich PCP configuration used in Kosny et al (2001) was two inches of rigid insulation in between two three inch layers of concrete connected by fiber composite connectors installed at 16 in on center. Kosny et al (2001) evaluated the Effective R-value based upon a clear wall R-value of 10.5 $\frac{\text{hr ft}^2 \text{ F}}{\text{Btu}}$, very similar to the Sandwich PCP system whole wall 10.6 $\frac{\text{hr ft}^2 \text{ F}}{\text{Btu}}$ used for this study.

Table 5.15. Effective R-value for the Sandwich PCP system compared to Kosny et al (2001) $\left(\frac{\text{hr}\ \ \text{ft}^2\ \ \text{F}}{\text{Btu}}\right)$

	Kosny	**Calculated**
Minneapolis	15.8	12.0
Denver	21.1	12.5
Washington	19.4	12.5
Atlanta	23.3	13.5
Phoenix	31.0	14.0
Miami	20.9	37.0

Similar to the ICF Effective R-value comparison in Table 5.14, Kosny et al (2001) calculated considerably larger Effective R-values than those for this study despite having a Sandwich PCP system with a smaller capacitance, $14.47\frac{\text{Btu}}{\text{ft}^2\ \ \text{F}}$, than the Sandwich PCP system for this study, $17.38\frac{\text{Btu}}{\text{ft}^2\ \ \text{F}}$. The best explanation for the consistently larger calculated Effective R-values of the references would be the differences in the house model used by Kosny et al (1999; 2001) and the prototypical house. Kosny et al (1999; 2001) used the typical single family residences designed by Huang et al (1987). In subsection 4.3.4, the internal heat gain by Huang et al (1987) was shown to be significantly lower then that from this study and that used in the Building America house (US DOE 2003). Also in subsection 5.1.2, the Huang et al (1999) study which was based upon Huang et al (1987) used the ASHRAE Fundamentals foundation heat loss method which has been proven to underestimate the heat flux through the foundation. Therefore, the wall component loads were much more significant in the house model used by Kosny et al (1999; 2001) than those in the prototypical house such that the performance benefits of the thermal mass walls were magnified. These discrepancies were probably the cause between the larger Effective R-values calculated by Kosny et al (1999; 2001). *These differences also illustrate the importance of the context within which the wall analysis is conducted. Different assumptions about the overall house performance can lead to different conclusions about the impact of the wall system performance.*

5.4 Conditioning Equipment Energy Savings

The following section evaluates the reduction in the prototypical house HVAC energy consumption by using the Energy Efficient Wood Frame, Sandwich PCP, and ICF wall systems

over the Conventional Wood Frame system. Subsection 5.4.1 analyzes the energy savings associated with the furnace and heating mode of the heat pump. Subsection 5.4.2 examines the energy savings associated with the CAC and cooling mode of the heat pump. Subsection 5.4.3 combines the heating and cooling energy consumption together to compare the total energy savings with the Energy Efficient Wood Frame, Sandwich PCP, and ICF wall systems against other published values.

It has been conjectured that the time delay in the maximum heating or cooling load provided by the thermally massive building envelopes would benefit a heat pump and CAC system by shifting their daily peak load to a time in the day where they would operate more efficiently. For example, a light weight, dynamic wood frame system would delay the maximum heating demand on the heat pump very little such that the heat pump would have to provide its maximum heating load when the outside weather conditions were close to the coldest temperature of the day. Conversely, a thermally massive wall system would delay the peak heating load to later in the day when the outside temperature was warmer and the heat pump could operate with a higher COP. If this physical scenario were valid, then both operations of the heat pump and CAC system would have a larger energy savings than that for the purchased heating and cooling savings shown in subsection 5.3.1. On the other hand, the efficiency of the furnace system should be relatively independent of the outside conditions.

5.4.1 Heating System Energy Consumption

Figure 5.38 shows the annual energy consumption savings for the heating mode of the heat pump with the Energy Efficient Wood Frame, Sandwich PCP, and ICF wall systems including the supplemental heat and defrost mode of the heat pump. Figure 5.39 shows the furnace annual energy consumption savings with the Sandwich PCP, Energy Efficient Wood Frame, and ICF wall systems for each prototypical house location. Both Figure 5.38 and Figure 5.39 exclude the fan energy consumption.

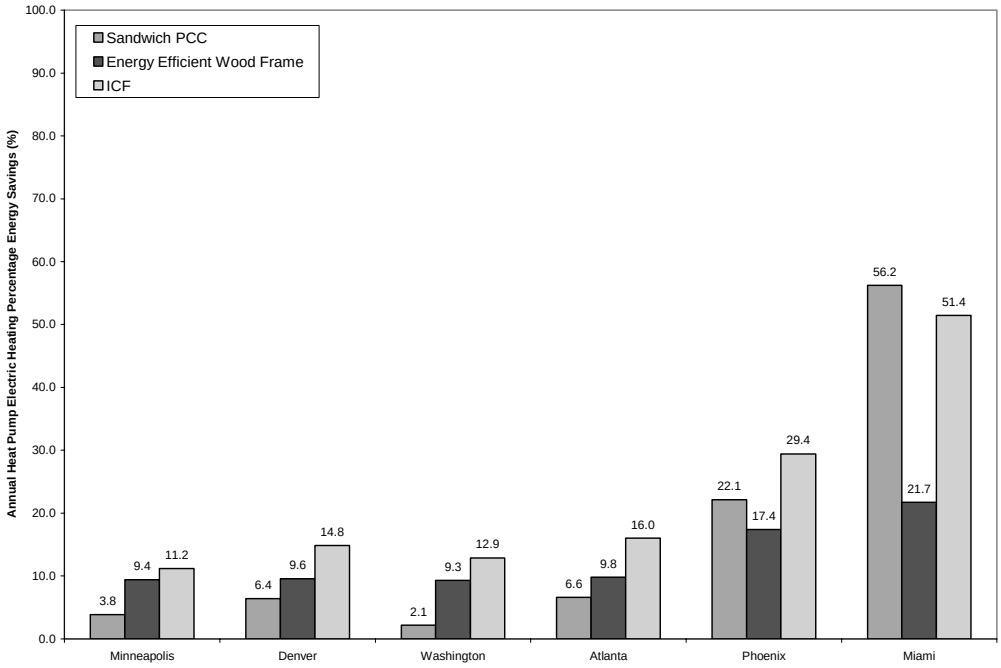

Figure 5.38. Annual heat pump heating mode energy savings with the Sandwich PCP, Energy Efficient Wood Frame, and ICF wall systems over the Conventional Wood Frame system

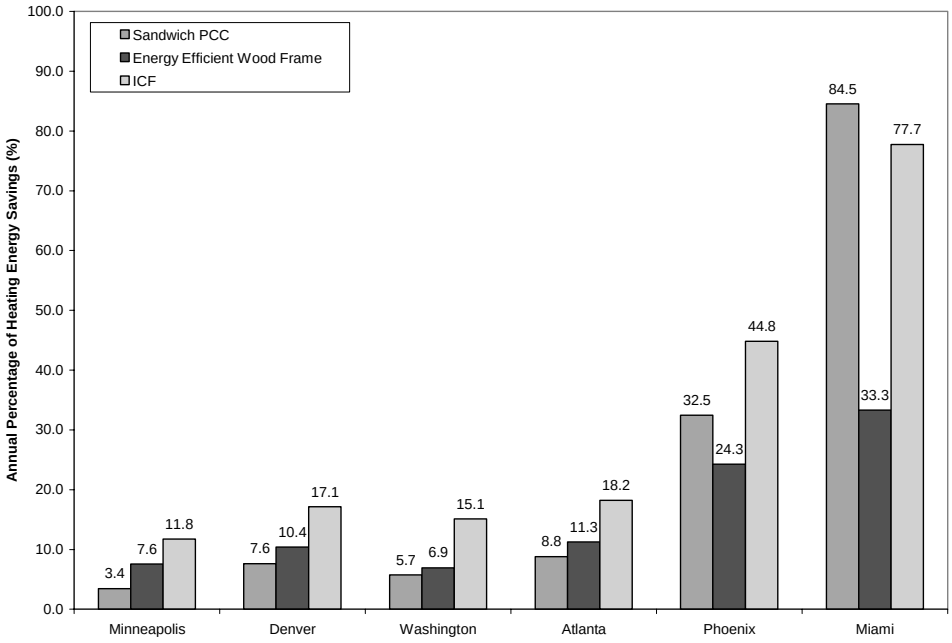

Figure 5.39. Annual furnace energy savings with the sandwich PCP, energy efficient wood frame, and ICF wall systems over the conventional wood frame system

Although, some of the savings vary by a few percent, the general heat pump heating mode and furnace energy saving trends in Figure 5.38 and Figure 5.39, respectively, are identical to those shown in the heating "purchased air" energy savings in Figure 5.30. The thermal mass benefits are only evident in the hot climates where the Sandwich PCP system performs better than the Energy Efficient Wood Frame system. In general the furnace energy savings are larger than the savings for the heating mode of the heat pump.

5.4.2 Cooling System Energy Consumption

Figure 5.40 shows the annual energy consumption savings for the cooling mode of the heat pump with the Energy Efficient Wood Frame, Sandwich PCP, and ICF wall systems for each prototypical house location. Figure 5.41 shows the CAC annual energy consumption savings with the Energy Efficient Wood Frame, Sandwich PCP, and ICF wall systems for each prototypical house location. Note that the fan electrical energy is not included in the results for either of Figure 5.40 and Figure 5.41.

The heat pump and CAC cooling energy savings have identical trends as the cooling "purchased air" energy savings shown in Figure 5.31 except in Phoenix. For the Phoenix purchased cooling savings, the Energy Efficient Wood Frame system has the same performance as the Sandwich PCP system. Yet when evaluated using an overall system model (heat pump or CAC cooling), the Sandwich PCP system has a higher performance than the Energy Efficient Wood Frame system. This result is attributable to the CAC and heat pump cooling operation working at an average higher efficiency throughout the year due to the daily thermal peak delay provided by the Sandwich PCP system as described in the beginning of this section. As expected in the temperate and colder cities, the cooling energy savings for the CAC system are slightly larger than those for the heat pump because the heat pump was sized to meet the larger heating demand therefore oversizing the cooling mode. As a result, the heat pump cooling energy in these colder climates is dominated by part load inefficiencies mitigating the effects on the energy savings. For the hot climates, the CAC and heat pump cooling energy savings are roughly the same. In general, the cooling energy savings are considerably smaller than the heating energy savings shown in Figure 5.38 and Figure 5.39 since the wall component load comprises a smaller portion of the total cooling energy load.

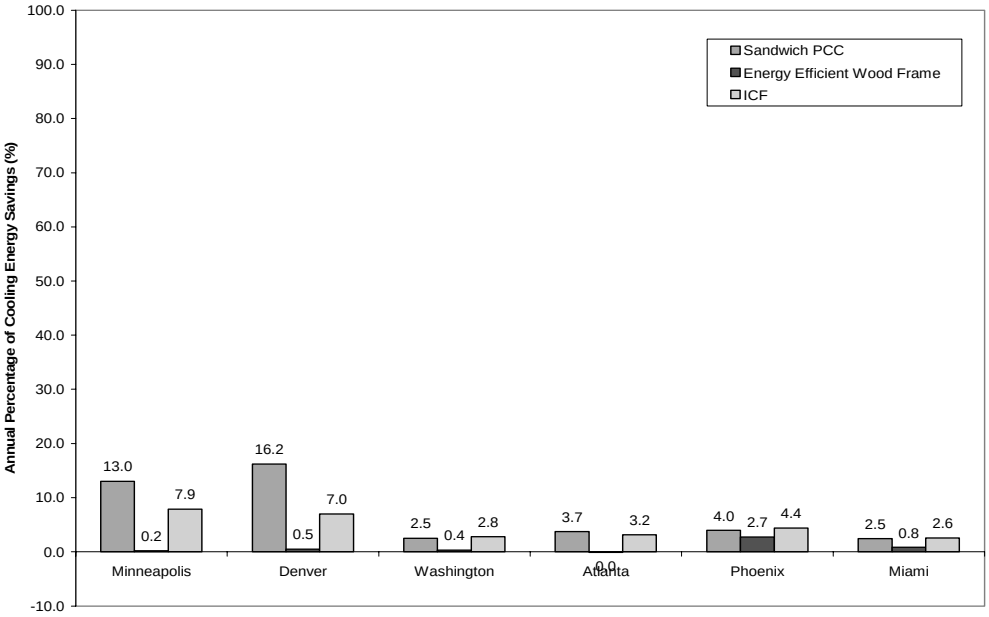

Figure 5.40. Annual heat pump cooling mode energy savings with the Sandwich PCP, Energy Efficient Wood Frame, and ICF wall systems over the Conventional Wood Frame system

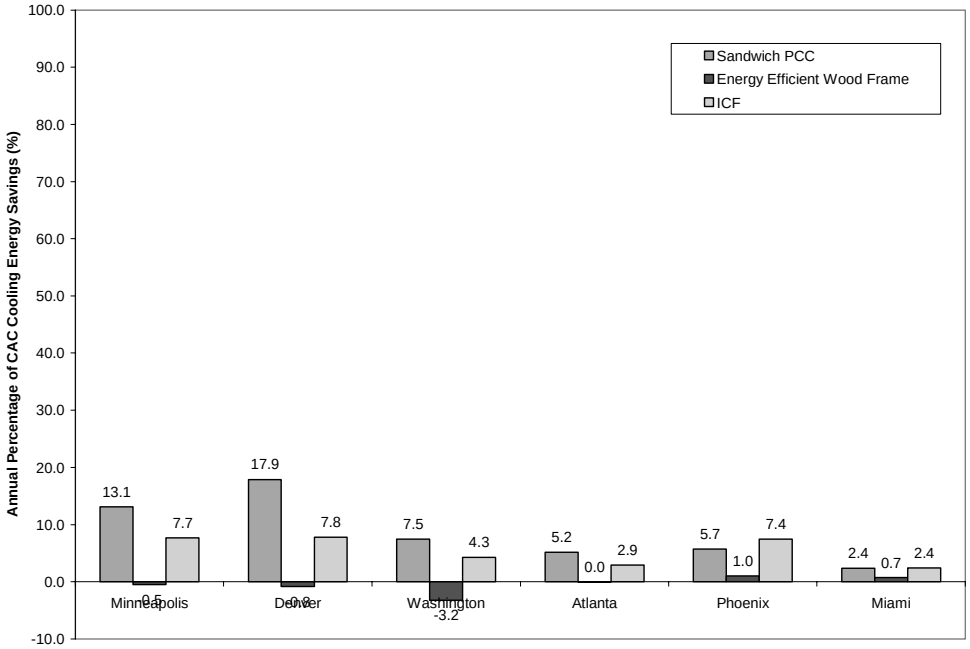

Figure 5.41. Annual CAC energy savings with the Sandwich PCP, Energy Efficient Wood Frame, and ICF wall systems over the Conventional Wood Frame system

5.4.3 Total Energy Consumption

Figure 5.42 shows the annual heat pump energy consumption including the fan energy for each wall system in all the prototypical house locations. Figure 5.43 shows the annual furnace/CAC energy consumption including the fan energy for each wall system in all the prototypical house locations. For the Sandwich PCP, Energy Efficient Wood Frame, and ICF wall systems, the percentage energy savings with respect to the Conventional Wood Frame system is shown above each bar.

For the cold and temperate climates, the relative energy savings directly correlates to the relative R-value of the wall system; the larger the R-value, the greater the energy savings. Only in the hot climates does the effect of thermal capacitance become more significant. In these hot climates, the Sandwich PCP system performs better than the Energy Efficient Wood Frame system and almost as well as the ICF system. Unfortunately, the energy savings magnitude is less the warmer the climate since the wall component load is only a small portion of the total cooling energy load. Therefore, for Miami where the greatest relative performance of the Sandwich PCP system occurs, the energy savings is roughly 3%.

Regarding the conjecture that the behavior of thermally massive walls would improve the operating efficiency of the heat pump and CAC systems, Figure 5.38, Figure 5.40, and Figure 5.41 give evidence that such a synergistic relationship does not exist. In Figure 5.38 and Figure 5.39, the furnace achieved a greater energy savings than the heating mode of the heat pump. Similarly, in Figure 5.40 and Figure 5.41, the cooling energy savings with the heat pump and CAC system alternated at being larger and smaller than the purchased air cooling energy savings in Figure 5.31. If a synergistic relationship did exist, the heat pump heating mode and the CAC/heat pump cooling mode should have saved noticeably more energy than the furnace system and purchased heating systems, respectively. The Phoenix cooling season was the only occasion where the Sandwich PCP and CAC or heat pump cooling mode combination saved more energy than the Sandwich PCP and purchased cooling feature combination.

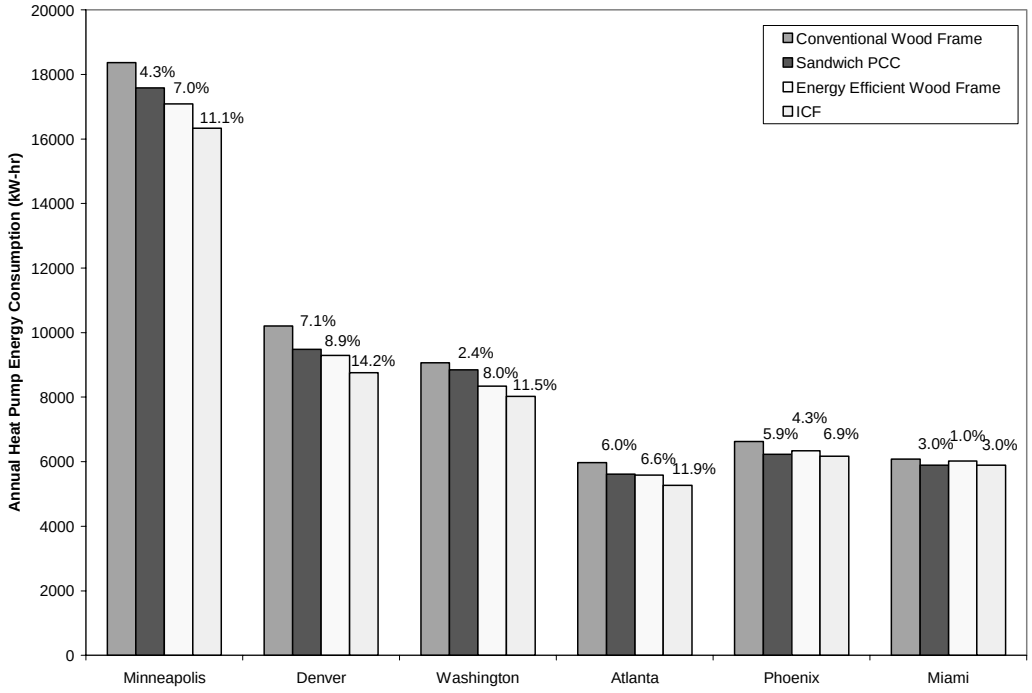

Figure 5.42. Heat pump annual energy consumption and savings for the different wall systems in each of the prototypical house locations

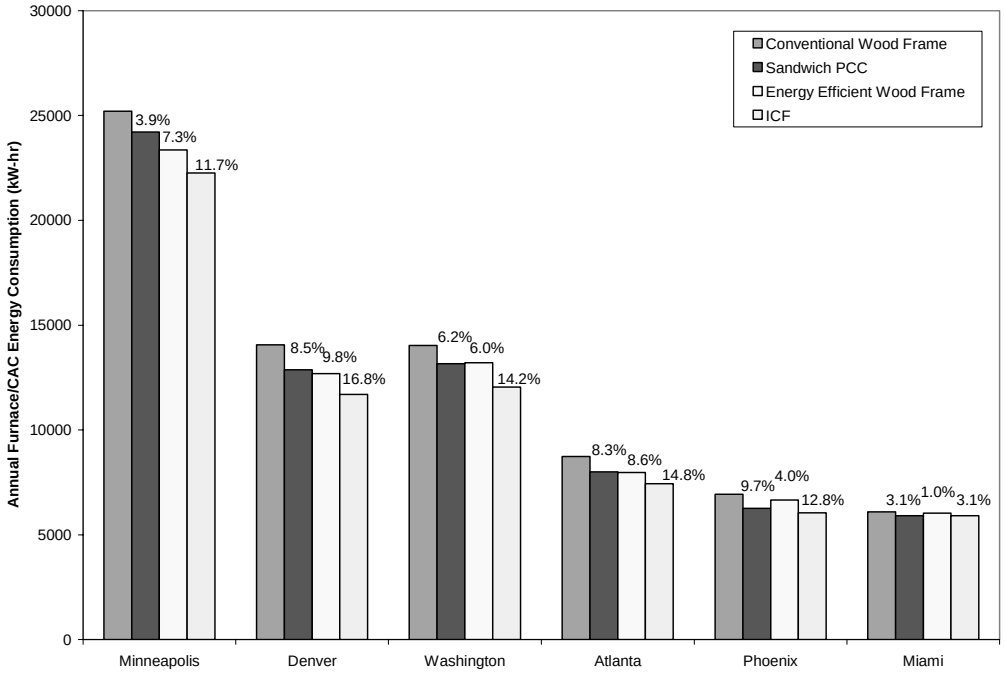

Figure 5.43. Furnace/CAC annual energy consumption and savings for the different wall systems in each of the prototypical house locations

Compared to three references which evaluate the HVAC energy savings associated with ICF and Sandwich PCP systems versuses standard wood frame systems, the total energy savings calculated in this study are consistently smaller. The most similar analysis to this study was conducted for the Portland Cement Association to evaluate the furnace/CAC energy savings associated with various exterior walls including a conventional wood frame system, flat ICF system, and a sandwich PCP system within the context of a standard, newly constructed home (Gajda 2001). Regardless of the wall system or climate, the typical house was identical except for the exterior walls. Table 5.16 compares the most important characteristics of the typical house used by Gajda (2001) and the prototypical house used for this study.

Table 5.16. Comparison of the basic features between the house used in Gajda (2001) and the prototypical house used in this study

	House used in Gajda (2001)	**Prototypical House used for this study**
Number of Stories	2	1
Conditioned Area	2450 ft^2	2275 ft^2
Window Area	392 ft^2	267 ft^2
Foundation	Slab-on-Grade	Basement

Although Gajda (2001) evaluated the same wall system types as this study, certain features were different. Table 5.17 compares the R-value and capacitance of the wall systems used in Gajda (2001) and in this study (using the whole wall analysis values). Even though Gadja (2001) evaluated the house in 25 different cities in the U.S., Minneapolis, Denver, and Washington were not simulated. Therefore, the Boulder and Baltimore results were used to compare against Denver and Washington DC, respectively, since they experience roughly the same climate conditions. Unfortunately, there was no alternative city close enough in climate for Minneapolis.

Table 5.17. Comparison of the wall systems modeled in Gajda (2001) and this study

	R-value $\left(\frac{hr\ ft^2\ F}{Btu}\right)$		**Capacitance** $\left(\frac{Btu}{ft^2\ F}\right)$	
	Gajda (2001)	Prototypical House	Gajda (2001)	Prototypical House
Conventional Wood Frame	12.8	9.5	< 1.0	2.5
Flat ICF	21.7	16.6	18.5	12.6
Sandwich PCP	11.1	10.6	29.0	17.4

As shown in Table 5.17, Gajda used R-value that were typically higher which possibly reflected clear wall values. Also, Gajda used thermal capacitances for the ICF and Sandwich PCP walls that were significantly larger than that used for this study because Gajda modeled ICF and Sandwich PCP configuration with considerably more concrete. Consequently, the wall systems evaluated in the current study should be more representative of their actual thermal performance for two reasons. First, the whole wall analysis was used thereby incorporating the wall detail effects other than the clear wall section. Second, the ICF and Sandwich PCP systems were modeled from commercially available products currently on the market. The thickness used by Gadja to obtain the larger thermal capacitance seems excessive compared to realistic wall dimensions.

Finally Table 5.18 compares the total energy savings for the furnace/CAC system for the ICF and Sandwich PCP systems in reference to the Conventional Wood Frame System between Gadja (2001) and this study. The ICF system energy savings between the two studies were close. On the other hand, results for the Sandwich PCP system differed significantly between the two studies. Although the Sandwich PCP R-values were similar, as shown in Table 5.17, this study calculated lower energy savings compared to Gadja (2001). Therefore, the considerably greater capacitance modeled with the ICF system in Gadja resulted in larger thermal mass effects.

Table 5.18. Comparison of furnace/CAC system energy savings (with respect to the Convetional Wood Frame system) for the ICF and Sandwich PCP systems reported in Gadja (2001) and this study

	ICF		**Sandwich PCP**	
	Gadja (2001)	**Prototypical House**	**Gadja (2001)**	**Prototypical House**
Denver/Boulder	14%	17%	11%	8%
Washington/Baltimore	13%	14%	9%	6%
Atlanta	16%	15%	14%	8%
Phoenix	10%	13%	10%	10%
Miami	11%	3%	9%	3%

The second study to which the current results are compared was a NAHB study (NAHB Research Center 1999) in which three identical residences were constructed side-by-side in Chestertown, Maryland with different wall systems, an ICF plank system, an ICF block system, and a conventional 2x4 wood frame system. From conducting an extensive investigation concerning the heating and cooling energy consumption and thermal loads on the building, the study concluded that the heat pump system in the ICF homes consumed approximately 20% less energy than the heat pump in the wood frame home. The study also addressed infiltration using blower door and tracer gas tests and concluded that there was no significant difference in the air leakage between the three homes. Since Washington DC and Chestertown, Maryland have similar climates, the current prototypical house was compared to the NAHB study. The results show that the prototypical house model predicts somewhat lower energy savings (11.5% than the NAHB study of 20%).

Based on the conclusions drawn in the NAHB study, there is a reasonable explanation for the discrepancy between the NAHB energy savings and those calculated for the prototypical house. The higher energy performance of the two ICF homes was attributed to two aspects; the higher R-value of the ICF over the wood frame system and the direct contact between the slab and foundation block for the wood frame home compared to the ICF homes which contained a continuous insulation layer from footer to roof line. This poorly designed wall-slab connection detail in the wood frame house resulted in “greater heat loss in February and greater heat gain in August as evidenced by the wood-frame home’s more pronounced and direct response to outdoor temperature changes” (NAHB Research Center 1999). Therefore, the prototypical house

modeled with conventional wood frame construction exhibited a greater energy performance than the base house in the NAHB study because the foundation for the typical house was a basement which provided better insulation than the extremely detrimental wall detail in the NAHB study.

The third study to which the current results are compared was based on an energy survey obtained from 29 pairs of houses, each pair representing an ICF and Wood Frame home in the same general location and with similar construction features (VanderWerf 1997). The energy consumption information was obtained from monthly utility bills in which the standard used in energy research to discriminate building energy bills into the heating, cooling, and appliance energy consumptions was applied. Since the study was based upon survey data, the characteristics of the homes varied appreciably from the prototypical house. Yet, the study by VanderWerf (1997) was a useful comparison because it represented the general residential building industry perception of energy savings associated with ICF construction.

Table 5.19 shows the average, lower, and upper percent of annual energy consumption savings of ICF systems over Conventional Wood Frame systems based on a 95% confidence interval as published in VanderWerf (1997).

Table **5.20** shows the average, low, and high annual energy consumption for the furnace/CAC system in the prototypical house. One simple reason explains the discrepancy between
Table **5.19** and

Table **5.20**. The ICF system energy savings in the prototypical house did not account for any infiltration reduction which has been sited as a major thermal performance benefit of ICF walls (Kosny et al. 1999; VanderWerf 1998).

Table 5.19. Annual heating and cooling energy savings obtained from an energy survey comparing the performance of ICF and wood frame systems published in VanderWerf (1997)

	95% Confidence Interval		
	Average	**Lower Bound**	**Upper Bound**

Energy Consumption Savings	41.9%	33.9%	50.0%

Table 5.20. Annual heating and cooling energy savings for the ICF system from the prototypical house model

	Average	**Lower Bound**	**Upper Bound**
Energy Consumption Savings	12.2%	3.1%	16.8%

5.5 Infiltration Reduction Effects

Summarized in subsection 4.3.6, there is considerable controversy regarding whether concrete wall technologies like the ICF and Sandwich PCP systems reduce the ELA such that the infiltration load is significantly reduced. As stated in subsection 5.4.3, the NAHB Research Center determined that there was no difference in infiltration between the wood frame and 2 ICF homes built for the study. Yet the authors did claim that the lack of difference in infiltration rates could be due to the fact that the homes were extremely small, roughly 1098 ft^2, and had a slab-on-grade foundation. In other words, for a larger home with a basement foundation, the air leakage associated with the exterior walls would be more significant such that an ICF system could have a noticeable impact on the infiltration rate.

Conversely, a study conducted by an infrared camera company evaluated the leakage area for seven ICF homes in southwestern U.S (Thompson 1995). Table 5.21 shows the resultant normalized leakage areas (ELA_N) calculated for each of the seven ICF homes. As evident in Table 5.21, the ELA_Ns are well below the leakage area distribution modeled in the prototypical house with a 1.21 ELA_N. Therefore, the energy savings of the prototypical house constructed with the ICF and Sandwich PCP systems with a reduced leakage area distribution were calculated with respect to the Conventional Wood Frame system with the original leakage area distribution. The new leakage area distribution had a 0.76 ELA_N based upon the same air leakage distribution as the original case except all the leakages associated with the exterior walls reduced from the maximum to best estimate ELA. This leakage area corresponded well to the

leakage area ranges specified for tightly constructed homes according to ASHRAE Standard 119 shown in Table 4.11. Although the new leakage area is still larger then those shown in Table 5.21, any further reduction would result in an infiltration rate well below the minimum required for proper ventilation. Therefore, a smaller leakage area would require mechanical ventilation which is described later in this section. For future reference, the 1.21 ELA_N and 0.76 ELA_N will be referred to as the maximum ELA and best estimate ELA, respectively.

Table 5.21. ELA_N calculated in Thompson (1995) for seven ICF homes in southwestern U.S.

Home	ELA_N
1	0.35
2	0.60
3	0.48
4	0.44
5	0.33
6	0.38
7	0.27

Figure 5.44 shows the average annual infiltration rate for the maximum ELA and best estimate ELA for each of the prototypical house locations. The red line corresponds to the minimum infiltration rate of 0.35 ACH specified by ASHRAE Standard 62 (1999) for proper ventilation in a home. Consequently, the maximum ELA meets the minimum ventilation requirement for all the cities except Phoenix. The best estimate ELA, on the other hand, does not meet the minimum ventilation rate for any of the prototypical house locations indicating that supplemental ventilation would be required.

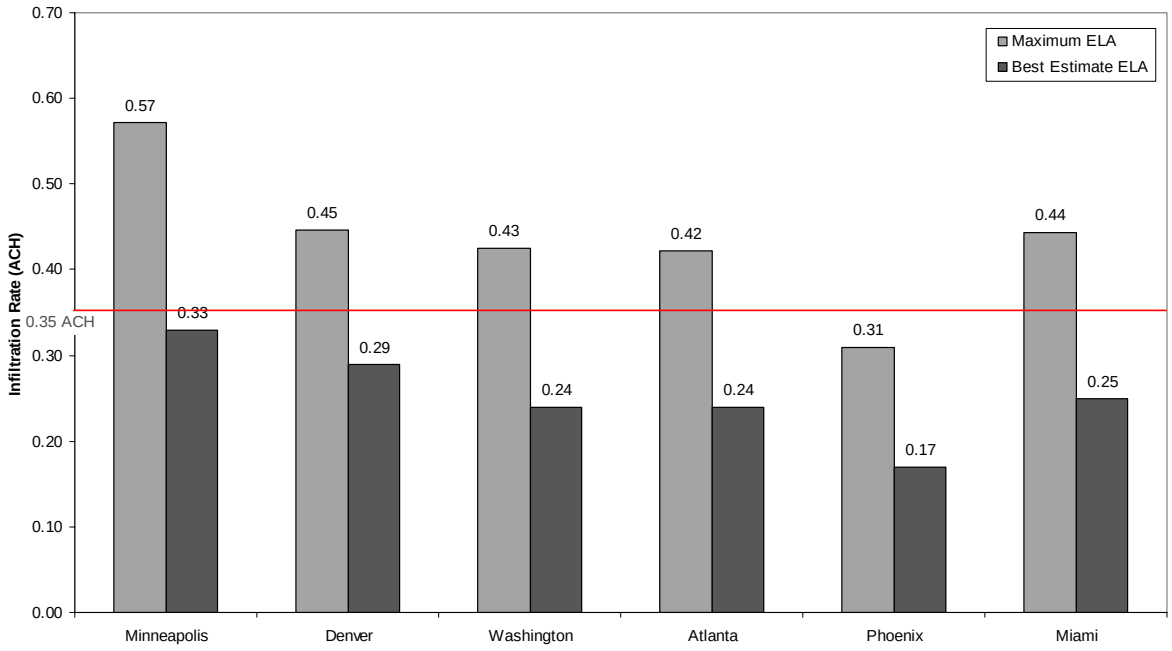

Figure 5.44. Annual average infiltration rate for each prototypical house location for the maximum ELA and best estimate ELA

The inability of a home to meet the minimum ventilation rate strictly through infiltration has been cited as a major problem with newer construction resulting in what is called "sick" buildings (ECCO 1999). The emission of toxins into the air from standard building materials and the operation of typical household appliances can have a detrimental effect on the health of the occupants in a home. This is the reason that Canada is requiring mechanical ventilation in all new residential construction (ASHRAE 2001a). Yet the installation of mechanical ventilation in the U.S. is rare since most builders assume that the house is loose enough to meet the minimum 0.35 ACH.

There are essentially two choices for mechanical ventilation to be implemented into the HVAC system of a home. The cheapest way is to attach a small inlet pipe that brings in a certain amount of outside air that mixes with the return air before entering the HVAC system. Although this method is cheap, roughly an extra $200 installation cost, it can significantly increase the energy consumption of the HVAC system since the mixed return air is no longer near the conditioned space conditions. The other method is to install an air-to-air heat exchanger which warms the outside air brought into the return air using the air exhaust from the house. Although

this method has a large installation cost due to the purchasing of the heat exchanger, between $1000 to $2000, it increases the energy consumption of the HVAC system much less (Sherman and Matson 1998) than direct introduction of outside air.

The effect of reduced infiltration on energy was evaluated by assuming that the ELA was reduced to the best estimate and that supplemental ventilation was either not provided or that is was provided through an air-to-air heat exchanger so that the energy effect of the supplemental ventilation was small. Table 5.22 shows the total energy savings including the fan energy of the heat pump system for the ICF and Sandwich PCP systems with the best estimate ELA over the Conventional Wood Frame system with the maximum ELA. Table 5.23 shows the total energy savings including the fan energy of the furnace/CAC for the ICF and Sandwich PCP systems with the best estimate ELA over the Conventional Wood Frame system with the maximum ELA for each city.

Table 5.22. ICF and Sandwich PCP system heat pump energy savings with reduced infiltration over the Conventional Wood Frame system

	Minneapolis	**Denver**	**Washington**	**Atlanta**	**Phoenix**	**Miami**
Sandwich PCP	22%	24%	22%	22%	1%	11%
ICF	29%	31%	30%	27%	9%	11%

Table 5.23. ICF and Sandwich system furnace/CAC energy savings with reduced infiltration over the Conventional Wood Frame system

	Minneapolis	**Denver**	**Washington**	**Atlanta**	**Phoenix**	**Miami**
Sandwich PCP	27%	31%	28%	30%	6%	12%
ICF	35%	39%	36%	36%	15%	12%

As shown in Table 5.22 and Table 5.23, the energy savings associated with both the heat pump and furnace/CAC systems increases considerably when including the reduction infiltration. The results also show that the furnace/CAC system consistently experiences a larger energy savings than that for the heat pump system for both the Sandwich PCP and ICF technologies for all the cities. Compared to the energy savings in VanderWerf (1997), the prototypical house with reduced infiltration still has lower energy savings but significantly closer than the energy savings without the infiltration reduction. This suggests that the energy savings reported for concrete

wall technologies may be largely due to reduced infiltration. The amount that the infiltration rate is reduced depends directly on the leakage area distribution and will most likely vary depending on the construction. As stated in the 2001 ASHRAE Fundamentals Handbook (ASHRAE 2001a), the lack of quality control at a construction site can lead to a wide range of leakage area.

5.6 Cost Analysis

The total energy savings shown in sections 5.4 and 5.5 were used to determine the annual conditioning energy monetary savings of the Energy Efficient Wood Frame, Sandwich PCP, and ICF systems over the Conventional Wood Frame system for each prototypical house location. The price per energy unit of electricity and gas for each prototypical house location, by state, was obtained from the 2003 Energy Databook (US DOE 2002) and is shown in Table 5.24.

Table 5.25 shows the heat pump and furnace/CAC annual energy cost including the fan energy consumption for the Conventional Wood Frame system which represented the base case to calculate the energy savings associated with the other wall systems.

Table 5.24. Electricity and gas prices per energy unit (US DOE 2002)

	Electricity Price (Cents per Kilowatthour)	**Gas Price** (Dollars per MMBtu)
Minnesota	7.49	8.73
Colorado	7.37	7.61
Washington	7.82	13.27
Georgia	7.63	12.06
Arizona	8.27	10.98
Florida	8.16	16.43

Table 5.25. Annual heat pump and furnace/CAC energy bill for the Conventional Wood Frame system for each of the prototypical house locations

	Minneapolis	**Denver**	**Washington**	**Atlanta**	**Phoenix**	**Miami**
Heat Pump	$1,376	$752	$709	$456	$548	$496
Furnace/CAC	$798	$411	$687	$435	$535	$497

This analysis included another wall system which was a modification to the Sandwich PCP system. Based upon the energy saving results, it was deemed necessary to compare the energy cost savings of a Sandwich Panel wall system with roughly the same amount of insulation as the

ICF system. Therefore, the new Sandwich PCP system incorporated 5" of rigid insulation in between two layers of concrete compared to the original 3" insulation layer. This is the maximum amount of insulation commercially available for Sandwich PCP systems since the wider the space between the two concrete layers, the longer the composite fiber connectors have to be (Composite Technologies 2004). For future reference, the Original Sandwich PCP system refers to the wall system with 3" of insulation and Modified Sandwich PCP system refers to the wall system with 5" of insulation. Rather then evaluating the steady state and dynamic performance of all the wall details, the Modified Sandwich PCP system whole wall R-value, capacitance, and capacitance distribution was calculated for the clear wall and changed by the same percentage as that of the clear wall to whole wall Original Sandwich PCP system.

Table 5.26 shows the increase in the annual mortgage payment from the increased exterior wall construction cost associated with the Energy Efficient Wood Frame, ICF, and Sandwich PCP systems with respect to the Conventional Wood Frame exterior wall construction cost. The mortgage is assumed to be over 30 years at a 7% interest rate. Since the ICF and Sandwich PCP wall technologies are relatively new compared to wood frame systems, they have a low to high estimate for the increase in the annual mortgage payment since they have greater cost variability mainly dependent on the experience by the contractor and construction crew. For the Sandwich PCP system, the low to middle range represents a stucco exterior façade and the mid to high range represents a brick or stone façade (Long 2004). The cost difference between the Original and Modified Sandwich PCP was considered negligible because the cost range of the Sandwich PCP system was so wide. The low to high range for the ICF system represents the typical cost range of construction for a semi-experienced crew across the country (ICFA 2004) and includes a vinyl siding finish.

Table 5.26. Increase in annual mortgage payment due to the increase in the construction cost associated with the Energy Efficient Wood Frame, ICF, and Sandwich PCP systems with respective to the construction cost for the Conventional Wood Frame system

Energy Efficient Wood Frame	ICF		Sandwich PCP		
	Low	High	Low	Middle	High
$50	$312	$520	$267	$475	$683

Figure 5.45 (a) and (b) compares the annual furnace/CAC and heat pump energy savings, respectively, of the Sandwich PCP system to the range of additional annual mortgage payment for each of the prototypical house locations. The first bar for each city shows the energy savings associated with the original Sandwich PCP system which incorporated 3" of rigid insulation subdivided into the thermal mass and increased insulation benefits. The second bar for each city shows the energy savings associated with a modified Sandwich PCP system which incorporates 5" of rigid insulation also subdivided into the thermal mass and increased insulation benefits. The third bar represents the possible energy savings if the Modified Sandwich PCP construction has a lower leakage area distribution and therefore, reduces the infiltration rate as discussed in subsection 4.3.6. More specifically, this bar is the energy savings of the modified Sandwich PCP system modeled with the best estimate ELA compared to the Conventional Wood Frame system modeled with the maximum ELA.

Figure 5.46 (a) and (b) compares the annual funace/CAC and heat pump energy savings, respectively, of the ICF system to the range of additional annual mortgage payment for each of the prototypical house locations. The first bar for each city shows the energy savings with the ICF system broken down into the thermal mass and increased insulation benefits. The second bar represents the possible energy savings if the ICF construction modeled with the best estimate ELA with respect to the Conventional Wood Frame construction modeled with the maximum ELA. Finally, Figure 5.47 shows the furnace/CAC and heat pump energy savings associated with the Energy Efficient Wood Frame system for each of the prototypical house locations.

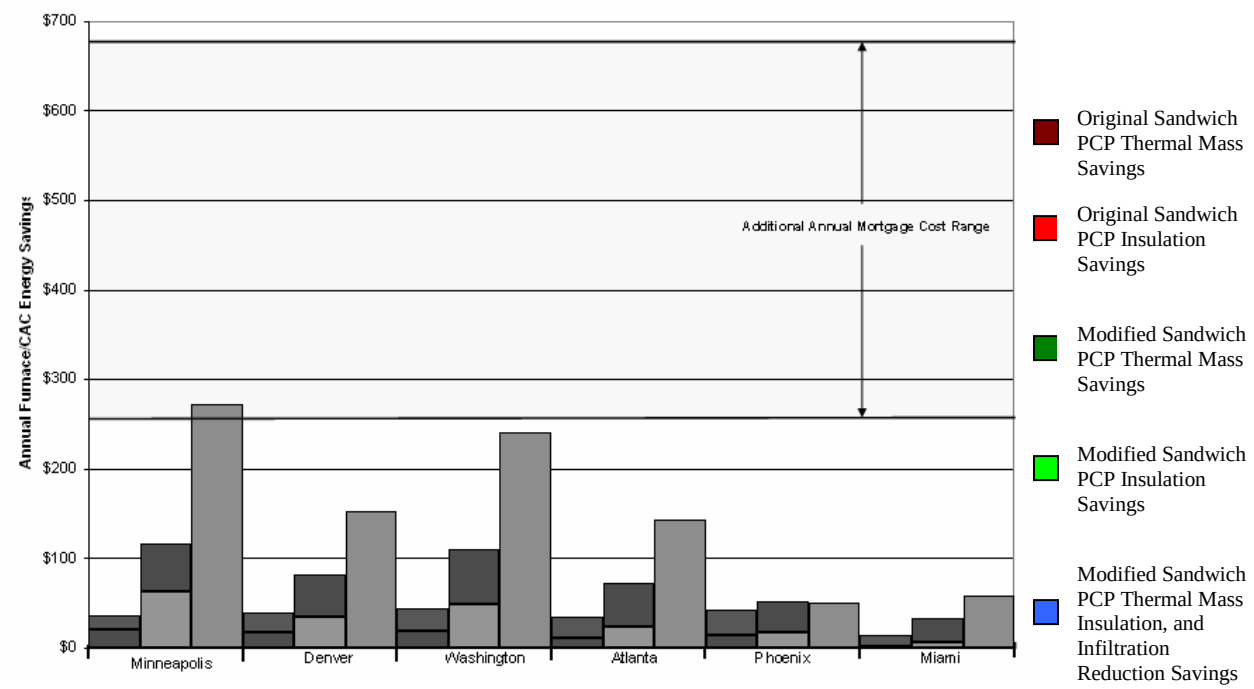

(a) Furnace/CAC System Energy Savings

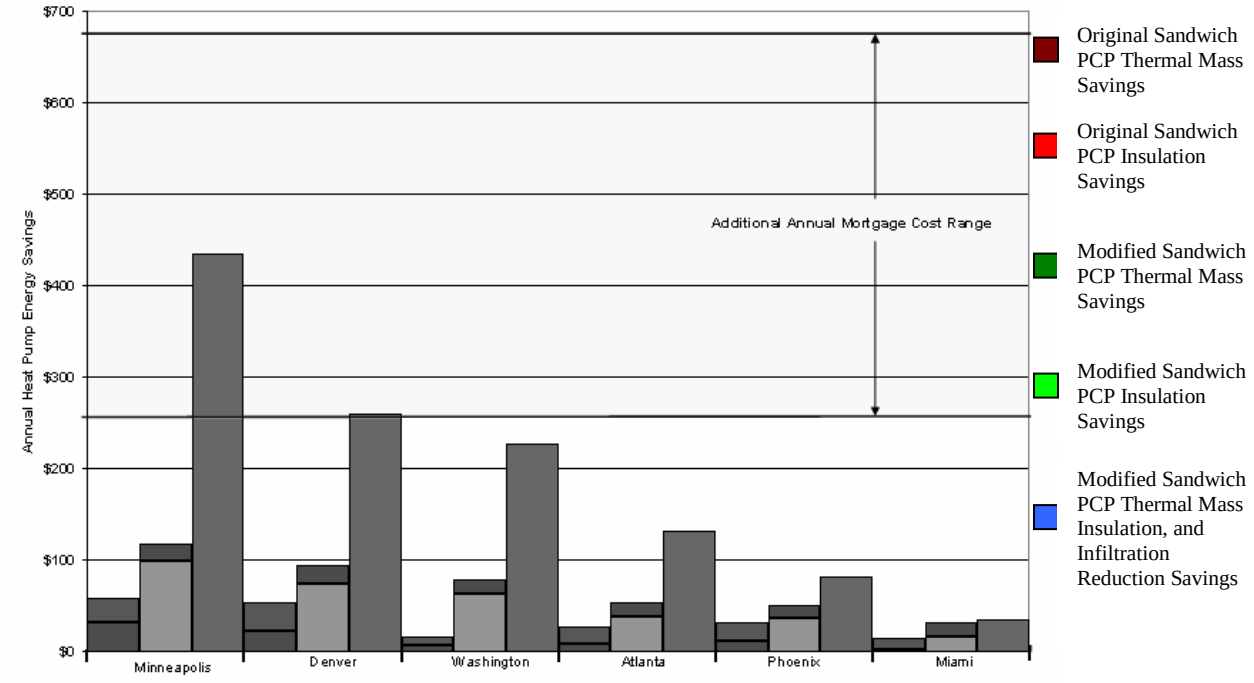

(b) Heat Pump System Energy Savings

Figure 5.45. Original and Modified Sandwich PCP annual furnace/CAC energy savings broken down into thermal mass, insulation, and infiltration reduction benefits

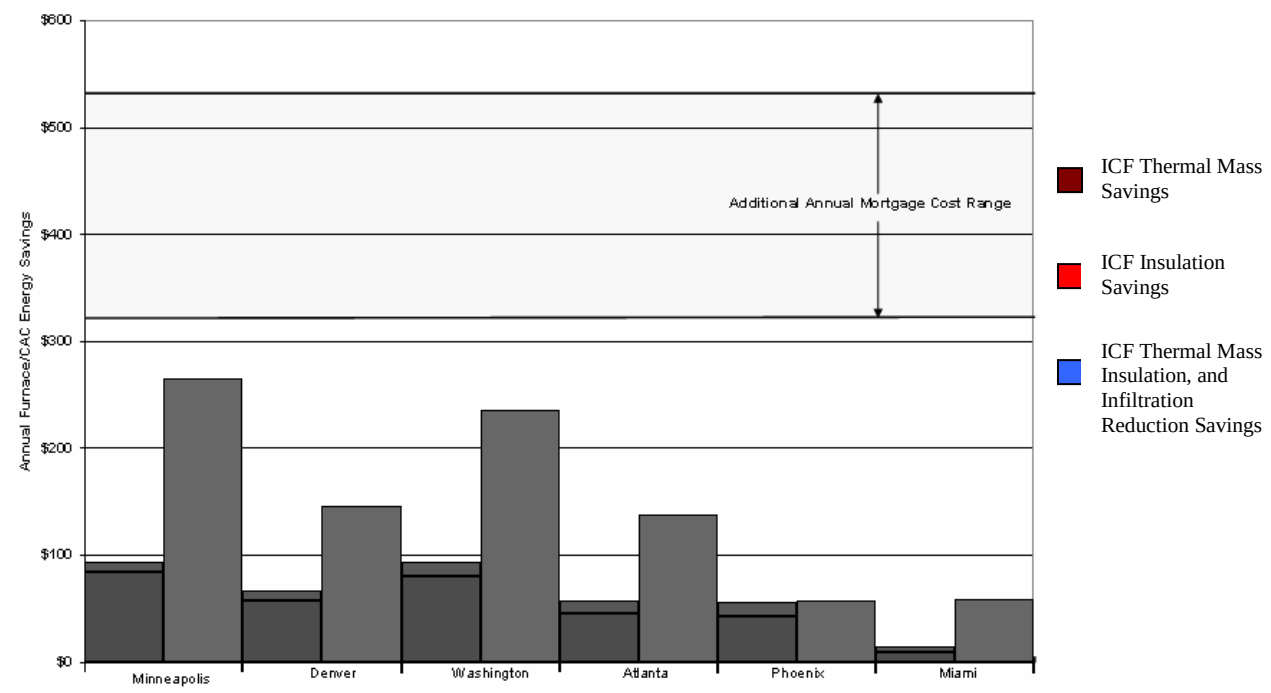

(a) Furnace/CAC System Energy Savings

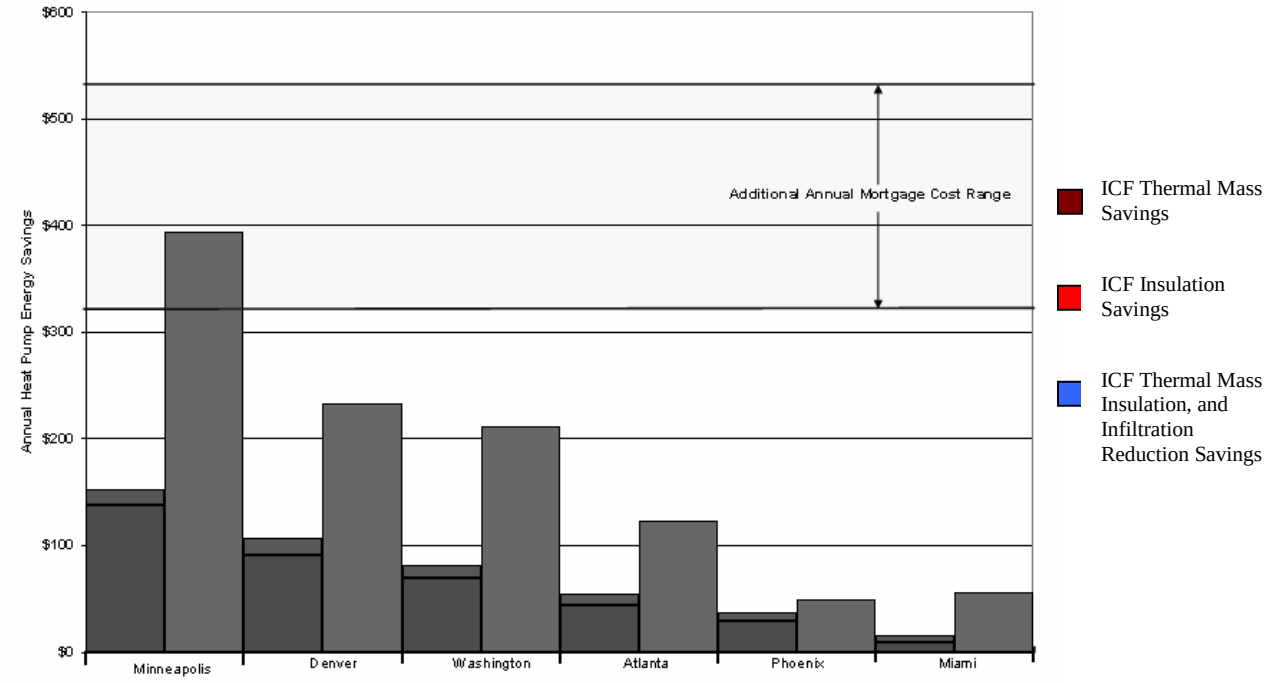

(b) Heat Pump System Energy Savings

Figure 5.46. ICF annual furnace/CAC energy savings divided into thermal mass, insulation, and infiltration reduction benefits

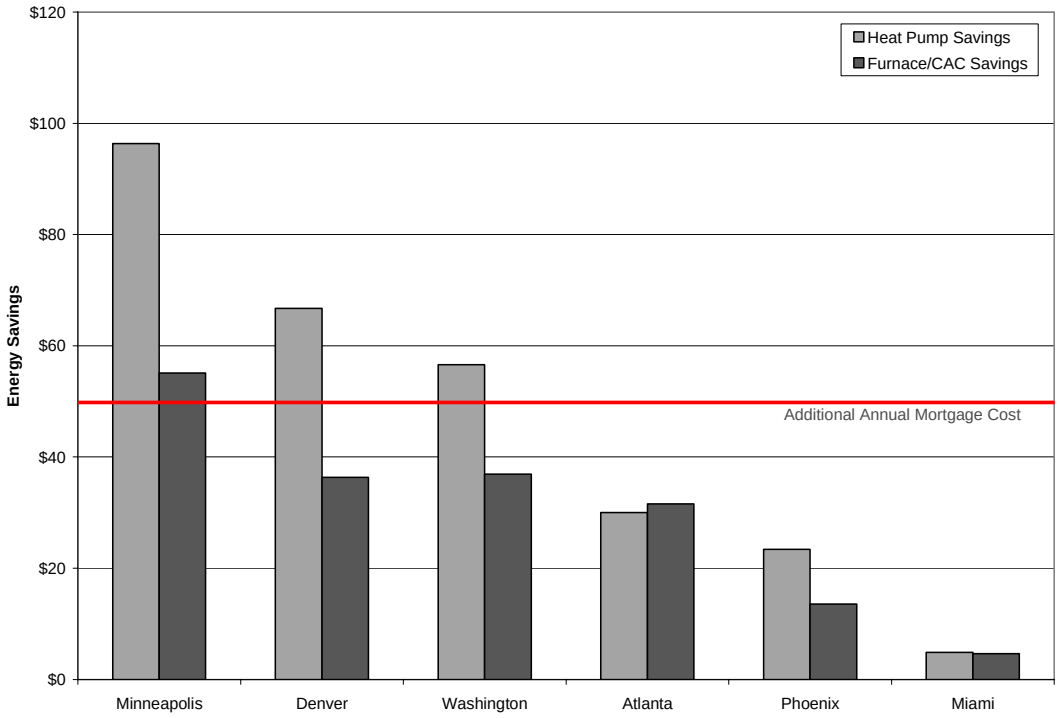

Figure 5.47. Energy Efficient Wood Frame annual heat pump and furnace/CAC energy savings

Figure 5.45 (a) and (b) indicate that the Sandwich PCP system only approaches the lower range of the additional annual mortgage cost range for the colder climates with the modified, 5" insulation system and assuming that the system will provide infiltration reduction. Figure 5.46 (a) and (b) shows the same trend with the ICF system. Therefore, both the ICF and Sandwich PCP systems only become cost effective in colder climates if they do provide infiltration reduction. The thermal mass benefits for the ICF and Sandwich PCP were negligible compared to the energy savings provided by the increased insulation over the Conventional Wood Frame system. Other then the cold climates where heat pumps perform poorly, the energy savings between the furnace/CAC and heat pump systems were similar.

Figure 5.47 shows that the Energy Efficient Wood Frame system was cost effective for colder climates. The energy savings associated with the Energy Efficient Wood Frame system was much smaller compared to that of the ICF and Sandwich PCP systems. However, it becomes an economical alternative because the increase in the cost of construction is much less than that of the concrete systems.

CHAPTER 6: CONCLUSION

The main conclusion from the work presented here is that precast concrete panel (PCP) wall technologies can improve the heating and cooling energy performance of detached, single family homes. Yet this conclusion is subject to three important qualifications.

First, the PCP wall design must maintain a nearly continuous insulation barrier surrounding the entire conditioned space with as little thermal bridging as possible. For the clear wall, floor, and ceiling areas, the PCP structural elements that consist of highly conductive concrete and metal must not penetrate the insulation layer. The ICF and Sandwich PCP systems are prime examples of how to minimize any degradation to the insulation layer by incorporating low conductive fiber composite connectors to attach the various layers. On the other hand, the Waffle PCP technology provides an example of how a concrete support and even a 16 gage steel nailer that spans across the insulation barrier can drastically reduce the thermal performance of the overall wall system.

A good guideline is to keep the clear wall R-value within 5% of the center-of-cavity R-value. This figure sets a much higher standard than the 15% center-of-cavity to clear wall R-value reduction of wood frame systems. The ICF system obtained a 4% reduction while the Sandwich PCP system achieved an impressive reduction of less then 1%. Note that the slightly greater reduction by the ICF system can be explained by its larger R-value. The greater the R-value of the wall system, the more magnified any thermal bridge effect will be.

In addition to the clear wall, more attention should be paid towards designing wall details to minimize breaks in the insulation barrier. Current design approaches often disregard the thermal performance of wall details because their effects on the overall wall system insulative behavior is considered to be negligible. In actuality, the application of the detail influence factor (DIF) showed that wall details normally account for roughly 50% of the overall wall thermal performance since the effects of the thermal bridges propagate well into the clear wall area. The wall details typically experience more thermal bridging than the clear wall area. Therefore, the larger the clear wall DIF, the better the overall wall performance will be. The wall details to pay

particular attention to are the wall/window connections because they affect the largest clear wall area and the wall/floor connections because they are directly connected to the foundation construction which essentially acts as a heat sink. Again, the ICF and Sandwich PCP systems exemplify well designed wall details with properly configured insulation to reduce wall detail thermal bridging effects. Conversely, the Waffle PCP system shows that wall details that have significant thermal bridging can have a considerable detrimental impact on the overall wall thermal performance.

For the whole wall, a good design objective is to maintain the whole wall R-value within 20% of the center-of-cavity R-value. Note that the whole wall R-value will vary depending on the detail of the house construction. Using the same wall technology, a simple rectangular home will have a smaller reduction than a complex house configuration since the later will have a much larger wall detail to clear wall area ratio. All the wall systems analyzed in this study, except for the Waffle PCP system, experienced approximately a 20% reduction from clear wall to whole wall R-value. Getting much below this value would be extremely difficult because some penetrations to the insulation barrier must occur for structural support of the exterior finish.

The second qualification to the observation that concrete wall systems improve energy performance concerns thermal capacitance effects. Although the prototypical house simulation results did show thermal capacitance benefits, a wall system should never be designed with equal emphasis on R-value and capacitance. In other words, the insulation configuration should not be compromised to incorporate thermal capacitance. Massive materials such as concrete should always be designed around the insulation specifications. The wall thermal performance during the dominant season will depend almost entirely on the R-value. Therefore, the insulation barrier is the most important in cold and temperate climates while the conditioning system is heating and hot climates while the conditioning system is cooling. Although there are slight thermal capacitance benefits during the primary season of a house, the main benefit occurs during the secondary season.

Interestingly, a higher R-value of a wood frame system increases the cooling loads for cold and temperate climates. The reason for this behavior is that the solar and internal gains from

appliances and occupants is so large that cooling occurs even when the outside temperature is lower than the inside temperature. During these times, the walls act as heat sinks transferring heat from the conditioned spaces. Consequently, the larger the R-value, the lower the transfer of heat out of the zone. High mass walls change this behavior by absorbing a greater amount of energy which is then slowly transfered to the outside while the interior temperature is higher than the outside temperature. Essentially, the more energy absorbed by the walls, the less energy the air conditioner or heat pump has to use to cool the space. Therefore, thermal mass is most beneficial inside the insulation barrier so it has greater access to heat surges inside the conditioned spaces. This is why the Sandwich PCP houses, which had a lower R-value but a higher capacitance that was distributed mostly inside the insulation barrier, consumed less cooling energy than the ICF houses in the cold and temperate climates.

As a result, to improve the thermal performance of a wall system in addition to a large R-value, a significant amount of mass should be incorporated inside the insulation barrier. The reduced energy consumption will vary depending on the climate and the operating condition of the house. For climates with extremely small secondary seasons, such as heating in Miami, thermal capacitance can completely eliminate the need for a secondary conditioning system. For climates with a more considerable secondary season, such as cooling in Minneapolis, the energy savings ranges from 5% to 15%. The more equally balanced the heating and cooling seasons become (i.e. temperate climates) the smaller the thermal mass benefits become.

The conclusions from this study concerning thermal capacitance agree with the general perception regarding the benefits of thermal capacitance but disagree with common perceptions regarding the climates that are aptly suited for these benefits. It has been understood for some time that thermal capacitance performs best when the daily outdoor temperature range swings into the setpoint temperature deadband. This coincides well with the greatest thermal capacitance benefits occurring in secondary seasons of a climate where the outside temperature most frequently swings in and out of the setpoint temperature deadband. Yet thermal capacitance benefits are thought to be maximized in temperature climates rather than extreme climates. The results from this study contradict that thinking showing that extreme climates are

best suited for thermal capacitance since the mass will reduce the conditioning during the secondary season.

The third qualification to the observation that concrete wall systems improve energy performance involves infiltration reduction. Few studies have focused on whether concrete wall systems reduce infiltration and those that do, contradict one another. One unanimous conclusion made by many publications is that the wall system itself comprises a small portion of the total envelope leakage area. The published estimate that 35% of the leakage area distribution is attributable to the wall (ASHRAE 2001a) is mainly comprised of the cracks in the wall/ceiling and wall/floor connections. Therefore, to consider that ICF and PCP systems reduce infiltration, most of the leakage area reduction must be in these connection details. This is another area where PCP systems have a much greater potential than ICF systems since precast systems which are manufactured in a quality controlled environment can result in a much tighter construction compared to cast-in-place systems where there is a much higher likelihood for loose connections.

The results of this study showed that if concrete wall systems reduce leakage area, much larger energy savings can be realized at the expense of meeting proper ventilation requirements. Wood frame construction, which has become much tighter, currently provides infiltration that marginally meets minimum ventilation requirements. Consequently, concrete wall systems that further tighten the building envelope should incorporate mechanical ventilation to provide enough fresh outside air for the occupants. If a concrete home is experiencing energy savings around 40%, infiltration tests should be conducted to determine whether a mechanical ventilation system should be installed. Installing a simple system to mix a certain amount of outside air with the return air is inexpensive, roughly $200, but would significantly decrease energy savings. Although more expensive, between $1000 to $2000, an air-to-air heat exchanger would ensure proper ventilation while not sacrificing energy savings.

Concerning the validity of the prototypical house model, several comparisons showed the heating and cooling energy consumption to be mainly conservative. Compared to the REC survey, the prototypical house heating energy consumption was usually smaller while the cooling energy consumption varied. These discrepancies were mainly due to the high performance

features of the prototypical house other then the wall constructions, such as the highly insulated windows, which resulted in a more energy efficient house than those that comprised the REC survey results. In reference to the heating and cooling component loads obtained from DOE2.1 simulations in Huang et al (1999), the prototypical house component loads compared well. The main discrepancy was the significant difference in the internal heat gain since the Huang et al (1999) miscellaneous electronic equipment energy consumptions were unrealistically low. Another large discrepancy was that Huang et al (1999) used the ASHRAE Fundamentals foundation heat transfer method which has been shown to underestimate heat loss through the foundation. These differences also illustrate the importance of the context within which the wall analysis is conducted. Different assumptions about the overall house performance can lead to different conclusions about the impact of the wall system performance.

The ICF wall system energy savings were lower than published savings from two separate studies. One analysis (VanderWerf 1997), based upon utility bills from ICF and wood frame houses determined much larger energy savings, with an average of 40%. The main reason for this discrepancy was the lack of infiltration reduction accounted for in the present ICF analysis. Compared to a study of three homes, a wood frame and two ICF constructions, conducted by the NAHB Research Center (1999), the ICF energy savings from this study were slightly low. This study that was conducted in Maryland determined a 20% energy savings which was larger than the 11% energy savings calculated from the Washington DC ICF prototypical house in this study. The reason for this discrepancy was that the slab-on-grade construction of the wood frame house had an insulation break between the slab-on-grade and wall connection which accounted for a significant part of the total conditioning load. The ICF houses did not have this insulation break and therefore had a higher performance relative to the wood frame house.

The cost calculations concerning the various wall systems showed that the energy savings associated with ICF and PCP systems can contribute to offsetting the added annual mortgage cost associated with the increased construction costs. Yet to be economically justifiable, the other attractive features of ICF and PCP systems such as greater durability and disaster resistance must be quantified and factored into the annual savings as well.

Based upon the literature review and the results and conclusions from this study, several other areas of analysis should be pursued to further investigate the thermal performance benefits of concrete wall systems for detached, single family homes. These recommendations are itemized in the following list.

1. Too few studies have assessed the impact of concrete wall systems on building envelope leakage. Yet based upon the results from this study, infiltration reduction may be the greatest energy saving benefit of concrete wall systems-more important than improved insulation configuration or thermal mass. As a result, the effect of concrete wall systems on the building envelope leakage area should be assessed through experimental analyses (blower door or tracer gas tests). These investigations should focus on what air leakage components the concrete wall systems affect (presumably wall/floor and wall/ceiling connections). Practices that yield consistent reductions in infiltration should be identified. In addition, standard recommendations should be defined for the home construction industry to properly measure the infiltration rate of concrete homes and install the necessary mechanical ventilation equipment to maintain the necessary air quality without compromising energy savings.
2. A sensitivity analysis should be conducted to further investigate parameters that affect thermal mass benefits. Several references claim that operating conditions such as thermostat setback and ventilation can have a considerable effect on the energy savings associated with thermal capacitance. According to Huang et al (1987), a greater dynamic response of the thermal mass to interior conditions can increase thermal mass benefits. Therefore, the simulation of the physical parameters affecting the response of the thermal mass specifically the surface convective and radiative heat transfer coefficient and increased conductivity of the concrete should be assessed.
3. Using the EnergyPlus thermal comfort calculations, a study should determine whether thermally massive wall systems provide increased comfort to the occupants. If such an effect exists, then the energy savings associated with altering the temperature setpoint deadband while still meeting a minimum thermal comfort range should be evaluated.
4. According to Kosny (2004), the thermal mass effects can be the largest in the ceiling surface thereby damping the large temperature fluctuations that a roof typically

experiences. Consequently, the energy savings effects of increased thermal mass in the ceiling surface should be assessed.

5. Several references (Kossecka and Kosny 2002; Kossecka 1999; ASHRAE 2001d) define correlations between the structure factors of the equivalent wall and the parameters defined in the frequency response method in Carslaw and Jaeger (1959). The relationships between the frequency response parameters and the structure factors should be further characterized. As a result, the dynamic behavior of various wall systems can be better understood and a reversal in the wall design methodology can occur where wall systems can be designed based upon the desired dynamic behavior, most importantly thermal delay. In most cases, wall systems should ideally delay an exterior thermal event 12 hours until it propagates through the wall to the interior surface. Understanding the relationship between the structural factors and the frequency response method, a designer could determine the proper wall arrangement to achieve this optimum behavior.
6. Finally, further research in "phase change materials" should be conducted to determine ways to incorporate thermal mass benefits using phase change materials instead of concrete.

REFERENCES

Akins, R.E., J.A. Peterka, and J.E. Cermak. 1979. *Averaged pressure coefficients for rectangular buildings*, Wind Engineering, Proc. Fifth International Conference 7:369-80, Fort Collins, CO. Pergamon Press, NY.

Alspach, P. 2004. Project Engineer - Ove Arup Corporation. Personal Correspondence.

Arasteh, D., B. Griffith, and P. LaBerge. 1994. Integrated Window Systems: An Advanced Energy-Efficient Residential Fenestration Product. Building Technologies Program, Windows and Daylighting Group, Energy and Environment Division. Lawrence Berkeley Laboratory. University of California, Berkeley, California.

ARI. 2004. "Air-Conditioning and Refrigeration Institute." Online posting. http://www.ari.org/.

ASCE. 1998. Minimum Design Loads for Buildings and Other Structures. Standard 7-1998. American Society of Civil Engineers, New York.

ASHRAE. 1988. ASHRAE Standard 119 – Air Leakage Performance for Detached Single-Family Residential Buildings. Atlanta: American Society of Heating, Refrigerating and Air-Conditioning Engineers, Inc.

ASHRAE. 1992. ASHRAE Standard 55 – Thermal Environmental Conditions for Human Occupancy. Atlanta: American Society of Heating, Refrigerating and Air-Conditioning Engineers, Inc.

ASHRAE. 1999. Ventilation for Acceptable Indoor Air Quality. ANSI/ASHRAE Standard 62-1999.

ASHRAE. 2000. A Method of Determining Air Change Rates in Detached Dwellings. ANSI/ASHRAE Standard 136-2000.

ASHRAE, 2004. ASHRAE Standard 152P - Method of Test for Determining the Design and Seasonal Efficiencies of Residential Thermal Distribution Systems. Atlanta: American Society of Heating, Refrigerating and Air-Conditioning Engineers, Inc.

ASHRAE. 1989. *1989 ASHRAE Handbook – Fundamentals*. Atlanta: American Society of Heating, Refrigerating and Air-Conditioning Engineers, Inc.

ASHRAE, American Society of Heating, Refrigeration, and Air-Conditioning Engineers. 1991. "Service Water Heating," in ASHRAE Handbook of HVAC Applications. Atlanta: ASHRAE.

ASHRAE 2000. ASHRAE Analytical Test Suite – Building Fabric, 1052RP Draft Final Report, December 2000.

ASHRAE. 2001a. *2001 ASHRAE Handbook – Fundamentals*. Atlanta: American Society of Heating, Refrigerating and Air-Conditioning Engineers, Inc.

ASHRAE. 2001b. ASHRAE Standard 90.2: Energy-Efficient Design of Low-Rise Residential Buildings. Atlanta: American Society of Heating, Refrigerating and Air-Conditioning Engineers, Inc.

ASHRAE. 2001c. ASHRAE Standard 140, Standard Method of Test for the Evaluation of Building Energy Analysis Computer Programs, August 2001.

ASHRAE. 2001d. ASHRAE Project 1145-TRP. Part 1 Draft Final Report: Modeling Two- and Three- Dimensional Heat Transfer Through Composite Wall and Roof Assemblies in Hourly Energy Simulation Programs. Atlanta: American Society of Heating, Refrigerating and Air-Conditioning Engineers, Inc.

ASTM 1993. Standard C236-89. "Standard Test Method for Steady-State Thermal Performance of Building Assemblies by Means of a Guarded Hot Box," Vol. 4.06, ASTM, Conshohocken, PA., pp. 53-63.

Azer, N.Z., Hsu, S., "The prediction of Thermal Sensation from Simple model of Human Physiological Regulatory Response", ASHRAE Trans., Vol. 83, Pt 1, 1977.

BEPAC 1993. B.H. Bland, Conduction Tests for the Validation of Dynamic Thermal Models of Buildings, Technical Note 93/1, August 1993.

Bergtold, G. Senior Development Specialist – DOW Chemical Company. Personal Correspondence.

Bursey, T., G.H. Green. 1970 Combined Thermal and Air Leakage Performance of Double Windows. ASHRAE Transactions 215-226.

Carpenter, Stephen. 2001. "Advances in Modeling Thermal Bridges in Building Envelopes," Enermodal Engineering Limited. Kitchener, ON, Canada.

Carrier Air Conditioning Company. 1965. "Handbook of Air Conditioning System Design," pp 1-100, Table 48. McGraw Hill.

Carrier Air Conditioning Company. 2004. "Furnace, Central Air Conditioning, and Heat Pump Manufacturing Performance Information" Online Posting. http://www.commercial.carrier.com/wcs/proddesc_display/0,1179,CLI1_DIV41_ETI4926_PRD697,00.html?SMSESSION=NO

Carslaw, H.S. and J.C. Jaeger. 1959. Conduction of Heat in Solids, Oxford University Press, Oxford.

Ceylan, H.T., and G.E. Myers. 1980. Long-time Solutions to Heat Conduction Transients with Time-Dependent Inputs. ASME Journal of Heat Transfer, Volume 102, No. 1, pp. 115-120.

Christian, J.E., "Thermal Mass Credits Relating to Building Envelope Energy Standards," ASHRAE, Transactions 1991, Vol. 97, Pt. 2.

Christian, J.E., and J. Kosny J. 1996. "Thermal Performance and Wall Ratings. ASHRAE Journal, March.

Colliver, D.G., W.E. Murphy, and W. Sun. 1992. Evaluation of the techniques for the measurement of air leakage of building components. Final Report of ASHRAE Research Project RP-438. University of Kentucky, Lexington.

Composite Technologies Inc. 2004. Wall Construction Detail Schematics. http://www.thermomass.com/downloads/default.htm.

Cornelissen, Alicje. 1998. Concrete Houses Reduce CO_2 - Fact or Fiction?. International Symposium on Sustainable Development of the Cement and Concrete Industry. Canadian Portland Cement Association. Ottawa, Canada.

Crawley, D.B., F.C. Winkelmann, L.K. Lawrie, and C.O. Pedersen. "EnergyPlus: A New-Generation Building Energy Simulation Program." Proc "Building Simulation '99," VolumeI, pp. 81-88, September 1999, Kyoto, Japan, IBPSA.

Donahey, Rex. 2004. Director of Engineering – Composite Technologies Corporation. Personal Correspondence.

ECCO. 1999. "Environmental Council of Concrete Organizations Information Article: What's Your IAQ I.Q.?" Skokie, Ill.

Electronic RECS. 2001. "Electronic RECS 99: Beta Version 3.1 Build 35" Pacific Northwest Laboratory. Richland Washington.

Ellis, M. 2001. "Whole-house Design through the Application of Multi-functional Precast Panels." NSF Research Proposal.

EMPA Duebendorf, Department of building physics. 1999. "Analysis, selection and statistical treatment of thermal properties of building material for the preparation of harmonized Design Values" CEN Technical Committee TC 89. Deubendorf, Switzerland.

Energy Information Administration (EIA). 1999. Residential Energy Consumption Survey (RECS) 1997.

EnergyPlus. 2004a. “Input Output Reference: The Encyclopedia Reference to EnergyPlus Input and Output”. Building Simulation Group. Lawrence Berkeley National Laboratory. Berkeley, California.

EnergyPlus. 2004b. “Engineering Documentation: The Reference to EnergyPlus Calculations”. Building Simulation Group. Lawrence Berkeley National Laboratory. Berkeley, California.

Fanger, P.O. 1986. “Radiation and Discomfort”, ASHRAE Journal. February 1986.

Fanger, P.O. 1970. “Thermal Comfort-Analysis and Applications in Environmental Engineering, Danish Technical Press, Copenhagen.

Fanger, P.O. 1967. “Calculation of Thermal Comfort: Introduction of a Basic Comfort Equation”, ASHRAE Trans., Vol. 73, Pt 2.

Feustel, H.E. and A. Raynor-Hoosen, eds. 1990 Fundamentals of the multizone air flow model-COMIS. Technical Note 29. Air Infiltration and Ventilation Centre, Coventry, Great Britain.

Feustel, H.E. and B.V. Smitth. 1997 COMIS 3.0-User’s Guide. University of California, Berkeley, California.

Gagge, A.P., Fobelets, A.P., Berglund, L.G., “A Standard Predictive Index of Human Response to the Thermal Environment”, ASHRAE Trans., Vol. 92, Pt 2, 1986.

Gajda, J. 2001. “Energy Use of Single-Family Houses with Various Exterior Walls,” Portland Cement Association.

Giaconia, C., A. Orioli.2000 “On the Reliability of ASHRAE Conduction Transfer Function Coefficients of Walls,” Applied Thermal Engineering. 21-47.

Grimsrud, D.T., M.H. Sherman, and R.C. Sonderegger. 1982. Calculating infiltration: Implications for a construction quality standard. Proceedings of the *ASHRAE-DOE Conference on the Thermal Performance of the Exterior Envelope of Buildings II*, p. 422. Las Vegas, NV.

Grot, R.A. and R.E. Clark. 1979 Air leakage charactersitcs and weatherization techniques for low income housing. Proceedings of the *ASHRAE-DOE Conference on the Thermal Performance of the Exterior Envelope of Buildings II*, p. 178. Orlando, FL.

Harrje, D.T. and G.J. Born. 1982. Cataloguing Air Leakage Components in Houses. Proceedings of the ACEEE 1982 Summer Study, Santa Cruz, CA. American Council for an Energy-Efficient Economy, Washington, D.C.

Hittle, D.C. 1979. Calculating Building Heating and Cooling Loads Using the Frequency Response of Multilayered Slabs, Ph. D. Thesis, University of Illinois, Urbana, IL.

Hittle, D.C. and R. Bishop. 1983. An Improved Root-Finding Procedure for Use in Calculating Transient Heat Flow Through Multilayered Slabs. International Journal of Heat and Mass Transfer, Vol. 26, No. 11, pp 1685-1693.

Hoke, J.R., Jr. "Architectural Graphic Standards," The American Institute of Architects, John Wiley and Sons, ISBN 0-471-81148-3.

Holmes, J.D. 1986. Wind loads on low-rise buildings: The structural and environmental effects of wind on buildings and structures, Chapter 12. Faculty of Engineering, Monash University, Melbourne, Australia.

Honma, H. 1975. *Ventilation of dwellings and its disturbances*. Faibo Grafiska, Stockholm.

Hsu, S., "A Thermoregulatory Model for Heat Acclimation and Some of its Application", Ph. D. Dissertation, Kansas State University, 1977.

Huang, Y.J., R. Ritschard, J. Bull, S. Byrne, I. Turiel, D. Wilson, C. Hsui, D. Foley. 1987, "*Methodology and Assumptions for Evaluating Heating and Cooling Energy Requirements in New Single-Family Residential Buildings*. Technical Support Document for the PEAR Microcomputer Program". Lawrence Berkeley National Laboratory. LBL-19128, Berkeley, CA.

Huang, Y.J., L.S. Shen, J.C. Bull, L.F. Goldberg. 1988, "Whole-House Simulation of Foundation Heat Flows using the DOE-2.1C Program". Lawrence Berkeley National Laboratory. Berkeley, CA.

Huang, J., J. Hanford, and Fuqiang Yang. 1999, "Residential Heating and Cooling Loads Component Analysis", Building Technologies Department. Lawrence Berkeley National Laboratory. Berkeley, CA.

Huang, J., and Gu, L. 2002, "Prototypical Residential Buildings to Represent the US Housing Stock", draft internal report. Lawrence Berkeley National Laboratory. Berkeley, CA.

IEA 1994. K.J. Lomas, C. Matrin, H. Eppel, M. Watson, and D. Bloomfield, Empirical Validation of Thermal Building Simulation Programs Using Test Room Data, Volume 2: Empirical Validation Package, September 1994.

ICFA. 2004. "Insulated Concrete Form Association – Insulated Concrete Form Costs." Online posting. http://www.forms.org/product_info/brief_costs.html.

Kosny, J. 2004. Scientist at Oak Ridge National Lab. Personal Correspondence.

Kosny, J. 2001. "Advances in Residential Wall Technologies-Simple Ways of Decreasing the Whole Building Energy Consumption". Oak Ridge National Laboratory, Building Technology Center.

Kosny, J. P Childs, and A. Desjarlais. 2001. Thermal Performance of Prefabricated Concrete Sandwich Wall Panels. Building Technology Center, Oak Ridge National Laboratory. TN.

Kosny, J., P. Childs. 2000. "Validation of Heating 7.2 Simulations Using Hot Box Test Data for RASTRA Wall Form System with Expanded Polystyrene-Beads. Oak Ridge National Laboratory, Building Technology Center.

Kosny, J., J.E. Christian, A.O. Desjarlais, E. Kossecka, and L. Berrenberg. 1999. Performance Check Between Whole Building Thermal Performance Criteria and Exterior Wall Measured Clear Wall R-Value, Thermal Bridging, Thermal Mass, and Airtightness. ASHRAE Transactions 104 (2), pp. 1379-1389.

Kosny, J., J.E. Christian. 1995 "Thermal Evaluation of Several Configurations of Insulation and Structural Materials for some Metal Stud Walls." Energy and Building 22. 157-163.

Kosny, J., A.O. Desjarlais. 1994 "Influence of Architectural Details on the Overall Thermal Performance of Residential Wall Systems. Oak Ridge National Laboratory, Building Technology Center.

Kosny, J., E. Kossecka. 2002. "Multi-Dimensional Heat Transfer through Complex Building Envelope Assemblies in Hourly Energy Simulation Programs." Energy and Buildings 34 445-454.

Kossecka, E., J. Kosny. 1996. "Relations between Structural and Dynamic Thermal Characteristics of Building Walls." Proceedings of 1996 International Symposium of CIB W67 "Energy and Mass flow in the Life cycle of Buildings", Vienna, 4-10 August 1996, pp. 627-632.

Kossecka, E., J. Kosny. 1997. "Equivalent Wall as a Dynamic Model of a Complex Thermal Structure." Thermal Insulation and Building Envelopes. Volume 20-January 1997.

Kossecka, E., J. Kosny. 2002. "Influence of Insulation Configuration on Heating and Cooling Loads in a Continuously used Building." Energy and Buildings 34 321-331.

Kossecka E. 1992. "Heat transfer through building wall elements of complex structure", Arch. Civ. Engn., 38(1-2), 117-126

Kossecka E. 1998. "Relationships Between Structure Factors, Response Factors, and Z-Transfer Function Coefficients for Multilayer Walls." ASHRAE Transactions Vol. 104(1A), 68-77.

Kossecka, E. 1999. “Correlations Between Structure Dependent and Dynamic Thermal Characteristics of Building Walls”, Journal of Thermal Insulation and Building Science, Vol. 22, 315-333.

Kreith, F., and R. Eisenstadt. 1957. *Pressure drop and flow characteristics of short capillary tubes at low Reynolds numbers*. ASME Transactions, pp. 1070-1078.

Latta, J.K. and G.G. Boileau. 1969. Heat losses from house basements Canadian Builiding 19(10):39.

Lau, A. P.E. 2004. Professor at Penn State University. Personal Correspondence.

Lee, Jaewook and Richard K. Strand. 2001. "An Analysis of the Effect of the Building Envelope on Thermal Comfort using the EnergyPlus Program," Association of Collegiate Schools of Architecture, *Proceedings of the ACSA Technology Conference*, Austin, Texas, 13-16 July 2001.

Long, Scott. 2004. Sales Manager – Long-Visio Technologies, Inc. Personal Correspondence.

Marino Industries Corporation, 1992. “NAHB Resource Conservation House-Construction Drawings,” January.

Mayflower Transit. 2004. “Table of Measurements” Fenton, MO.

McGowan, A.G. and A.O. Desjarlais, "An Investigation of Common Thermal Bridges in Walls,” ASHRAE Transactions. Vol. 103, part 1, January 1997.

Mitalas, G.P. Calculation of Basement Heat Loss. ASHRAE Trans., 89 (1) (1983) 420-438.

NAHB Research Center. 1997 Insulating Concrete Forms for Residential Construction Demonstration Homes. Washington, DC: U.S. Government Printing Office.

NAHB Research Center. 1998 Insulated Concrete Forms Construction Prescriptive Requirements. Washington, DC: U.S. Government Printing Office.

NAHB Research Center. 1999 Insulating Concrete Forms: Comparitive Thermal Performance. Washington, DC: U.S. Government Printing Office.

NAHB Research Center. 2001 Costs and Benefits of Insulating Concrete Forms for Residential Construction Washington, DC: U.S. Government Printing Office.

NFRC (National Fenestration Rating Council) 2002 “NFRC 100:2001 Procedure for Determining Fenestration Product U-factors” November, Silver Spring, MD.

Navigant Consulting (September 2003), "U.S. Lighting Market Characterization: Volume 1: National Lighting Inventory and Energy Consumption Estimate".

Neilsen. 1987. The 1987 Neilsen Report. Neilsen Media Research Company.

Neymark, J., and R. Judkoff. 2002. International Energy Agency Solar Heating and Cooling Programme Task 22 Building Energy Simulation Test and Diagnostic Method for HVAC Equipment Models (HVAC BESTEST), National Renewable Energy Laboratory, Golden, Colorado, NREL/TP-550-30152, January 2002.

Ouyang, K., and F. Haghighat. 1991. A Procedure for Calculating Thermal Response Factors of Multi-layered Walls—State Space Method. Building and Environment, Vol. 26, No. 2, pp. 173-177.

Parker, G.B., M. McSorley, and J.Harris. 1990. The Northwest Residential Infiltration Survey: A field study of ventilation in new houses in the Pacific Northwest. In *Air change rate and airtightness in buildings*, pp. 93-103. ASTM STP 1067. M.H. Sherman, ed.

Patankar, Suhas. 1980. Numerical Heat Transfer and Fluid Flow. Hemisphere Publishing Corporation. New York, New York.

Peony, B.A., F.J. Powell, and D.M. Burch. 1979. Dynamic thermal performance of an experimental masonry building. NBS Report 10 664, National Institute of Standards and Technology, Gaithersburg, MD.

Resfen 3.1. 2001. "Resfen 3.1: for Calculating the Heating and Cooling Energy Use of Windows in Residential Buildings. Building Technologies Program, Windows and Daylighting Group, Energy and Environment Division. Lawrence Berkeley Laboratory. University of California, Berkeley, California.

Reward Wall Systems. 2004. Wall Construction Detail Schematics. http://www.rewardwalls.com/install/iform_s5.pdf.

Ritschard, R.I., and Y.J. Huang 1989. Multi-family Heating and Cooling Requirements: Assumptions, Methods, and Summary Results. Topical Report No. GRI-88/0239, Gas Research Institute, Chicago, IL.

RSMeans. 2003. Residential Cost Data, 22nd Annual Edition.

Seem, J.E. 1987. Modeling of Heat Transfer in Buildings, Ph.D. Thesis, University of Wisconsin, Madison, WI.

Shen, L.S., J. Poliakova, and Y.J. Huang. 1988. Calculation of Building Foundation heat Loss using Superposition and Numerical Scaling, ASHRAE Trans., 94 (2) 917-935.

Sherman, M., and D. Dickerhoff. 1998. Air-Tightness of U.S. Dwellings. Energy Performance of Buildings Group, Energy and Environmental Division LBNL. University of California. Berkeley, CA.

Sherman, M.H., and D.T. Grimsrud. 1980. *Infiltration-pressurization correlation: Simplified physical modeling*. ASHRAE Transactions 86(1): 778-807.

Sherman, M.H. and D.T. Grimsrud, 1980 "The Measurement of Infiltration Using Fan Pressurization and Weather Data," In Proceedings, First AIC Conference: Air Infiltration Instrumentation and Measurement Techniques, Bracknell, Berkshire, Great Britain:Air Infiltration Centre, pp. 277-322. LBL-10752.

Sherman M and N. Matson. 1998. Residential Ventilation and Energy Characteristics. Energy Performance of Buildings Group, Energy and Environmental Division LBNL. University of California. Berkeley, CA.

Siegel J, McWilliams J, Walker I. (2002) Comparison Between Predicted Duct Effectiveness from Proposed ASHRAE Standard 152P and Measured Field Data for Residential Forced Air Cooling Systems. Berkeley: Lawrence Berkeley National Laboratory report #50008.

Strand, R.K. 1995. Heat Source Transfer Functions and Their Application to Low Temperature Radiant Heating Systems, Ph.D. Thesis, University of Illinois, Urbana, IL.

Sobotka P, Yoshino H, Matsumoto S. (1994) Thermal performance of three deep basements: a comparison of measurements with ASHRAE Fundamentals and the Mitalas method, the European Standard and two-dimensional FEM program. Energy and Buildings, 21 (1994) 23-34.

Thompson, G.L. 1995. Airtightness tests for the American Polysteel form houses, Contract # SW1547AF. Southwest Infrared Inc.

Tuluca A.N., D. Lahiri, J.H. Zaidi. 1997. “Calculation Methods and Insulation Techniques for Steel Stud Walls in Low-Rise Multifamily Housing,” ASHRAE Transactions. Vol. 103, part 1, January 1997.

US DOE, U.S. Department of Energy. 1990b. Technical Support Document: Energy Conservation Standards for Consumer Products: Dishwashers, Clothes Washers, and Clothes Dryers. DOE/CE-0299P. U.S. Department of Energy, Assistant Secretary, Conservation and Renewable Energy, Building Equipment Division.

US DOE, U.S. Department of Energy. 1993c. *Technical Support Document: Energy Efficiency Standards for Consumer Products: Room Air Conditioners, Water Heaters, Direct Heating Equipment, Mobile Home Furnaces, Kitchen Ranges and Ovens, Pool Heaters, Fluorescent Lamp Ballasts, and Television Sets.* DOE/EE-0009. U.S. Department of Energy, Assistant Secretary, Energy Efficiency and Renewable Energy, Office of Codes and Standards.

US DOE, U.S. Department of Energy. 1995a. *Household Energy Consumption and Expenditures 1995, Part 1: National Data*, Washington, DC: Energy Information Administration. DOE/EIA-0321/1(95).

US DOE, U.S. Department of Energy. 1995b. *Residential Energy Consumption Survey: Housing Characteristics 1993 and 1993 Public Use Data Tape*. DOE/EIA-0314(93). October.

US DOE, U.S. Department of Energy. 1995c. Technical Support Document: Energy Efficiency Standards for Consumer Products: Refrigerators, Refrigerator-Freezers, and Freezers. U.S. Department of Energy, Assistant Secretary, Energy Efficiency and Renewable Energy, Office of Codes and Standards.

US DOE, U.S. Department of Energy. 1995d. *Annual Energy Outlook 1995 With Projections to 2010.* DOE/EIA-0383(95). Energy Information Administration. December.

US DOE, U.S. Department of Energy. 1997. *Residential Energy Consumption Survey: Housing Characteristics 1995 and 1995 Public Use Data Tape*. DOE/EIA-0314(93). October.

US DOE, U.S. Department of Energy. 2002, "2003 Building Energy Databook", http://buildingsdatabook.eere.energy.gov/frame.asp?p=/bookdisplay.asp.

US DOE, U.S. Department of Energy. 2003, "Building America Research Benchmark Definition, Version 3.1", http://www.eere.energy.gov/buildings/building_america/pdfs/benchmark_def_ver3.pdf

VanderWerf, Pieter. 1997. Energy Comparisons of Concrete Homes Versus Wood Frame Homes. Building Works. Portland Cement Association.

VanderWerf, Pieter. 1998. Foam Forms Bring Concrete Results. Home Energy Magazine.

Walker, I.S., D.J.Wilson., and M.H. Sherman. 1997. *A comparison of the power law to quadratic formulations for air infiltration calculations*. Energy and Buildings 27 (3).

Walton, G.N. 1987. Estimating 3-D Heat Loss from Rectangular Basements and Slabs using 2-D Calculations. ASHRAE Trans., 93 (1). 791-797.

Wenzel, T.P., J.G. Koomey, G.J. Rosenquist, M. Sanchez, J.W. Hanford. 1997. *Energy Data Sourcebook for the U.S. Residential Sector*. Lawrence Berkeley National Laboratory. LBL-40297.

Windows 5.0. 2001. "Window 5.0 User Manual: For Analyzing Window Thermal Performance" Building Technologies Program. Lawrence Berkeley National Laboratory. Berkeley, CA.

Witte, Michael J., Robert H. Henninger, Jason Glazer, and Drury B. Crawley. 2001. "Testing and Validation of a New Building Energy Simulation Program" in *Proceedings of Building Simulation 2001*, pp. 353-360. Rio de Janeiro, Brazil, August 2001. IBPSA.

APPENDIX A: PROTOTYPICAL HOUSE SPECIFICATIONS

Tables A1 – A12 show the breakdown of the REC survey data for all single family detached homes surveyed and those just built after 1990 (US DOE 1995b).

Table A1. Number of Stories

	All Years		1990-1993	
	Homes	Percentage	Homes	Percentage
Split Level	151	3	18	3
One Story	2717	62	285	55
Two Story	1446	33	201	39
Three Story	74	2	16	3

Table A2. Neighborhood

	All Years		1990-1993	
	Homes	Percentage	Homes	Percentage
City	1576	36	124	24
Town	817	19	81	16
Surburbs	990	23	176	34
Rural	1006	23	138	27

Table A3. Number of Bedrooms

	All Years		1990-1993	
	Homes	Percentage	Homes	Percentage
0	6	0	0	0
1	98	2	7	1
2	881	20	34	6
3	2322	53	326	62
4	907	21	135	26
5	144	3	18	3
6	33	1	4	1
7	10	0	0	0

Table A4. Number of Full Bathrooms

	All Years		1990-1993	
	Homes	Percentage	Homes	Percentage
0	13	0	0	0
1	2224	51	62	12
2	1843	42	379	73
3	275	6	65	12
4	30	1	11	2
5	12	0	5	1

Table A5. Number of Half Bathrooms

	All Years		1990-1993	
	Homes	Percentage	Homes	Percentage
0	2941	67	304	59
1	1376	31	203	39
2	70	2	11	2
3	5	0	0	0
4	1	0	0	0

Table A6. Number of Other Rooms

	All Years		1990-1993	
	Homes	Percentage	Homes	Percentage
0	0	0	0	0
1	55	1	17	3
2	1089	25	121	23
3	1589	36	174	33
4	1064	24	131	25
5	380	9	48	9
6	127	3	20	4
7	95	2	15	3

Table A7. Heated Floor Area

	All Years		1990-1993	
	Homes	Percentage	Homes	Percentage
500	59	1	3	1
1000	487	11	20	4
1500	1021	23	105	20
2000	930	21	110	21
2500	743	17	81	15
3000	446	10	63	12
3500	304	7	53	10
4000	174	4	31	6
Over 4000	257	6	64	12

Table A8. Unheated Floor Area

	All Years		1990-1993	
	Homes	Percentage	Homes	Percentage
0	1875	42	153	29
100	126	3	8	1
200	184	4	12	2
300	277	6	31	6
400	319	7	44	8
500	374	8	85	16
1000	880	20	145	27
1500	222	5	31	6
2000	94	2	12	2
2500	34	1	5	1
3000	21	0	5	1
Over 3000	17	0	5	1

Table A9. Number of Windows

	All Years		1990-1993	
	Number	**Percentage**	**Number**	**Percentage**
0-4	4	0	4	1
5 to 9	912	21	110	21
10 to 14	1595	36	162	32
15 to 19	971	22	91	18
20 to 24	479	11	81	16
over 25	174	4	64	13

Table A10. Winter thermostat set point during occupied hours

	All Years		1990-1993	
	Number	**Percentage**	**Number**	**Percentage**
50-55	9	0	0	0
55-60	99	2	0	0
60-65	383	9	15	3
66	75	2	11	2
67	75	2	20	4
68	991	23	137	27
69	118	3	17	3
70	1329	30	149	29
71	71	2	10	2
72	518	12	54	11
73	52	1	12	2
74	61	1	8	2
75	247	6	18	4
76-80	159	4	38	7
80-85	9	0	3	1
85-90	79	2	0	0
Over 90	0	0	0	0
Heat Off	79	2	2	0
No Answer	75	2	1	0
NA	31	1	1	0

Table A11. Winter thermostat set point during unoccupied hours

	All Years		1990-1993	
	Number	**Percentage**	**Number**	**Percentage**
Under 50	86	2	8	2
50-55	97	2	11	2
55-60	506	12	63	12
61	11	0		
62	160	4	25	5
63	38	1	7	1
64	76	2	8	2
65	582	13	87	17
66	79	2	10	2
67	43	1	12	2
68	680	16	78	15
69	68	2	78	15
70	712	16	74	14
71	35	1	8	2
72	264	6	32	6
73	25	1	4	1
74	29	1	0	0
75	91	2	8	2
76-80	74	2	11	2
80-85	3	0	0	0
85-90	3	0	0	0
Over 90	0	0	0	0
Heat Off	631	14	49	10
No Answer	61	1	1	0
NA	31	1	1	0

Table A12. Winter thermostat set point during sleeping hours

	All Years		1990-1993	
	Number	**Percentage**	**Number**	**Percentage**
Under 50	50	1	5	1
50-55	76	2	4	1
55-60	457	10	39	8
61	10	0	1	0
62	153	3	22	4
63	51	1	8	2
64	88	2	10	2
65	620	14	80	16
66	103	2	14	3
67	71	2	17	3
68	768	18	101	20
69	77	2	14	3
70	810	18	99	19
71	32	1	6	1
72	295	7	35	7
73	26	1	7	1
74	32	1	3	1
75	111	3	11	2
76-80	89	2	14	3
80-85	5	0	0	0
85-90	2	0	0	0
Over 90	0	0	0	0
Heat Off	360	8	20	4
No Answer	68	2	1	0
NA	31	1	1	0

APPENDIX B: INTERNAL LOADS

Appendix B specifies each appliance and component that contributed to the overall residential internal heat gain, describing the particulars about the heat emitted from each and where that information was ascertained. The tables at the end of many of the sections, similar to those in Appendix A, are information gained from the 1997 REC survey.

People

Since the end purpose of this study was focused on human comfort in residences, the description of the condition of the occupants was very specific to most accurately model their interaction with the space conditions. Several schedules were necessary to completely define the inhabitants within the prototypical house. The first and most obvious schedule was used to define the number of inhabitants that lived within the residence and their hourly location within the different thermal zones of the house. From the information shown in Table B1 below, 3 individuals, an adult male, an adult female, and a child were specified within the house with identical routines. During the week, the inhabitants occupied the bedroom from 10 pm to 8 am and the living room from 8 to 9 am and 6 to 10 pm. During the weekends, they occupied the bedroom zone from 11 pm to 10 am and the living zone the rest of the day.

TableB1. Number of occupants per household (US DOE 1995c)

	All Years		1990-1993	
	Number	**Percentage**	**Number**	**Percentage**
1	630	14	31	6
2	1506	34	179	35
3	817	19	105	21
4	838	19	122	24
5	406	9	55	11
6	115	3	14	3
7	38	1	3	1
8	14	0	2	0
9	7	0	1	0

A second schedule was used to define the amount of heat in watts emitted by an occupant during each hour based on their activity level. When occupying the living zone, the inhabitants were assumed to be sitting and relaxing such that their metabolic rates were $60\,W/m^2$ of skin surface area. While in the bedroom zone, the inhabitants were assumed to emit $40\,W/m^2$ of skin surface to model sleeping (ASHRAE 2001). To calculate the total heat transfer from the occupants, these metabolic rates were multiplied by the estimated total skin surface area of 1.8 m^2, 1.6 m^2, and 1.4 m^2 for the adult male, adult female, and child respectively (Carrier Air 1965). The heat emitted by the occupants was split between latent and sensible heat based upon equations B1 and B2 (EnergyPlus 2004a):

$$\begin{aligned} Sen = {} & 6.461927 + 0.946892(met) + 0.0000255737(met)^2 + \\ & 7.139322(T_{inside}) - 0.0627909(T_{inside})(met) + 0.0000589172(T_{inside})(met)^2 - \\ & 0.198550(T_{inside})^2 + 0.000940018(T_{inside})(met) - 0.00000149532(T_{inside})^2(met)^2 \end{aligned} \quad \text{(B1)}$$

$$Lat = met - Sen \quad \text{(B2)}$$

where:

Sen is the sensible heat gain (W),

T_{inside} is the inside air temperature (°C),

met is the metabolic rate (W), and

Lat is the latent heat gain (W).

Of the sensible heat gain, 30% was emitted as long wave radiation while the rest was convected to the air.

A third schedule was used to describe the type of attire worn at different times during the day as quantified by the unit “clo”. During the cooling season that spanned from May 15 to September 30, the clothing value was set to 0.5 clo which represented the inhabitants wearing fitted trousers and a short sleeve tee-shirt. For the rest of the year, the clothing value was set to 1.01 clo representing an ensemble that consisted of loose trousers, a long-sleeve shirt, a long-sleeve sweater, and a T-shirt (ASHRAE 1989).

The fourth schedule was used to approximate the velocity of the zone air past each occupant during the day. From Table B2 below, the prototypical house had 1 ceiling fan. Consequently, a ceiling fan was modeled in the living zone by increasing the air velocity past the inhabitants during their hours of occupation of this zone. Based on the relationship between air velocity, ambient temperature, and activity level shown in the 1989 ASHRAE Fundamentals, the air velocity past the inhabitants with and without the fan was assumed to be 40 and 20 feet per minute (fpm) respectively.

Table B2. Number of ceiling fans used (US DOE 1995c)

	All Years		1990-1993	
	Number	**Percentage**	**Number**	**Percentage**
1	1007	23	101	20
2	668	15	78	15
3	451	10	66	13
4	350	8	84	16
5	218	5	39	8
6	91	2	15	3
7	0	0	15	3
NA	0	0	114	22

The last schedule was used to determine what percentage of the energy generated by each occupant was converted to heat rather then mechanical energy. For simplicity, all the energy created by the inhabitants was assumed to result in the emission of heat.

Lights

The lighting information for the prototypical house was based on the benchmark home developed by the DOE Building America program (US DOE 2003). The conditioned zones yearly light energy consumption was based upon the equation below (Navigant 2003):

$$\text{Interior Lighting} = (0.8 * \text{Conditioned Floor Space}) + 455. \qquad \text{(B3)}$$

Consequently, the conditioned zones consumed 2275 kWhr/yr, 90% incandescent and 10% fluorescent. Of that total energy, the living and bedroom zones consumed 63% and 37%

respectively (Navigant 2003). The energy consumed by the exterior, garage, and basement lights was 250, 100, and 0 kWhr/yr, respectively, all of which were incandescent (Navigant 2003). The load shape used for all the lighting was based on a modified draft of a LBNL report by Huang and Gu (Huang 2002) and is shown in Figure B1 below.

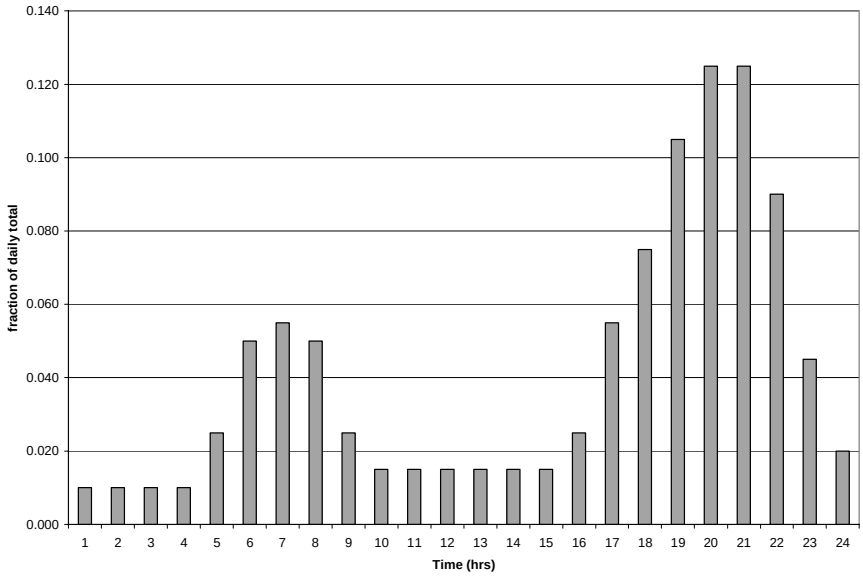

Figure B1. Daily load shape for all light energy consumption (Huang 2002)

All of the energy given off by the lights was split between convected heat and radiation. For the incandescent lights: 72% was long wave radiation, 10% was short wave radiation, and 18% was convected to the air (Kaufman 2-42). For the fluorescent lights: 30.7% was long wave radiation, 19.4% was short wave radiation, and 49.9% was convected to the air (Kaufman 2-42).

Water Heater

The modeling of the water heater was difficult due to the complexity of quantifying its: level of usage, behavioral impacts, climatic impacts, and energy impacts on different parts of the house. As shown in Table B5 below, the majority of households use a water heater with a capacity between 31 and 49 gallons. Therefore the water heater in the prototypical house had a 40 gallon storage capacity. The hot water consumption per day was set to 64.3 gallons based on a DOE test procedure for water heaters (ASHRAE 1991). The amount of energy consumed by the water heater to supply 64.3 gallons at a set point temperature of 120°F varied by location since the incoming water temperature changed with the climate. A calculation method developed by the

Building America program (US DOE 2003) provided the means to calculate the monthly incoming water main temperature for each of the prototypical house locations which is shown in Table B3 below. The annual energy consumption by the hot water heater independent of its efficiency was calculated using equation B4,

$$E_{HW} = \frac{V_{HW} * \Delta T_{rise} * C_W}{\frac{EF}{100}} * \frac{365 \text{ days}}{1 \text{ year}} * \frac{1 \text{ MMBtu}}{1{,}000{,}000 \text{ Btu}} \qquad \text{(B4)}$$

where:

E_{HW} is the hot water energy consumed per day (Btu),

V_{HW} is the gallons of hot water consumed per day (64.3 gallons),

ΔT_{rise} is the annual average temperature difference between the incoming cold water and the tank set point temperature (120°F), and

C_W is the specific heat of water (8.2928 Btu/gal-°F).

Table B3. Monthly inlet water main temperature for each prototypical house location

	Atlanta	Denver	Miami	Minneapolis	Phoenix	Washington DC
January	56.7	46.9	76.7	40.8	65.1	48.8
February	56.3	45.6	77.2	38.6	66.0	47.6
March	58.6	47.0	78.9	39.8	70.3	49.6
April	63.0	50.6	81.4	43.9	76.6	54.2
May	68.4	55.6	84.0	49.8	83.5	60.2
June	73.2	60.6	86.0	56.1	89.0	66.0
July	76.4	64.4	86.9	61.1	91.9	70.2
August	77.0	66.0	86.5	63.5	91.2	71.6
September	74.8	64.8	84.9	62.6	87.2	69.9
October	70.6	61.4	82.4	58.8	81.0	65.5
November	65.3	56.4	79.8	52.9	74.1	59.6
December	60.3	51.3	77.8	46.6	68.3	53.6

When the prototypical house contained a gas furnace, the hot water heater consumed gas. The gas water heater performance was simplified using two factors, the energy factor (EF) and the recovery efficiency (RE), defined by the equations below:

$$EF = \frac{E_{Delivered}}{E_{Total}} \tag{B5}$$

$$RE = \frac{E_{Delivered} + E_{Standby}}{E_{Total}} \tag{B6}$$

where:

$E_{Delivered}$ is the energy content of the hot water delivered (Btu),

E_{Total} is the total energy used to heat the water (Btu), and

$E_{Standby}$ is the standby loss-constant loss associated with keeping the water in the tank hot and ready for use (Btu).

Since the information from Table B6 showed that the age of hot water heaters are within two years of newly constructed homes, the prototypical house will have a hot water heater built after the 1990 energy efficiency standards. Therefore the energy factor and recovery efficiency were set to 54% and 76%, respectively (Wenzel et al. 1997) (US DOE 1993c). Knowing the recovery efficiency, energy factor, and total energy consumption, the standby loss was determined and represented the amount of heat distributed equally over the year to the basement zone where the hot water heater was located, 50% long wave radiation and 50% convected. The remaining energy that did not reach the tap was lost to the outside through the gas exhaust.

When the prototypical house contained a heat pump, the hot water heater consumed electrical energy. The electric water heater efficiency was set to 88% (Wenzel et al. 1997). The lost 12% energy was modeled as standby losses, distributed equally over the year to the basement zone where the hot water heater was located, 50% long wave radiation and 50% convected.

Table B4. Water heating fuel used (US DOE 1995c)

	All Years		1990-1993	
	Number	Percentage	Number	Percentage
Don't Use Hot Water	12	0	0	0
Piped Gas	2227	51	250	49
LPG or Propane	219	5	33	6
Fuel oil	235	5	25	5
Kerosene	1	0	1	0
Electricity	1659	38	203	40
Coal or Coke	3	0	0	0
Wood	5	0	0	0
Solar	24	1	0	0
Other	0	0	0	0

Table B5. Size of water heater (US DOE 1995c)

	All Years		1990-1993	
	Number	Percentage	Number	Percentage
No Water Heater	63	1	5	1
Small (less 30 gallons)	686	16	36	7
Medium (31-49 gallons)	2218	51	270	53
Large (over 50 gallons)	1181	27	175	34
Don't Know	217	5	26	5
NA	20	0	0	0

Table B6. Age of water heater (US DOE 1995c)

	All Years		1990-1993	
	Number	Percentage	Number	Percentage
No Water Heater	63	1	5	1
under 2 years	692	16	259	51
2-4 years	818	19	230	45
5-9 years	1180	27	11	2
10-19 years	920	21	0	0
over 20 years	354	8	0	0
Don't Know	338	8	7	1
NA	20	0	0	0

Dishwasher

Table B7 below indicates that the majority of homes have an automatic dishwasher. Dishwashers primarily impact residential energy use by consuming hot water. The total energy use attributable to a dishwasher can be divided into the energy needed to heat the incoming water and the electrical energy needed for the motor, dryer, and booster heater. From the baseline "Standard Water Heating Dishwasher" unit (US DOE 1990b), the dishwasher was assumed to operate for 229 cycles per year and to use 0.78 kWhr/cycle of electrical energy and 11.90 gallons/cycle of hot water from the water heater. Assuming each cycle lasted 1 hour and averaging 229 cycles over 365 days, the dishwasher used 489 W of electric energy per day from 8:00 to 9:00 pm everyday. Of this energy, 30% was convected to the air, 15% was emitted as latent heat, 30% was emitted as long wave radiation, and 25% was lost down the drain (US DOE 2003). All the energy contained in the hot water used by the dishwasher was assumed to be lost down the drain.

Table B7. Use of an automatic dishwasher (US DOE 1995c)

	All Years		1990-1993	
	Number	**Percentage**	**Number**	**Percentage**
No	1969	45	84	16
Yes	2416	55	428	84

Refrigerator

Refrigerators are typically the largest consumer of electricity among typical residential appliances. Base on the information in TablesB8, B9, and B10 below, the prototypical house has one 22 ft^3 refrigerator including an automatic freezer stacked on top of the main cooling compartment. Table B11 indicates that the prototypical house does not have a separate freezer. With Table B12 showing that new homes contain refrigerators built within 2 years of the construction time, the prototypical house contained the most recent top-freezer automatic defrost unit which used 649 kWhr/year (Wenzel 1997). Although the energy consumption from a refrigerator can be affected from 5-20% by a few degree change in the ambient room temperature, this variable behavior was considered negligible for the purpose of this study. Consequently, the average power of the refrigerator was kept at a constant 74 W throughout the

year. All the refrigerator power was assumed to be released as sensible heat into the living area where the refrigerator was located, 50% convected and 50% long wave radiation (US DOE 2003).

TableB8. Number of refrigerators per household (US DOE 1995c)

	All Years		1990-1993	
	Number	**Percentage**	**Number**	**Percentage**
0	3	0		
1	3462	79	437	85
2	872	20	73	14
Over 3	48	1	2	0

Table B9. Size of refrigerator (US DOE 1995c)

	All Years		1990-1993	
	Number	**Percentage**	**Number**	**Percentage**
less then 10 ft3	29	1	0	0
11-14 ft3	237	5	14	3
15-18 ft3	2134	49	203	40
19-22 ft3	1720	39	232	45
over 23 ft3	262	6	63	12
NA	3	0	0	0

Table B10. Type of refrigerator (US DOE 1995c)

	All Years		1990-1993	
	Number	**Percentage**	**Number**	**Percentage**
Half size or quarter	5	0	1	0
Reg with 1 door	217	5	6	1
Top and Bottom doors	3056	70	304	59
Side by Side Doors	1081	25	196	38
Other	23	1	5	1
NA	3	0	0	0

Table B11. Ownership of a separator freezer (US DOE 1995c)

	All Years		1990-1993	
	Number	Percentage	Number	Percentage
No	2320	53	312	61
Yes	2065	47	200	39

Table B12. Age of refrigerator (US DOE 1995c)

	All Years		1990-1993	
	Number	Percentage	Number	Percentage
Under 2	619	14	207	40
2-4 years	833	19	183	36
5-9 years	1343	31	73	14
10-19 years	1171	27	37	7
Over 20	314	7	7	1
Don't Know	102	2	5	1
NA	3	0	0	0

Clothes Washer

Table B13 below indicates that almost all homes have an automatic clothes washer. Much like a dishwasher, the contribution of the clothes washer to the household energy consumption was through using hot water. Based on the "Standard Clothes Washer" unit (US DOE 1990b), the clothes washer was assumed to run 380 cycles/year and to use 0.27 kWhr/cycle for the motor and 12.8 gallons/cycle of hot water from the water heater. Assuming that each cycle took 30 minutes to run and averaging 380 cycles over 365 days, the clothes washer used 562 W per day of electrical energy from 8:00 to 8:30 pm everyday. All the 3886 W of hot water energy consumed by the clothes washer during its operation was assumed to be lost down the drain. Of the motor energy, 80% was released into the basement zone where the clothes washer was located, 50% convected to the air and 50% as long wave radiation (US DOE 2003).

Table B13. Use of an automatic clothes washer (US DOE 1995c)

	All Years		1990-1993	
	Number	Percentage	Number	Percentage
No	255	6	7	1
Yes	4130	94	505	99

Clothes Dryer

Based upon Tables B14 and B15, the prototypical house contained an electric automatic clothes dryer. Using the "Standard Clothes Dryer" unit (US DOE 1990b), the clothes dryer ran 359 cycles/year, consuming 2.79 kWhr/cycle of electric energy. Therefore, the clothes dryer consumed 2744 W from 9:00 to 10:00 pm everyday. Of the electric energy consumed, 15% entered the basement zone as sensible heat, 50% convected and 50% by long range radiation, 5% entered the basement zone as latent heat, and 80% was lost to the outside (US DOE 2003).

Table B14. Ownership of a clothes dryer (US DOE 1995c)

	All Years		1990-1993	
	Number	Percentage	Number	Percentage
No	488	11	11	2
Yes	3897	89	501	98

Table B15. Fuel used for clothes dryer (US DOE 1995c)

	All Years		1990-1993	
	Number	Percentage	Number	Percentage
Electric	3183	73	422	82
Ugas	663	15	68	13
LPG	53	1	11	2

Shower

After accounting for the hot water used for the dish washer (7.57 gallons/day) and clothes washer (13.51 gallons/day), the remaining 43.22 gallons/day of hot water was assumed to be consumed for showers. Estimating an energy content of 498 Btu/gal of hot water determined from the gallons of water consumed per day and the hot water heater energy that was not lost through the flu or by standby losses, the shower consumed 5.78 kWhr per day. A simple experiment was

conducted in a bathroom of similar size, air conditions, and using an exhaust fan, indicated by Table B16, as that in the prototypical house to determine the amount of heat released to the conditioned zone. The resultant data, shown in Appendix C, determined that 10.77% and 1.55% of the total energy from the shower was released as latent and convective heat respectively. Using Table B17 below, each individual in the prototypical house took one 10 minute shower a day in succession such that the shower was on from 9:00 to 9:30 pm. Therefore, during that half an hour, 623 Whr and 90 Whr was emitted to the bedroom zone where the showers were located as latent and convective heat respectively. The remaining shower energy was assumed to be discharged down the drain.

TableB16. Use of an exhaust fan in the bathroom (US DOE 1995c)

	All Years		1990-1993	
	Number	**Percentage**	**Number**	**Percentage**
No	1616	37	64	13
Yes	2769	63	448	88

Table B17. Number of showers taken per week (US DOE 1995c)

	All Years		1990-1993	
	Number	**Percentage**	**Number**	**Percentage**
Under 10	965	22	45	9
10 to 20	1962	45	266	52
Over 20	1446	33	201	39
NA	12	0	0	0

Cooking Appliances

Using the information from Tables B18 and B19 below, the prototypical house used an electric range/oven and a microwave for cooking. These cooking appliances can account for 7% of the residential electricity consumption. From the Energy Data Sourcebook, electric ranges/ovens consume 822 kWhr/year and microwaves consume 132 kWhr/year. Using Table B20 below, the prototypical home was estimated to use the electric range/oven from 6:00 to 7:00 pm everyday consuming 2252 W during that time. Similarly, using Table B21 below, the microwave was used twice a day between 7:00 to 8:00 am and 6:00 to 7:00 pm, for fifteen minutes each, resulting in an average power of 723 W. Of the energy used by the range/oven and microwave,

30%, 20%, and 20% was emitted as latent heat, convective heat, and long wave radiation respectively, while the remaining 30% was released outside due to the existence of an exhaust fan indicated in Table B22 below (US DOE 2003).

Table B18. Fuel used for cooking (US DOE 1995c)

	All Years		1990-1993	
	Number	Percentage	Number	Percentage
No Cooking Done	2	0	0	0
Piped Gas	1221	28	118	23
LPG	225	5	23	4
Fuel Oil	1	0	0	0
Kerosene or Coal Oil	0	0	0	0
Electricity	2929	67	370	72
Coal or Coke	1	0	0	0
Wood	6	0	1	0

Table B19. Ownership of a microwave (US DOE 1995c)

	All Years		1990-1993	
	Number	Percentage	Number	Percentage
No	450	10	21	4
Yes	3933	90	491	96
NA	2	0	0	0

Table B20. Number of cooked meals a day (US DOE 1995c)

	All Years		1990-1993	
	Number	Percentage	Number	Percentage
2 or more per day	1628	37	162	32
once a day	2045	47	247	48
few times a week	611	14	89	17
once a week	55	1	8	2
under once a week	44	1	6	1
NA	2	0	0	0

Table B21. Frequency of microwave use for cooking (US DOE 1995c)

	All Years		1990-1993	
	Number	Percentage	Number	Percentage
Most or All	175	4	24	5
about half	659	15	95	19
some or little	1124	26	149	29
snack/defrost/reheat	1975	45	223	44
NA	452	10	21	4

Table B22. Use of an exhaust fan in the kitchen (US DOE 1995c)

	All Years		1990-1993	
	Number	Percentage	Number	Percentage
No	1616	37	64	13
Yes	2769	63	448	88

Television

Due to the large number of TV sets and the number of hours they are in use today, television can account for about 5% of the total electricity usage in the residential sector. From Table B23 below, the prototypical house had two TVs, a 27" using 276 kWhr/year and 20" using 199 kWhr/year (Wenzel et al. 1997). With the average household having at least one TV in operation over 7 hours a day (Neilson 1987), the 27" TV was set in the living zone and operated 4 hours a day, from 5:00 to 9:00 pm everyday, and the 20" TV was set in the bedroom zone and operated 3 hours a day, from 7:00 to 8:00 am and 9:00 to 11:00 pm everyday. Distributing the annual energy use specified by the REC survey data over the assumed operating schedule, the 27" and 20" televisions used 190 W and 182 W respectively. All of this energy was assumed to be emitted in their respective zones as sensible heat, 50% convected and 50% long wave radiation.

Table B23. Number of televisions per household (US DOE 1995c)

	All Years		1990-1993	
	Number	**Percentage**	**Number**	**Percentage**
0	68	2	4	1
1	1403	32	120	23
2	1671	38	216	42
3	868	20	119	23
4	271	6	39	8
over 5	104	2	14	3

Miscellaneous Electrical Equipment

Between one quarter to half of the residential appliance electric energy consumption is attributable to miscellaneous electrical equipment (Wenzel et al. 1997). Rather then get extremely specific, miscellaneous electrical equipment consumption in the prototypical house was set to 25 percent of the total electrical energy consumption. The resultant 2000 kWhr/year of electrical energy consumption by miscellaneous equipment was distributed evenly between the living and bedroom zones. Uniformly spread across each day of the year, 5.48 kWhr of electrical energy was consumed each day according to the distribution shown in Figure B2 below. All of this energy was assumed to be transferred to the respective zones, 45%, 45%, and 10% as convective heat, long wave radiation, and latent heat respectively (US DOE 2003).

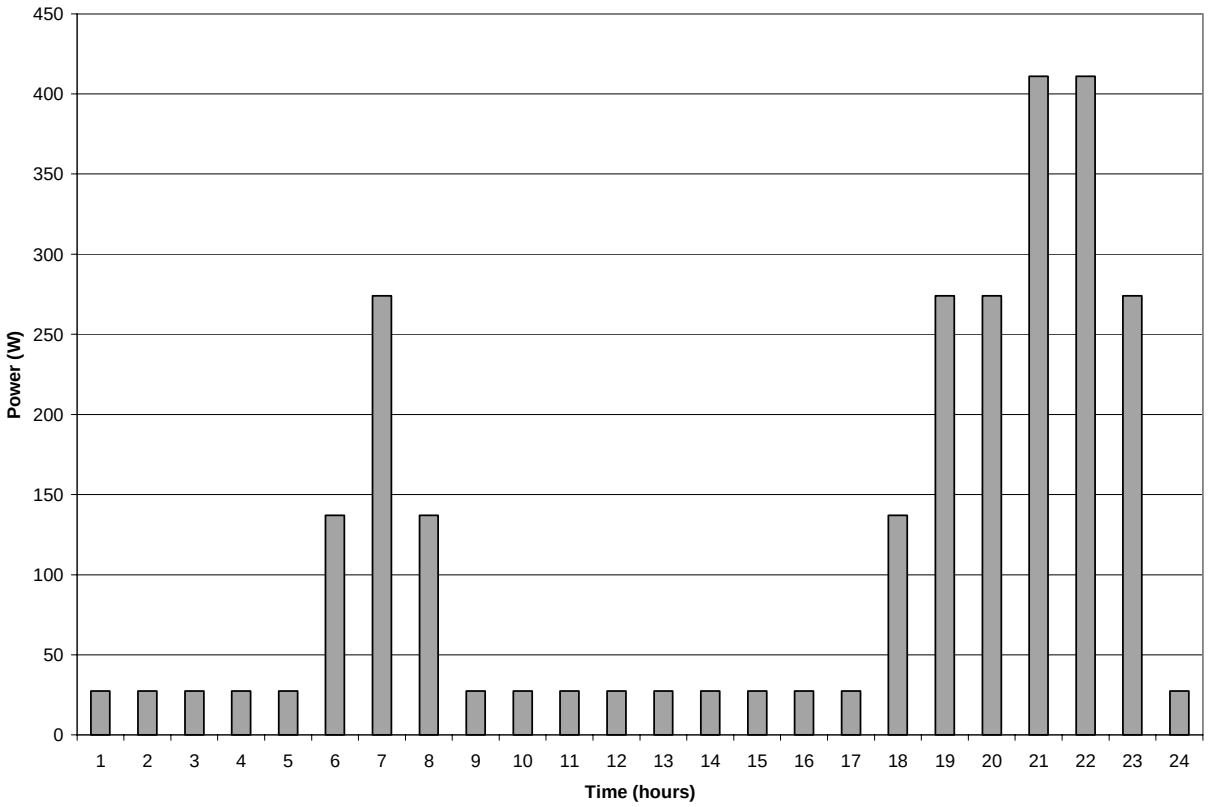

Figure B2. Hourly distribution of miscellaneous electric equipment energy consumption

Shower Test

Experiment

	Before Shower	After Shower
Dry-Bulb	25 (77)	31.11 (88)
Wet-Bulb	22.22 (72)	31.11 (88)

Water Temperature = 42.78 (109)

Drainage Temperature = 37.22 (99)

Water Consumption = 15.75 gallons

Calculations

1. Humidity Ratio of initial bathroom air

$T_{wet-bulb} = 22.22\ C$ therefore $P_{sat,wet-bulb} = 2.671\ kPa$

$h_{fg,,wet-bulb} = 2449.38\ kJ/kg$

$h_{f,wet-bulb} = 93.25\ kJ/kg$

$T_{dry-bulb} = 25\ C$ therefore $P_{sat,dry-bulb} = 3.169\ kPa$

$h_{g,dry-bulb} = 2547.2\ kJ/kg$

$$v_{sat,wet-bulb} = \frac{0.622\ P_{sat,wet-bulb}}{P_{atm} - P_{sat,wet-bulb}}$$

$$= \frac{(0.622)(2.671)}{101.325 - 2.671}$$

$$= 0.0168\ \text{kg H20 / kg air}$$

$$v_{initial\_air} = \frac{C_p (T_{wet-bulb} - T_{dry-bulb}) + v_{sat,wet-bulb} h_{fg,wet-bulb}}{h_{g,dry-bulb} - h_{f,wet-bulb}}$$

$$= \frac{(1.005\ kJ/kg\ C)(22.22\ C - 25\ C) + (0.0168)(2449.38\ kJ/kg)}{2547.2\ kJ/kg - 83.33\ kJ/kg}$$

= 0.0156 kg H20 / kg air

$$f = \frac{v_{initial\_air} P_{atm}}{(0.622 + v_{initial\_air}) P_{sat,dry-bulb}}$$

$$= \frac{(0.0156\ kgH20/kgAir)(101.325\ kPa)}{(0.622 + 0.0156\ kgH20/kgAir)\ 3.169\ kPa} =$$

= 78.2%

2. Water in Air

Before: 25°C at 78.2% R.H.

After: 31.11° at 100% R.H.

Room Volume: 16.99 m3

Air Mass: 21.24 kg air

a. Before shower

$$m_{water,before} = (w_{initial\_air})(AirMass) = (0.0156\ kg\ H2O/kg\ air)(21.24\ kg\ air)$$

= 0.3313 kg H2O

b. After shower

$$v_{final\_air} = \frac{0.622\ P_{sat,final\_air}}{P_{atm} - P_{sat,final\_air}} = \frac{(0.622)(4.553\ kPa)}{101.325\ kPa - 4.553\ kPa} = 0.0262\ \ kg\ H2O/kg\ air$$

$$m_{water,after} = (w_{final\_air})(AirMass) = (0.0262 \text{ kg H2O / kg air})(21.24 \text{ kg air})$$

=0.6202 kg H2O

3. Change in Air Latent Energy

$T_{dry\_bulb,initial} = 25$ C $\qquad h_{fg,initial} = 2442.3$ kJ/kg

$h_{f,initial} = 104.89$ kJ/kg

$T_{dry\_bulb,final} = 31.11$ C $\qquad h_{fg,initial} = 2418.6$ kJ/kg

$h_{f,final} = 130.43$ kJ/kg

$$E_{latent} = m_{water,final}(h_{f,final} + h_{fg,final}) - m_{water,before}(h_{f,initial} + h_{fg,initial})$$

= (0.6202 kg H2O) (130.43 kJ/kg + 2418.6 kJ/kg) – (0.3313 kg H20) (104.89 kJ/kg+2442.3 kJ/kg)

= 737.02 kJ

4. Change in Air Sensible Energy

$$E_{sensible} = m_{air}Cp_{air}(T_{final} - T_{initial}) = (21.24 \text{ kg air})(1.005 \text{ kJ/kg°C})\ (31.11°C\text{-}25°C)$$

= 130 kJ

5. Total Energy from Shower

$T_{water,entering} = 42.78$ C $\qquad h_f = 179.18$ kJ/kg

$$m_{water} = r_{water}Volume_{water} = (1000 \text{ kg / m3})(0.0596 \text{ m3}) = 59.6 \text{ kg}$$

$$E_{water} = h_f m_{water} = (179.18 \text{ kJ / kg})(59.6 \text{ kg}) = 10679.128 \text{ kJ}$$

6. Power Generated

$$P_{water} = \frac{E_{water}}{10 \text{ min}} = \frac{10679.128 \text{ kJ}}{600 \text{ s}} = 17.80 \text{ kW}$$

$$P_{latent} = \frac{E_{latent}}{10\ \text{min}} = \frac{737.02\ \text{kJ}}{600\ \text{s}} = 1.23\ \text{kW (6.91\% of total water power)}$$

$$P_{sensible} = \frac{E_{sensible}}{10\ \text{min}} = \frac{130\ \text{kJ}}{600\ \text{s}} = 0.22\ \text{kW (1.24\% of total water power)}$$

7. Water Heat Released

$$E_{water} = m_{water} Cp_{water} (T_{initial} - T_{idrainage}) = (59.6\ \text{kg})(4.18\ \text{kJ/kg C})(42.78\ \text{C} - 37.22\ )$$

$$= 1385\ \text{kJ}$$

$$P_{water} = \frac{E_{water}}{10\ \text{min}} = \frac{1385\ \text{kJ}}{600\ \text{s}} = 2.31\ \text{kW}$$

Model

	Before Shower	After Shower
Dry-Bulb	23.33 (74)	31.11 (88)
Relative Humidity	50	100

Water Temperature = 42.78 (109)

Drainage Temperature = 37.22 (99)

Water Consumption = 15.75 gallons

Room Volume: 16.99 m3

Air Mass: 21.24 kg air

1. Water in Air

a. Before shower

$T_{before} = 23.33\ \text{C}$ $\qquad$ $P_{g,before} = 2.616\ \text{kPa}$

$$w_{before} = \frac{0.622 f_{before} P_{g,before}}{P_{atm} - P_{g,before}} = \frac{(0.622)(0.50)(2.616\ \text{kPa})}{101.325\ \text{kPa} - 2.616\ \text{kPa}} = 0.00824\ \text{kg H20/kg air}$$

$$m_{water,before} = (w_{before})(AirMass) = (0.00824 \text{ kg H2O / kg air})(21.24 \text{ kg air})$$

$$= 0.175 \text{ kg H2O}$$

b. After shower

$T_{after} = 31.11$ C $\qquad P_{g,after} = 4.553$ kPa

$$w_{after} = \frac{0.622 f_{after} P_{g,after}}{P_{atm} - P_{g,after}} = \frac{(0.622)(1.0)(4.553 \text{ kPa})}{101.325 \text{ kPa} - 4.553 \text{ kPa}} = 0.0293 \text{ kg H20/kg air}$$

$$m_{water,after} = (w_{after})(AirMass) = (0.0293 \text{ kg H2O / kg air})(21.24 \text{ kg air})$$

$$=0.6223 \text{ kg H2O}$$

2. Change in Air Latent Energy

$T_{dry\_bulb,initial} = 23.33$ C $\qquad h_{g,before} = 2544.16$ kJ/kg

$T_{dry\_bulb,final} = 31.11$ C $\qquad h_{g,after} = 2558.30$ kJ/kg

$$E_{latent} = m_{water,after} h_{g,after} - m_{water,before} h_{g,before}$$

$$= (0.6223 \text{ kg H2O}) (2558.30 \text{ kJ/kg})-(0.175 \text{ kg H2O}) (2544.16 \text{ kJ/kg})$$

$$= 1146.80 \text{ kJ}$$

3. Change in Air Sensible Energy

$$E_{sensible} = m_{air} Cp_{air} (T_{final} - T_{initial}) = (21.24 \text{ kg air}) (1.005 \text{ kJ/kg°C}) (31.11°C-23.33°C)$$

$$= 166.07 \text{ kJ}$$

4. Total Energy from Shower

$T_{water,entering} = 42.78\ C$ $\qquad$ $h_f = 179.18\ kJ/kg$

$$m_{water} = r_{water} Volume_{water} = (1000\ kg/m3)(0.0596\ m3) = 59.6\ kg$$

$$E_{water} = h_f m_{water} = (179.18\ kJ/kg)(59.6\ kg) = 10679.128\ kJ$$

5. Power Generated

$$P_{water} = \frac{E_{water}}{10\ min} = \frac{10679.128\ kJ}{600\ s} = 17.80\ kW$$

$$P_{latent} = \frac{E_{latent}}{10\ min} = \frac{1146.80\ kJ}{600\ s} = 1.911\ kW\ (10.7\%\ of\ total\ water\ power)$$

$$P_{sensible} = \frac{E_{sensible}}{10\ min} = \frac{166.07\ kJ}{600\ s} = 0.28\ kW\ (1.55\%\ of\ total\ water\ power)$$

6. Water Heat Released

$$E_{water} = m_{water} Cp_{water} (T_{initial} - T_{idrainage}) = (59.6\ kg)(4.18\ kJ/kg\ C)(42.78\ C - 37.22\ )$$

$$= 1385\ kJ$$

$$P_{water} = \frac{E_{water}}{10\ min} = \frac{1385\ kJ}{600\ s} = 2.31\ kW$$

APPENDIX C: INFILTRATION INFORMATION

COMIS Capabilities

The following is a list of what COMIS can and can not do.

Can Do

2. Air flow through cracks in exterior or interzone surfaces
3. Air flow through cracks around windows and doors
4. Natural ventilation, i.e., air flow through open (or partially open) exterior windows and doors.
5. Control of natural ventilation based on inside/outside temperature or enthalpy difference.
6. Modulation of natural ventilation to prevent large temperature swings.
7. Interzone air flow, i.e., air flow through open interzone windows and doors, and through cracks in interzone surfaces.
8. Account for how air flow depends on buoyancy effects and wind pressure.
9. Account for how wind pressure depends on wind speed, wind direction, and surface orientation

Cannot Do

1. Account for the effect of outdoor supply-air and/or return-air flows in a zone when an HVAC air system is present and is operating. This means that the COMIS air flow simulation will give reliable answers only if: there is no HVAC system, the HVAC system is off, the HVAC system just recirculates air, or the HVAC system is hydronic.
2. Bi-directional flow through large horizontal openings.
3. Air circulation and/or temperature stratification within a thermal zone
4. Flow through ducts or other elements of an HVAC air system.
5. Pollutant transport
6. Air-flow networks that are not connected such that air flow can not be modeled in two or more separate groups of zones.

COMIS Wind Inputs

The wind specifications required by COMIS were descriptions of how the wind conditions would affect the exterior pressure surrounding the prototypical house. First, the height at which the wind speeds from the weather files was measured and the exponent of the wind velocity profile were set to 10 m and 0.14 respectively. These inputs allowed COMIS to generate the power law function that determines the wind velocity at different heights above the ground.

The next set of inputs defined the characteristics of the wind from the four different cardinal directions. For simplicity, all the following inputs were the same for all four directions. The density of the surrounding buildings over a reference area from a radius of 10 to 25 times the prototypical house height was set to 0.25, in between 0.0 and 0.5 representing an open field and a densely populated housing development respectively. The wind velocity profile exponent was set to 0.22 to represent rolling grassland broken by numerous obstructions such as trees or small houses. The surrounding building height was set to the prototypical house height.

The last set of wind data defined the wind pressure coefficient (Cp) value on each exterior surface of the prototypical house for each wind direction. The wind pressure coefficient is the ratio of the surface pressure to the dynamic pressure in the undisturbed flow pattern measured at a reference height. The Cp values used for the vertical surfaces were obtained from a study on the average pressure coefficients for rectangular buildings which determined the wind pressure coefficients based upon the length to width ratio of each wall (Akins et al, 1979). Figure C1 below shows the Cp values for the prototypical house walls facing each of the cardinal directions. The Cp values used for the north and south facing roofs were based upon a combination of the Akins study and research conducted for the Australian Housing Research Council (Holmes, 1986). Figure C2 below shows the Cp values for the north and south facing roofs of the prototypical house.

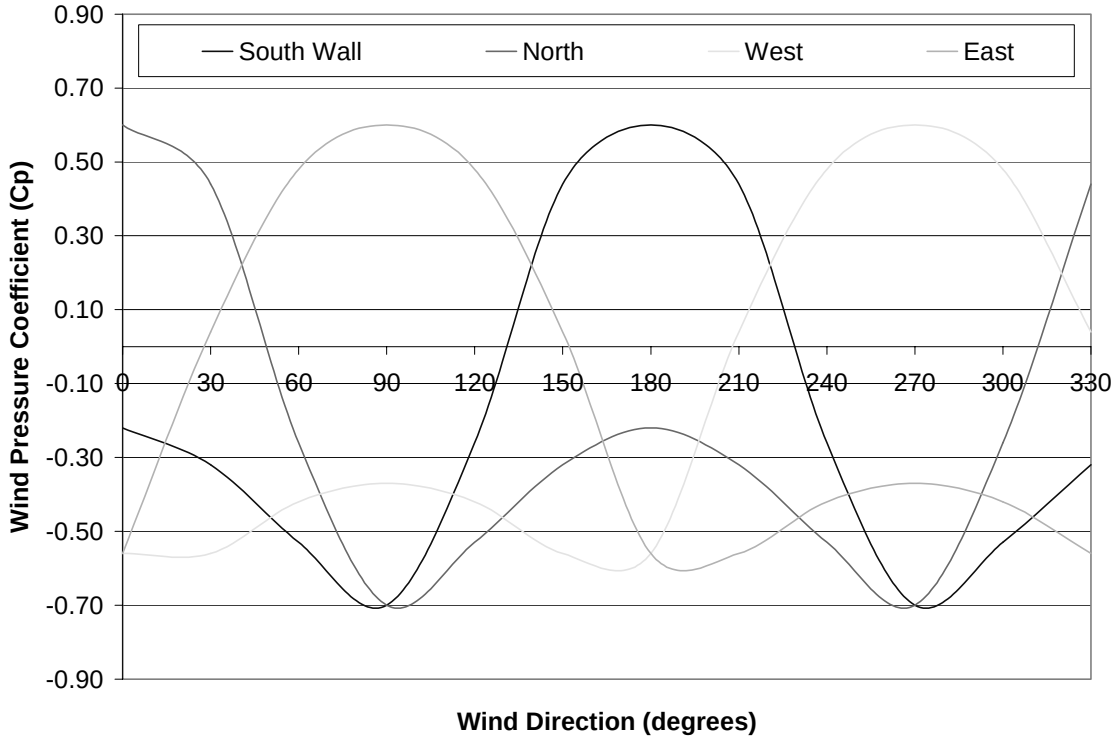

Figure C1. Wind pressure coefficient values for the prototypical house walls

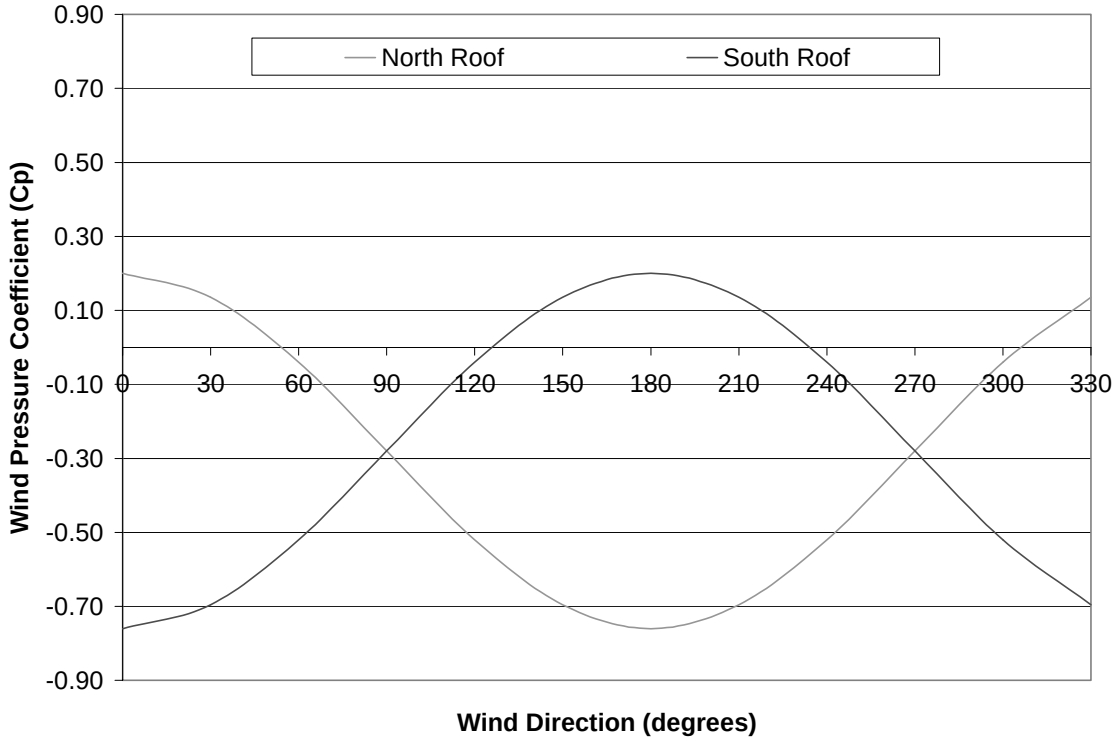

Figure C2. Wind pressure coefficient values for the prototypical house roofs

COMIS Crack Parameters

Once the crack ELA for each surface of the prototypical house was determined, a couple more calculations were made to convert that information to the correct input parameters for the COMIS program. The flow rate through each ELA was calculated for a reference pressure of 0.016 in of water and C_D =1.0 using equation 14

$$Q = C_D A_L \sqrt{\frac{2\Delta p_{ref}}{\rho_{air}}} \qquad \text{(C1)}$$

where:

Q is the flow rate (m3/s),

A_L is the ELA (m2),

Δp_{ref} is the reference pressure difference (Pa), and

ρ_{air} is the density of air at standard temperature and pressure (STP).

COMIS uses the power law equation to calculate the air flow through a crack based upon the pressure difference across it, as shown in equation 15

$$Q = C_Q (\Delta P)^n \qquad \text{(C2)}$$

where:

C_Q is the air mass flow coefficient (kg/s- Pa^n),

ΔP is the pressure difference across the crack (Pa), and

n is the air flow exponent.

As a result, the air mass flow coefficient for each building component was calculated based upon the air flow rate from equation 14, the reference pressure difference of 0.016 in of water, and a typical air flow exponent value. Although measurements of single cracks have shown that n can vary if ΔP changes over a wide range (Honma 1975, Krieth et al. 1957), Walker et all. (1997) has shown that for the arrays of cracks in a building envelope over the range of pressures acting during infiltration, n is constant. Consequently, based on whole house pressurization tests, the air flow exponent value was set to the typical value of 0.65 (ASHRAE 2001). Therefore, a crack assigned to each surface in the prototypical house was modeled with an air flow exponent of 0.65 and an air mass flow coefficient based upon the effective leakage area for that particular surface. These crack characteristics were assumed to be valid for standard temperature, barometric pressure, and humidity conditions of 20°C, 101.325 kPa, and 0 g/kg respectively.

APPENDIX D: CONDITIONING EQUIPMENT PERFORMANCE CURVES

CAC Performance Curves

1. Equation D1 below calculates the cooling capacity available (Cap_{Temp}) based upon the wetbulb temperature of the air entering the cooling coil (T_{wet}) and the drybulb temperature of the air entering the air-cooled condenser (T_{dry}).

$$Cap_{Temp} = Cap_{Rated}\left[0.9426 + 0.0095(T_{wet}) + 0.0007(T_{wet})^2 - 0.0110(T_{dry}) + 0.0(T_{dry})^2 - 0.0(T_{wet})(T_{dry})\right] \quad \text{D1}$$

2. Equation D2 below calculates the further reduction in the cooling capacity ($Cap_{Temp,Flow}$) from equation D1 based upon the ratio of the actual air flow rate across the cooling coil (R_{Flow}) to the rated air flow rate.

$$Cap_{Temp,Flow} = Cap_{Temp}\left[0.8 + 0.2(R_{Flow}) + 0.0(R_{Flow})^2\right] \quad \text{D2}$$

3. Equation D3 below calculates the reduction in the COP (COP_{Temp}) based upon the wetbulb temperature of the air entering the cooling coil (T_{wet}) and the drybulb temperature of the air entering the air-cooled condenser (T_{dry}).

$$\frac{1}{COP_{Temp}} = \frac{1}{COP_{Rated}}\left[0.3424 + 0.0349(T_{wet}) - 0.0006(T_{wet})^2 + 0.0050(T_{dry}) + 0.0004(T_{dry})^2 - 0.0007(T_{wet})(T_{dry})\right] \quad \text{D3}$$

4. Equation D4 below calculates the further reduction in the COP from equation D3 (COP_{Temp}) based upon the ratio of the actual air flow rate across the cooling coil to the rated air flow rate (R_{Flow}).

$$\frac{1}{COP_{Temp,Flow}} = \frac{1}{COP_{Temp}} \left[1.1552 - 0.1808(R_{Flow}) + 0.0256(R_{Flow})^2\right] \qquad D4$$

5. Equation D5 below reduces the COP from equation D4 further $(COP_{Temp,Flow,PLR})$ based upon the inefficiencies associated with the compressor cycling which is numerical specified by the part load ratio (R_{PLR}), sensible cooling load to steady-state sensible cooling capacity.

$$\frac{1}{COP_{Temp,Flow,PLR}} = \frac{1}{COP_{Temp,Flow}} \left[0.75 + 0.25(R_{PLR}) + 0.0(R_{PLR})^2\right] \qquad D5$$

Air-to-Air Heat Pump Heating Mode Performance Curves

1. Equation D6 below calculates the heating capacity available (Cap_{Temp}) based upon the outdoor drybulb temperature of the air (T_{dry}) entering the evaporator.

$$Cap_{Temp} = Cap_{Rated} \left[0.758746 + 0.027626(T_{dry}) + 0.000148716(T_{dry})^2 + 0.0000034992(T_{dry})^3\right]$$

D6

2. Equation D7 below calculates the final heating capacity availability $(Cap_{Temp,Flow})$ based upon the ratio of the actual air flow rate across the heating coil to the rated air flow rate (R_{Flow}).

$$Cap_{Temp,Flow} = Cap_{Temp} \left[0.84 + 0.16(R_{Flow}) + 0.0(R_{Flow})^2 + 0.0(R_{Flow})^3\right] \qquad D7$$

3. Equation D8 below calculates the reduction in the rated COP (COP_{Temp}) based upon the drybulb temperature of the air (T_{dry}) entering the evaporator.

$$\frac{1}{COP_{Temp}} = \frac{1}{COP_{Rated}} \left[1.1925 - 0.0300(T_{dry}) + 0.0010(T_{dry})^2 - 0.0000(T_{dry})^3\right] \quad \text{D8}$$

4. Equation D9 below calculates the final COP available $(COP_{Temp,Flow})$ based upon the ratio of the actual air flow rate across the heating coil to the rated air flow rate (R_{Flow}).

$$\frac{1}{COP_{Temp,Flow}} = \frac{1}{COP_{Temp}} \left[1.3824 - 0.4336(R_{Flow}) + 0.0512(R_{Flow})^2\right] \quad \text{D9}$$

5. Equation D10 below reduces the COP from equation D9 further $(COP_{Temp,Flow,PLR})$ based upon the inefficiencies associated with the compressor cycling which is numerical specified by the part load ratio (R_{PLR}) (sensible heating load / steady-state sensible heating capacity).

$$\frac{1}{COP_{Temp,Flow,PLR}} = \frac{1}{COP_{Temp,Flow}} \left[0.75 + 0.25(R_{PLR}) + 0.0(R_{PLR})^2\right] \quad \text{D10}$$

6. Equation D11 specifies the COP of the heat pump when it is operated in reverse during the defrost mode $(COP_{Defrost})$ based upon the outdoor air dry-bulb temperature (T_{dry}) and the air wet bulb temperature entering the heating coil (T_{wet}).

$$\frac{1}{COP_{Defrost}} = \frac{1}{COP_{Rated}} \left[0.0583 + 0.0(T_{dry}) + 0.0(T_{dry})^2 + 0.0(T_{wet}) + 0.0(T_{wet})^2 + 0.0(T_{wet})(T_{dry})\right]$$

D11

Air-to-Air Heat Pump Cooling Mode Performance Curves

1. Equation D12 below calculates the cooling capacity available (Cap_{Temp}) based upon the wetbulb temperature of the air entering the cooling coil (T_{wet}) and the drybulb temperature of the air entering the air-cooled condenser (T_{dry}).

$$Cap_{Temp} = Cap_{Rated}\left[0.7670 + 0.0108(T_{wet}) + 0.0(T_{wet})^2 + 0.0013(T_{dry}) - 0.0003(T_{dry})^2 + 0.0005(T_{dry})(T_{wet})\right] \quad \text{D12}$$

2. Equation D13 below calculates the further reduction in the cooling capacity ($Cap_{Temp,Flow}$) from equation D12 based upon the ratio of the actual air flow rate across the cooling coil (R_{Flow}) to the rated air flow rate.

$$Cap_{Temp,Flow} = Cap_{Temp}\left[0.8 + 0.2(R_{Flow}) + 0.0(R_{Flow})^2\right] \quad \text{D13}$$

3. Equation D14 below calculates the reduction in the COP (COP_{Temp}) based upon the wetbulb temperature of the air entering the cooling coil (T_{wet}) and the drybulb temperature of the air entering the air-cooled condenser (T_{dry}).

$$\frac{1}{COP_{Temp}} = \frac{1}{COP_{Rated}}\left[0.2971 + 0.0431(T_{wet}) - 0.0007(T_{wet})^2 + 0.0060(T_{dry}) + 0.0005(T_{dry})^2 - 0.0010(T_{wet})(T_{dry})\right] \quad \text{D14}$$

4. Equation D15 below calculates the further reduction in the COP from equation D15 (COP_{Temp}) based upon the ratio of the actual air flow rate across the cooling coil to the rated air flow rate (R_{Flow}).

$$\frac{1}{COP_{Temp,Flow}} = \frac{1}{COP_{Temp}}\left[1.156 - 0.1816(R_{Flow}) + 0.0256(R_{Flow})^2\right] \quad \text{D15}$$

5. Equation D16 below reduces the COP from equation D15 further ($COP_{Temp,Flow,PLR}$) based upon the inefficiencies associated with the compressor cycling which is numerical specified by the part load ratio (R_{PLR}), sensible cooling load to steady-state sensible cooling capacity.

$$\frac{1}{COP_{Temp,Flow,PLR}} = \frac{1}{COP_{Temp,Flow}} \left[0.75 + 0.25(R_{PLR}) + 0.0(R_{PLR})^2\right]$$